

Analysis of the Wnt receptors Ror, Otk and Otk2 during nervous system development in *Drosophila melanogaster*

Dissertation
for the award of the degree
“Doctor rerum naturalium”
within the doctoral program *Genes and Development*
of the Georg-August University Göttingen,
Faculty of Biology

submitted by

Caroline Ripp

Born in Stuttgart, Germany

Göttingen 2014

PhD Thesis Committee

Prof. Dr. Andreas Wodarz

Department for Anatomy and Cell Biology/Stem Cell Biology

Georg-August-University, Göttingen

Prof. Dr. Sigrid Hoyer-Fender

Department of Developmental Biology

Johann-Friedrich-Blumenbach-Institute of Zoology and Anthropology

Georg-August-University, Göttingen

PD Dr. Halyna Sherbata (MPI-bpc)

Gene expression and Signaling

Max Planck Institute for Biophysical Chemistry, Göttingen

AFFIDAVIT

I hereby declare that I prepared the thesis “Analysis of the Wnt receptors Ror, Otk and Otk2 during nervous system development in *Drosophila melanogaster*” on my own with no other sources and aids than quoted.

Caroline Ripp

Göttingen, December 31st, 2014

Table of Contents

Table of Contents

1. Introduction	1
1.1 Wnt signaling	1
1.1.1 The molecular basis of β -catenin dependent Wnt signaling	4
1.1.2 Establishment of PCP	6
1.2 Wnt ligands	9
1.2.1 Wingless is involved in patterning of the embryo and larval imaginal discs....	10
1.2.2 <i>Drosophila</i> Wnt2 functions in testes morphogenesis, tracheal development and indirect flight muscle attachment.....	12
1.2.3 Wnt4 can antagonize Wg signaling, elicit similar responses to Wg or have completely distinct functions.....	13
1.2.4 Wnt5 is involved in axon guidance and muscle attachment site selection.....	14
1.2.5 Other <i>Drosophila</i> Wnt proteins	15
1.3 The specificity of Wnt responses depends on ligand and receptors.....	16
1.4 Wnt receptors	18
1.4.1 Frizzled proteins are considered the primary Wnt receptors	18
1.4.2 LRP family receptors	20
1.4.3 Ryk proteins acts as guidance receptors	20
1.4.4 PTK7 and its <i>Drosophila</i> orthologs.....	22
1.4.5 Ror proteins	24
1.4.5.1 Structural features	24
1.4.5.2 Developmental functions.....	25
1.4.5.3 Intracellular responses.....	26
1.4.5.4 Kinase activity	27
1.4.5.5 Association with Frizzled receptors	28
1.4.5.6 <i>Drosophila</i> Ror family members	28
1.5 Scope of this Thesis.....	28
2. Material and Methods	30
2.1 Chemicals and enzymes	30
2.1.1 Chemicals and reagents	30
2.1.2 Enzymes	30
2.2 Antibodies and antisera	30

Table of Contents

2.3 <i>Drosophila melanogaster</i> stocks	32
2.4 Bacterial strains and cell culture lines.....	35
2.5 Synthetic oligonucleotides	36
2.6 Vectors and Constructs	37
2.7 Model organism <i>Drosophila melanogaster</i>	39
2.7.1 Culturing of <i>Drosophila melanogaster</i>	39
2.7.2 Crosses of <i>Drosophila melanogaster</i> strains.....	40
2.7.3 Fertility test for <i>Drosophila melanogaster</i> males and females.....	40
2.7.4 Viability test.....	40
2.7.5 Directed gene expression using the UAS-Gal4-System.....	40
2.8 Isolation of nucleic acids	41
2.8.1 Mini preparation of plasmid DNA from <i>Escherichia coli</i> (alkaline lysis method)	41
2.8.2. Midi Preparation of plasmid DNA from <i>Escherichia coli</i>	42
2.8.3 Preparation of genomic DNA from <i>Drosophila melanogaster</i>	43
2.8.4 Preparation of genomic DNA from single flies.....	43
2.8.5 Isolation of total RNA from <i>Drosophila melanogaster</i> embryos	44
2.9 Amplification and cloning of nucleic acids.....	45
2.9.1 Amplification of DNA using polymerase chain reaction (PCR).....	45
2.9.2 Colony PCR	46
2.9.3 Restriction of DNA.....	47
2.9.4 Cloning of PCR products in the Entry vector	47
2.9.5 Cloning of PCR products via Gateway® Cloning (Invitrogen)	48
2.9.6 Generation of GFP fusion proteins via Recombineering (recombination- mediated genetic engineering)	49
2.9.6.1 Transformation of BAC clone in SW102 cells.....	50
2.9.6.2 Amplification of GFP selection cassette.....	50
2.9.6.3 Recombination of GFP selection cassette into BAC containing gene of interest	51
2.9.6.4 Removal of the kanamycin cassette via Cre-recombination	52
2.9.6.5 Copy number induction of positive clones and large construct preparation	52

Table of Contents

2.9.7 Transformation of DNA into chemically competent <i>Escherichia coli</i>	53
2.9.8 Electroporation of DNA into electrocompetent <i>E.coli</i> cells.....	54
2.9.9 Preparation of <i>Escherichia coli</i> stab cultures.....	54
2.10 Analyses of DNA.....	54
2.10.1 Electrophoretic separation of DNA (Sambrook et al., 1989).....	54
2.10.2 DNA extraction from agarose gels.....	55
2.10.3 Ethanol precipitation of DNA.....	55
2.10.4 Photometric determination of DNA concentrations	56
2.10.5 Sequencing of DNA sequences	56
2.11 Histological methods	57
2.11.1 Formaldehyde fixation of <i>Drosophila</i> embryos	57
2.11.2 Antibody stainings on <i>Drosophila</i> embryos and third instar larval imaginal discs.....	58
2.11.3 Immunoperoxidase staining and dissection of the embryonic CNS.....	58
2.11.4 Dissection and staining of third instar larval brains	59
2.11.5 Dissection and analysis of pupal <i>Drosophila</i> genital discs.....	60
2.11.6 Preparation of adult <i>Drosophila</i> wings	60
2.11.7 Cuticle preparations of <i>Drosophila</i> embryos.....	60
2.11.8 Analysis of PCP defects in adult <i>Drosophila</i> eyes	61
2.12 Cell culture	61
2.12.1 Culturing <i>Drosophila</i> Schneider cells	61
2.12.2 Transfection of <i>Drosophila</i> Schneider cells.....	62
2.13 Biochemical methods.....	62
2.13.1 Preparation of cell lysates from <i>Drosophila</i> embryos	62
2.13.2 Determination of Protein concentration	63
2.13.3 Co-immunoprecipitation.....	63
2.13.4 SDS-PAGE	64
2.13.5 Western Blot	64
2.14 Transcriptome analysis	65
2.14.1 RNA isolation.....	65
2.14.2 Sample preparation and sequencing.....	65
2.14.3 Processing and analysis pipeline.....	66

Table of Contents

2.14.4 Venn Diagrams	67
2.14.5 Cluster network analysis	67
2.15 Imaging	67
2.15.1 Confocal microscopy	67
2.15.2 Lightsheet fluorescence microscopy (LSFM)	68
2.15.3 Light microscopy	68
2.15.4 Image processing	68
3. Results	69
3.1 Expression pattern of <i>Ror</i> > <i>Ror</i> -eGFP	69
3.1.1 <i>Ror</i> -eGFP is expressed in the embryonic nervous system	69
3.1.2 <i>Ror</i> -eGFP is expressed throughout the larval nervous system	72
3.1.3 <i>Ror</i> -eGFP is expressed in larval imaginal discs	74
3.2 Localization of <i>Ror</i> -eGFP is not affected in a <i>Wnt</i> mutant background	77
3.3 Generation of a null allele for <i>Ror</i>	78
3.4 Characterization of the <i>Ror</i> null allele <i>Ror</i> ⁴	80
3.4.1 The absence of <i>Ror</i> alone has no effect on viability but many <i>Ror</i> , <i>otk</i> , <i>otk2</i> triple mutants do not develop into adulthood	80
3.4.2 The embryonic nervous system of homozygous <i>Ror</i> ⁴ embryos displays a mild CNS phenotype	82
3.4.3 Adult <i>Ror</i> ⁴ mutant flies display no obvious defects in planar cell polarity	87
3.5 <i>Ror</i> interacts with members of the Wnt pathways	90
3.5.1 <i>Ror</i> genetically interacts with the ligand Wnt5	90
3.5.2 <i>Ror</i> binds to the Wnt ligands Wg, Wnt2 and Wnt4	93
3.5.3 <i>Ror</i> binds to the Wnt receptors Fz and Dfz2 and the Wnt co-receptors Otk and Otk2	94
3.6. Overexpression of <i>Ror</i>	95
3.6.1 <i>Ror</i> -Myc overexpression using the Gal4-UAS system	95
3.6.2 Viability is not affected by <i>Ror</i> overexpression	96
3.6.3 <i>Ror</i> overexpression does not lead to any PCP defects in adult flies	97
3.6.4 Overexpression of <i>Ror</i> -Myc does not affect nervous system development ..	100
3.7. Transcriptome analysis	103
3.7.1 Nearly all reads could be mapped to the <i>Drosophila</i> genome	104

Table of Contents

3.7.2 The mapped reads in the genomic regions of <i>Ror</i> , <i>otk</i> and <i>otk2</i> correspond to the genotypes of the used fly lines.....	105
3.7.3 Differentially expressed genes in <i>Ror</i> and <i>otk</i> , <i>otk2</i> mutant embryos	106
3.7.4 Cytoscape analysis	108
4. Discussion.....	113
4.1 Expression of <i>Ror</i> > <i>Ror</i> -eGFP	113
4.1.1 <i>Ror</i> > <i>Ror</i> -eGFP is primarily expressed in the nervous system.....	113
4.1.2 <i>Ror</i> -eGFP expression does not depend on Wg, Wnt2, Wnt4 or Wnt5.....	115
4.2 Loss-of-function and overexpression of <i>Ror</i>	115
4.2.1 <i>Ror</i> loss of function does not lead to lethality but results in a mild fasciculation defect while overexpression does not affect development.....	115
4.2.2 Neither <i>Ror</i> loss of function nor <i>Ror</i> overexpression affect PCP.....	118
4.2.3 The combined loss of <i>Ror</i> , <i>Otk</i> and <i>Otk2</i> increases the lethality rate and some embryos display CNS defects.....	118
4.3 <i>Ror</i> acts as receptor for Wnt ligands	119
4.3.1 <i>Ror</i> genetically interacts with Wnt5	119
4.3.2 Biochemical interactions with other Wnt family members.....	120
4.4 Possible signal transduction mechanism of <i>Drosophila</i> <i>Ror</i>	121
4.5 Transcriptomic analysis.....	123
4.5.1 The forkhead domain protein Fd59A is upregulated in <i>Ror</i> ⁴ mutant embryos	123
4.5.2 The microtubule-binding protein Tektin C is downregulated in <i>Ror</i> ⁴ mutant embryos as well as in <i>Df(otk, otk2)</i> D72 embryos	124
4.5.3 A potential zinc-finger transcription factor encoded by the gene CG32581 is downregulated in <i>Df(otk, otk2)</i> D72 embryos.....	125
5. References.....	127
6. Appendix	150
7. Curriculum vitae.....	173

Acknowledgements

Acknowledgements

First of all, I would like to express my gratitude towards my supervisor Prof. Dr. Andreas Wodarz for accommodating me in his group and for giving me an interesting project to work on. Thank you for your guidance, for supporting me always and for giving me the opportunity to bring forward and realize my own ideas.

Furthermore, I want to thank Prof. Dr. Sigrid Hoyer-Fender and Dr. Halyna Sherbata for being part of my thesis committee, being a great support during discussion of my results and conclusions and for providing input from different perspectives. Prof. Dr. Sigrid Hoyer-Fender I want to thank for writing the external review as well.

Dr. Reinhard Schuh, Prof. Dr. Heidi Hahn and Prof. Dr. Gregor Bucher I want to thank for taking part as members of my extended thesis committee during my defense.

Thanks also go to Prof. Dr. Jasprien Noordermeer for providing the *Ror4* mutant fly-line.

In addition, I would like to thank Dr. Marita Büscher for introducing me into the art of CNS dissection and for discussing aspects of *Drosophila* CNS development with me.

I would like to thank all present and former members of the Stem Cell Biology department and the members of the Kaffeerunde for four years I thoroughly enjoyed.

I am especially grateful to Dr. Manu Tiwari. Not only for performing the analyses of my initial RNA-Sequencing data and for discussing the drawn conclusions (even during the holidays!), but also for our many inspiring conversations in the evenings and for sharing your worldly wisdom with me.

Dr. Karen Linnemannstöns, my Wnt-companion, I want to thank for carefully reading the manuscript of my thesis as well as for discussing the outline of the thesis with me. I am also thankful for your friendship, support and encouragement and for always pointing me in the right direction when I was about to make something much more complicated than it really was.

An enormous amount of gratitude goes to Mona Honemann-Capito, who was a great help in performing numerous molecular biological experiments to support my thesis and to me is the heart and soul of our group. Thank you for being so organized, and for being so much fun to work with.

Julia Loth receives my thanks for performing a copious amount of co-immunoprecipitation experiments and transfections for me, for flipping my many flies when I couldn't get around to it, for rousing myself to get some exercise every now and then, for your friendship and maturity and for the many laughs we had.

Patricia Räke I thank for guiding me through the jungle of all my paperwork and especially for standing by me when I really needed somebody as assertive and understanding as you.

Claudia Buabe I thank for excellent technical support and taking care of my zoo.

I also want to express my gratitude towards Dr. Hamze Beati, whose ideas and discussions were a great help during all phases of my project. You gave me Lemmy, made me run and showed me how to keep ants. Thank you for always being so enthusiastic about everything and for inspiring the same enthusiasm in me.

Sascha Neubauer I want to thank for all the good times, for always lightening the atmosphere in the lab and for bequeathing your water tank to me (Hauste!).

Very special thanks go to Stefan for always being at my side, for your many valuable comments, for putting up with me, and for providing me with many excellent meals.

To my family I will always be thankful for always being there and for believing in me.

Last, I would like to thank the GGNB program "Genes and Development" for helpful discussion and support during my project, as well as for funding (GGNB and DFG).

Abstract

In vertebrates and also in *Drosophila*, Wnt signaling regulates many developmental and adult physiological processes. On the intracellular level, this functional diversity is achieved through the activation of several distinct Wnt pathways. The outcome is determined by a specific combination of a Wnt ligand and one or several Wnt receptors. Ror receptor tyrosine kinases are evolutionary conserved Wnt receptors. In vertebrates they function in many developmental processes including skeletal and neuronal development, cell movement and cell polarity. They are able to activate and repress transcription of Wnt target genes and also act during the establishment of planar cell polarity. So far, no phenotypic or functional data for the *Drosophila* Ror family member were available.

Using a fly line expressing Ror-eGFP under the endogenous promoter, we could show that *Drosophila* Ror is expressed in the nervous system. Ror-eGFP localizes to the plasma membrane. The expression commences after germ band retraction and persists throughout embryonic development within the ventral nerve cord and the brain. Besides the CNS, it can also be observed in the sensory organs of PNS. In the larval CNS Ror-eGFP it is visible in the membrane of all neuronal cells and not in glia. In larval imaginal discs Ror-eGFP can be observed in distinct cell clusters possibly representing proneuronal clusters.

Embryos mutant for *Ror* display a mild CNS defect. The axons forming the longitudinal pathways are not tightly associated and have a frayed appearance. A number of embryos in which the two PTK7 homologs Otk and Otk2 were removed as well, display an even stronger CNS phenotype and exhibit increased larval lethality. Furthermore, we could demonstrate that Ror genetically interacts with the ligand Wnt5 and is able to bind to Wg, Wnt2, Wnt4, as well as to the main Wnt receptors Fz and Fz2 and to Otk and Otk2. To identify downstream targets of Ror-, Otk/Otk2- and possibly also Ror/Otk/Otk2-signaling, we performed a transcriptome analysis and compared differentially expressed genes in the respective single, double and triple mutants. We have identified various genes, which are up- or downregulated including several transcription factors and proteins involved in nervous system development. Future analyses of this data set will enable us to define the functions of Ror, Otk and Otk2 during *Drosophila* development.

List of Figures

Figure 1: The three major Wnt signaling pathways.	3
Figure 2: Overview of β -catenin dependent Wnt signaling.	6
Figure 3: The PCP core proteins and their intracellular effectors.	9
Figure 4: Structure of human Wnt-1.	10
Figure 5: Specification of segmental boundaries and denticle secretion by Wntless signaling in the embryonic epidermis.	11
Figure 6: Different Wnt-receptor combinations.	17
Figure 7: Structure of Ror receptors in vertebrates and Invertebrates.	25
Figure 8: Mouse Ror mutants exhibit severe developmental defects.	26
Figure 9: Targeted gene expression with the UAS/Gal4 system.	41
Figure 10: Directional Topo Cloning.	48
Figure 11: Gateway® Cloning.	49
Figure 12: Generation of a C-terminal tagged GFP- fusion construct via Recombineering.	53
Figure 13: Expression of a Ror-eGFP fusion protein expressed under the endogenous <i>ror</i> promoter in <i>Drosophila</i> embryos imaged by confocal microscopy.	70
Figure 14: Lightsheet fluorescence microscopy of fixed and stained <i>Ror</i> > <i>Ror</i> -eGFP embryos.	71
Figure 15: Ventral nerve cord of a stage 16 <i>Ror</i> -eGFP embryo stained against GFP, Miranda and Elav.	72
Figure 16: <i>Ror</i> -eGFP expression in the central nervous system of third instar larvae.	73
Figure 17: <i>Ror</i> -eGFP is not expressed in glial cells within the central nervous system of third instar larvae.	74
Figure 18: <i>Ror</i> -eGFP expression in third instar larval imaginal discs.	77
Figure 19: The expression of <i>Ror</i> -eGFP is not reduced in homozygous <i>Wnt</i> mutant embryos.	78
Figure 20: The <i>Ror</i> allele <i>Ror</i> ^{E267} was generated via imprecise excision of a P-element. ..	79
Figure 21: The <i>Ror</i> allele <i>Ror</i> ⁴ was generated via transdeletion between two P-elements.	80
Figure 22: Embryonic viability of <i>Ror</i> mutants and <i>Ror</i> , <i>otk</i> , <i>otk2</i> triple mutants compared to wild type and homozygous <i>otk</i> , <i>otk2</i> double mutants.	81
Figure 23: The morphology of the ventral nerve cord in wild type embryos compared to <i>Ror</i> , <i>otk</i> and <i>otk2</i> mutants.	85
Figure 24: The number of CNS segments with disrupted fascicles in <i>Ror</i> and <i>otk,otk2</i> mutant embryos is not statistically relevant.	86
Figure 25: The PNS in <i>Ror</i> ⁴ mutant embryos is not affected.	86
Figure 26: Planar cell polarity in <i>Ror</i> mutant eyes is not disturbed.	88
Figure 27: Planar cell polarity in <i>Ror</i> mutant wings is not disturbed.	89
Figure 28: <i>Ror</i> -GFP binds to Myc-tagged Wg, Wnt2 and Wnt4.	94
Figure 29: <i>Ror</i> -GFP binds to Myc-tagged Fz, Fz2, Otk and Otk2.	95
Figure 30: <i>Ror</i> -Myc overexpression via the UAS-Gal4 system.	96
Figure 31: Embryonic viability of <i>Ror</i> -Myc overexpressing embryos compared to the used Gal4 driver and UAS line.	97
Figure 32: Planar cell polarity in wings of <i>Ror</i> -Myc overexpressing flies is not affected. .	98

List of Figures

Figure 33: Planar cell polarity in the eyes of Ror-Myc overexpressing flies is not disturbed.....	99
Figure 34: The morphology of the ventral nerve cord in filleted Ror-Myc overexpressing embryos compared to wild type embryos.....	101
Figure 35: The PNS of Ror-Myc overexpressing embryos.....	102
Figure 36: Central nervous system of a third instar <i>da>Gal4/UAS-Ror-Myc</i> larva.....	103
Figure 37: Number of mapped reads in all RNA-Sequencing samples.	104
Figure 38: IGV views of the genomic loci for <i>otk</i> , <i>otk2</i> and <i>Ror</i> in a triple mutant RNA-Seq sample.....	106
Figure 39: Venn diagrams of up- and downregulated genes.....	108
Figure 40: Cluster networks analysis of transcripts up- or downregulated in <i>Ror⁴</i> mutant embryos compared to the wild type.	109
Figure 41: Cluster networks analysis of transcripts up- or downregulated in <i>Df(otk, otk2)D72</i> double mutant embryos compared to the wild type.	111
Figure 42: Cluster networks analysis of transcripts up- or downregulated in <i>Ror⁴, Df(otk, otk2)D72</i> triple mutant embryos compared to the wild type.	112

List of Tables

List of Tables

Table 1: Primary antibodies used in this study	30
Table 2: Secondary antibodies used in this study	31
Table 3: <i>D. melanogaster</i> stocks used in this study	32
Table 4: Bacterial strains used in this study	35
Table 5: <i>Drosophila</i> cell lines used in this study.....	35
Table 6: Primers used in this study	36
Table 7: Vectors used in this study	37
Table 8: Constructs used in this study.....	37
Table 9: Ror genetically interacts with Wnt5.....	91
Table 10: Number of transcripts up- or downregulated in <i>Ror</i> , <i>otk</i> and <i>otk2</i> mutant embryos.....	107

1. Introduction

1.1 Wnt signaling

During the development of all organisms a tight control of cell-cell communication is required to ensure normal embryonic development. All key events during development are governed by the joint action of different signal transduction pathways (Basson, 2012). Among them, Wnt signaling is fundamental for the coordination of the complex cell behaviors that affect multiple traits and occur throughout development (Wodarz et al., 1998).

The first Wnt gene, *int-1*, was identified by the observation that the integration of MMTV (mouse mammary tumor virus) into the genome activates the *int-1* gene and induces mammary tumors in mice (Nusse and Varmus, 1982). Later it turned out that *Int-1* is the mouse ortholog of *Drosophila* Wingless (Wg) and the term Wnt signaling was introduced (Rijsewijk et al., 1987; Nusse et al., 1991).

Wnt signaling is highly conserved across a wide range of species. All metazoans have a complete set of Wnt ligands and the origin of Wnt signaling can be traced to pre-bilaterians (Holstein, 2012). On a cellular level, it is essential for cell proliferation (including stem cells), cell polarity, cell fate determination and cell migration (Logan and Nusse, 2004). At the organismal level, it is important for tissue homeostasis and tissue regeneration (Logan and Nusse, 2004; Reya and Clevers, 2005; Clevers, 2006).

During embryonic development, Wnt signaling plays diverse roles such as specification of the body axis, establishment of segment polarity, neural patterning and organ development (Cadigan and Nusse, 1997; Yamaguchi, 2001; Komiya and Habas, 2008; Hikasa and Sokol, 2013). Consequently, deregulated Wnt signaling leads to diverse developmental phenotypes ranging from embryonic lethality and defects in the central nervous system to defects in organ and limb development (Clevers, 2006; Wang et al., 2012; Herr et al., 2012). In adults, aberrant Wnt signaling results in the loss of controlled cell growth and impaired cell differentiation. For instance, in degenerative diseases such as osteoporosis the Wnt signaling level is too low, whereas Wnt signaling is elevated in

proliferative diseases such as cancers (Patel and Karsenty, 2002; Polakis 2012; Logan and Nusse, 2004).

Signaling by Wnt proteins activates several different intracellular signaling cascades. The pathway best understood is the β -catenin dependent, so-called canonical Wnt pathway, which acts through the regulation of β -catenin levels in the cytosol to activate target gene expression (Figure 1 B, detailed in 1.1.1). In the absence of a Wnt ligand, β -catenin is not able to accumulate in the cytoplasm because of ubiquitylation by a multi-protein destruction complex. Activation of Wnt activity by binding of a Wnt ligand to the receptors Frizzled (Fz) and LRP5/6, prevents targeting of β -catenin for proteasomal degradation (Ikeda et al., 1998; Kikuchi et al., 1999; He et al., 2004). It can then activate target gene transcription in the nucleus (Hurlstone and Clevers, 2002).

Besides the β -catenin dependent pathway there are other divergent downstream pathways, collectively termed β -catenin independent or non-canonical Wnt signaling pathways. The Wnt/ Ca^{2+} pathway is characterized by the increase of the intracellular calcium concentration (Figure 1 C). Binding of the Wnt ligand to the cell surface activates phospholipase C (PLC), which leads to calcium release. Subsequently, calcium/calmodulin-dependent protein kinase II (CAMKII), protein kinase C (PKC) and the protein phosphatase Calcineurin become activated. Calcineurin activates the transcriptional regulator nuclear factor associated with T cells (NFAT) resulting in the transcription of genes controlling cell fate and cell migration. PKC acts through Cdc42 to mediate cell movements and CAMKII activates other kinases, which antagonize β -catenin dependent Wnt signaling. This pathway has been shown to control the development of dorso–ventral polarity, morphogenetic movements during gastrulation, organ formation, and is also involved in inflammatory response and cancer (Kühl et al., 2000; Komiya and Habas, 2008; De, 2011).

Another β -catenin independent pathway is the planar cell polarity (PCP) pathway (Figure 1 A). In *Drosophila*, it regulates the polarity of cells within an epithelium (Adler and Lee, 2001). Its vertebrate counterpart regulates cell motility and morphogenetic movements (Simons and Mlodzik, 2008). Upon Wnt binding to the receptor, the cytoplasmic protein Dishevelled (Dvl/Dsh) becomes activated, which in turn, activates two pathway branches. The small GTPase RhoA activates Rho kinase (ROCK) leading to changes in the

Introduction

cytoskeleton and Rac1 activates c-Jun N-terminal kinase (JNK), which activates target gene transcription (Komiya and Habas, 2008; Niehrs, 2012).

Both the PCP and the Ca^{2+} pathway have been shown to antagonize β -catenin dependent signaling at various levels (Niehrs, 2012). And all Wnt pathways intersect with other intracellular signaling pathways. The Hippo pathway, which regulates tissue growth for example, intersects with the β -catenin dependent Wnt pathway on several levels (Konsavage and Yochum, 2013).

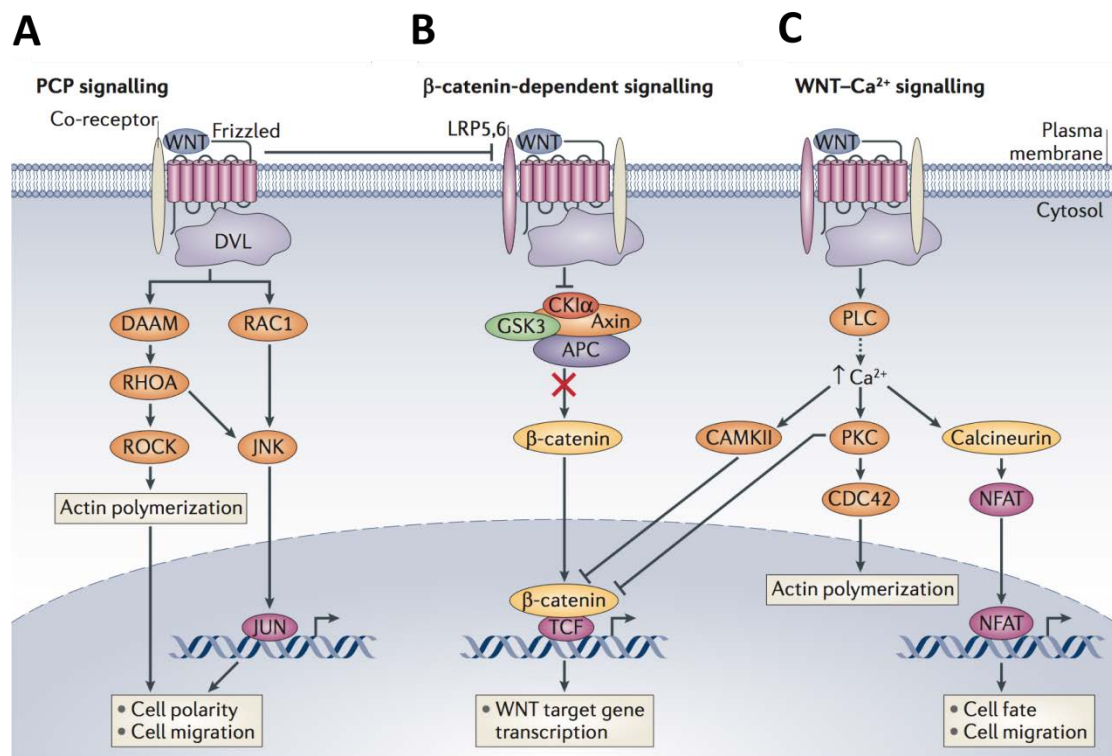


Figure 1: The three major Wnt signaling pathways. (A) The PCP pathway acts β -catenin independently and regulates cell polarity and cell motility through the kinases ROCK and JNK. (B) The β -catenin dependent Wnt signaling pathway regulates target gene transcription through the stabilization of intracellular β -catenin. (C) The Wnt/ Ca^{2+} pathway operates via the increase of the intracellular calcium levels and affects the cytoskeletal organization and gene expression. Taken from (Niehrs, 2012).

Dvl is the only intracellular component shared by all three pathways. While *Drosophila* has only one Dvl protein, mammals have three - Dvl-1, Dvl-2 and Dvl-3. The structure of Dvl is highly conserved and consists of the three main domains DIX, PDZ and DEP (Wallingford and Habas, 2005). However, the detailed mechanism of Dvl action has not been completely solved although it has been demonstrated that it becomes phosphorylated in response to Wnt binding and its nuclear localization is important for β -catenin dependent Wnt signaling (Yanagawa et al., 1995; Willert et al., 1997; Itoh et

al., 2005). Also, for different signal transduction pathways, different protein domains are used. For different Dvl domains are important for different Wnt pathways: for β -catenin dependent signaling, all three domains are necessary, while for Wnt/ Ca^{2+} and PCP signaling, only the PDZ and the DEP domain are needed (Wallingford and Habas, 2005).

1.1.1 The molecular basis of β -catenin dependent Wnt signaling

After the function of β -catenin (Armadillo [Arm] in *Drosophila*) as a signaling molecule was discovered, further studies were conducted in *Drosophila* and other model organisms that have led to the identification of the basic molecular signaling mechanism (Siegfried et al., 1994). As briefly mentioned earlier, the defining event in this Wnt pathway is the cytosolic accumulation and the subsequent translocation of β -catenin into the nucleus.

Under steady conditions, when no Wnt ligand is bound to the receptor, the β -catenin level in the cytosol is low. It is targeted for degradation by a destruction complex consisting of four core components Axin, adenomatous polyposis coli (APC), and the serine/threonine kinases glycogen synthasekinase-3 α/β (GSK3 α/β) (in *Drosophila* Shaggy/Zeste-white3) and casein kinase 1 α (CK1 α) (Clevers, 2006; MacDonald, 2009). These two kinases phosphorylate β -catenin (Amit et al., 2002; Liu, 2002; Yanagawa et al., 2002) and this interaction is facilitated by Axin and APC, which act as scaffolding proteins (Hart et al., 1998, Kishida et al., 1998). The phosphorylated β -catenin is then recognized by the E3 ubiquitin ligase β -TrCP (β -transducin repeats-containing protein, *Drosophila* ortholog Slimb [Slmb]), and subsequently degraded by the proteasome (Aberle et al., 1997; Jiang and Struhl, 1998; Marikawa et al., 1998; Latres et al., 1999). Consequently, in the nuclear absence of β -catenin, the transcription factor TCF (T cell factor) acts as a repressor together with members of the Groucho/TLE family and histone deacetylases to repress Wnt-responsive genes (Cavallo et al., 1998; Hurlstone and Clevers, 2002).

Binding of a Wnt ligand to Frizzled and its co-receptor LRP5/6 (low-density lipoprotein receptor-related protein, Arrow in *Drosophila*) has been proposed to mediate a physical interaction between the two receptors (Gordon and Nusse, 2006). After Wnt binding, Frizzled recruits the cytosolic Dvl to the membrane (Axelrod et al., 1998). The manner in which Dvl then transduces the signal is not fully understood. It has been established that Dvl becomes phosphorylated, but the role of this phosphorylation remains to be

Introduction

elucidated (Lee et al., 1999; Yanagawa et al., 1995; Willert et al., 1997; Sun, 2001). Additionally, phosphorylation of the co-receptor LRP5/6 by CK1 γ and GSK3 is also critical for signal transduction and mediates the binding of Axin (Davidson et al., 2005; Zeng et al., 2005; Mao et al., 2001). This membrane recruitment of Axin has been suggested to be sufficient to activate Wnt signaling (Brennan et al., 2004). For the subsequent steps leading to β -catenin stabilization, several models have been proposed. It has been suggested that the destruction complex dissociates either because Axin binds to LRP5/6 and Dvl (Liu, 2005; Logan and Nusse, 2004), or because Axin becomes degraded (Tolwinski et al., 2003). Other findings indicate that β -catenin can no longer be phosphorylated due to GSK3 inhibition (Cselenyi et al., 2008; Piao et al., 2008), or that it simply becomes dephosphorylated (Su et al., 2008). Interestingly, most of these models are based on physical dissociation of the destruction complex and/or interference with the phosphorylation of β -catenin (MacDonald et al., 2009). A more recent study however proposes an alternate model in which the phosphorylated β -catenin accumulates in the intact complex while β -TrCP dissociates upon pathway induction. Consequently, β -catenin is no longer ubiquitinated and degraded (Li et al., 2012). The stabilized cytoplasmic β -catenin then translocates into the nucleus and converts TCF/LEF into transcriptional activators by displacing Groucho and thereby, activating Wnt responsive genes (Molenaar et al., 1996; Behrens et al., 1996; Daniels and Weis 2005) (Figure 2). Additionally, in *Drosophila*, the activity of β -catenin also depends on Legless (Lgs) (ortholog of human BCL9) and Pygopus (Pygo, human PYGO1/2), which bind directly to β -catenin in the nucleus (Kramps et al., 2002; Hoffmans et al., 2005). Complexes of β -catenin with other proteins in the nucleus are cell-type dependent.

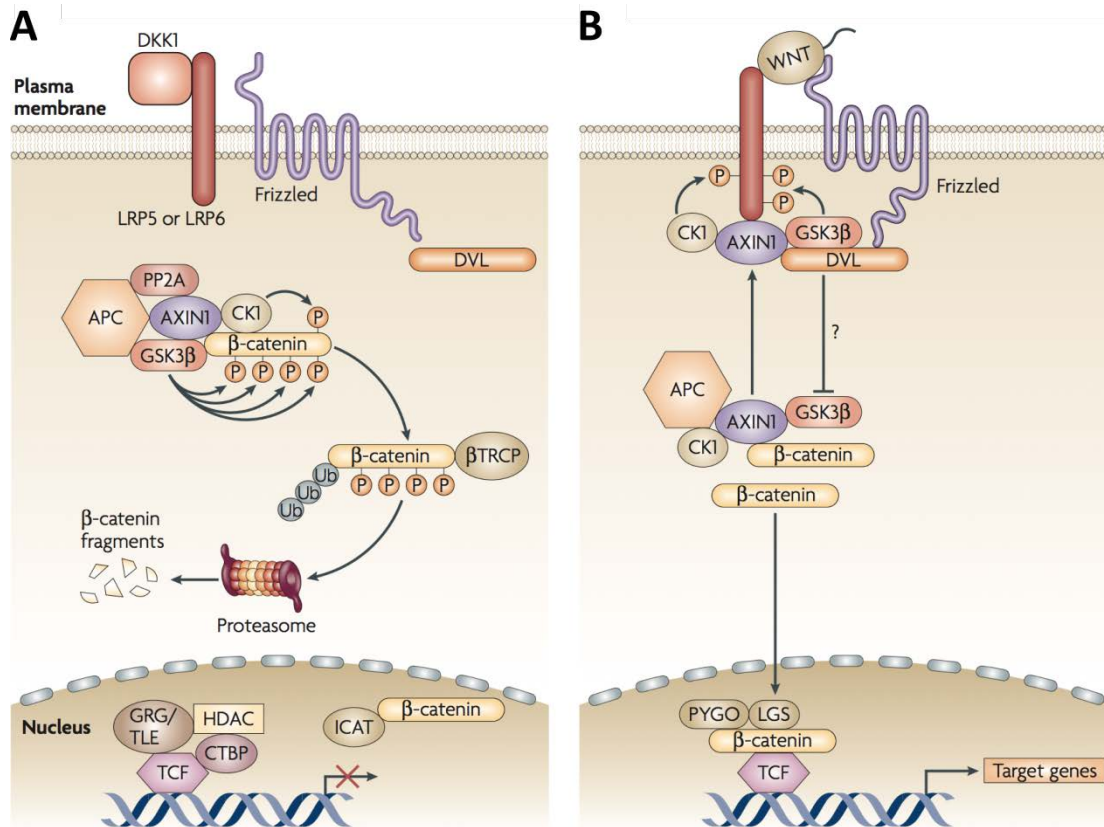


Figure 2: Overview of β -catenin dependent Wnt signaling. (A) In the absence of a Wnt ligand, the secreted Wnt inhibitor Dickkopf (DKK) is bound to the LRP5/6 co-receptor (see 1.4.2). The kinases of the destruction complex, CK1 and GSK3 β phosphorylate β -catenin, which is recognized by β -TRCP, part of an E3 ubiquitin ligase complex and subsequently degraded by the proteasome. In the nucleus, Groucho (Grg)/TLE repressors inhibit the transcription of Wnt target genes. **(B)** After Wnt binding to the receptor, Fz interacts with Dvl resulting in the phosphorylation of Dvl and the co-receptor LRP5/6. Axin becomes recruited away from the destruction complex, which leads to the inactivation of the complex. In the nucleus β -catenin binds and activates TCF/LEF transcription factors leading to target gene transcription. Taken from (Staal et al., 2008).

1.1.2 Establishment of PCP

As mentioned earlier, PCP signaling coordinates the polarity of cells through the organization of their cytoskeletal elements to bring about the patterning of tissues (Boutros and Mlodzik, 1999; Adler and Lee, 2001). In *Drosophila*, it controls cellular polarity within the plane of an epithelium, perpendicular to the apical-basal polarity of the cell. This manifests in the regulation of the orientation of hairs on the wings, legs and thorax and the chirality of ommatidia in the eye (Adler and Lee, 2001; Strutt, 2001). It is also required for the regulation of asymmetric cell divisions of a subset of neuroblasts (Adler and Taylor, 2001).

Introduction

Studies in *Xenopus*, Zebrafish and mice have shown that the vertebrate equivalent of this β -catenin independent signaling pathway plays an essential role in convergent extension movements during gastrulation, coordinated cell movements during neurulation, limb and skeletal development as well as tissue and organ morphogenesis (Heisenberg, 2000; Tada and Smith, 2000; Wallingford and Harland, 2001; Keller et al., 2002; Gong et al., 2004; Wang et al., 2005; Matsuyama et al., 2009; Wang et al., 2011).

PCP signaling shares the Frizzled receptors and Dishevelled with the β -catenin dependent pathway but otherwise utilizes a distinct set of proteins including a set of so-called core PCP proteins which were found through genetic analyses in *Drosophila*. This group consists of the sevenpass transmembrane cadherin Flamingo (Fmi), the fourpass transmembrane protein Van Gogh/Strabismus (Vang/Stbm) and the cytoplasmic proteins Diego (Dgo) and Prickle (Pk). In *Drosophila*, lack of any of these proteins results in similar polarity defects in wing, eye and other tissues (Strutt, 2003). In mice, mutations in almost all core PCP genes lead to characteristic neural tube closure defects (Kibar et al. 2011; Curtin et al. 2003; Wang et al. 2006b). Additionally, the lack of some proteins as for example the mouse Flamingo ortholog Celsr1 or the Vang/Stbm ortholog Vangl2 can disturb the orientation of stereociliary bundles in the cochlea, another manifestation of planar polarity in vertebrates (Curtin et al., 2003; Wang et al., 2006b). Mutations in the two human Van Gogh orthologs, Vangl1 and Vangl2 have also been shown to result in neural tube closure defects (Kibar et al., 2011).

On a cellular level, the establishment of PCP has been best studied in *Drosophila*. For cell polarization, the asymmetric subcellular localization of the core PCP proteins is required. It has been proposed that this is first initiated by an upstream signal from the two proto-cadherins Fat (Ft) and Dachshous (Ds) and the Golgi resident protein Four-jointed (Fj), but the activity of all core PCP proteins and mutual antagonism between the complexes is also required (Strutt, 2002). As a result, the core PCP proteins assemble into two complimentary apical subdomains. Fz, Dvl and Dgo localize to the posterior/distal side of the cell and Stbm and Pk localize to the anterior/proximal side of the cell; Fmi is present at both the locations (Figure 3). This asymmetric localization has been observed in several tissues in *Drosophila* as well as in the mouse inner ear and leads to the polarization of individual cells as well as coordinated polarization of the neighboring cells (Zallen, 2007). For individual cells to reorganize the cytoskeleton and undergo the

Introduction

complex morphological changes during polarization, the activity of downstream effectors is necessary (Adler, 2002; Axelrod and McNeill, 2002). In *Drosophila* these effectors include the small GTPases RhoA, Rac1 and Cdc42, the RhoA effector Drok as well as the STE20-like kinase Misshapen (Msn) and JNK (Klein and Mlodzik, 2005). In addition to these downstream effectors, in *Xenopus* the Formin homology protein Daam1 has been proposed to transduce the signal from Dsh to RhoA (Habas et al., 2001). The activity of these proteins is cell-type dependent. Also, in different tissues, specific effector modules are active. Consequently, in some tissues, PCP signaling results in cytoskeletal reorganization, while in others in transcriptional gene activation (Klein and Mlodzik 2005). For a long time it was not clear if the Fz/Dsh-mediated PCP pathway in *Drosophila* was in fact regulated through Wnt ligands. In other model organisms the involvement of Wnts has been demonstrated, for example Wnt11 in *Xenopus* and zebrafish or Wnt5a in mice (Heisenberg et al., 2000; Tada and Smith, 2000; Qian et al., 2007). However, it was shown recently that Wg and Wnt4 act redundantly to determine PCP in the *Drosophila* wing by modulating the interaction between Fz and Vang (Wu et al., 2013). There are also some developmental processes in which the cells display a planar polarity but the process itself does not require the PCP core proteins. This occurs, for instance, during germband extension in *Drosophila*, which is independent of Fz and Dsh (Zallen and Wieschaus, 2004). Similarly, in *Xenopus*, the planar oriented cell divisions in the developing neural epithelium are also PCP-independent (Kieserman and Wallingford, 2009).

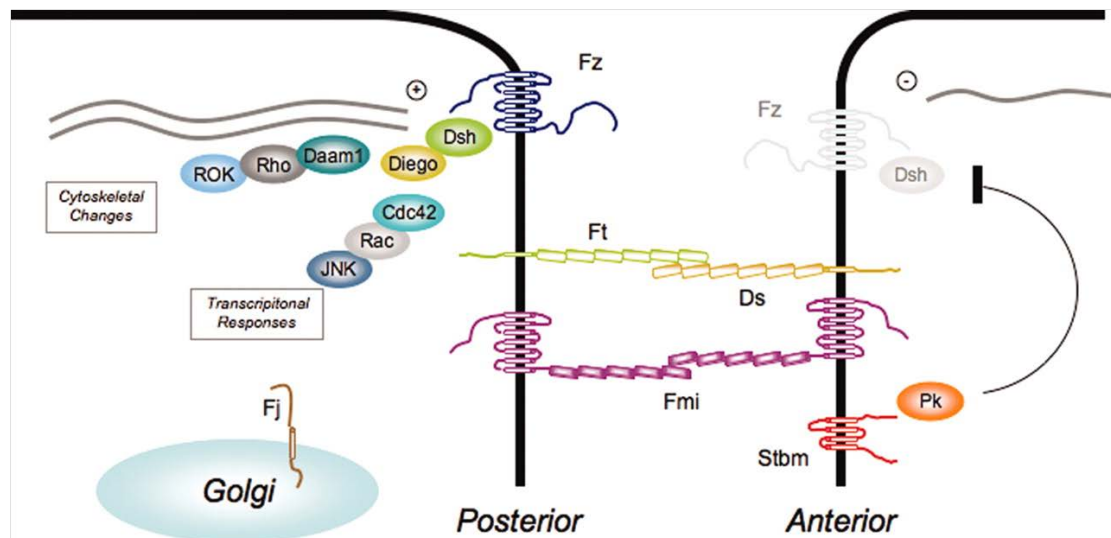


Figure 3: The PCP core proteins and their intracellular effectors. Two cells which display planar polarity. The asymmetric localization of the core PCP proteins is triggered by interactions of Ft and Ds. After polarized assembly of the core PCP proteins on opposite sides of the cell, cytoskeletal rearrangements and transcriptional responses are mediated by tissue-specific effectors. Taken from (Benzing et al., 2007).

1.2 Wnt ligands

Members of the Wnt protein family are secreted proteins that can act both as short-range signaling molecules and long-range morphogens, depending on the developmental context (Gonzalez et al., 1991; Neumann et al., 1997). In general, Wnts are expressed locally, secreted to the extracellular space where they establish a concentration gradient, which then induces distinct responses in the signal-receiving cells. They are highly conserved in organisms from *Drosophila* (7 Wnt proteins) to human (19 Wnt proteins), and the protein family is defined by sequence homology rather than by function (Nusse and Varmus, 1982; Van Ooyen and Nusse, 1984; Logan and Nusse, 2004). Wnts are hydrophobic proteins consisting of 350-400 amino acid residues and harbor an N-terminal signal peptide for secretion and four glycosylation sites. In addition, they have 22-24 highly conserved cysteine residues (Fung et al., 1985; Van Ooyen et al., 1985; Brown et al., 1987; Harterink and Korswagen, 2012). Wnt proteins are lipid-modified on two conserved residues: palmitoylation of a cysteine is important for the activity of the protein (Willert et al., 2003; Komekado et al., 2007; Kurayoshi et al., 2007) and palmitoylation of a conserved serine residue is necessary for Wnt secretion (Takada et al., 2006; Ching et al., 2008).

Figure 4 depicts the structure of human Wnt-1 as an example for all Wnt proteins.

Introduction

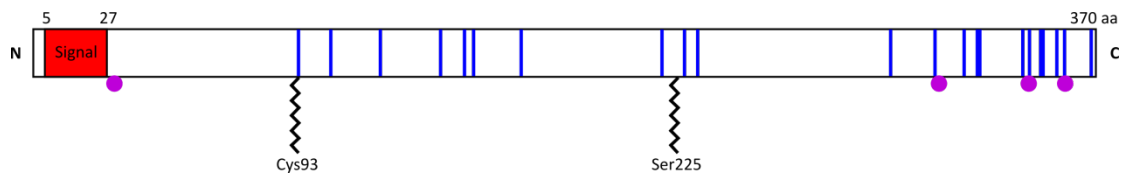


Figure 4: Structure of human Wnt-1. The signal peptide (red) is located at the N-terminus of the protein. The highly conserved cysteine residues are indicated as blue lines. One conserved cysteine residue and one serine are lipid modified by palmitoylation (black). Pink dots indicate glycosylation sites. Modified from (Herr et al., 2012).

For Wnt secretion the cargo receptor Evenness interrupted/Wntless (Evi/Wls) binds to their palmitate modification and transports them to the plasma membrane (Bänziger et al., 2006; Bartscherer et al., 2006). Subsequently, their extracellular transport can occur in at least two different ways. The lipoprotein particle SWIM (secreted wingless-interacting molecule) binds to secreted *Drosophila* Wingless via its lipid-modifications and facilitates transport through the extracellular matrix (Panáková et al., 2005; Mulligan et al., 2012). A similar process has also been demonstrated for mammalian Wnt3a, which is released by high-density lipoprotein particles (Neumann et al., 2009). A second mechanism proposed for extracellular Wnt protein transport is secretion on exosomes (Gross et al., 2012).

In the following sections, the developmental functions of the *Drosophila* Wnt ligands will be described.

1.2.1 Wingless is involved in patterning of the embryo and larval imaginal discs

Initially, Wingless (Wg) was identified through the hypomorphic allele *wg*¹, which transforms the adult wings into thoracic notum (Sharma and Chopra, 1976). Later, a lethal loss-of-function allele was found, in which the pattern of the larval cuticle is affected (Nüsslein-Vollhardt and Wieschaus, 1980). In the wild type larval cuticle, the anterior region of each segment contains a denticle band and the posterior region consists of naked cuticle. In *wg* mutant embryos the naked cuticle is absent and replaced by a lawn of denticles (Bejsovec and Martinez-Arias, 1991). The denticle arrangement is the consequence of correct establishment of segment polarity and specific cell fate

within segments. This is achieved through interplay between short-range Wg and Hedgehog (Hh) signaling. Before segments are formed, a set of repeating developmental units termed parasegments is established. Each parasegment consists of a posterior compartment of one segment and an anterior compartment of the next segment (Martinez-Arias and Lawrence, 1985). During germband extension, the cells at the anterior boundary of each parasegment express Wg and the adjacent cells at the posterior end of the next parasegment express the segment polarity gene *engrailed* (*en*) and secrete Hh. While the expression of Wg maintains *en* expression, Hh in turn maintains Wg expression (DiNardo et al., 1994). After the establishment of two additional expression domains (*serrate* and *rhomboid*) in each parasegment, a segmental groove is formed at the posterior edge of each *en/hh* domain (Swarup and Verheyen 2012). This groove defines the boundary of the segments. The decision between the presence or the absence of denticles depends on the expression of *shaven baby* (*svb*). Wg expression, in turn, represses *svb* and thereby specifies naked cuticle (Payre et al., 1999) (Figure 5). Mutations in *armadillo*, *arrow* and *dvl* resemble the *wg* phenotype, whereas *zw3* (GSK3 ortholog) displays a *wg* gain-of-function phenotype with an excess of naked cuticle (Siegfried et al., 1994).

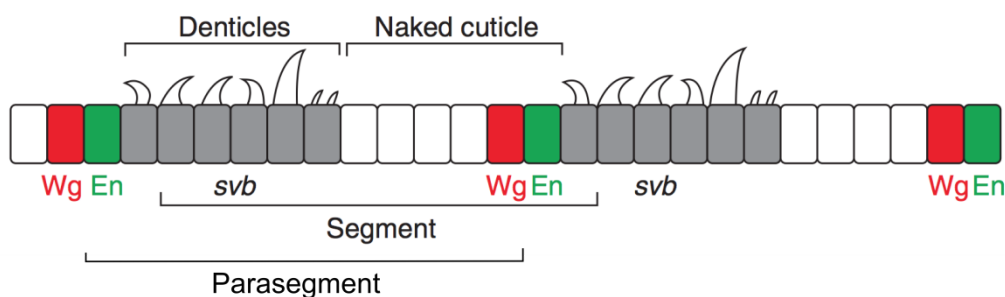


Figure 5: Specification of segmental boundaries and denticle secretion by Wingless signaling in the embryonic epidermis. Expression of Wingless and Engrailed in adjacent rows of cells specifies the parasegmental and segmental boundaries. One row posterior and four rows of cells anterior to the Wg expressing cells, the transcription factor *svb* is repressed and naked cuticle is produced. In the remaining rows of cells, *svb* expression directs denticle formation. Modified from (Swarup and Verheyen, 2012).

During later stages of embryogenesis, Wg signaling is required for head development (Schmitt-Ott and Technau, 1992) as well as patterning of the midgut (Immerglück et al, 1990; Bienz, 1994). During heart morphogenesis, it is needed for the specification of a subset of myoblasts (Park et al., 1996) and during CNS development it acts non-autonomously during cell fate specification and delamination of a subset of neurons in each segment (Chu-Lagraff and Doe, 1993; Bhat, 1996). Another function of Wg signaling during embryogenesis is to promote self-renewal of intestinal stem cells (Lin et al., 2008).

During larval development, Wg signaling is involved in the patterning of wing, leg and eye imaginal discs (Struhl and Basler, 1993). In the wing disc for example, Wg is expressed in a narrow stripe and diffuses along the dorsoventral axis to define patterns of target gene expression (Neumann and Cohen, 1997). During these processes, Wg also acts at longer distances and its morphological effects appear to be concentration-dependent.

Mice deficient for Wnt-1, the vertebrate ortholog of Wg display midbrain and hindbrain abnormalities (Thomas and Capecchi, 1990). *Wnt1/Wnt3a* double mutants show an additional deficiency of neural crest derivatives (Ikeya et al., 1997).

1.2.2 *Drosophila* Wnt2 functions in testes morphogenesis, tracheal development and indirect flight muscle attachment

Drosophila Wnt2 was first discovered in a screen for more Wnt orthologs using a probe derived from mouse Wnt3 cDNA. In the embryo, it is expressed in segmental patches in the abdominal and thoracic segments as well as in the gonadal precursors (Russel et al., 1992). It is required for the morphogenesis of testes and for the specification of cells in the testis sheath. In Wnt2 mutants, the pigment cells forming the outer layer of the sheath are absent and the smooth muscle cells composing the inner layer fail to migrate and ensheath the gonad. The testes themselves have an abnormal shape and are moderately to severely reduced in size (Kozopas et al., 1998). The male-specific expression of Wnt2 within the male gonad initiates pigment cell precursor formation from surrounding cells (DeFalco et al., 2008a). Recently, I could show that Wnt2 binds to

the presumptive Wnt co-receptors Otk and Otk2 and proposed that they function together in assuring male fertility, although their phenotypes are different. Additionally, I could demonstrate that Wnt2 signaling stabilizes Otk at the posttranscriptional level (Linnemannstöns et al., 2014). During tracheal development, Wnt2 together with Wg induces formation of the main tracheal trunk through the activation of the β -catenin dependent Wnt pathway. In *wg/wnt2* double mutants, the dorsal trunk is missing (Lliamargas and Lawrence, 2001). Wnt2 signaling also plays a role in the interaction of muscle and epidermal cells during muscle attachment site selection in pupae. In mutant flies, a subset of direct flight muscles are missing or fail to attach to the epidermis (Kozopas and Nusse, 2002).

In mice, signaling regulated by the Wnt2 homolog Wnt7a is required for the sexually dimorphic development of the Müllerian duct. Mutant flies are male and female sterile because males fail to undergo regression of the Müllerian duct and in females the uterus and the oviduct develop abnormally (Parr and McMahon, 1998). Additionally, Wnt7a acts as a dorsalizing signal in dorsal-ventral limb patterning and is also involved in anterior-posterior patterning of the limb (Parr and McMahon, 1995).

1.2.3 Wnt4 can antagonize Wg signaling, elicit similar responses to Wg or have completely distinct functions

The embryonic expression patterns of Wg and Wnt4 overlap in many parts of the embryo, especially at the parasegmental boundaries in the ventral ectoderm and in the visceral mesoderm (Graba et al., 1995). Since the two genes are adjacent to each other, it has been proposed that they share *cis*-regulatory elements (Gieseler et al., 1995). The functional relationship of Wnt4 and Wg is dependent on the tissue and the position within. In the ventral epidermis Wnt4 can antagonize Wg signaling, in dorsal parts of the embryonic epidermis they have distinct activities, while they exhibit similar responses during imaginal development (Gieseler et al., 1999; Buratovich et al., 2000). Ectopic Wnt4 expression along the A/P boundary of the wing disc instead of the D/V boundary affects the formation of adult appendages including notum-to-wing transformation, which resembles *wg* overexpression. In addition, Wnt4 can rescue Wg function in

antenna and haltere morphogenesis (Gieseler et al., 2001). Furthermore, Wnt4 has been shown to regulate cell motility through the regulation of focal adhesions during ovarian morphogenesis. This function also requires Fz2, Dsh and PKC, and has been proposed to occur through a pathway distinct from the β -catenin dependent or the Wnt/PCP pathway (Cohen et al., 2002). Other functions of Wnt4 include the regulation of dorsoventral specificity during projection of retinal axons into the lamina (Sato et al., 2006) and as a local repulsive cue during synaptic targeting (Inaki et al., 2007).

1.2.4 Wnt5 is involved in axon guidance and muscle attachment site selection

Drosophila Wnt5 is unusual compared to other Wnt ligands. Its N-terminal region is longer than in other Wnts and it also carries an insert in the C-terminal region. The primary translation product of Wnt5 is 112 kDa, more than twice as large as the other Wnt family members (Eisenberg et al., 1992; Russel et al., 1992). Earlier in development, Wnt5 protein is found in the limb and appendage primordia, later it can be observed in the axon tracts of the CNS and in the embryonic brain but is primarily enriched in the posterior commissures (PC) (Fradkin et al., 1995; Fradkin et al., 2004). Wnt5 plays a role in axon guidance by acting as a ligand for the atypical receptor tyrosine kinase Derailed (Drl). Drl is expressed on the growth cones and axons of neurons crossing the midline through the anterior commissure (AC) and Wnt5 acts as a repulsive ligand for the Drl-expressing axons at the PC. In *wnt5* and in *drl* mutants, the commissures appear disorganized, AC axons project abnormally and the mature AC is very thin, while the PC axons are not affected. Wnt5 misexpression at the midline results in the loss of the AC (Bonkowsky et al., 1999; Yoshikawa et al., 2003). This Wnt5/Drl-mediated axon repulsion also requires the Src family kinase Src64B and probably does not activate the β -catenin dependent Wnt pathway (Wouda et al., 2008). A second requirement for Wnt5 during embryonic CNS development is during the formation of the lateral and intermediate longitudinal axon tracts. In *wnt5* mutant embryos the selective defasciculation of axons to pioneer new pathways is disturbed and they display thinning or disruptions in the lateral and intermediate longitudinal fascicles (Fradkin et al., 2004). Moreover, Wnt5 signals via Drl and Doughnut (Dnt) during embryonic muscle attachment site selection. In

wnt5 mutant embryos, the lateral transverse muscles overshoot their target attachment sites and form ectopic contacts (Lahaye et al., 2012).

In the post-embryonic CNS, Wnt5 is required within mushroom body (MB) neurons and interacts with Drl expressed in non-MB neurons to establish the adult MB. The lack of Wnt5 leads to overextension of the medial lobes and reduction or disappearance of the vertical lobes (Grillenzoni et al., 2007). Furthermore, Wnt5 and Drl play roles in antennal lobe (AL) development while mutation of *wnt5* leads to a derangement of the glomerular pattern, overexpression results in the formation of ectopic midline glomeruli (Yao et al., 2007). During MB and AL development, Wnt5 and Drl appear to have antagonistic roles since Drl overexpression phenocopies the *wnt5* mutant phenotype. It has been proposed that Drl sequesters Wnt5 so it cannot interact with other Wnt receptors (Moreau-Fauvarque et al., 1998; Grillenzoni et al., 2007; Yao et al., 2007; Sakurai et al., 2009).

Null mutants of the mouse homolog Wnt5a exhibit prenatal lethality and fail to extend multiple structures that grow out from the primary body axis (see 1.4.5) (Yamaguchi et al., 1999).

1.2.5 Other *Drosophila* Wnt proteins

Drosophila has three more Wnt proteins: Wnt6, Wnt10 and WntD (Wnt8). Interestingly, the *wnt6* and *wnt10* genes are located very close to *wg* and *wnt4* on chromosome 2. While *wnt6* transcript expression is very weak in embryos, it resembles Wg expression in third instar imaginal discs. Therefore it has been proposed that the imaginal expression of the two genes is controlled by the same enhancer element or that earlier Wg expression regulates *wnt6*. Wnt10 is only very weakly expressed in imaginal discs, but during embryonic development its transcript can be observed in the mesoderm, the gut and the CNS (Janson et al., 2001). So far, no loss-of-function studies have been reported for these two genes.

WntD is the only Wnt protein that is not lipid-modified. It has also been shown that in contrast to all other Wnts its secretion is independent of the cargo receptor Evi/Wls and the O-acyltransferase porcupine (Por) (Ching et al., 2008). WntD acts as a feedback inhibitor of the *Drosophila* NF- κ B homolog Dorsal during embryonic patterning and the

innate immune response. Maternal overexpression of WntD is lethal and *wntD* mutants exhibit defects in embryonic *dorsal* regulation and are immunocompromised. This function is most probably independent of β -catenin (Gordon et al., 2005; Ganguly et al., 2005).

1.3 The specificity of Wnt responses depends on ligand and receptors

An outstanding question is how the specificity of activating a certain intracellular signaling cascade is regulated in a temporally and spatially controlled manner.

Initially, Wnt proteins were subdivided into two functional classes. The first class was able to induce a second dorsal-ventral axis in *Xenopus* embryos when ectopically expressed (McMahon and Moon, 1989; Moon, 1993) and to morphologically transform C57MG mammary tumor cells (Jue et al., 1992; Wong et al., 1994). This class includes Wingless, XWnt1, XWnt3a and XWnt8 (Moon, 1993). These properties have been correlated with the activation of the β -catenin dependent Wnt pathway (Shimizu et al., 1997) and so the first group was termed canonical Wnts. The second class includes XWnt4, XWnt5a and XWnt11 as well as mWnt4, mWnt5a and mWnt6 and does not have the same properties as the first group (Moon, 1993; Du et al., 1995). Instead, they affect morphogenetic movements. Wnt5 and Wnt11 for example have been shown to be required for convergent extension movements in *Xenopus* and zebrafish (Heisenberg et al., 2000; Kilian et al., 2003). This second group was termed non-canonical Wnts. Based on these classifications of Wnt ligands it was proposed that the canonical Wnts activate the β -catenin dependent Wnt pathway and the non-canonical Wnts the β -catenin independent pathways.

However, further research suggests that this classification is entirely subjective and that Wnt ligands of either group can activate several Wnt pathways. For example Wnt5a, which has been shown to be involved in β -catenin independent signaling (Wallingford and Harland, 2001; Qian et al., 2007). When co-injected with hFz5 in *Xenopus* embryos, Wnt5a induces axis duplication and in cultured cells transfected with Wnt5a, mFz4 and LRP5, a β -catenin responsive luciferase reporter was activated (He et al., 1997; Mikels and Nusse, 2006). In addition, Wnt11, which is associated with convergent extension movements in zebrafish (Heisenberg et al., 2000), has been shown to activate the β -

catenin dependent pathway in early *Xenopus* embryos (Tao et al., 2005). Thus, a Wnt ligand might prefer binding to a certain receptor, but in another context is able to bind a different receptor to activate a different signaling cascade.

The primary receptor elements of Wnt signaling belong to the Frizzled family. Some Wnt pathways but not all of them require co-receptors in addition to Fz, such as LRP5/6 (*Drosophila* Arrow) for the activation of the β -catenin dependent cascade (Wehrli et al., 2000; Tamai et al., 2000). Besides Frizzleds and LRPs, several other protein families can also serve as Wnt receptors. These include the receptor tyrosine kinase families Ryk (Keeble and Cooper, 2006), Ror (Hikasa et al., 2002) and PTK7 (Peradziryi et al., 2011), as well as the muscle skeletal receptor tyrosine kinase MuSK (Jing et al., 2009) and the Heparan sulphate proteoglycan (HSPGs) subfamilies glypicans and syndecans (Muñoz et al., 2006; Sakane et al., 2012). Some of these receptors have only been shown to activate one downstream pathway, while others are able to activate several distinct pathways (Figure 6).

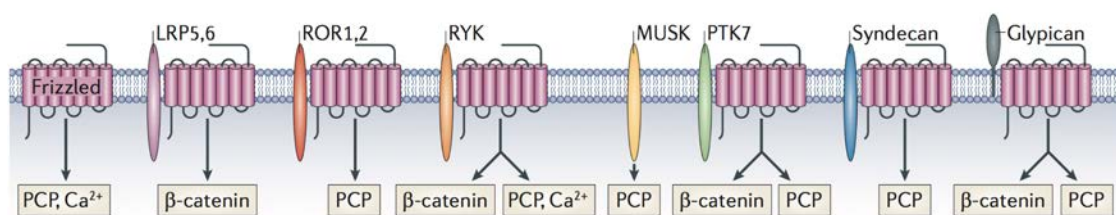


Figure 6: Different Wnt-receptor combinations. The outcome, which downstream signaling cascade becomes activated is determined by a distinct combination of a Wnt ligand and the receptors. Taken from (Niehrs, 2012).

Ultimately, a new model was proposed, in which the outcome is not based on properties intrinsic to the Wnt ligands but rather by a specific combination of a ligand with the receptors expressed at the cell surface (Mikels and Nusse, 2006; Van Amerongen et al., 2008; Angers and Moon, 2009; Niehrs, 2012).

The receptor families Frizzled, LRP, Ryk, PTK7 and Ror are described in the following sections.

1.4 Wnt receptors

1.4.1 Frizzled proteins are considered the primary Wnt receptors

As mentioned above Frizzled proteins can transduce β -catenin dependent and independent signaling. Structurally, they are sevenpass transmembrane proteins with a conserved cysteine-rich CRD domain in their extracellular part and a cytoplasmic tail (Vinson et al., 1989). The CRD domain is necessary and sufficient for Wnt binding and can bind Wnts with nanomolar affinity (Cadigan et al., 1998; Wu and Nusse, 2002). Although there has been some evidence indicating that the CRD might be dispensable for Wg signal transduction (Hsieh et al., 1999; Chen et al., 2004). Within the cytoplasmic tail is a conserved KTXXXW motif with which they can bind to Dishevelled proteins and transduce signals (Umbhauer et al., 2000; Wong et al., 2003).

Frizzleds were first implicated as Wnt receptors, when it was shown that *Drosophila* S2 cells transfected with Dfz2 were able to bind Wg and activate downstream β -catenin signaling (Bhanot et al., 1996). Additionally it was demonstrated that a dominant-negative form of Fz2 was able to block Wg signaling in the wing imaginal disc and Fz2 overexpression resembles overexpression of Wg (Cadigan et al., 1998).

Drosophila Fz (Dfz1) and Fz2 (Dfz2) are both expressed in embryos and larvae (Adler et al., 1990; Bhanot et al., 1996), Fz also has a maternal component (Park et al., 1994).

Fz is required for the establishment of planar cell polarity (see 1.1.2), but mutants display no defects in embryonic patterning (Gubb and Garcia-Bellido, 1982; Vinson et al., 1989; Zheng et al., 1995). And homozygous Fz2 mutant flies, although developmentally delayed and sterile, are normally proportioned and do not display any patterning or PCP defects (Chen and Struhl, 1999). However, the mutation of *fz1* and *fz2* together results in a *wingless*-like phenotype and in cultured cells transfection of either Fz or Fz2 is sufficient to elicit a response to Wg (Kennerdell and Carthew, 1998; Bhanot et al., 1999; Chen et al., 1999). Therefore, there is functional redundancy between Fz and Fz2 in β -catenin-dependent Wnt signaling. However, when overexpressed in imaginal discs, the two proteins display distinct signaling abilities. While Fz overexpression in eye and wing disc leads to PCP phenotypes, Fz2 does not. Contrarily, Fz2 overexpression in wing discs leads to ectopic bristles while Fz overexpression does not result in this Wg gain-of-

function phenotype (Boutros et al., 2000). So although generally both receptors are able to activate both pathways (but with different efficiencies), the current model states that Fz is mainly involved in the establishment of PCP, while Fz2 activates β -catenin dependent signaling. This is supported by the fact that *Drosophila* Frizzleds bind to Wnts with different affinities. The CRD domain of Fz2 for instance has a 10-fold higher affinity to Wg than the CRD of Fz (Rulifson et al., 2000). Nevertheless, the properties which distinguish the different Frizzled receptors from each other do not lie only in the CRD but within the entire protein (Strapps and Tomlinson, 2000).

Besides *fz* and *fz2*, there are two additional *frizzled* genes in *Drosophila*, whose function has not been thoroughly analyzed. Fz3 (Dfz3) mutants do not display any obvious defects (Sato et al., 1999; Sivasankaran et al., 2000). Fz3 is positively regulated by Wg signaling and its absence has been demonstrated to suppress the effects of hypomorphic *wg* mutants. Its *wg* signal transduction efficiency seems to be much less efficient than Fz2 (Sato et al., 1999). During embryonic development Fz4 is expressed in foregut, midgut and CNS (Janson et al., 2001). (Dfz4) Its CRD has been shown to only bind to Wnt4 and WntD and not to Wg, Wnt2 or Wnt5 (Wu and Nusse, 2002). Fz4 (Dfz4) mutants are also viable and fertile and heterozygosity of the alleles is able to suppress the overexpression phenotype of WntD (McElwain et al., 2011).

In humans and mice, ten *frizzled* genes have been found. Similar to the *Drosophila* Frizzleds they have also been shown to activate distinct pathways. Mouse Fz3 and Fz6 for instance seem to activate the PCP pathway. While *fz3* mutants display axonal growth and guidance defects in the CNS and *fz6* mutants have aberrant hair patterning, *fz3 fz6* double mutants exhibit neural tube closure defects and PCP defects in the inner ear (Wang et al., 2006; Guo et al., 2004; Wang et al., 2006b). The analysis of the individual functions of all vertebrate Frizzleds is complicated because of the high number of homologs and many redundancies.

Recently, the three-dimensional structure of *Xenopus* Wnt8 in complex with the mFz8 CRD has been solved. It shows that Wnt8 binds Fz8 as a monomer and that Wnt8 has a structure with two finger-like domains termed lipid thumb and index finger that grasp the Fz8 CRD at two sites. The region of the CRD where the Wnt index finger binds contains some residues, which are not conserved and has been proposed to mediate binding specificity (Janda et al., 2012).

1.4.2 LRP family receptors

Low-density lipoprotein receptor-related proteins (LRPs) are single-pass transmembrane proteins acting as co-receptors in β -catenin dependent Wnt signaling. Mutants for the *Drosophila* homolog *arrow* (*arr*) cannot be distinguished from *wg* mutants since Arrow is required for all Wg signaling events, but they do not display the *fz* PCP phenotype (Wehrli et al., 2000). In vertebrates, LRP5 and LRP6 are also critical for Wnt signaling. In mice, LRP6 is required for the signal transduction of several Wnt ligands. Knock-out mice display developmental defects reflecting composite phenotypes of several Wnts (Pinson et al., 2000). And in *Xenopus*, LRP6 RNA injection results in dorsal axis duplication and expands neural crest progenitors (Tamai et al., 2000). Although Wnt ligand binding to both Fz and LRPs has been shown (Tamai et al., 2000), it has been suggested that the capture of the ligand is mainly performed by Frizzled receptors since they are able to bind Wg at the cell surface and this could not be shown for Arrow (Bhanot et al., 1996; Wu and Nusse, 2002). Consistent with this it has been proposed that the binding of the ligand mediates physical interaction between the two receptors thereby constructing a ternary complex (Gordon and Nusse, 2006). Several extracellular secreted Wnt signaling modulators have been shown to bind to LRPs. For example members of the Dickkopf protein family (Dkk) whose binding blocks the ligand-receptor interaction and inhibits signal transduction and the protein Wise, which has been shown to activate or inhibit Wnt signaling in a context-dependent manner (Glinka et al., 1998; Itasaki et al., 2003).

1.4.3 Ryk proteins acts as guidance receptors

RYK proteins belong to a family of conserved transmembrane proteins. Their extracellular Wnt binding domain resembles the extracellular Wnt agonist WIF (Wnt inhibitory factor) (Hsieh et al., 1999a; Patthy, 2000; Fradkin et al., 2010). They carry a tyrosine kinase domain in their cytoplasmic part, but are characterized as dead kinases since they contain amino acid substitutions, which likely render them inactive and no kinase activity could be demonstrated (Hovens et al., 1992; Stacker et al., 1993; Yoshikawa et al., 2001).

Introduction

In contrast to mammalian genomes which only harbor one Ryk family member, in *Drosophila* three Ryk receptors have been identified: Derailed (Drl, also known as Linotte), Derailed-2 (Drl-2) and Doughnut (Dnt) (Hovens et al., 1992; Callahan et al., 1995; Oates et al., 1998; Savant-Bhonsale et al., 1999). Drl was originally found in a screen for mutants with defects in axon pathfinding in the embryo (Callahan et al., 1995) and also in a screen for learning and memory in the adult (Dura et al., 1993). Within the embryonic ventral nerve cord, Drl is expressed exclusively in neurons projecting in the anterior commissure (AC), after leaving the AC, Drl is downregulated and the axons extend medially and anteriorly within the connectives (Bonkowsky et al., 1999). Drl is necessary and sufficient to promote axon crossing at the AC, in mutants many axons cross abnormally between the AC and the posterior commissure (PC). Misexpression of Drl in PC neurons results in their axons also crossing at the AC (Callahan et al., 1995; Bonkowsky et al., 1999; Moreau-Fauvarque et al., 2002). As ligand for Drl Wnt5 has been identified. Together, they are involved in the guidance of axons and myotubes (see 1.2.4). In the antennal lobes (ALs) and mushroom body (MB) the intracellular part of Drl is not required, therefore it is likely that Drl does not actively transduce the signal in these tissues (Yao et al., 2007). In the AL the Wnt5 overexpression phenotype is attenuated in Drl-2 mutants, therefore it has been concluded that Drl-2 also mediates Wnt5 signaling. Drl-2 has also been shown to oppose Drl during AL development (Sakurai et al., 2009).

In mammals Ryk is also important for the development of the nervous system. In mice it was shown that Ryk activates the β -catenin dependent pathway together with Wnt3a and Wnt1 to regulate neurite outgrowth (Lu et al., 2004a). And together with Wnt5a Ryk mediates axon guidance in the mouse spinal cord and brain (Keeble et al., 2006). Mouse Ryk was also shown to be involved in Wnt/PCP signaling. Ryk mutant mice display typical PCP defects such as the misorientation of stereocilia in the inner ear and in zebrafish, genetic interaction with Wnt11 during PCP establishment was demonstrated (Macheda et al., 2012).

Mouse Ryk has been shown to function as co-receptor together with Fz and in *Drosophila* and *C. elegans* the kinase activity is dispensable for its function, while the WIF domain is required (Lu et al., 2004a; Yoshikawa et al., 2001; Taillebourg et al., 2005). During *Xenopus* gastrulation Ryk cooperates with Fz7 and Wnt11, which also suggests

they interact with each other (Kim et al., 2008). However, during vulval development the *C. elegans* Ryk Lin-18 and the Fz homolog Lin-17 function in two independent pathways (Inoue et al., 2004). It is possible that context-dependently, Ryk receptors either act as co-receptor with Fz or as an independent primary signal transducing receptor.

1.4.4 PTK7 and its *Drosophila* orthologs

Protein tyrosine kinase 7 (PTK7) belongs to a family of receptor protein tyrosine kinases whose structure is conserved in vertebrates and invertebrates. All proteins of this family contain seven extracellular immunoglobulin-like (Ig) domains, a transmembrane domain, and a tyrosine kinase homology domain (Jung et al., 2002). The kinase homology domain of all PTK7 orthologs lacks at least one conserved catalytic residue and no kinase activity has been demonstrated (Miller and Steele, 2000; Kroiher et al., 2001).

In vertebrates, the loss of PTK7 leads to characteristic PCP phenotypes. Mutant mice display craniorachischisis, a severe form of neural tube closure defect and misorientation of the stereociliary bundles in the inner ear, as well as phenotypes consistent for defects in convergent extension such as a shortened body axis and a broader floor plate (Lu et al., 2004; Yen et al., 2009; Paudyal et al., 2010). Downregulation of PTK7 in *Xenopus* embryos and in zebrafish also leads to defects in convergent extension movements during gastrulation and neural tube closure (Lu et al., 2004; Hayes et al., 2013) and PTK7 is frequently deregulated in human cancers (Easty et al., 1997; Endoh et al., 2004; Müller-Tidow et al., 2004). In addition to the PCP phenotypes, genetic interactions with Vangl2 and Celsr1 have been demonstrated (Lu et al., 2004; Paudyal et al., 2010).

Xenopus PTK7 co-precipitates with Wnt3a and Wnt8 (Peradziryi et al., 2011). Moreover, it is part of a Fz/Dsh complex and can recruit Dsh to the cell membrane, which is necessary for PCP signaling. Interestingly, the inactive kinase homology domain is required for this interaction (Shnitsar and Borchers, 2008; Wehner et al., 2011). It has been proposed that PTK7 might exert its signaling activity through interactions with functional kinases at the plasma membrane (Boudeau et al., 2006).

In addition to the involvement in PCP signaling, PTK7 has also been implicated to regulate β -catenin dependent Wnt signaling. Its function however is unclear since investigations remain inconclusive. In three independent analyses, no Wnt/beta-catenin

dependent patterning defects were observed in PTK7 mutant mice (Lu et al., 2004; Yen et al., 2009; Paudyal et al., 2010). But has been shown that in addition to the defects mentioned above, PTK7 morphant *Xenopus* embryos display a reduced activity of the Spemann organizer whose formation is β -catenin dependent. And PTK7 deficient cells display a weakened β -catenin/TCF transcriptional activity, thus PTK7 has been suggested to potentiate β -catenin signaling (Puppo et al., 2011). Nevertheless, another group has demonstrated that PTK7 overexpression in *Xenopus* embryos inhibits Wnt8-induced second axis formation and that PTK7 loss-of-function activates β -catenin signaling. They suggested that PTK7 activates PCP signaling by turning off the β -catenin-dependent signaling branch (Peradziryi et al., 2011). In zebrafish a role for PTK7 in attenuating β -catenin signaling has also been demonstrated *in vivo* (Hayes et al., 2013). It has been proposed that these inconsistencies exist due to several PTK7 isoforms with different subcellular localization and function and that they might differentially regulate β -catenin dependent or independent signaling in a cell-context-specific manner (Bin-Nun et al., 2014).

Loss-of-function of the *Drosophila* ortholog of PTK7, Off-track (Otk) has been reported to be lethal and affect the lamina-specific targeting of photoreceptor axons. In *otk* mutant clones, many R1-R6 axons connect abnormally to the medulla instead of the lamina (Pulido et al., 1992; Cafferty et al., 2004). However, we have already observed this axon targeting phenotype in a wild-type rough- τ -lacZ reporter line (Linnemannstöns, 2012). Additionally, Otk has been proposed to function downstream of Semaphorin-1a (Sema-1a) to regulate axon guidance of motor neurons to their muscle targets in the embryo (Winberg et al., 2001). The data on which this hypothesis is based on is not completely convincing as well, since the depicted images were not all taken in the same focal plane. Furthermore, it has been shown that Otk interacts with Wnt4 and that *otk* mutant embryos display defects in embryonic patterning similar to *wg* overexpression. Moreover, mutation of *otk* was proposed to suppress the development of ectopic denticles upon *wnt4* overexpression indicating that Otk and Wnt4 function together during patterning of the embryo (Peradziryi et al., 2011). We could also not reproduce these data and instead found that overexpression of *wnt4* alone already leads to the phenotype described for the co-overexpression of *otk* and *wnt4* (Linnemannstöns,

2012). Recently, we have reinvestigated the role of Otk during development and found that there are in fact two PTK7 homologs in *Drosophila*, Otk and Otk2 (Off-track2). We have generated new null mutant fly lines for both genes and revealed that single and double mutants are all viable and do not display any PCP defects. They also did not display any cuticular defects as was described for the *otk* allele used in the previous studies. Therefore we concluded that the previous findings concerning *otk* function are misleading and are most probably based on an allele carrying an additional lethal mutation (Linnemannstöns et al., 2014).

Using our newly generated null mutants, we could show that *otk*, *otk2* double mutants are male-sterile due to an abnormal development of the ejaculatory duct while Otk overexpression leads to female sterility. Our data indicate that Otk and Otk2 act as co-receptors for Wnt2 during genital tract development (Linnemannstöns et al., 2014).

1.4.5 Ror proteins

1.4.5.1 Structural features

Ror proteins belong to the family of receptor tyrosine kinases (RTKs) and are evolutionary conserved in vertebrates and invertebrates. Characteristic of all Ror proteins are an extracellular Frizzled-like cysteine-rich domain (CRD), a single transmembrane domain, a membrane-proximal kringle domain and an intracellular tyrosine kinase domain. The structure of other domains varies between species. All but the *Drosophila* Rors (Dror and Dnrk) possess immunoglobulin (Ig)-like domains in their extracellular regions (Figure 7) (Masiakowski and Carroll, 1992; Oishi et al., 1999; Forrester et al., 2002; Yoda et al., 2003). These domains are also found in PTK7 orthologs (see 1.4.4) and MuSK receptors (Jing et al., 2009). The kringle domain is thought to mediate protein-protein interactions and to function as recognition module for Wnt ligands and the Ig domains also possibly contribute to binding of ligands and other signaling molecules (Minami et al., 2010). Mammalian Rors additionally possess a proline-rich domain and two serine/threonine-rich domains in their cytoplasmic tails (Masiakowski and Carroll, 1992; Oishi et al., 1999; Yoda et al., 2003).

Introduction

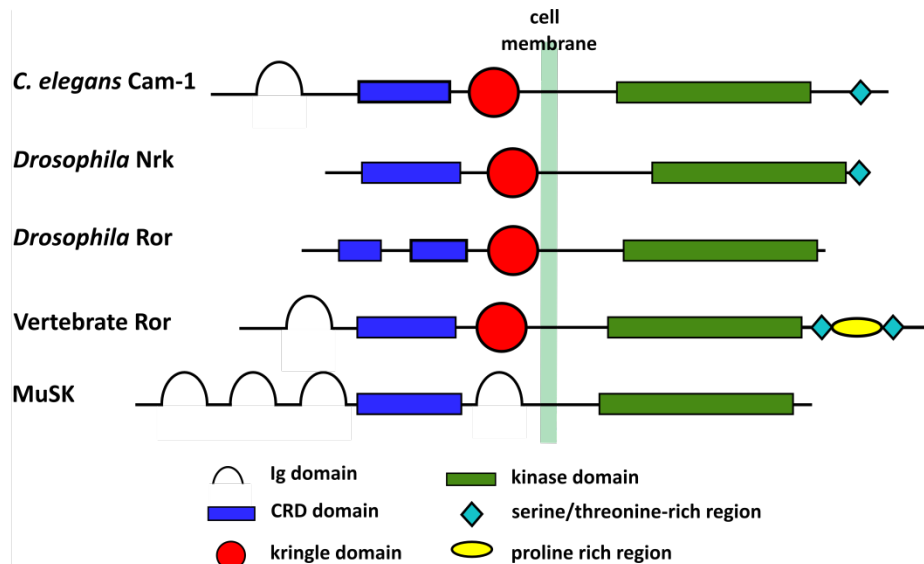


Figure 7: Structure of Ror receptors in vertebrates and invertebrates. All Ror receptors contain a CRD domain and a kringle domain in their extracellular part and a tyrosine kinase domain within their intracellular part. The two *Drosophila* Rors terminate shortly after the kinase domain. All invertebrate Rors do not possess a proline-rich region, but *Drosophila* NrK and *C. elegans* Cam-1 both have a short serine/threonine-rich domain at their C-terminus. Modified from (Forrester et al., 2002).

1.4.5.2 Developmental functions

In humans, mutations in Ror2 have been associated with two skeletal disorders, brachydactyly B and Robinow syndrome (Oldridge et al., 2000). More insights into the function of Ror proteins have been gained from mouse and *C. elegans* Ror mutants and from studies in *Xenopus* embryos and cultured cells. In *Xenopus*, XWnt5a and Xror2 regulate convergent extension movements through the activation of JNK signaling via Cdc42 and PI3K (Phosphoinositide 3 kinase). This is considered a distinct β -catenin independent Wnt signaling branch not related to PCP signaling via XWnt11 (Schambony and Wedlich 2007). Overexpression of Ror2 in *Xenopus* embryos results in a short body axis with dorsal bending and abnormal head structures. This is due to defects in neural plate closure and convergent extension (Hikasa et al., 2002). Depletion of *Xenopus* Ror2 blocks constriction of Keller explants and thereby phenocopies Wnt5a loss-of-function (Schambony and Wedlich, 2007).

Mice deficient for Ror2 die perinatally and display widespread skeletal abnormalities including facial malformations, shortened limbs and caudal axis and heart defects (Takeuchi et al., 2000; Ho et al., 2012). Homozygous Ror1 mutant mice on the other hand are viable at birth and cannot be distinguished from heterozygous animals.

However, in *Ror1/2* double mutant mice, the defects are more severe than in *Ror2* single mutants. They exhibit system-wide tissue elongation defects, edema in the trunk region as well as innervation defects of several organs and occasionally also encephaly (Figure 8 A) (Ho et al., 2012). In addition, they display the classical PCP phenotype in the inner ear where the orientation of ciliary bundles of sensory hair cells in the inner ear is disturbed (Figure 8 B) (Yamamoto et al., 2008). As observed in *Xenopus* as well, these phenotypes are significantly similar to those of homozygous *Wnt5a* mutant mice (Yamaguchi et al., 1999; Ho et al., 2012). Thus, Rors have been proposed to constitute the primary receptors for *Wnt5a* in vertebrates and *Wnt5a/Ror2* signaling seems to play a general role in morphogenetic processes.

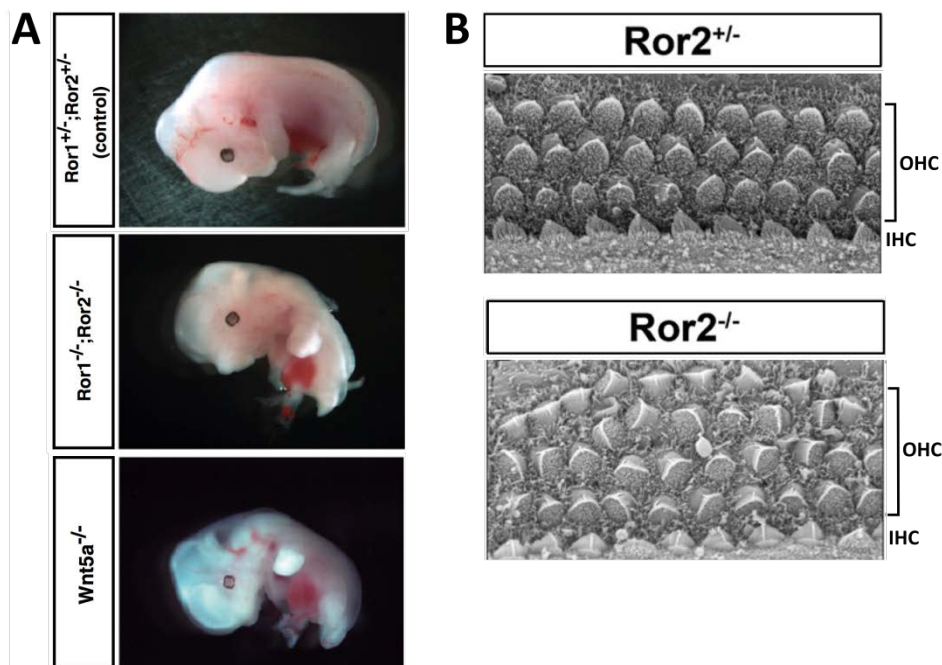


Figure 8: Mouse *Ror* mutants exhibit severe developmental defects. (A) *Ror1/Ror2* double mutant mice exhibit the same defects as *Wnt5a* deficient mice. This includes overall shortening of the A-P axis and malformations of face, limbs and tail. **(B)** The alignment and orientation of sensory hair cells of homozygous *Ror2* mice is disturbed. OHC: outer hair cells; IHC: inner hair cells. Modified from (Ho et al., 2012) (A) and (Yamamoto et al., 2008) (B).

1.4.5.3 Intracellular responses

Rors have been shown to modulate several intracellular responses. In cultured cells, *Wnt5a* signaling mediated by *Ror2* can directly inhibit β -catenin dependent signaling without affecting the stabilization of β -catenin (Mikels and Nusse, 2006). And in human

osteoblastic cells Ror2 has been shown to inhibit the stabilization of β -catenin and Wnt3-induced reporter activation, although Wnt1-induced activation was enhanced (Billiard et al., 2005). Ror signaling has also been demonstrated to activate JNK signaling, for instance in cultured cells where Ror2 can potentiate Wnt5a-induced JNK activation or in wound healing assays (Oishi et al., 2003; Nomachi et al., 2008). Another downstream mechanism activated by Ror is the phosphorylation of Dvl. In mouse embryonic fibroblasts (MEFs), mouse L cells and in embryos Wnt5a-induced Dvl2 phosphorylation is dependent on the level of Ror expression (Ho et al., 2012; Nishita et al., 2010). Ror proteins have also been suggested to antagonize Wnt signaling by simply sequestering the ligands, limiting the amount of Wnts to reach their destined receptor and thereby inhibiting their function (Green et al., 2007; Billiard et al., 2005).

1.4.5.4 Kinase activity

In *Xenopus* the Wnt5a/Ror2 mediated transcriptional regulation of XPAPC (paraxial protocadherin) requires kinase activity (Schambony and Wedlich, 2007). Likewise for the inhibition of Wnt3a-induced β -catenin signaling in HEK-293 cells (Mikels and Nusse, 2006). But this is not the case for all functions of Ror proteins. The overexpression phenotype of Ror2 in *Xenopus* is less severe without a kinase domain but not abolished, which indicates that Ror2 has kinase-dependent and -independent functions (Hikasa et al., 2002). Similarly, in *Xenopus* ectodermal explants, convergent extension movements are still synergistically inhibited to some extent when Wnt5a is co-expressed with a Ror2 construct lacking the cytoplasmic region (Oishi et al., 2003). *C. elegans* Cam-1 has also been demonstrated to have tyrosine kinase-dependent as well as -independent functions. While the regulation of cell migration is independent of kinase activity, it is necessary for asymmetric cell division (Forrester et al., 1999; Kim and Forrester, 2003). For vertebrate Ror1 proteins it is unclear if they constitute active tyrosine kinases. While human Ror2 was shown to be active although it displays five deviations from the tyrosine kinase domain consensus sequence, Ror1 displays seven deviations and no obvious autophosphorylation activity has been observed (Masiakowski and Carroll, 1992).

1.4.5.5 Association with Frizzled receptors

For vertebrate Rors it has been demonstrated that their CRD domain can bind Wnt ligands and Frizzled receptors (Oishi et al., 2003). Human Ror2 for instance co-immunoprecipitates with Wnt1, Wnt3, and several other Wnts, and the ectodomain of *Xenopus* Ror2 co-precipitates Wnt11, Wnt5a as well as Wnt8 (Billiard et al., 2005; Hikasa et al., 2002). In mouse fibroblast L cells, Wnt5a/Ror2 signaling regulates polymerization of Dvl2 and activation of the AP-1 promoter. This requires complex formation with Fz7 (Nishita et al., 2010). And murine Ror2 has also been shown to form a complex with soluble forms of rat Fz2 and human Fz5 (Oishi et al., 2003). It is not fully clear however, if Ror proteins always signal as a co-receptor together with Fz or in some contexts as an alternative principal Wnt receptor.

1.4.5.6 *Drosophila* Ror family members

Like vertebrates, *Drosophila* has two Ror orthologs, Ror and NrK. NrK displays a considerable sequence similarity to MuSK and has been proposed to be evolutionarily distinct from the other Ror family members (Sossin, 2006; Green et al., 2008). While in mice, Ror proteins are expressed in a variety of tissues including face, limbs, heart, brain and lungs (Matsuda et al., 2001; Oishi et al., 1999; DeChiara et al., 2000), transcripts of the *Drosophila* family members are found mainly in the embryonic nervous system and have been suggested to function during neural development. NrK has been demonstrated to possess autophosphorylation activity *in vitro* but at the same time *Drosophila* Ror is lacking a conserved lysine residue, which is usually target for autophosphorylation (Oishi et al., 1997; Wilson et al., 1993). Loss-of-function phenotypes for both have not been described yet.

1.5 Scope of this Thesis

The goal of this work was to study the developmental function of *Drosophila* Ror by generating a null mutant and the subsequent analysis of developmental defects observed upon loss and overexpression of Ror. Additionally, I planned to establish a Ror>Ror-eGFP reporter fly line, which reflects the endogenous Ror expression and

Introduction

analyze the developmental and subcellular expression pattern with regard to different Wnt ligands as well as receptors. Moreover, I intended to elucidate the mechanism of Ror function by the identification of the Ror ligands and analysis of genetic interactions with ligands and other Wnt receptors.

Since the vertebrate Otk homolog PTK7 is also known to be involved in the regulation of polarized cell migration during development and Otk as well as Otk2 are both also expressed within the fly nervous system, I further analyzed whether Ror, Otk and Otk2 act together in some aspects of *Drosophila* development or possibly perform redundant functions.

To get more insight into the processes downstream of Ror and Otk/Otk2 signaling, I performed a transcriptome analysis and aimed to identify genes which are differentially expressed in corresponding single, double and triple mutant embryos.

2. Material and Methods

2.1 Chemicals and enzymes

2.1.1 Chemicals and reagents

All chemicals used in this study were purchased from following companies: Biomol (Hamburg, Germany), Bio-Rad (Munich, Germany), Biozym (Oldendorf, Germany), BioVision (Lyon, France), Difco (Detroit, USA), Fluka (Buchs, Switzerland), Gibco/BRL Life Technologies (Karlsruhe, Germany), Merck (Darmstadt, Germany), Roth (Karlsruhe, Germany), Serva (Heidelberg, Germany), Sigma-Aldrich (Steinheim, Germany), Macherey-Nagel (Düren, Germany), QIAGEN (Hilden, Germany).

All buffers and solutions were prepared with distilled water and if necessary autoclaved before use.

2.1.2 Enzymes

All enzymes used in this study were purchased from the following companies: Bioline (Luckenwalde, Germany), ThermoScientific (St. Leon-Rot, Germany), Genecraft (Lüdingshausen, Germany), Roche (Mannheim, Germany).

2.2 Antibodies and antisera

All primary antibodies used for immunofluorescence staining, immunoperoxidase staining, Western blotting and immunoprecipitation, are listed in Table 1. All secondary antibodies conjugated to fluorochromes or peroxidases are listed in Table 2.

Table 1: Primary antibodies used in this study

Epitope	Species	Dilution	Application	Reference/Source
Actin	rabbit	1:2000	WB	Sigma A2066
BP 102	mouse	1:50	IF	DSHB, BP102
β -Galactosidase	mouse	1:20	IF	DSHB, JIE7

Material and Methods

β-Galactosidase	rabbit	1:3000	IF	Cappel
C-Myc	mouse	1:20	WB, IF, IP	DSHB, 9E10
DE-Cadherin	rat	1:5	WB, IF	DSHB, DCAD 2
Elav	mouse	1:30	IF	DSHB, 9F8A9
FasciclinII	mouse	1:20	IF	DSHB, 1D4
FasciclinIII	mouse	1:20	IF	DSHB, 7G10
Futsch	mouse	1:20	IF	DSHB, 22C10
GFP	rabbit	1:1000	WB, IF, IP	Invitrogen Molecular Probes A11122
HA	mouse	1:2000	WB	Roche 11 583 816 001
Miranda	guinea pig	1:1000	IF	Kim et al., 2009, DE02120, SA120
Otk	guinea pig	1:1000	WB, IF	Linnemannstöns et al., 2014
Otk2 (CG8964)	rabbit	1:100	WB, IF	Linnemannstöns et al., 2014
Repo	mouse	1:20	IF	DSHB, 8D12
Repo	rabbit	1:1000	IF	B. Altenheim, Mainz (unpublished)
Robo-2	goat	1:100	IF	Santa Cruz, sc-19720
Tubulin α	mouse	1:20	WB	DSHB, 12G10
Wingless	mouse	1:20	WB	DSHB, 4D4

DSHB: Developmental Studies Hybridoma Bank

IF: Immunofluorescence

IP: Immunoprecipitation

WB: Western Blot

Table 2: Secondary antibodies used in this study

Epitope	Conjugate	Species	Dilution	Application	Source/Company
Guinea Pig IgG	HRP	goat	1:10000	WB	Jackson ImmunoResearch 106-035-003
Rabbit IgG	HRP	goat	1:10000	WB	Jackson ImmunoResearch 111-035-144
Mouse IgG	HRP	goat	1:10000	WB	Jackson ImmunoResearch 115-035-068
Mouse IgG	Biotin-SP	donkey	1:500	IPS	Jackson ImmunoResearch 715-065-151
Rabbit IgG	Alexa-488	goat	1:200	IF	Molecular Probes A11008
Rabbit IgG	Cy3	donkey	1:200	IF	Jackson ImmunoResearch 711-165-152
Rabbit IgG	Alexa-647	goat	1:200	IF	Molecular Probes A21245
Mouse IgG	Alexa-488	goat	1:200	IF	Molecular Probes A11029
Mouse IgG	Alexa-555	goat	1:200	IF	Molecular Probes A21422
Mouse IgG	Cy5	goat	1:200	IF	Molecular Probes A21236
Rat IgG	Alexa-555	goat	1:200	IF	Molecular Probes A21434
Rat IgG	Alexa-647	goat	1:200	IF	Molecular Probes A21247
Guinea Pig IgG	Alexa-488	goat	1:200	IF	Molecular Probes A21435
Guinea Pig IgG	Cy3	donkey	1:200	IF	Jackson ImmunoResearch 706-165-148
Guinea Pig IgG	Alexa-647	goat	1:200	IF	Molecular Probes A21450

IPS: Immunoperoxidase staining

2.3 *Drosophila melanogaster* stocks

Table 3: *D. melanogaster* stocks used in this study

Stock	Genotype	Description	Reference
wild type Oregon R	wild type	Red-eyed wild type strain	Stock collection AG Wodarz
white-	w[1118]	white eyes	BL 5905
Mga/FM7(act>GFP); Sp/CyO	Mga/FM7 P[act>GFP]; Sp/CyO	Balancer 1st and 2nd chromosome	Stock collection AG Wodarz
Gla/CyO (fz>lacZ)	Gla/CyO P[ftz>lacZ]	Balancer 2nd chromosome	Stock collection AG Wodarz
Gla/CyO (tw>GFP)	w[1118]; In(2LR)Gla, wg[Gla-1]/CyO, P{w[+mC]=GAL4- twi.G}2.2, P{UAS- 2xEGFP}AH2.2	Balancer 2nd chromosome	BL 6662
IF/CyO; MKRS/TM6b	w; If/CyO; MKRS/TM6B	Balancer 2nd and 3rd chromosome	Stock collection AG Wodarz
IF/CyO(tw>GFP); MKRS/TM6b	w[1118]; If/CyO, P(twGFP); MKRS/TM6B[Tb1]	Balancer 2nd and 3rd chromosome	Stock collection AG Wodarz
Bl/CyO; TM2/TM6b	w; Bl/CyO; TM2/TM6B	Balancer 2nd and 3rd chromosome	Stock collection AG Wodarz
TM3(fz>lacZ)/TM6	w;;TM3(ftz>lacZ)ce, Ser/TM6B, e, Tu, Ser	Balancer 3rd chromosome	Stock collection AG Wodarz
TM3(tw>GFP)/TM6	TM3, P[tw>GFP]/TM6	Balancer 3rd chromosome	Stock collection AG Wodarz
Mga/FM7act-GFP; sp/CyO Mef2-RFP	Mga/FM7, P[act>GFP]; sp/CyO, P[Mef2::RFP]	Balancer 1st and 2nd chromosome	Stock collection AG Wodarz
daughterless Gal4	w[1118]; P{da>GAL4.w[-]}3	Gal4 driver line; ubiquitous expression under control of daughterless promotor; 3rd chromosome	BL 8641
actin Gal4	y[1] w[*]; IF/CyO; P{w[+mC]=Act5C- GAL4}17bFO1/TM6B, Tb[1]	Gal4 driver line; ubiquitous expression under control of daughterless promotor; 3rd chromosome	Stock collection AG Wodarz

Material and Methods

tubulin Gal4	y[1] w[*]; P{w[+mC]=tubP- GAL4}LL7/TM3, Sb[1]	Gal4 driver line; ubiquitous expression under control of daughterless promotor; 3rd chromosome	BL 5138
otk, otk2 Gal4		Gal4 driver line; expression under control of otk, otk2 promotor; 3rd chromosome	VDRC VT015409
P{EP}	y ¹ w [*] ; P{EP}G8235	P{EP} insertion at position 2L:10251808 (-), upstream of Ror locus, used for generation of Ror allele E267	BL 27979
P{GSV3}	y[1] w[67c23]; P{w[+mC]=GSV3}GS8107 / SM1	P{GSV3} insertion at position 2L:10,251,860, in Ror locus 5'UTR, used as control in transcriptome analysis	DGRC 201394
PBac{RB}e03992	PBac{RB}e03992	piggyBac insertion at position 2R:11,999,690 [-], downstream of otk locus, used as control in transcriptome analysis	Exelixis collection, Harvard
PBac{PB}c01790	PBac{PB}c01790	piggyBac insertion at position 2R:12,027,235 ..12,027,288 [-], upstream of otk2 locus, used as control in transcriptome analysis	Exelixis collection, Harvard
P{XP}d01360	P{XP}d01360	piggyBac insertion at position 2R:12,019,858 [-], upstream of otk locus, used as control in transcriptome analysis	Exelixis collection, Harvard
Ror RNAi v932	w ¹¹¹⁸ ; P{GD40}v932	Ror RNAi line, 2nd chromosome	VDRC 932
Ror RNAi v29930	w ¹¹¹⁸ ; P{GD14377}v29930	Ror RNAi line, 1st chromosome	VDRC 29930
Nrk RNAi 36284	w ¹¹¹⁸ ; P{GD14403}v36284	Nrk RNAi line, 3rd chromosome	VDRC 36284
Nrk RNAi 42442	w ¹¹¹⁸ ; P{GD14403}v42442	Nrk RNAi line, 3rd chromosome	VDRC 42442
otk ^{A1}	w; otk ^{A1}	null allele for otk, homozygous viable	Linnemannstöns et al., 2014

Material and Methods

otk2 ^{C26}	w; otk ^{C26}	null allele for otk2 (CG8964), homozygous viable	Linnemannstöns et al., 2014
Df(otk,otk2)D72	w; Df(otk,otk2)D72/CyO	null allele for otk and otk2 (CG8964), homozygous viable, male sterile	Linnemannstöns et al., 2014
Ror ⁴	w ¹¹¹⁸ ; Ror ⁴	Ror mutant allele, aa 1 - 281 deleted, homozygous viable	PhD thesis I. Petrova, Leiden University, 2014
Ror ⁴ , Df(otk,otk2)D72	w ¹¹¹⁸ ; Ror ⁴ , Df(otk,otk2)D72	null allele for Ror, otk and otk2 (CG8964), generated via mitotic recombination between Df(otk,otk2)D72 and Ror ⁴	this study
Ror ^{E267}	w ¹¹¹⁸ ; Ror ^{E267}	Ror mutant allele, not verified, homozygous viable	this study
wg ^{CX4}	wg[l-17] b[1] pr[1]/CyO	wg null allele	BL 2980
wnt2 ^O	Wnt2[O]/CyO, amos [Roi-1]	wnt2 null allele	BL 6958
wnt2 ^L	w[1118]; Wnt2[L]/CyO, amos[Roi-1]	wnt2 null allele	BL 6909
wnt4 ^{C1}	w[1118]; Wnt4[C1]/CyO	wnt4 null allele	BL 6651
wnt5 ⁴⁰⁰		wnt5 null allele	Fradkin et al., 2004
fz ^{J22}	fz ^{J22} /TM6C	fz allele, autonomous	gift from Paul Adler
fz ^{P21}	fz ^{P21} th st/TM6C	fz allele, non-autonomous	gift from Paul Adler
fz ^{R52}	fz ^{R52} th st/TM6C	fz allele, non-autonomous	gift from Ken Cadigan
Dfz2 C2	Dfz2-C2/TM6	Dfz2 null allele	gift from Gary Struhl
Df(3L)469-2	Df(3L)469-2/TM6	Deficiency line, removes <i>Dfz2</i>	Bhanot et al., 1999
Df(2L)ED729	Df(2L)ED729/SM6a	Deficiency line, removes <i>Dror</i>	BL 24134
Ror>Ror-eGFP	w;; Ror>Ror-eGFP	Ror-GFP under control of endogenous Ror promoter	this study
UAS-mCD8-GFP	w[*]; P{y[+t7.7] w[+mC]=10XUAS-mCD8::GFP}attP2	mCD8-GFP under control of UAS element, 2nd chromosome	BL 32184
UAS<Otk-GFP	w;; UAS<OtkGFP	Otk-GFP under control of UAS< promoter, 3rd chromosome	Linnemannstöns et al., 2014

Material and Methods

UAS-Ror-Myc	Ror-Myc under control of UAS promoter, 3rd chromosome	gift from L. Fradkin
-------------	---	----------------------

BL: Bloomington Drosophila Stock Center
 DGRC: Drosophila Genetic Resource Center (Kjoto)
 VDRC: Vienna Drosophila RNAi Center
 Exelixis at Harvard Medical School

2.4 Bacterial strains and cell culture lines

Table 4: Bacterial strains used in this study

Strain	Genotype	Application/Reference
DH5 α	Φ 80lacZ Δ M15, Δ lacZYA-argF)U169, deoR, recA1, endA1, hsdR17(rk-, mk+), phoA, supE44, λ -, thi-1, gyrA96, relA1	Amplification of plasmid DNA
TOP10	F' [lacIq, Tn10(TetR)]mcrA Δ (mrr-hsdRMS-mcrBC) Φ 80lacZ Δ M15, Δ lacX74, recA1, araD139, Δ (araleu), 7697 galUgalK rpsL (Str ^R) endA1 nupG	Cloning of PCR fragments in pENTR
XL1-Blue	endA1, gyrA96(nalR), thi-1, recA1,relA1, lac, glnV44, F'[Tn10 proAB+lacIq Δ (lacZ)M15], hsdR17(rk-, mk+)	Site-directed mutagenesis
SW-102	F- mcrA Δ (mrr-hsdRMS-mcrBC) Φ 80dlacZ M15 Δ lacX74 deoR recA1 endA1 araD139 Δ (ara, leu) 7649 galU galK rpsL nupG [λ cl857 (cro-bioA) <> tet]	Recombineering of linear DNA into BAC clones, Warming et al., 2005
SW-106	F- mcrA Δ (mrr-hsdRMS-mcrBC) Φ 80dlacZ M15 Δ lacX74 deoR recA1 endA1 araD139 Δ (ara, leu) 7649 galU galK rpsL nupG [λ cl857 (cro-bioA) <> tet] [(cro-bioA) <> araC-PBADcre]	Cre recombination between two loxP sites, Warming et al., 2005
TransforMax TM EPI300 TM	F ⁻ mcrA Δ (mrr-hsdRMS-mcrBC) Φ 80dlacZ Δ M15 Δ lacX74 recA1 endA1 araD139 Δ (ara, leu)7697 galU galK λ ⁻ rpsL (Str ^R) nupG trfA dhfr	High copy number induction of BAC clones using the CopyControl TM Cloning System (Epicentre)

Table 5: *Drosophila* cell lines used in this study

Cell line	Application	Description	Description/Reference
S2	Cell Binding Assay	made on Oregon R embryos on the verge of hatching, no Dfz2 expression	Schneider, 1972
S2R+	Co-Immunoprecipitation	S2 Receptor plus cells, express DFz1 and Dfz2	Yanagawa et al., 1998

2.5 Synthetic oligonucleotides

Table 6: Primers used in this study

Primer name	Sequence (5'- 3')	Application
RorC-end-loxP-F	GTCTCAAACTTGGCACGAGGGCCACTTTAAG GCCAGTAATCCAGAAATGGCAGCCCAATTCCG ATCATATTCAATAACCCTTAATATAA	Amplification of GFP-loxP selection cassette
RorC-3'-GFP-rev	TTTACAGTCCATTTGTTGAAAATACATATGTA TGTGTAAAATCTTATGTCTTGACAGCTCGTCC ATGCCGAGAGTGATCCCGGCGGCG	Amplification of GFP-loxP selection cassette
Ror-C-rec-F	CAATCAGGAAGTAATCAATCTCATCC	Verification and sequencing of Ror-eGFP construct
Ror-C-rec-R	CCATATGGTTATTACGAACAAATCTCAC	Verification and sequencing of Ror-eGFP construct
Kan-seq-F	TCTATCGCCTTCTTGACGAG	Verification of Ror-eGFP construct
Kan-seq-R	TCTTGTTCAATGGCCGATC	Verification of Ror-eGFP construct
GFP-Forward	GTAAACGGCCACAAGTTCA	Verification of existence of GFP ORF in Ror-eGFP construct
GFP-Reverse	TTACTTGTACAGCTCGTCCA	Verification of existence of GFP ORF in Ror-eGFP construct
CG31717-Ex2-fw	TCAGCGAGGAACTGCATTT	Verification of location of P-element P{EP}G8235
Pry4	CAATCATATCGCTGTCTCACTCA	Verification of location of P-element P{EP}G8235
CG31717-Ex2-fw1	ACCCGATAAGTTCAGCTTTCC	Genotyping of imprecise P-element P{EP}G8235 excision lines
CG31717-genotype-fw	GAAATACACAGCGATATGAGGACGGTTG	Genotyping of imprecise P-element P{EP}G8235 excision lines
Ror-Ex2-rev2	CCTTTAATCGCTCCTCAAATCGTTC	Genotyping of imprecise P-element P{EP}G8235 excision lines
UP-primer	GACGGGACCACCTTATGTTATTTTCATCATG	Genotyping of imprecise P-element P{EP}G8235 excision lines
Ror-upstream-fw	AACAACCCCAACGACTTCGTGCG	Verification of imprecise P-element excision of P{EP}G8235 to generate Ror ^{E267}
Ror-Ex1-fw	CGCGAAAGGATAAAATACAAAATATTTTCGG	Verification of imprecise P-element excision of P{EP}G8235 to generate Ror ^{E267}
Ror-mut-check-fw	CCTTTGTTCCGAGTCATAGCA	Verification of imprecise P-element excision of P{EP}G8235 to generate Ror ^{E267}
CG5676-Ex1-rev	GCTTATTGGCGTTTCATCAGG	Verification of imprecise P-element excision of P{EP}G8235 to generate Ror ^{E267}
Pten-upstream-rev	GTTGTGCAAAGCATACAGGA	Verification of imprecise P-element excision of P{EP}G8235 to generate Ror ^{E267}
Pten_reg_rev	CCTGAAGCAGAATGTGTCTT	Verification of imprecise P-element excision of P{EP}G8235 to generate Ror ^{E267}

Material and Methods

00884L	TCGGCAATGAAGTGGAACCTCT	Quality control of cDNA
00884R	AGGCAAAGGCATCAAACCTCGTC	Quality control of cDNA
Wnt2-check-fw	TATTGTGGCTCTACAGGGTG	Verification of point mutations in Wnt2 alleles
Wnt2-check-rev	GTGCGTATCTGCGGTTGTAA	Verification of point mutations in Wnt2 alleles
Otk-Exon4-fw	ATGATGGAGTCCTGGGACAAAC	Test RNA-Seq samples for otk transcript
Otk-Exon5-rev2	GTGGCATTATCTGTCCTTGGC	Test RNA-Seq samples for otk transcript
Otk2-Exon1-fw2	CTGAACGGAAGACGACGATTG	Test RNA-Seq samples for otk2 transcript
Otk2-Exon3-rev	CACAAAGTACAGGAAGGCCAG	Test RNA-Seq samples for otk2 transcript

2.6 Vectors and Constructs

Table 7: Vectors used in this study

Vector name	Description	Reference or Source
pENTR™/D-TOPO®	Entry vector for directional Gateway Cloning	Invitrogen, Carlsbad, Germany
pAWG	Expression vector, Actin5C promoter, C-terminal GFP tag	Murphy lab, Baltimore, USA
pAWM	Expression vector, Actin5C promoter, C-terminal Myc tag	Murphy lab, Baltimore, USA
pAWH	Expression vector, Actin5C promoter, C-terminal HA tag	Murphy lab, Baltimore, USA
pcDNA3W	used for in vitro transcription of RNA probes, MCS is flanked by SP6 and T7 promoter sequences	Plasmid collection AG Wodarz

Table 8: Constructs used in this study

Construct name	Description	Reference
Ror-pENTR	full length Ror in pENTR	Dissertation Karen Linnemannstöns, 2012
Ror-pAWG	full length Ror, Actin promoter, C-terminal GFP-tag	Dissertation Karen Linnemannstöns, 2012
Ror-pAWH	full length Ror, Actin promoter, C-terminal HA-tag	Dissertation Karen Linnemannstöns, 2012
Ror-pAWM	full length Ror, Actin promoter, C-terminal Myc-tag	Dissertation Karen Linnemannstöns, 2012
BAC CH322-82M14	attB-P[acman]-Cm ^R -BW harboring a 25kb insert including the ORFs of Ror, bsk, CG31717, CG5676, Pten and Rsf1	BACPAC Resources Center; Venken et al., 2009
Fz1-pENTR	full length Fz1 in pENTR	Dissertation Karen Linnemannstöns, 2012

Material and Methods

Fz1-pAWM	full length Fz1, Actin promoter, C-terminal Myc-tag	Dissertation Karen Linnemannstöns, 2012
Fz2-pENTR	full length Fz2 in pENTR	Dissertation Karen Linnemannstöns, 2012
Fz2-pAWM	full length Fz2, Actin promoter, C-terminal Myc-tag	Dissertation Karen Linnemannstöns, 2012
Otk-pAWM	full length Otk, Actin promoter, C-terminal Myc-tag	Dissertation Karen Linnemannstöns, 2012
Otk2-pAWM	full length Otk2, Actin promoter, C-terminal Myc-tag	Dissertation Karen Linnemannstöns, 2012
Wg-pAWM	full length Wg, Actin promoter, C-terminal Myc-tag	Plasmid collection AG Wodarz
Wnt2-pAWM	full length Wnt2, Actin promoter, C-terminal Myc-tag	Dissertation Karen Linnemannstöns, 2012
Wnt4-pAWM	full length Wnt4, Actin promoter, C-terminal Myc-tag	Plasmid collection AG Wodarz
Wnt5-pAWM	full length Wnt5, Actin promoter, C-terminal Myc-tag	Plasmid collection AG Wodarz
pUAS-mCD8-GFP	full length mouse CD8, UAS enhancer sequence, C-terminal GFP-tag	Lee and Luo, 1999
PL-452-C-eGFP	PL-452 vector with Kanamycin resistance gene flanked by loxP sites and GFP ORF, used as template vector to amplify recombineering selection cassettes	Addgene plasmid 19178, Venken et al., 2008

2.7 Model organism *Drosophila melanogaster*

2.7.1 Culturing of *Drosophila melanogaster*

Drosophila melanogaster stocks were maintained at 18°C or room temperature. The stocks were raised on a cornmeal-based standard medium as described in Ashburner, 2004. Every two to four weeks the flies were transferred into fresh culture bottles. For handling and dissection, adult flies were anaesthetized with CO₂. For embryo collection, flies were kept in collection cages on an apple juice agar plate with a small amount of yeast paste.

Drosophila medium: 712 g cornmeal

95 g soy flour

168 g dry yeast

450 g malt extract

150 ml 10% Nipagin

(700 ml ethanol (99%), 300 ml H₂O, 100 g Nipagin)

45 ml propionic acid

50 g agar

400 g sugar beet syrup

add 9.75 l ddH₂O

Apple juice plates: 40 g agar

1 l H₂O

340 ml apple juice

17 g sugar

20 ml 10% Nipagin

Material and Methods

2.7.2 Crosses of *Drosophila melanogaster* strains

Drosophila virgin females were collected within 4-6 h after the vial had been cleaned of adult flies. For each cross, virgins and male flies (2:1) were put together into a fresh vial and incubated at 25°C.

2.7.3 Fertility test for *Drosophila melanogaster* males and females

To assess if the males or females of a fly line are sterile, single pair crosses were performed. For this purpose, young adult males were placed individually with three wild-type virgin females of the *white*⁻ strain, or vice versa. The crosses were then incubated at 25°C and scored for offspring after two weeks. At least ten individuals of one fly line were tested.

2.7.4 Viability test

To test the viability of a fly line, 3 times 100 single embryos were aligned on an apple juice agar plate with yeast paste. To prevent other flies from laying eggs onto this plate, it was covered with a small cage. The plate was then incubated at 25°C. After at least 24 h, hatching rates were recorded.

2.7.5 Directed gene expression using the UAS-Gal4-System

The UAS/Gal4 system is employed for targeted gene expression in a temporal and spatial fashion. It is based on the yeast transcription factor Gal4 and its specific binding to the UAS (upstream activating sequence) which is analogous to an enhancer element. The binding of Gal4 to the UAS is essential for the transcriptional activation of Gal4-controlled genes.

Expression of the gene of interest is controlled by the presence of an UAS element located upstream of the gene. To achieve expression of the gene of interest, UAS flies are mated to flies expressing Gal4 under a specific promoter, termed the driver line (**Figure 9**). Expression of the gene of interest in the resulting progeny then reflects the Gal4 expression pattern of the driver line (Brand and Perrimon, 1993).

Material and Methods

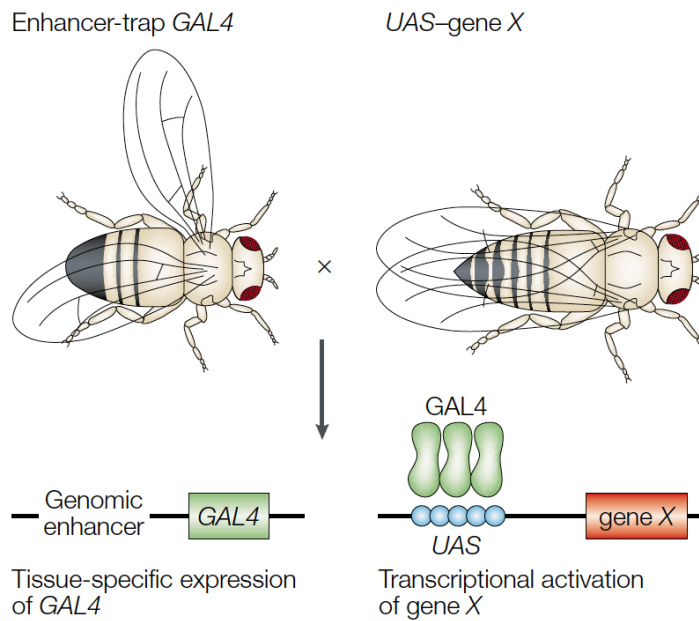


Figure 9: Targeted gene expression with the UAS/Gal4 system. Expression of a gene of interest is controlled by the presence of an UAS element. To activate transcription, a Gal4 driver line and UAS-gene of interest lines are crossed together. Taken from (St Johnston, 2002).

2.8 Isolation of nucleic acids

2.8.1 Mini preparation of plasmid DNA from *Escherichia coli* (alkaline lysis method)

One bacterial colony was inoculated in 3 ml LB medium and the appropriate antibiotics and incubated at 37°C overnight on a shaker. The next day, the cell suspension was centrifuged for 1 min at 13,000 rpm. Afterwards, the cells were resuspended in 200 µl buffer S1, followed by cell lysis for 5 min at RT in 200 µl buffer S2. For neutralization, 200 µl buffer S3 were added and the tube gently inverted. After a 20 min centrifugation step at 13,000 rpm, the supernatant was transferred into a fresh 1.5 ml reaction tube and the DNA was precipitated by adding 400 µl isopropanol. By centrifugation for 30 min at 4°C and 13,000 rpm the DNA was pelleted. This DNA pellet was then washed with 200 µl ethanol (70%) for 5 min at 13,000 rpm. After drying, the pellet was resuspended in 20 µl ddH₂O. The isolated DNA was stored at -20°C.

Material and Methods

Buffer S1 50 mM Tris-HCl (pH 8)
 10 mM EDTA
 100 µg/ml RNaseA
 store at 4°C

Buffer S2 0.2 M NaOH
 1% (w/v) SDS
 store at RT

Buffer S3 3 M KAc pH 5.5
 store at RT

2.8.2. Midi Preparation of plasmid DNA from *Escherichia coli*

This method utilizes the different characteristics of chromosomal and plasmid DNA during the change of the pH value from acidic to basic. The NucleoBond Xtra Midi Kit from Macherey-Nagel was used according to the manufacturers instructions.

For preparation of high DNA amounts, 100 ml LB medium were inoculated with 50 µl bacterial culture including appropriate antibiotics and incubated over night at 37°C on a shaker. The bacteria culture was then transferred to fresh 50 ml falcons and pelleted in a centrifuge (Eppendorf) for 15 min at 4°C (5000 rpm). Meanwhile, the column and the filter were equilibrated with 12 ml buffer EQU. After centrifugation, the supernatant was discarded and the cell pellet was resuspended in 8 ml buffer RES. For cell lysis, further denaturation of DNA and degradation of RNA, 8 ml buffer LYS were added, mixed, and the cell suspension was then incubated for 5 min at RT. Afterwards, 8 ml neutralization buffer NEU were added and the sample was inverted several times to precipitate chromosomal DNA and proteins. The lysate was then loaded onto the column with the filter and washed once with 5 ml buffer EQU. After discarding the filter paper and one washing step with 8 ml buffer WASH each followed. The plasmid DNA stays attached to the exchange matrix during these washing steps. Elution of the plasmid DNA was achieved by adding 5 ml buffer ELU to the column. The plasmid DNA was then

Material and Methods

precipitated with 3.5 ml isopropanol, pelleted by centrifugation (30 min at 13,000 rpm at 4°C) and washed with 2 ml 70% ethanol (10 min at 13,000 rpm). Finally, the pellet was dried at RT and solved in 50-100 µl TE-buffer (pH 8.0).

TE-buffer: 10 mM Tris-HCl pH 8.0
 1 mM EDTA pH 8.0

2.8.3 Preparation of genomic DNA from *Drosophila melanogaster*

Thirty flies were frozen for 10 min at -80°C. After adding 200 µl buffer A, the flies were homogenized using a biovortexer. After adding additional 200 µl buffer A, the homogenization was continued until only cuticles remained. The resulting extract was incubated for 30 minutes at 65°C. After addition of 800 µl LiCl / KAc solution (572 µl 6 M LiCl + 228 µl 5 M KAc), the mixture was incubated on ice for 15 minutes and centrifuged at 13.000 rpm for 15 minutes at RT. Then, 1 ml supernatant was transferred into a new reaction tube and 600 µl of isopropanol were added followed by another centrifugation step for 15 min at 13.000 rpm. The pellet was twice washed with 200 µl ice-cold 70% ethanol and air-dried. Finally, the genomic DNA was dissolved in 150 µl ddH₂O or TE-buffer and stored at -20°C for future use.

Buffer A: 100 mM Tris-HCl pH 7.5
 100 mM EDTA pH 8.0
 100 mM NaCl
 0.5 % SDS

2.8.4 Preparation of genomic DNA from single flies

One single fly was shock-frozen in liquid nitrogen. After adding 50 µl squishing buffer and 0.5 µl Proteinase K (200 µg/ml), the fly was homogenized using a biovortexer. The sample was incubated for 30 min at 37°C, then the Proteinase K was inactivated by

Material and Methods

another incubation step for 5 min at 95°C. After a final centrifugation step for 5 min at 13.000 rpm, the DNA was either stored at -20°C or 5 µl were directly used for PCR.

Squishing buffer: 10 mM Tris-HCl pH 8.0
 1 mM EDTA
 25 mM NaCl

2.8.5 Isolation of total RNA from *Drosophila melanogaster* embryos

Over night embryo collections were used and, if necessary embryos were aged afterwards at 25°C to reach the desired developmental stage. If applicable, embryos were sorted under a fluorescence stereomicroscope (i.e. if balanced over a GFP balancer). For each sample, 25 embryos were collected in a RNase-free tube. 100 µl NaCl solution (0.9 % in DEPC-H₂O) were added and the embryos quickly homogenized with a small pestle. After adding 800 µl TRIzol (QIAGEN) and mixing thoroughly, the sample was incubated at RT for 15 min to allow dissociation. Next, 160 µl chloroform were added, mixed vigorously for 30 sec and incubated for 3 min at RT. After a 20 min centrifugation step at 12.000 x g (4°C) the aqueous phase (upper phase) was cautiously transferred into a fresh RNase-free tube. To precipitate the RNA, 400 µl isopropanol and 2.2 µl GlycoBlue (Ambion®, Life Technologies AM9515) were added, vortexed for 15 sec and then the sample was incubated at -80°C over night. After 30 min centrifugation at 12.000 x g (4°C), the supernatant was removed and the RNA pellet was washed twice with 75% ethanol. Finally, the pellet was dried for 5 min at 37°C and dissolved in 20 µl RNase-free water. If used for transcriptome analysis, 2 µl of the sample were used to check RNA quality and quantity (NanoDrop, BioAnalyzer). The samples were stored at -80°C until further use.

2.9 Amplification and cloning of nucleic acids

2.9.1 Amplification of DNA using polymerase chain reaction (PCR)

The amplification of specific DNA fragments *in vitro* was achieved by polymerase chain reaction. For cloning purposes, a self-made proofreading PfuS polymerase was used, for other applications (i.e. screening PCRs), Taq polymerase (Biotherm™) was utilized. In general, the reactions were done in a total volume of 50 µl (PfuS) or 20 µl (Taq) by adding the following reaction components:

for PfuS polymerase: 5 µl genomic DNA (20-50 ng) or

- 1 µl plasmid DNA (200 ng)
- 2 µl forward primer (10 µM)
- 2 µl reverse primer (10 µM)
- 1.5 µl dNTPs (10 mM)
- 10 µl 5x HF-buffer (NEB)
- 1.5 µl PfuS polymerase
- ad 50 µl with ddH₂O

for Taq polymerase: 1 µl genomic DNA (20-50 ng) or

- 0.5 µl plasmid DNA (200 ng)
- 0.8 µl forward primer (10 µM)
- 0.8 µl reverse primer (10 µM)
- 0.2 µl dNTPs (10 mM)
- 2 µl 10x Taq-buffer (BioTherm™)
- 0.5 µl Taq polymerase (BioTherm™)
- ad 20 µl with ddH₂O

The appropriate PCR conditions were determined, depending on the product length, the DNA polymerase used, and the specific melting temperature of the oligonucleotides used as primers. The number of performed PCR cycles is dependent on the initial template concentration. The following standard conditions were regarded:

Material and Methods

Step 1: Initial denaturation:	5 min at 95°C
Step 2: Denaturation	30 sec at 95°C
Step 3: Primer annealing	30 sec at 50 - 65 °C
Step 4: Polymerization	30 sec /kb at 72°C
Step 5: final polymerization	10 min at 72°C
Storage	4°C

After completion of the DNA synthesis in step 4, the reaction was taken up again to step 2. In general, the cycle was repeated 35 times. After the reaction was complete it was stored at 4°C in the final step.

2.9.2 Colony PCR

In order to determine whether a certain DNA sequence is present or absent in a plasmid, colony PCRs can be used.

A mastermix was prepared for all reactions and distributed into tubes. Then, single colonies were picked with a sterile toothpick, added directly into the reaction tubes and then streaked out on an agar plate containing appropriate antibiotics. In general, the primers used for the colony PCR were the same primers already used to amplify the PCR fragment, same with the conditions for the reaction. Lysis of the bacteria occurred during the initial denaturation step in the PCR reaction. The reaction was performed in a total volume of 12.5 µl by adding the following components:

bacterial colony

0.25 µl forward primer (10 µM)

0.25 µl reverse primer (10 µM)

0.25µl dNTPs (10 mM)

1.25 µl Taq buffer (BioTherm™)

0.5 µl Taq polymerase (BioTherm™)

add up to 12.5 µl with ddH₂O

Material and Methods

As positive control, a plasmid containing the analyzed DNA sequence was used as template, as a negative control H₂O was added to the reaction.

2.9.3 Restriction of DNA

For test restriction of plasmids after Mini preparation, 3 µl of DNA were digested in a total volume of 20 µl, using 0.3 µl restriction enzyme and 2 µl of the 10x digestion buffer suited best for the restriction enzyme used. The restriction digestion was incubated at 37°C for 1 – 2 h and subsequently analyzed by agarose gel electrophoresis.

2.9.4 Cloning of PCR products in the Entry vector

To directionally clone PCR products into a vector and generate Entry clones, the pENTR/D-Topo[®] Cloning Kit (Invitrogen) was used. One important feature of this system is the topoisomerase I enzyme which is bound to two TOPO[®] recognition sites on each end of the double-stranded DNA fragment which will in the end be the vector backbone. Downstream of the 5' TOPO[®] recognition site is a GTGG overhang (Figure 10). After mixing the PCR product and the TOPO[®]-charged vector backbone, this overhang then invades the 5' end of the PCR product, which is required to be CACC, anneals and stabilizes the PCR product in the correct orientation. Topoisomerase I seals the phosphodiester chain and generates an Entry clone with the PCR product inserted in the correct orientation. In the pENTR[™]/D-TOPO[®] vector, the PCR product is flanked by attL recombination sites, making recombination into an attR site containing Gateway vector possible.

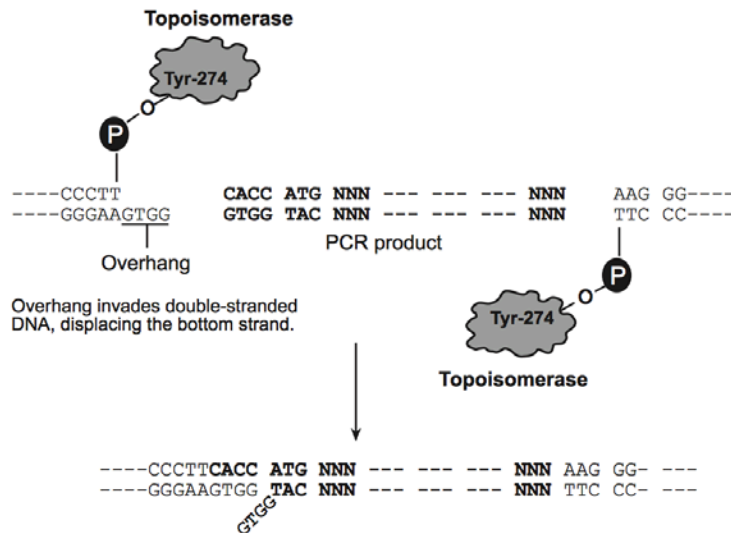


Figure 10: Directional Topo Cloning. A PCR product contains a CACC sequence motif at the 5' end. The Topo® vector backbone has a GTGG overhang at the 5' end. The enzyme topoisomerase I, which is covalently bound to the vector facilitates the directional cloning of the PCR product into the vector therefore generating an Entry clone. Taken from the pENTR/D-Topo® Cloning Kit User guide (Invitrogen).

A ENTR cloning reaction consisted of the following components:

2 µl PCR product (100ng/µl, freshly purified)

0.5 µl pENTR vector

0.5 µl salt solution

add up to 5 µl with ddH₂O

After incubation for 5-10 min at RT, the reaction was transformed into competent *E. coli* TOP10 cells.

2.9.5 Cloning of PCR products via Gateway® Cloning (Invitrogen)

For cloning of PCR products into expression vectors for functional analysis and protein expression, the Gateway® Cloning system was used. This system is based on the site-specific recombination properties of the bacteriophage lambda between DNA recombination sequences (att sites). After cloning of a PCR product into an Entry vector (see 2.9.4), the PCR product can easily be recombined into a collection of different Gateway destination vectors containing promoters and/or tags. In the Entry vector, the PCR product is flanked by two attL recombination sites. And the Gateway destination vectors contain two attR recombination sites, which flank the *ccdB* gene used for

Material and Methods

negative selection. The enzyme LR Clonase facilitates site-specific recombination between the attL and the attR sites leading to the replacement of the *ccdB* gene with the PCR product and the generation of hybrid attB sites in the expression clone and attP sites in the donor vector (Figure 11).

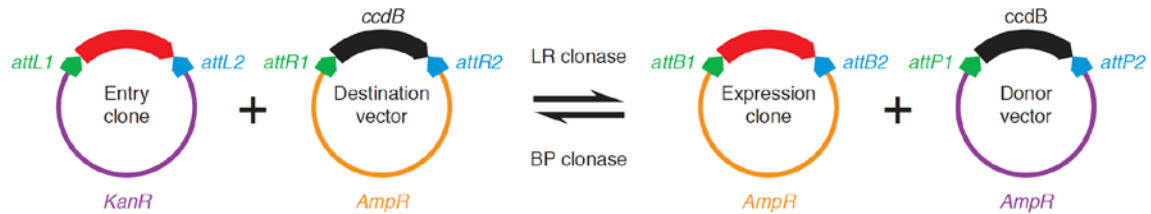


Figure 11: Gateway® Cloning. A PCR product (red) (i.e. a cloned gene) can be easily transferred into a collection of expression vectors using the Gateway® Cloning system. Taken from (Katzen et al., 2007).

A Gateway cloning reaction with the Gateway LR Clonase™ II Enzyme Mix (Invitrogen) consisted of the following components:

- 0.5 µl pENTR clone containing gene of interest (100ng/µl)
- 0.5 µl pDEST vector (150ng/µl)
- 3 µl TE-Buffer (pH 8.0)
- 1 µl LR Clonase II enzyme mix

After incubation for 1 h at 25°C, 0.5 µl of Proteinase K (2 µg/µl) was added and the sample was again incubated for 10 min at 37°C and transformed into competent *E. coli* cells.

2.9.6 Generation of GFP fusion proteins via Recombineering (recombination-mediated genetic engineering)

In this study a fly line expressing a GFP fusion protein under the control of the endogenous promoter was created using Recombineering (Venken et al., 2008). This method is based on homologous recombination in *E.coli* using recombination proteins provided from λ phage. Linear DNA with homology in the 5' and 3' ends to a target DNA molecule, which is already present in the bacteria can be introduced into heat-shocked

electrocompetent bacteria. The introduced linear DNA will then undergo homologous recombination with the target molecule.

The bacterial strains used for recombineering (SW102 and SW106) contain a defective λ prophage. The phage genes *exo* (5'-3' exonuclease), *beta* (generate recombination activity) and *gam* (protects linear DNA from nucleases) are under control of the λ PL promoter. This promoter is under tight control of the temperature-sensitive λ repressor cI857. When the bacteria are kept at <32°C, no recombination proteins are produced, but the recombination functions can transiently be supplied by a heat-shock at 42°C. The recombineering strains should always be grown at temperatures below 32°C, or they will lose the prophage.

2.9.6.1 Transformation of BAC clone in SW102 cells

After high copy number induction of the BAC clone harboring the genomic region of the gene of interest and subsequent plasmid preparation (see 2.8.1), 1 μ l was transformed into 80 μ l electrocompetent SW102 cells (see 2.9.8). The cells were incubated shaking at 30°C for at least 1 h, plated on LB-chloramphenicol plates and grown at 30°C for at least 24 h. Clones harboring the BAC were identified via colony PCR (see 2.9.2).

2.9.6.2 Amplification of GFP selection cassette

The template vector used for the amplification of the GFP selection cassette contains a kanamycin resistance gene, which is flanked by two loxP sites upstream of the GFP open reading frame. The primers for the amplification of the selection cassette each contained a 50 bp long sequence homologous to the destination sequence in the BAC. The forward primer contained the last 50 bp before the stop codon of the gene of interest and the reverse primer contained the first 50 bp of the 3'UTR. For the amplification of the cassette, the following PCR program was used:

Material and Methods

Step 1:	98°C	30 sec
Step 2:	98°C	10 sec
Step 3:	60-72 °C	30 sec
Step 4:	72°C	1 min 30 sec (go back to step 2, repeat 40 times)
Step 5:	72°C	10 min
store at 4°C		

Every cycle the annealing temperature was increased by 0.3°C and in the last cycle it reached the elongation temperature. The PCR product was purified over an agarose gel and freshly used for recombination.

2.9.6.3 Recombination of GFP selection cassette into BAC containing gene of interest

A starter culture of SW102 cells harboring the BAC was grown over night at 30°C. From this culture, two diluted cultures (1:10) were inoculated (induced sample + uninduced control) and grown at 30°C. After the culture reached an OD₆₀₀ of 0.4 - 0.6, the induced sample was incubated for 15 min at 42°C to activate the recombination functions. The uninduced control sample was kept at 30°C. Next, both samples were shaken in an ice-water slurry for 5 min before the cells were pelleted at 3220 rpm, 4°C for 10 min. The cells were washed twice with 25 ml ice-cold autoclaved ddH₂O and each time carefully resuspended by tapping. Then the cells were washed once with 10 % glycerol, spun down for 30 sec at 13.000 rpm and finally resuspended in a final volume of 160 µl 10 % glycerol. These fresh electrocompetent cells were divided into 2 samples and transformed with 100 ng purified GFP selection cassette via electroporation (see 2.9.8). After shaking at 30°C for 1.5 - 2 h, the cells were plated on chloramphenicol (BAC) + kanamycin (cassette) plates and incubated at 30°C for 36 h.

Recombination events of the selection cassette into the BAC clone were verified via colony PCRs using the primer pairs goi-rec-F + Kan-seq-R and Kan-seq-F + goi-3'-rec-R (Figure 12).

2.9.6.4 Removal of the kanamycin cassette via Cre-recombination

In order to remove the kanamycin cassette from the construct, a second recombination step has to be performed. Only then will the GFP be in-frame with the gene of interest. For this purpose the SW106 cells, which contain a tightly controlled arabinose-inducible *cre* gene were used. Cre recombinase can mediate recombination between two identical loxP sites.

After preparing DNA from BAC clones containing the GFP selection cassette, the construct was transformed into electrocompetent SW106 cells and positive clones were again verified by colony PCR. For Cre recombination, a fresh starter culture was inoculated in LB medium supplemented with chloramphenicol, but without kanamycin. After growing the cells at 30°C until they reached an OD₆₀₀ of 0.5, 0.1 % of filter-sterilized L-arabinose were added to induce expression of Cre recombinase. The cells were grown for an additional hour and several dilutions were plated on LB plates with chloramphenicol, but without kanamycin. To verify the absence of the kanamycin resistancy gene, 16 colonies were picked and streaked onto LB plates with kanamycin. This second recombination event was also verified via colony PCR with the primers goi-rec-F and goi-rec-R (Figure 12).

2.9.6.5 Copy number induction of positive clones and large construct preparation

After preparing DNA from clones harboring the BAC with GFP cassette and without the kanamycin cassette, the construct was transformed into electrocompetent TransforMax™ EPI300™ cells (Epicentre). After growing an over night culture at 37°C and diluting it 1:10, CopyControl™ induction solution (Epicentre) was added (1:1000) and the culture was incubated shaking for 5 h at 37°C. The induction solution induces the expression of a mutant *trfA* gene in the EPI300™ cells. This results in initiation of replication from the *oriV* high copy origin of the BAC clone and amplification of the construct. If this step is omitted, replication will originate from the low copy *oriS*. DNA preparation was performed with the QIAGEN Large Construct Kit according to the manufacturer's instructions. After verification of the construct by sequencing, the construct was send to Genetic Services Inc. (Cambridge, MA) for PhiC31 integrase-mediated integraton into the genome of fly embryos.

Material and Methods

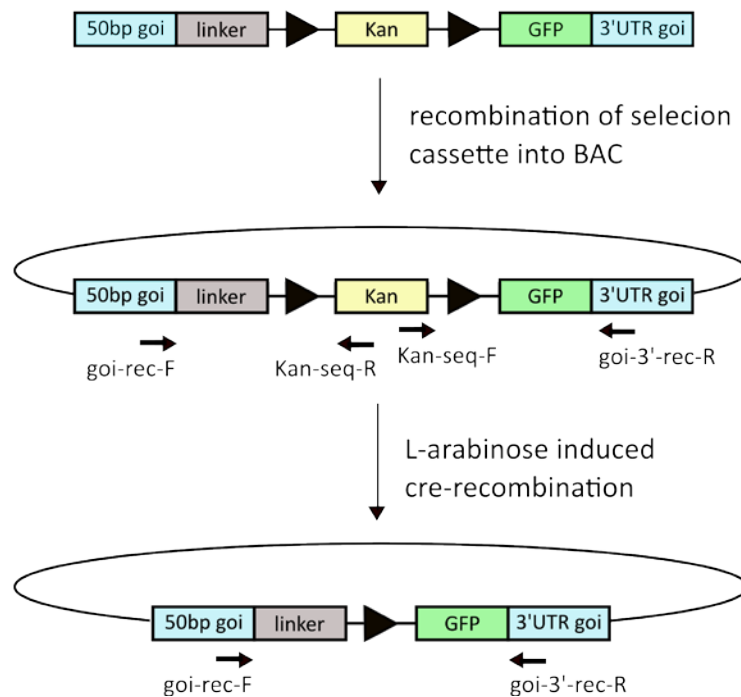


Figure 12: Generation of a C-terminal tagged GFP- fusion construct via Recombineering. A selection cassette containing two 50 bp long homology arms, a linker sequence, a kanamycin resistance gene flanked by two loxP sites and the eGFP open reading frame was integrated into the gene of interest (goi) which was located on a BAC clone, by recombination. Afterwards, the kanamycin cassette was removed in a second, cre-mediated recombination step. The primers used for colony PCRs are indicated.

2.9.7 Transformation of DNA into chemically competent *Escherichia coli*

For transformation of plasmid DNA, 50 µl of chemically competent *E. coli* cells were thawed on ice. The DNA sample was then carefully mixed with the cells and incubated on ice for 30 min. Afterwards, a heat shock for 30-45 sec at 42°C was performed, after which the cells were cooled down on ice for 2 min. Then, 200 µl of pre-warmed LB- or SOC medium was added to the suspension, followed by incubation for at least 1h at 37°C on a shaker. Finally, the suspension was plated on LB agar plates containing an antibiotic corresponding to the resistancy gene contained in the transformed construct. The plates were incubated over night at 37°C.

2.9.8 Electroporation of DNA into electrocompetent *E.coli* cells

For transformation of DNA into electrocompetent *E. coli* cells, 80 µl of competent cells were gently mixed with 1-2 µl DNA and transferred into a pre-cooled electroporation cuvette (Bio-Rad) without any air bubbles. Electroporation was performed using a Bio-Rad electroporator and the following parameters: Ec1 - 1.8 kV (200 Ω, 25 µF). Next, 150 µl pre-warmed SOC-medium was added and the bacterial suspension carefully transferred into a fresh tube. After shaking for 1 h at 37°C, the bacteria were plated on a LB agar plate containing appropriate antibiotics.

2.9.9 Preparation of *Escherichia coli* stab cultures

In order to transport *E. coli* cultures to other labs, solid stab cultures were prepared. LB-medium + 1 % agar was autoclaved and distributed into 2 ml screw-cap vials while still liquid. After solidification of the medium, a bacterial colony was transferred into the tube using a sterile toothpick through stabbing deep into the agar several times. After incubation at 37°C over night with the cap slightly loose, the stab culture was ready for shipment.

2.10 Analyses of DNA

2.10.1 Electrophoretic separation of DNA (Sambrook et al., 1989)

DNA molecules were separated based on size and electric charge by agarose gel electrophoresis. For proper separation based on the size of the DNA fragments, an agarose concentration of 1 % (w/v) in 1x TAE buffer was used. 1 µl of a 1 % ethidium bromide solution (Merck) was added per 100 ml agarose. The DNA samples were mixed with 6 x loading buffer and loaded onto the polymerized gel with a DNA ladder (Fermentas) in a separate lane. The electrophoresis was performed at 120 V for 20 - 30 min. Subsequently, the DNA was visualized via UV light exposure and a picture was taken.

Material and Methods

50x TAE buffer: 2 M Tris-Base
 50 mM EDTA pH 8.0
 acetic acid

6x DNA-loading buffer: 10 mM Tris-HCl pH 7.4
 60 mM EDTA pH 8.0
 60 % glycerol
 Bromphenol blue

2.10.2 DNA extraction from agarose gels

For the isolation of specific DNA fragments directly from agarose gels, the NucleoSpin[®] gel and PCR clean up kit (Macherey-Nagel) was used.

The gel slice containing the DNA fragment was excised under UV light and transferred into a 1.5 ml reaction tube. For each 100 mg gel slice, 200 µl buffer NTI were added. After 10 min shaking at 50°C to solubilize the gel piece, the mixture was loaded onto a spin column with a silica membrane. Afterwards, it was centrifuged for 1 min at 11.000 rpm and the flow-through was discarded. Two washing steps with 700 µl buffer NT3 followed. Drying of the silica membrane was achieved through another centrifugation step for 1 min at 11.000 rpm. Finally, the DNA was eluted by placing the column into a new tube, adding 20 µl buffer NE directly onto the membrane, incubation for 1 min at RT and centrifugation for 1 min at 11.000 rpm. The DNA was stored at -20°C.

2.10.3 Ethanol precipitation of DNA

For ethanol precipitation 2.5 volumes of 100% ethanol and 1/10 volume 3 M sodium acetate were added to the DNA solution and mixed. After incubation for at least 15 min at -20°C, a 15 min centrifugation step at 13.000 rpm followed. An incubation for at least 15 min at -20°C was followed by a 15 min centrifugation step at 13.000 rpm. Finally, the pellet was washed once with 70% ethanol, dried and resuspended in 20 - 40 µl of ddH₂O.

2.10.4 Photometric determination of DNA concentrations

Nucleic acids can be quantified due to their maximum absorption at the wavelength of $\lambda = 260$ nm using a spectrophotometer. From the maximum absorption of the measured solution at a specific wavelength the spectrophotometer can estimate the optical density (OD). Based on the OD the photometer can calculate the nucleic acid concentration of the solution. Using a UV micro cuvette (BRAND, 12.5 x 12.5 x 45 mm) and a dilution of 1:100 (sample in ddH₂O) the photometer displays the concentration in $\mu\text{g} / \mu\text{l}$.

2.10.5 Sequencing of DNA sequences

Sequencing of DNA was performed by the sequencing service at the Department of Developmental Biochemistry (AG Pieler). First, the sequencing reactions had to be performed. Reactions contained the following components:

For plasmids: 300 ng template
 8 pmol primer
 1.5 μl Seqmix (Applied Biosystems)
 1.5 μl Seqbuffer (Applied Biosystems)
 add to 10 μl with ddH₂O

For PCR products: 20 - 30 ng purified PCR product
 8 pmol primer
 1 μl Seqmix (Applied Biosystems)
 1 μl Seqbuffer (Applied Biosystems)
 add to 10 μl with ddH₂O

Material and Methods

Standard PCR program used for sequencing reactions:

Step 1:	2 min at 96°C
Step 2:	20 sec at 96°C
Step 3:	30 sec at 55 °C
Step 4:	4 min at 60°C
Repeat steps 2–4 26 times	
Step 5:	10 min at 72°C
Storage	12°C

After ethanol precipitation of the PCR product, the pellet was resuspended in 15 µl HiDi (Applied Biosystems). The sample was then handed to the sequencing service at the Department of Developmental Biochemistry.

2.11 Histological methods

2.11.1 Formaldehyde fixation of *Drosophila* embryos

After collecting the embryos on an agar plate containing apple juice and yeast, the embryos were washed off the surface using a brush and ddH₂O. Next, through adding sodium hypochloride (Klorix) the chorion was removed. This process can be observed by a glossy appearance of the embryos and the dorsal appendages coming off. Then, the embryos were transferred to a Netwell™ Insert (Corning Life Sciences, USA; 74 µm mesh size) and again washed with ddH₂O. After transferring the embryos into a glass vial containing 3 ml heptane and 3 ml 4% formaldehyde (in PBS), they were fixed by rocking them for 17 - 20 min. The lower phase (fixative) was removed from the vial, 3 ml methanol added and then the vial was shaken vigorously for 30 sec to remove the vitelline membrane. The fixed embryos sunk to the bottom of the vial, were transferred into a tube, washed three times with methanol and stored at -20°C or directly used for staining.

Material and Methods

PBS (1x)	140 mM NaCl
	10 mM KCl
	2 mM KH_2PO_4
	6.4 mM $\text{Na}_2\text{HPO}_4 \times 2\text{H}_2\text{O}$
	adjust pH to 7.3 and autoclave

2.11.2 Antibody stainings on *Drosophila* embryos and third instar larval imaginal discs

For immunostaining, embryos and imaginal discs were suspended to the same staining protocol. For staining of imaginal discs, wandering third instar larvae were collected and transferred to a glass dish with PBS. Then, their posterior ends were cut off and the whole larvae were turned inside out. The tissues were fixed for 20 min in 4 % formaldehyde/PBS. Embryos were also fixed prior to staining (see protocol 2.11.1).

The tissues were washed three times with PBTw and unspecific binding sites were blocked with PBTw + 5 % NHS (normal horse serum) for 30 min at RT. Incubation with the primary antibodies was performed over night at 4°C. After three washing steps with PBTw, the secondary antibodies were added and incubated for 2 h at RT. Next, the tissues were incubated with Hoechst in PBTw (1:200) for 20 min, followed by two more washing steps with PBTw. Embryos were then mounted in Mowiol. The imaginal discs were now dissected off the cuticula and transferred into a reaction tube with PBTw. Finally, after sinking to the bottom of the tube the PBTw was removed and the imaginal discs were mounted in 80 µl of Mowiol.

PBTw	PBS + 0.1% Tween20
------	--------------------

2.11.3 Immunoperoxidase staining and dissection of the embryonic CNS

For immunoperoxidase staining, embryos were fixed for 1 h according to the standard protocol (see 2.11.1). The next steps of the staining protocol up to the incubation with the secondary antibody resemble the protocol in 2.11.2. To achieve signal amplification, secondary antibodies conjugated to biotin were used. After 2h incubation at RT, the embryos were washed three times with PBTw. Before starting the first of these washing

steps, 10 µl of solution A and 10 µl of solution B of the VECTASTAIN® ABC Kit (Vector laboratories) were mixed with 500 µl PBTw and incubated for 30 min at RT. Solution A contains avidin DH and solution B contains biotinylated horseradish peroxidase (HRP) H. During the 30 min incubation, these form the Avidin/Biotinylated enzyme complex (ABC). Next, the embryos were incubated with the ABC complex for 1 h at RT. Since avidin has four binding sites for biotin, the complex is able to bind to the biotinylated secondary antibody, which amplifies the signal. After three more washing steps with PBTw, the embryos were washed once for 5 min with PBS. For the staining reaction, the embryos were transferred into a 12-well plate. The PBS was removed and replaced with 300 µl DAB (3,3'-diaminobenzidine) in PBS (1:3). Next, 1 µl 3 % H₂O₂ was added. In the presence of H₂O₂, DAB becomes oxidized by the HRP, which results in a brown precipitate. The staining reaction was stopped by washing several times with PBTw. Then the embryos were transferred to reaction tubes, the PBTw was removed and 200 µl 86 % glycerol were added. At this step the embryos can be stored at -20°C or at 4°C. To dissect the central nervous system, the embryos were transferred onto a glass slide. The anterior and the posterior part of the embryos were cut off with the tip of a 26 G needle and afterwards the dorsal side of the embryos was sliced open. Next, the lateral sides of the embryo were hinged to the side and the gut was removed. Finally, the stained and dissected nervous systems were transferred onto a fresh glass slide, mounted in 10 µl 50 % glycerol and covered with a 24 x 50 mm coverslip, which was fixed on the slide with nailpolish.

2.11.4 Dissection and staining of third instar larval brains

Brains from *Drosophila* wandering L3 larvae were dissected in *Drosophila* Ringer solution and collected on ice. After fixation with 4% formaldehyde in PBS for 20 min at RT, the brains were washed three times with PBTw, followed by a one hour blocking/permeabilization step in PBTx + 5% NHS. Incubation with the primary antibodies was performed in PBTw + 5% NHS, over night at 4°C. After three 10 min washing steps with PBTw, the brains were incubated with the secondary antibodies in PBTw + 5% NHS for 2h at RT. Next, the brains were Incubated with DAPI/Hoechst in PBTw for 20 min, washed twice with PBTw for 10 min and mounted in Mowiol.

Material and Methods

Ringer solution	182mM KCl 46mM NaCl 3mM CaCl ₂ 10mM Tris adjust pH to 7.2 with 1 N HCl
PBTx	PBS + 1% TritonX-100

2.11.5 Dissection and analysis of pupal *Drosophila* genital discs

After collecting pre-pupae, they were aged at 25°C until they reached the required developmental stage. The anterior halves of the pupae were then cut off with a scalpel and the pupal genital discs were dissected in PBS with the help of a tungsten dissecting needle. For the dissection of these small tissues, the standard stereomicroscopes were upgraded with EasyLED Spot M6 lighting and a 1,6x FWD 48mm lense (Carl Zeiss, Jena, Germany).

2.11.6 Preparation of adult *Drosophila* wings

After anaesthetizing adult flies, their wings were removed and dehydrated for 5 min in 100 % isopropanol. The wings were then transferred onto a glass slide and after the isopropanol was evaporated, the wings were mounted in a drop of Roti®-Histokitt (Roth) mounting medium.

2.11.7 Cuticle preparations of *Drosophila* embryos

For cuticle preparations, an overnight collection of embryos was incubated with yeast paste on the apple juice agar plate for at least 24 h at 25°C. After all hatched larvae were removed with the yeast paste, the remaining unhatched embryos were washed once with ddH₂O and mounted with one drop of Hoyer's mountant. After incubation of the slide at 65°C for 12 h or over night, the cuticle preparations were analyzed via light microscopy.

Material and Methods

Hoyers mountant: 30 g Gumarabic
50 ml H₂O
200 g Chloralhydrate
20 g Glycerol

Add gumarabic to H₂O and stir until completely dissolved. Keep stirring and add chloralhydrate slowly to avoid clumping. After adding the glycerol, centrifuge for at least 3 h, better over night at 12.000 x g until mountant is clear. Store at room temperature.

2.11.8 Analysis of PCP defects in adult *Drosophila* eyes

To analyze adult eyes for defects in planar cell polarity, the heads of anaesthetized flies were removed and immediately mounted in immersion oil (Zeiss) on a glass slide. To protect the heads from being squashed, the glass slide used for mounting had coverslips glued onto two sides to increase the space between slide and coverslip. The polarity of the photoreceptor cells was then analyzed by light microscopy.

2.12 Cell culture

2.12.1 Culturing *Drosophila* Schneider cells

For cell culture experiments in this study, the two Schneider cell lines S2 and S2R+ were used (Schneider, 1972). Both cell lines were made on Oregon R wild type embryos on the verge of hatching. The difference between the two lines is that in contrast to S2R+ cells, the S2 cells do not express the Wnt receptor Dfz2. The cells were maintained at 25°C in *Drosophila* S2 medium (Gibco), supplemented with 10 % FCS (fetal calf serum), 50 U/ml penicillin 50 µg/ml and streptomycin.

Material and Methods

2.12.2 Transfection of *Drosophila* Schneider cells

For each (co-)transfection, 2 wells with 2 million S2 cells each were transfected. The cells were counted using a Neubauer improved counting chamber and transferred into 6-well plates with S2 medium to reach a total volume of 2 ml per well. For two wells the transfection mix consisted of the following components:

For 2 wells: 188 μ l ddH₂O
 4 μ l DNA construct
 8 μ l FuGENE® HD transfection reagent (Promega, Madison, WI)

The DNA and ddH₂O were mixed and the solution was briefly vortexed, then the transfection reagent was added, followed by another brief vortexing step. After incubation for 15 min at RT, the transfection mix was carefully added to the cells and swayed gently to achieve an even distribution within the wells. The cells were incubated at 25°C for 48 h before they were transferred to cell culture flasks containing 6 ml fresh S2 medium. After another 72 hours growth at 25°C the cells were harvested.

2.13 Biochemical methods

2.13.1 Preparation of cell lysates from *Drosophila* embryos

An over night collection of embryos was dechorionated and washed with ddH₂O. After homogenizing the embryos in 200 μ l TNT-lysis buffer + protease inhibitors (see 2.13.3) with the help of a biovortexer, the volume was adjusted according to the amount of embryos. In general, lysis was performed in a total volume of 500 μ l – 1 ml. The lysates were shaken for 20 min on ice, followed by centrifugation for 10 min at 13.000 rpm at 4°C. After determination of the protein concentration, 2x SDS-loading buffer was added and the lysates were boiled at 95°C for 5 min and stored at -20°C until use.

TNT-lysis buffer: 150 mM NaCl
(pH 8.0) 50 mM Tris HCl
 1 % Triton X-100

2.13.2 Determination of Protein concentration

Protein concentration was determined with a photometer (Eppendorf Biophotometer). Bradford reagent (Roth) was diluted 1:5 with H₂O. After the blank measurement was taken, 2 µl of protein lysate were added and the OD₆₀₀ was measured. The measured value was multiplied by 10, which reflected the protein concentration in µg/µl.

2.13.3 Co-immunoprecipitation

For co-immunoprecipitation experiments, two wells with 2 million cells each were transiently transfected per sample. Two days after transfection, they were transferred into 75 cm² cell culture flasks. After another 72 h, the cells were harvested by centrifugation at 500 x g (4°C) and washed once with PBS. The cell pellets were then resuspended in 1 ml freshly prepared cold Co-IP buffer with protease inhibitors (Pefabloc (0.5 M in MeOH), Aprotinin (1 mg/ml, in H₂O), Leupeptin (1 mg/ml, in H₂O), Pepstatin (1 mg/ml in H₂O) all 1:500) and phosphatase inhibitor (Halt™ Phosphatase Inhibitor Cocktail, ThermoScientific, 1:100). After homogenization by pushing the lysates 5x through a 26 G insulin syringe, the lysates were sonicated at medium power for 10 min in a waterbath to destroy the DNA. This was followed by centrifugation for 10–15 min at 13.000 rpm. Next, the lysates were transferred to new reaction tubes and precleared with 30 µl prewashed ProteinA/G sepharose beads (BioVision) on a rotator for 2 h at 4°C. After removal of the beads, 25 µl input was taken from each sample, boiled with 2x SDS-loading buffer and stored at -20°C. The antibody-antigen reaction was performed over night at 4°C (rabbit anti-GFP, 1:1000). Next, 15 µl ProteinA/G beads were added to the lysates, and incubated for 2 h at 4°C on a rotator. After the beads were washed five times with 800 µl Co-IP buffer, all remaining liquid was removed with a syringe, the beads were boiled with 2x SDS-loading buffer and stored at -20°C or used directly for SDS-PAGE and Western blot.

Co-IP-Buffer: 50 mM Tris-HCl
 150 mM NaCl
 0.5 % NP-40

Material and Methods

0.5 % CHAPS

2.13.4 SDS-PAGE

In order to separate proteins according to their size, SDS-PAGE (sodium dodecyl sulfate polyacrylamide gel electrophoresis) was performed. This was done with the BioRad system. In general, gels with a thickness of 0.75 mm were prepared. After polymerization of the acrylamide, the electrophoresis chamber was filled with 1x SDS-running buffer and the samples were loaded onto the gel with 4 µl PageRuler Prestained Protein Ladder (Fermentas) to determine the size of the proteins. Electrophoresis was performed at 200 V for approximately 1 h.

2x SDS-loading buffer:	0.2 % Bromophenolblue
	200 mM beta-mercaptoethanol
	20 % glycerol
	4 % SDS
	100 mM Tris HCl pH 6.8

1x SDS-running buffer:	192 mM glycine
	25 mM Tris base
	0.1 % SDS

2.13.5 Western Blot

To transfer proteins, which were separated by size via SDS-PAGE onto a nitrocellulose membrane, the BioRad system was used. The gel and the membrane were assembled in a blotting chamber surrounded by two layers of Whatman paper and a plastik mat on each side. The transfer occurred for 1 h at 4°C in 1x transfer buffer. Afterwards, unspecific binding sites on the membrane were blocked with blocking buffer for at least 30 min. Incubation with the primary antibody was performed in blocking buffer, over night at 4°C. Next, the membrane was washed three times with TBST, followed by a 2 h incubation with a HRP-coupled secondary antibody (1:10000) at RT. After three more

Material and Methods

washing steps with TBST, the membrane was incubated for 1 min with POD substrate (1 ml solution A with 10 µl solution B, Roche). Finally, the chemiluminescence signal was detected using X-Ray films (Fuji) and developed with a developing machine (typon Optimax).

1x Transfer buffer:	25 mM TrisHCl
	192 mM glycine
	20 % (v/v) methanol

TBST:	150 mM NaCl
	1 mM Tris HCl
	0.2 % Tween20

Blocking buffer:	TBST
	3 % skim milk
	1 % BSA

2.14 Transcriptome analysis

2.14.1 RNA isolation

For each genotype, isolation of total RNA from triplicates of 25 embryos each (stage 16) was performed according to the protocol in 2.8.5. To analyze the RNA quality and quantity, analyses with the 2100 Bioanalyzer (Agilent Technologies) and NanoDrop (ThermoScientific) was performed at the [DNA Microarray and Deep-Sequencing Facility – Transkriptome analysis lab \(TAL\)](#), GZMB, Göttingen.

2.14.2 Sample preparation and sequencing

At the transcriptome analysis lab, the RNA-samples were prepared with the TruSeq RNA Sample Prep Kit v2 according to the manufacturer's instructions (Illumina). Sequencing was performed using HiSeq 2000 (Illumina). For each genotype three independent biological replicates were performed.

2.14.3 Processing and analysis pipeline

Data processing and analysis was performed simultaneously at the TAL (GZMB, Göttingen) and in our group (Dr. Manu Tiwari, MT) with the following pipeline:

Step 1: Demultiplexing using CASAVA v1.8.2, 1 mismatch allowed for index, indices different in at least 2 bases

Step 2: Quality assessment of fastq files by FastQC analysis (MT, version 0.11.2)

Step 3: Alignment of the fastq files to the *Drosophila* transcriptome with STAR (2.3.0), local alignment to the dm74 transcriptome reference of Ensembl (TAL) or the *Drosophila* reference genome BDGP 6.01 from Flybase (MT), 2 mismatches allowed

Step 4: Conversion and sorting via samtools 0.1.19

Step 5: Counting reads per gene using htseq-count version 0.5.4.p5 (TAL) and version 0.6.1 (MT)

Step 6: Normalisation and differential expression analysis was performed using the DESeq2 package 1.14.0 in R/Bioconductor (TAL: 3.0.2/2.13; MT: 3.1.1/2.14)

Genes were considered to be differentially expressed with the filters set to the following thresholds:

fold change (fc) >2 or < -2

false discovery rate (FDR, Benjamini Hochberg correction) < 0.05

Step 7: further annotation with ensembl biomaRt (2.18.0) via R

goseq (1.14.0), GO.db (2.10.1),: GO enrichment test on candidate genes

The lists of differentially expressed genes from both analyses were compared to each other using R version 3.1.1. The resulting lists with genes that are up- or downregulated in both analyses can be found in the appendix of this thesis.

2.14.4 Venn Diagrams

Venn diagrams displaying intersections between several data sets were prepared with the help of an online tool from the Bioinformatics and Evolutionary Genomics group at the University of Gent, Belgium (bioinformatics.psb.ugent.be).

2.14.5 Cluster network analysis

We used Cytoscape (v3.2.0) to integrate our expression data with known, related interactions. In each case, the list of differentially expressed genes was fed to the Cytoscape Interaction Database Universal Client (PSICQUIC registry) to fetch curated molecular interactions from the IntAct and DIP databases. After fetching and merging the interactions, we used the clusterMaker Community cluster (GLay) algorithm to cluster the interactions. Next, we overlaid the sub-networks with our expression data and used a custom style to view the clustering: green represents upregulation, red represents downregulation, and the intensity of the color corresponds to the \log_2 (fold-change) expression levels; cyan represents known interactions.

2.15 Imaging

2.15.1 Confocal microscopy

Confocal images were acquired with a LSM 510 Meta confocal laser scanning microscope (Carl Zeiss, Jena, Germany) using 25 x 0.8 NA Zeiss Plan-Neofluar, 63 x 1.4 NA Zeiss Plan-Apochromat oil immersion objectives and LSM 510 software (Carl Zeiss, Jena, Germany). The pinholes were set to 1 airy unit. In general, images were captured by 1024 x 1024 pixels using 2-line mean averaging.

Material and Methods

Images in Figure 15 were acquired with an inverse LSM 780 confocal laser scanning microscope (Carl Zeiss, Jena, Germany), a 63 x 1.4 NA Zeiss Plan-Apochromat oil immersion objective and Zen 2012 (black edition) software at the Department of Developmental Biochemistry, GZMB, Göttingen.

2.15.2 Lightsheet fluorescence microscopy (LSFM)

Images for Figure 14 were acquired with a Lightsheet Z.1 microscope (Carl Zeiss, Jena, Germany), provided by Zeiss for demonstration purposes at the GZMB, Göttingen in July 2013. The embryos were fixed and stained, then embedded in a tube made of 1 % low-melt agarose in H₂O and inserted into the sample chamber of the microscope, filled with PBS. A lightsheet Z.1 detection optics 20x/1.0 (water immersion) objective was used.

2.15.3 Light microscopy

All brightfield and phase contrast images were acquired with an Axio Imager.Z1 upright microscope (Carl Zeiss, Jena, Germany) using 10 x 0.3 NA Zeiss Plan-Neofluar, 25 x 0.8 NA Zeiss Plan-Neofluar and 63 x 1.4 NA Plan-Apochromat oil immersion objectives as well as Zen 2012 (blue edition) software from Zeiss.

2.15.4 Image processing

Single images were processed with Adobe Photoshop CS2 (Adobe Systems, San Jose, USA) software or GIMP, GNU General Public License (GPL). All figures were assembled using Inkscape, GNU General Public License (GPL).

3. Results

3.1 Expression pattern of *Ror*>*Ror*-eGFP

The expression pattern of *Drosophila* *Ror* has previously been described on the transcript level. *Ror* transcripts have been observed in the embryonic brain and central nervous system as well as in additional cells in the head and trunk of embryos (Wilson et al., 1993). To investigate the expression pattern on protein level and its subcellular localization, a fly line expressing a *Ror*-eGFP fusion protein under control of the endogenous *Ror* promoter (*Ror*>*Ror*-eGFP, *Ror*-eGFP) has been generated in this study (see 2.9.6).

3.1.1 *Ror*-eGFP is expressed in the embryonic nervous system

Figure 13 and Figure 14 depict the expression of the *Ror*-eGFP fusion protein in embryos stained with an anti-GFP antibody. The protein can first be detected in developmental stage 11 when the germ band is fully elongated (Figure 13 B, arrowheads). In this stage *Ror*-eGFP is visible as segmental patches colocalizing with the neuronal marker embryonic lethal abnormal vision (*Elav*) (data not shown). The expression level is weak when it first appears but increases in successive stages and persists throughout embryonic development. After completion of germband retraction, the protein can clearly be observed in the embryonic ventral nerve cord and in the brain (Figure 13 D) and becomes more prominent as the ventral nerve cord condenses into its final ladder-like structure (Figure 13 E-I). *Ror*-eGFP is not only expressed in the plasma membrane of cell bodies of neuronal cells (perikarya), but also in their axonal processes forming the commissures and connectives of the ventral nerve cord (Figure 13 I, Figure 14 B''). While it has been shown that expression of *Otk* and *Otk2* are both enriched at the anterior commissures when compared to the posterior commissures (Linnemannstöns et al., 2014), this is not the case for *Ror*-eGFP. The intensity of the GFP signal is evenly distributed throughout the ventral nerve cord (Figure 14 B'').

In addition to the expression in the central nervous system, *Ror*-eGFP is also expressed in the sensory cells of the embryonic peripheral nervous system (PNS) (Figure 14). This can

Results

be observed from developmental stage 13 onwards, but cannot be seen in Figure 13 since the PNS is in a different focal plane than the central nervous system (CNS). In stage 14 the sensilla, which differentiated in the first wave of differentiation can be seen (Figure 14 A/A'). In the abdominal segments of stage 16 embryos, Ror-eGFP can be observed at the cell membrane of neurons in all three clusters of sensory organs of the PNS (Figure 14 B''') including the sensory axons, which connect to the CNS. In addition to this, Ror-eGFP is expressed in the larval head sensory organs (Figure 13 F inset and Figure 14 B' arrow): the bolwig's organ, which represents the larval eye as well as in the dorsal, terminal and lateropharyngeal organs, all performing gustatory functions.

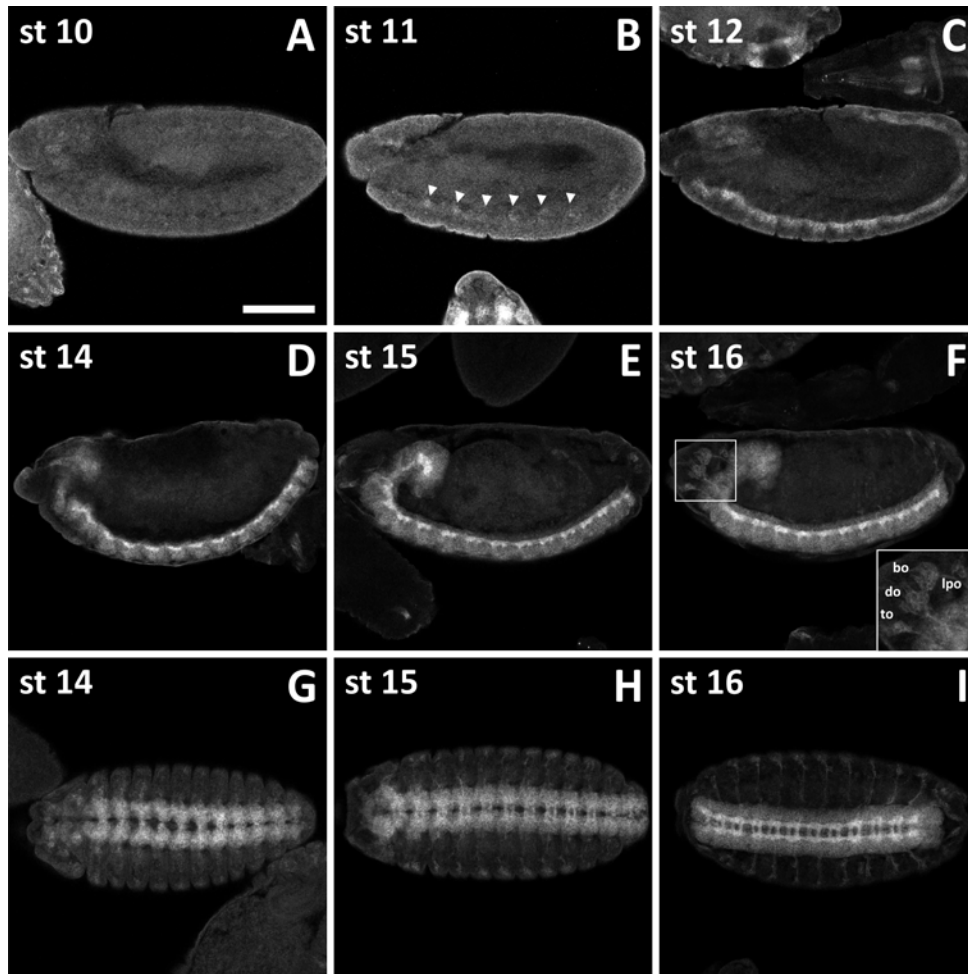


Figure 13: Expression of a Ror-eGFP fusion protein expressed under the endogenous *ror* promoter in *Drosophila* embryos imaged by confocal microscopy. Ror-eGFP expression can be observed from stage 11 onwards, primarily in the embryonic CNS and PNS. The developmental stages are indicated. **(A-F)** Lateral views of stage 10-12 and 14-16 embryos, the dorsal side is up. **(G-I)** Stage 14-16 embryos viewed from the ventral side. Anterior is to the left, scale bar = 50µm. Abbreviations: bo: bolwig's organ; do: dorsal organ; to: terminal organ; lpo: lateropharyngeal organ.

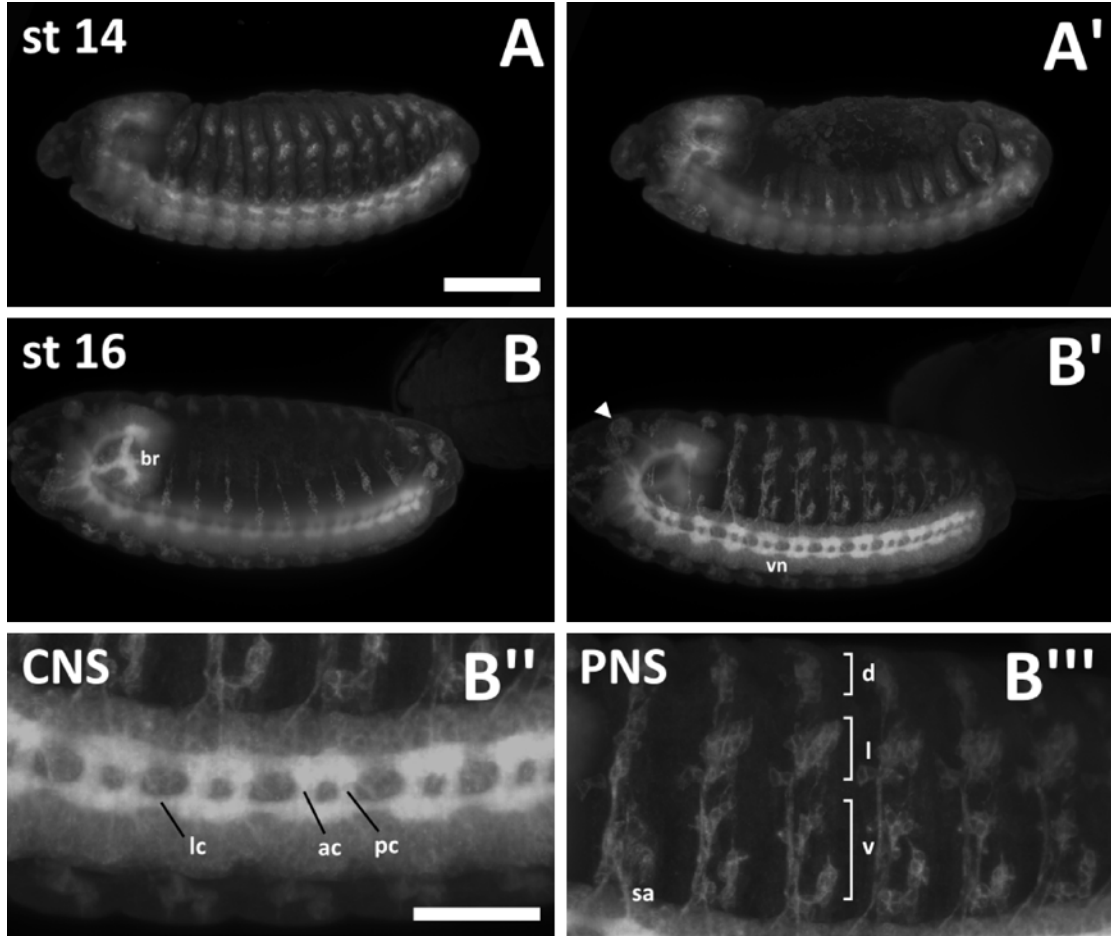


Figure 14: Lightsheet fluorescence microscopy of fixed and stained *Ror>Ror-eGFP* embryos. The images show maximum intensity projections of stacks taken from whole embryos. The left panels A/B and the right panels A'/B' show the same embryo, respectively, scanned from both sides. **(A, A')** In stage 14 embryos *Ror-eGFP* expression is strong in the embryonic CNS and already visible in the developing PNS. **(B, B')** In stage 16 embryos the protein is expressed throughout the entire nervous system. **(B'')** Enlarged view of the CNS seen in B'. **(B''')** Enlarged view of the PNS seen in B'. Anterior is to the left, the dorsal side is up. Scale bars: A-B' = 50µm; B''/B''' = 20 µm. Abbreviations: br: embryonic brain; vn: ventral nerve cord; lc: longitudinal connectives; ac: anterior commissures; pc: posterior commissures; sa: sensory axon; d: dorsal cluster; l: lateral cluster; v: ventral cluster.

To determine whether *Ror-eGFP* is expressed in all cells of the central nervous system or only in a certain subset, I stained embryos with the neuroblast marker *Miranda* (*Mira*) and the neuronal marker *Elav*. *Ror-eGFP* localizes to the cell membrane in an unpolarized manner. Figure 15 shows a section of the ventral nerve cord of a stage 16 embryo. The *Ror-eGFP* signal localizes to the membrane of all neurons, marked with *Elav* (Figure 15 A). In a higher magnification, the expression can clearly be detected at the membrane of a dividing neuroblast (Figure 15 A', asterisk).

Due to the weak expression of the protein, it was not possible to acquire any images with higher magnifications from developmental stages earlier than stage 16. Therefore,

Results

a final statement about Ror-eGFP expression in neuroblasts before this stage cannot be made.

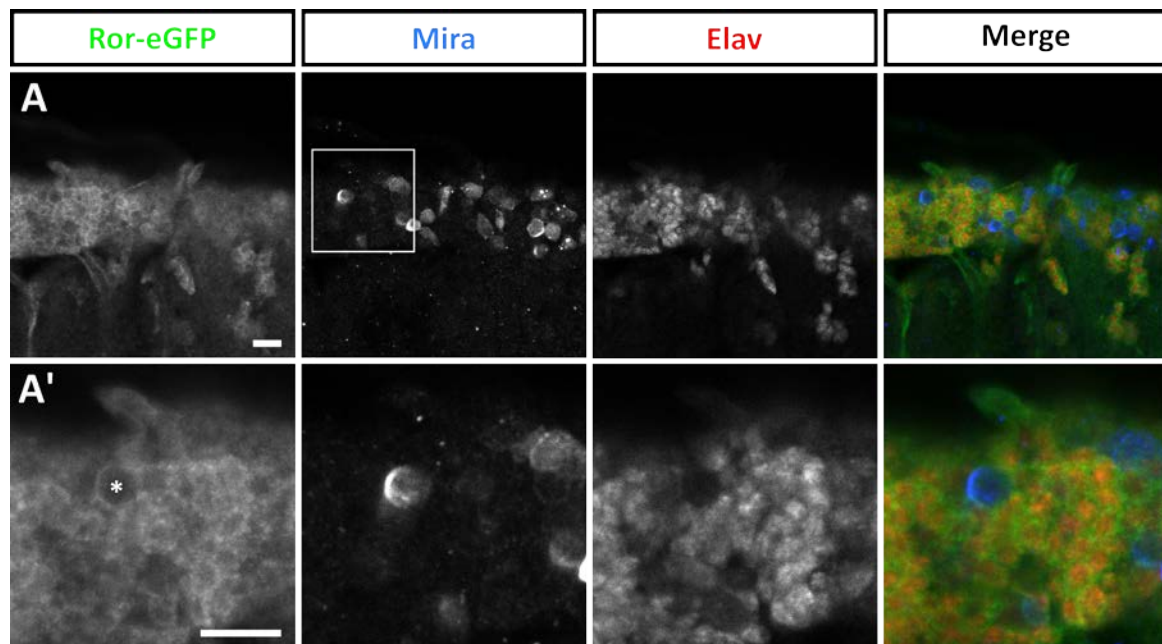


Figure 15: Ventral nerve cord of a stage 16 Ror-eGFP embryo stained against GFP, Miranda and Elav. (A) Ror-eGFP expression overlaps with the membrane of the Elav-expressing neurons. **(A')** A higher magnification shows that Ror-eGFP is also expressed in embryonic neuroblasts. Scale bars= 10µm.

3.1.2 Ror-eGFP is expressed throughout the larval nervous system

In order to analyze the expression pattern of Ror-eGFP in the larval central nervous system, I dissected larval brains from third instar larvae and stained them for the markers Mira and Elav. Each brain is composed of two symmetrical hemispheres, the brain lobes, which are attached to the ventral nerve cord (VNC).

Ror-eGFP expression can be seen throughout the larval central nervous system. It is not confined to a certain area but can be observed in the central brain, the optic lobe as well as the VNC (Figure 16 A). The expression in this tissue is much stronger compared to the expression in embryos. In all parts of the larval brain, the expression can be clearly detected in the cell membrane of neural stem cells (neuroblasts, NBs) as well as in their neuronal progeny marked by Elav (Figure 16 B/C). A closer look at neuroblasts and their progeny shows that Ror-eGFP is indeed expressed in all analyzed cell types. In the central part of the brain lobes and in the ventral nerve cord as well as in the central brain region it can be found in neuroblasts (Figure 16 D, asterisks) and in their progeny. Without

Results

additional markers the ganglion mother cells (GMCs) and intermediate progenitor cells (INPs) cannot be reliably identified.

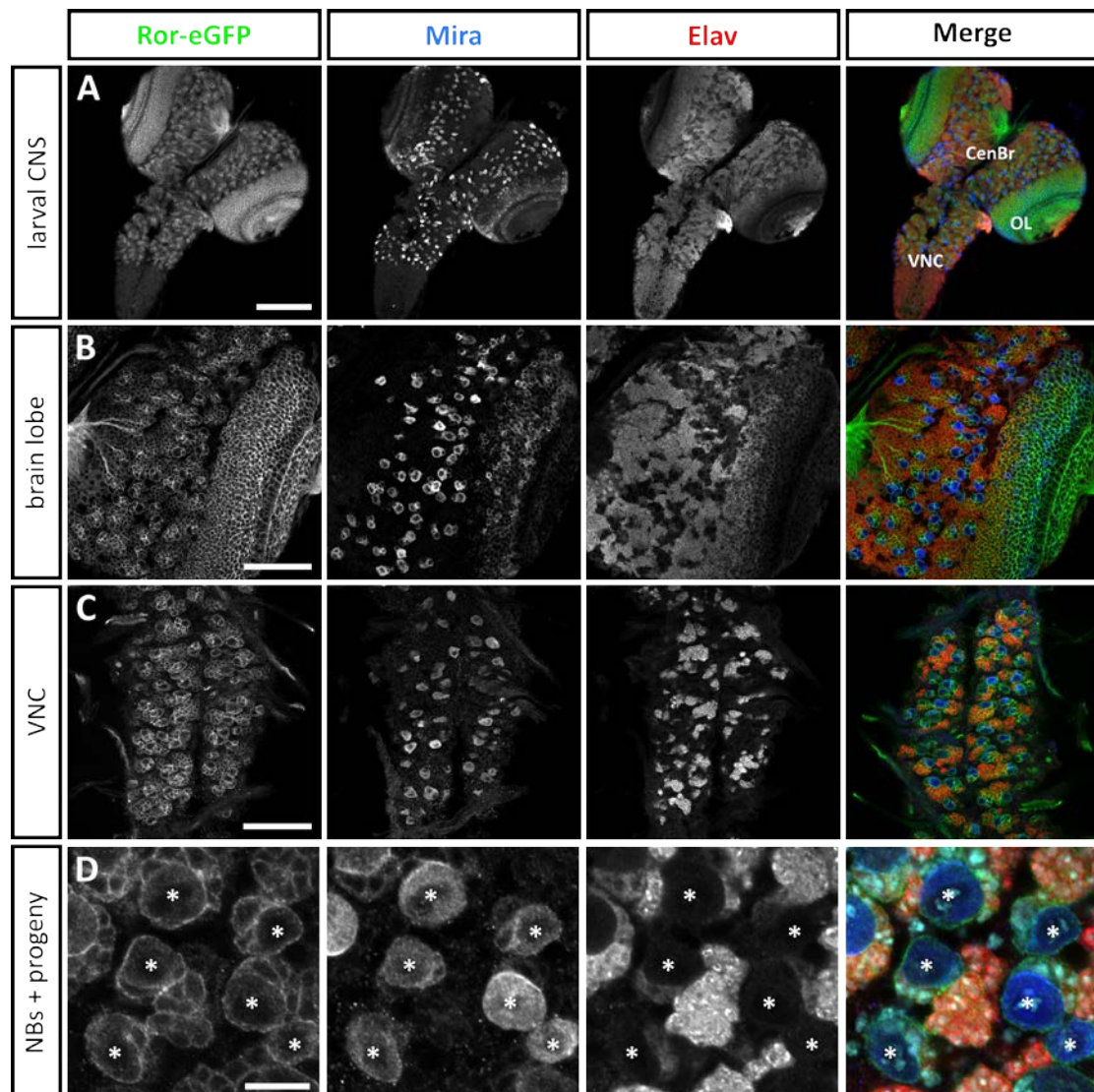


Figure 16: Ror-eGFP expression in the central nervous system of third instar larvae. (A) Overview of a larval central nervous system. Ror-eGFP is expressed in NBs and their neuronal progeny. (B) Larval brain lobe. (C) Larval ventral nerve cord. (D) Magnification of a section of a larval brain lobe including neuroblasts, neurons and most likely also GMCs. In D the Merge image additionally contains the Hoechst staining which labels the DNA. Scale bars: A =100µm; B/C = 50µm; D = 10µm. Abbreviations: CenBr: central brain; OL: optic lobe; VNC: ventral nerve cord; NB: neuroblast.

To investigate whether Ror-eGFP expression is restricted to neuronal cells, I additionally stained larval brains for the glial marker Repo (reversed polarity).

Figure 17 shows that while the protein is nicely visible in the membrane of all neuronal cells, it cannot be observed in the cell membrane of any glial cells (Figure 17 B, asterisks).

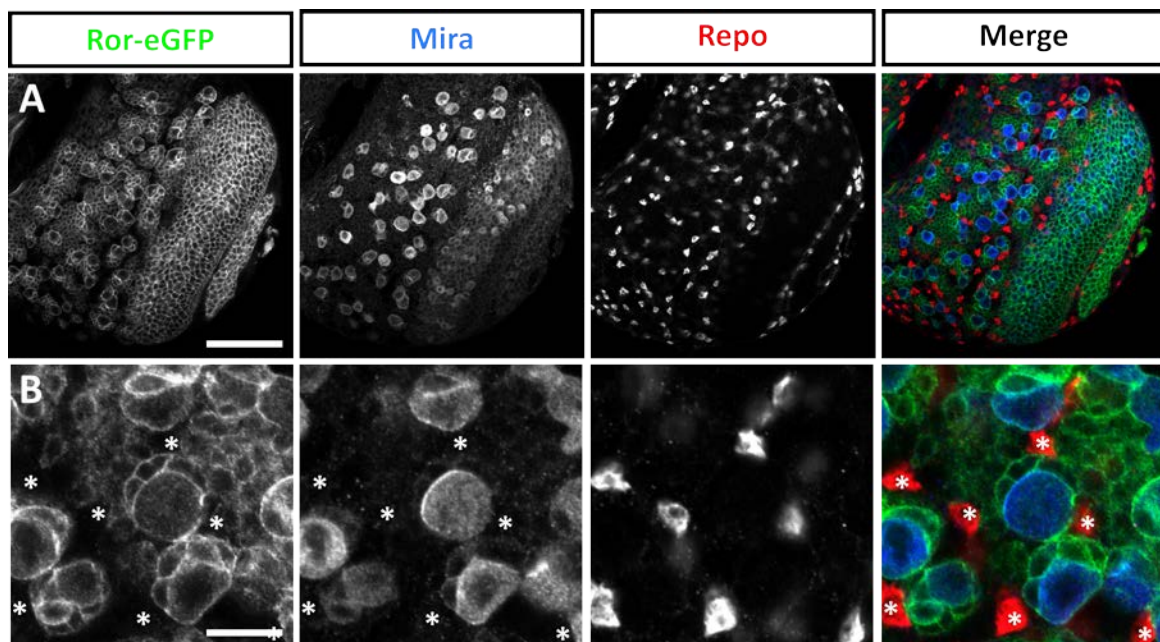


Figure 17: Ror-eGFP is not expressed in glial cells within the central nervous system of third instar larvae. (A) Overview of a larval brain lobe. **(B)** Higher magnification of the larval brain lobe, no Ror-eGFP signal can be seen in the membrane of glial cells. Scale bars: A = 50 μ m; B = 10 μ m.

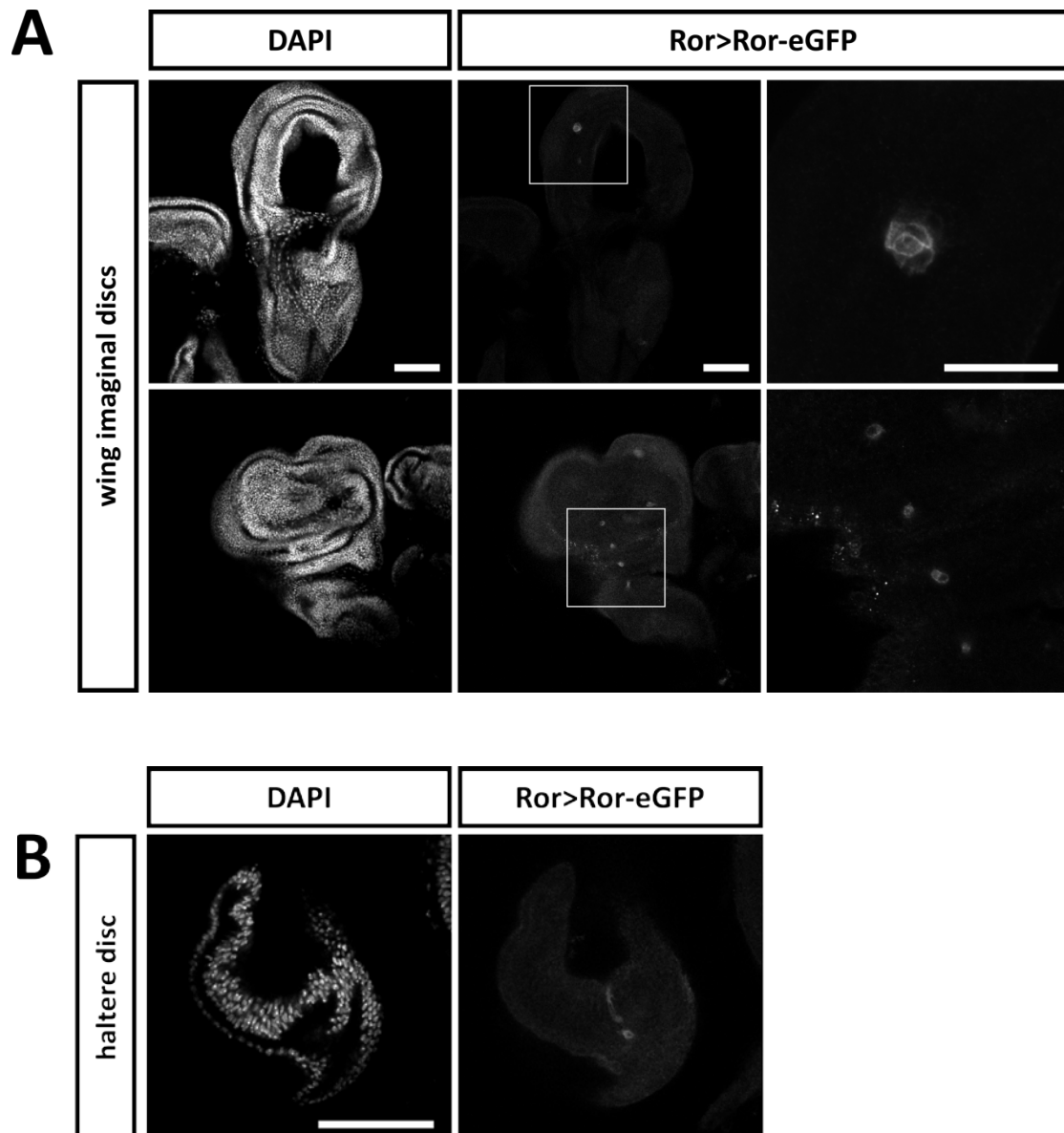
3.1.3 Ror-eGFP is expressed in larval imaginal discs

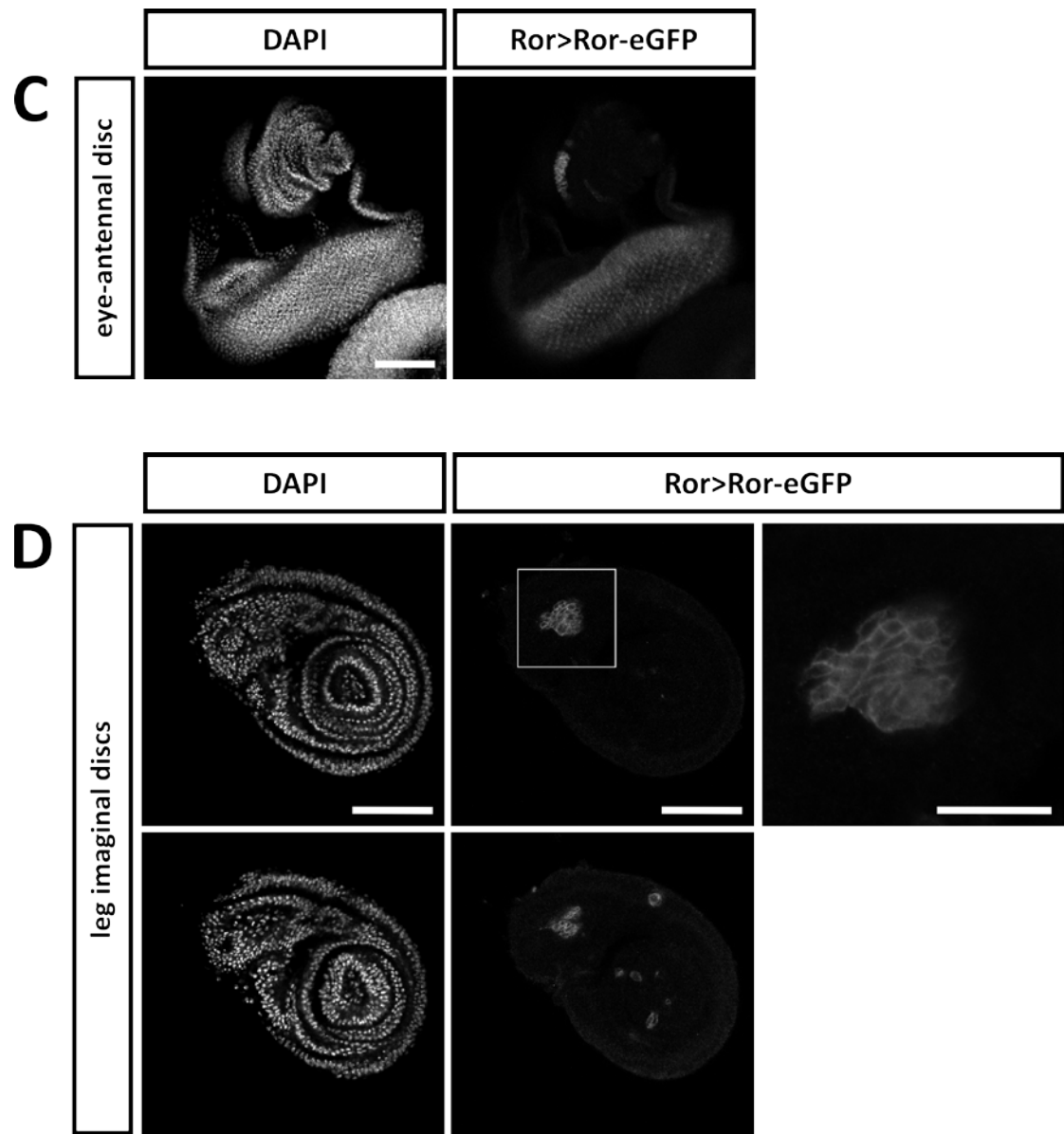
In third instar larvae, Ror-eGFP expression can also be found in imaginal discs. Imaginal discs are clusters of primordial cells already set-aside during embryogenesis which are precursors of the adult epidermal structures of head, thorax and external genitalia. During pupal metamorphosis, each disc differentiates into an adult appendage and the portion of body wall in which it resides. The wing imaginal disc for example develops into the adult wing and dorsal thorax while the eye-antennal imaginal disc develops into the adult eyes, antennae and head capsule including all bristles (Bate and Martinez-Arias, 1993).

I have analyzed Ror-eGFP expression in third instar wing discs, haltere discs, leg discs, eye-antennal discs and genital discs. In all these imaginal discs Ror-eGFP expression can be seen in a subset of cells. In wing imaginal discs the protein is visible in one cell cluster in a region of the disc corresponding to the adult ventral wing surface and in a row of smaller cell clusters along the proximal-distal axis of the disc (Figure 18 A). These cells likely represent proneural clusters or specified sensory organ precursor cells (SOPs). The Figure shows two separate wing imaginal discs in different stages of development. All cell clusters could be observed in both discs. In haltere imaginal discs, Ror-eGFP can be

Results

seen in several cells in the proximal part of the disc (Figure 18 B). In eye-antennal discs the protein is found in the developing photoreceptor cells and in the antennal portion of the eye-antennal disc. There, it is located in a cell cluster that might later account to sensory cells of the Johnston's organ, an auditory organ in the antenna (Figure 18 C). In leg imaginal discs Ror-eGFP is expressed in one bigger cell cluster probably representing sensory cells of the femoral chordotonal organ and in several smaller cell clusters within the disc (Figure 18 D). Ror-eGFP expression in genital discs, which later form the male and female terminalia (genitalia and analia) can be observed in four distinct cell clusters in both the female (Figure 18 E) and male genital disc (not shown).





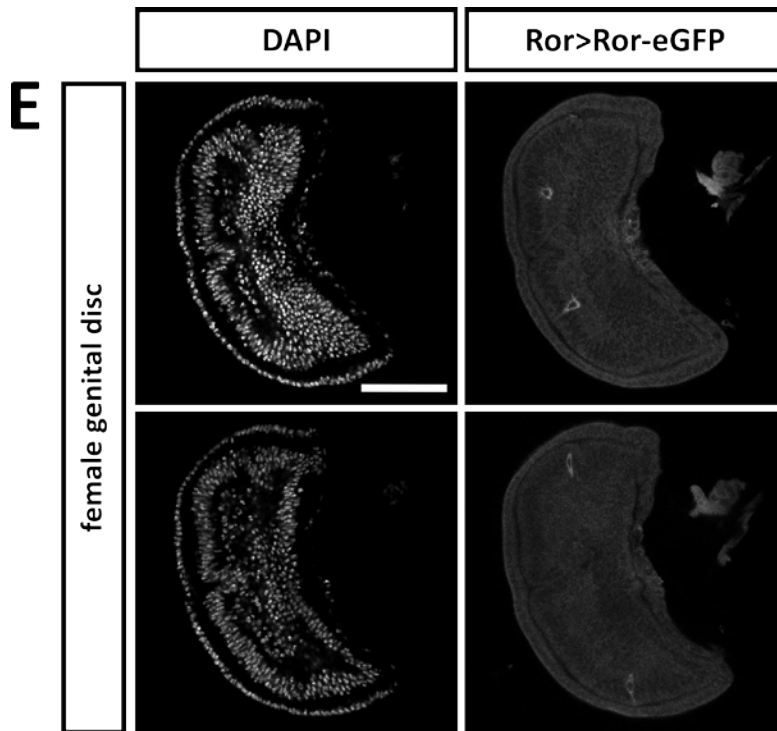


Figure 18: Ror-eGFP expression in third instar larval imaginal discs. The protein can be found in cell clusters within all analyzed imaginal discs. **(A)** Wing imaginal discs. Two different discs are shown, in each disc the expression in a different focal plane can be seen. **(B)** Haltere imaginal disc. **(C)** Eye-antennal imaginal disc. **(D)** Leg imaginal disc, two focal planes of the same imaginal disc are shown. **(E)** Female genital disc, two focal planes of the same imaginal disc are shown. Scale bars = 50 μ m; Scale bar in magnifications in A and D = 20 μ m.

3.2 Localization of Ror-eGFP is not affected in a *Wnt* mutant background

For Otk it has been shown that the expression of the protein is reduced within the central nervous system in embryos homozygous mutant for *Drosophila Wnt5* and greatly reduced in embryos homozygous mutant for *Drosophila Wnt2*. This indicates that Otk itself might be a target of Wnt signaling mediated by Wnt2 and Wnt5. Interestingly, this reduction has not been observed for expression of Otk2 (Linnemannstöns et al., 2014).

In order to analyze, whether the expression of Ror is also regulated by Wnt signaling, I crossed the Ror-eGFP transgene into several *Drosophila Wnt* mutant lines and compared the GFP expression in homozygous mutant embryos. It seems that the absence of neither Wg, nor Wnt2, Wnt4 or Wnt5 has any influence on the expression of Ror. While the reduction of Otk in the ventral nerve cord can be confirmed in homozygous *Wnt2* mutants (Figure 19 B), the Ror-eGFP signal is consistently strong in all analyzed *Wnt* mutant lines (Figure 19). While the morphology of the homozygous *wg^{CX4}* mutant

Results

embryo is so severely disturbed that the developmental stage cannot be determined, the Ror-eGFP signal in the central nervous system can clearly be identified (Figure 19 A).

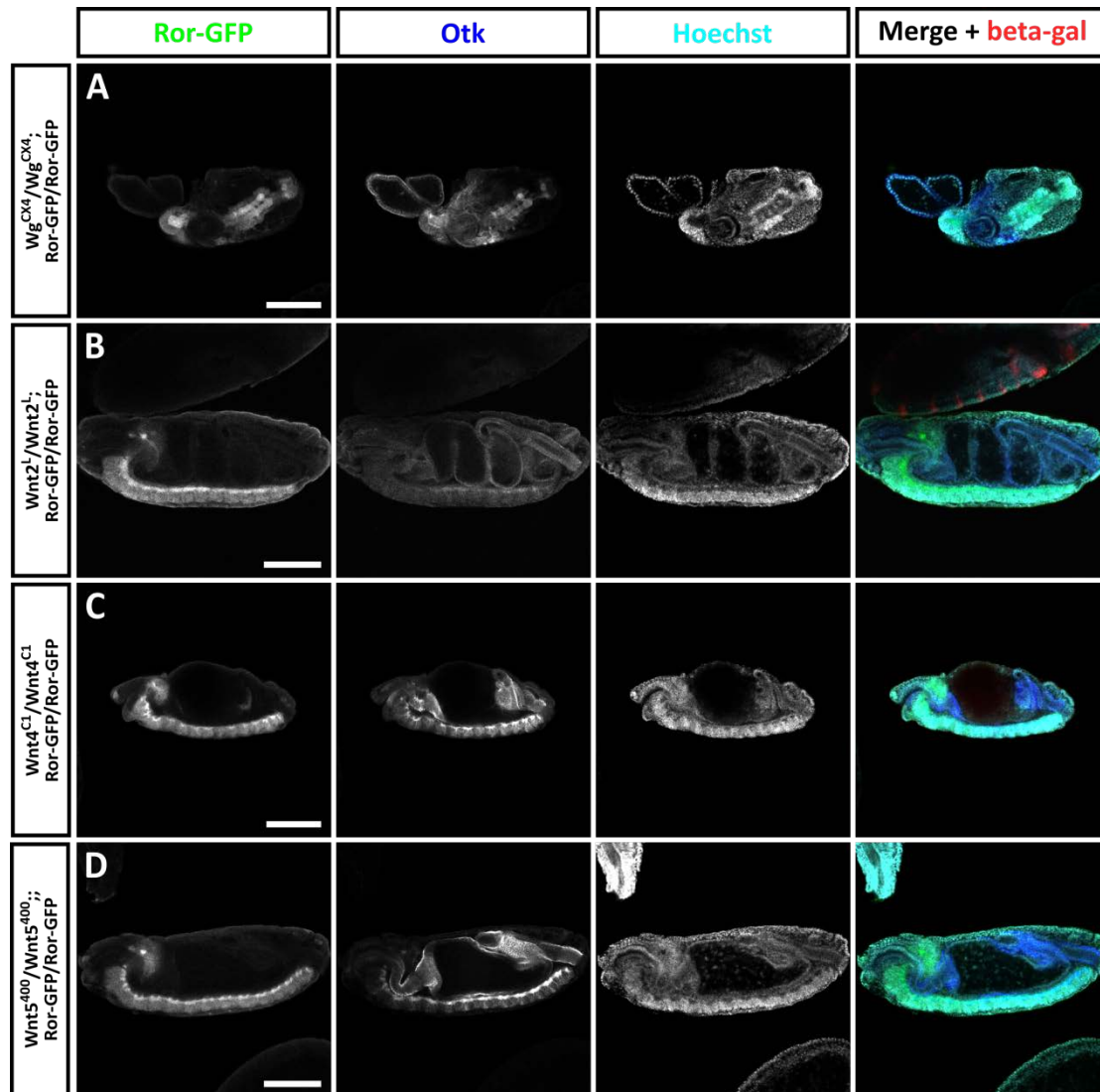


Figure 19: The expression of Ror-eGFP is not reduced in homozygous *Wnt* mutant embryos. Embryos were stained for GFP, Otk and β -galactosidase, which labels the balancer chromosome in heterozygous *Wnt* mutants. **(A)** Homozygous *Wg* mutant embryo. **(B)** Homozygous *Wnt2* mutant embryo, stage 16. **(C)** Homozygous *Wnt4* mutant embryo, stage 14. **(D)** Homozygous stage 15 embryo mutant for *Wnt5*. Anterior is to the left, the dorsal side is up. Scale bars = 100 μ m.

3.3 Generation of a null allele for *Ror*

In vertebrates, Ror proteins have been shown to play a role in many processes during development, including skeletal and neuronal development. To investigate the function of *Drosophila* Ror during development, I have generated a null allele for *Ror* via

Results

imprecise P-element excision. The P-element P{EP}G8235 is located 29 bp upstream of the *Ror* 5'UTR. Through crossing the P-element line with a fly line expressing P transposase, the P-element was mobilized. I established 936 excision lines, all selected by the absence of the *mini-white* gene. These lines were then screened via two PCRs with one primer each in the genomic region of *Ror* and the second primer binding to the inverted repeats within the P-element (Figure 20 A). The fly line termed *Ror*^{E267} has been identified as a fly line in which the P-element has been excised imprecisely and most likely removed part of the *Ror* locus. The region located upstream of the P-element is still intact, while the PCR fragment downstream of the P-element location cannot be amplified anymore (Figure 20).

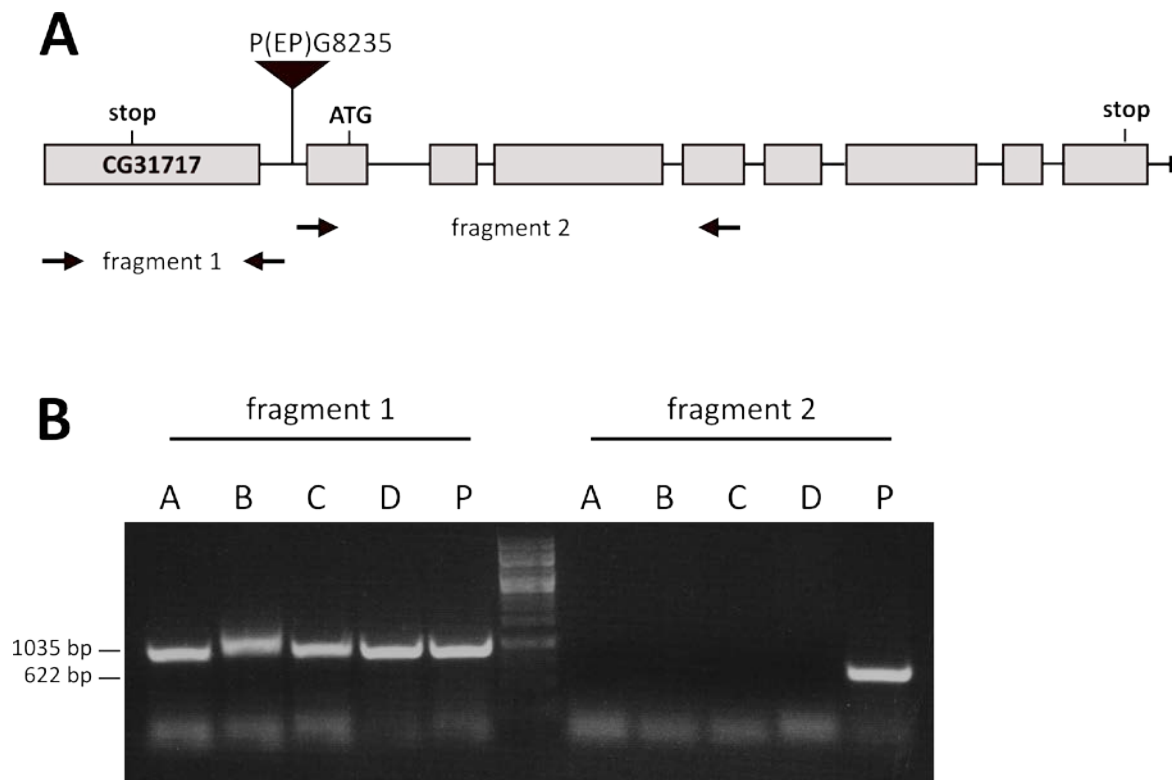


Figure 20: The *Ror* allele *Ror*^{E267} was generated via imprecise excision of a P-element. (A) The P-element P{EP}G8235 was mobilized by P-transposase and together with part of the P-element itself, very likely a section of the genomic *Ror* locus was removed. **(B)** Gel picture from screening via PCR. A-D represent four single *Ror*^{E267} flies. In these flies the region upstream of the P-element is still intact (fragment 1), while the region downstream could not be amplified because it has been excised (fragment 2). As positive control (P) the P-element line P{EP}G8235 was used.

3.4 Characterization of the *Ror* null allele *Ror*⁴

Due to problems in the process of verifying which parts of the *Ror* gene were excised in the *Ror*^{E267} allele and the limited time frame of this study, a different *Ror* allele was used for all phenotypic analyses in this study. This allele, termed *Ror*⁴ was generously provided by the group of Jasprien Noordermeer from the Leiden University Medical Center. The *Ror*⁴ fly line was generated by letting the P-element P{GSV3}GS8107 (located in the *Ror* 5'UTR) integrate into the coding region of *Ror*(P{GSV3}GS8107-Hop), followed by transposase-mediated excision of the genomic region present in between the two P-elements. With this approach, 1045 bp have been removed including the *Ror* start codon and most of the first three exons (Figure 21). Due to the lack of the start codon, the generated fly line likely represents a null allele. *Ror*⁴ mutant flies are homozygous viable and fertile.

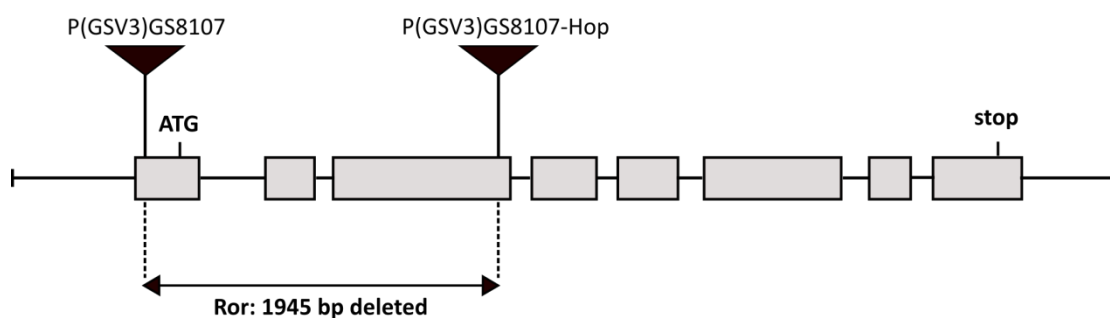


Figure 21: The *Ror* allele *Ror*⁴ was generated via transdeletion between two P-elements. The P-element P{GSV3}GS8107 was first mobilized using P-transposase and re-integrated into the third exon of the *Ror* coding region. Then the region between the two P-elements was excised in a second transposase-mediated step.

3.4.1 The absence of *Ror* alone has no effect on viability but many *Ror*, *otk*, *otk2* triple mutants do not develop into adulthood

In a co-immunoprecipitation experiment (see 3.6.1) I have observed that *Drosophila* *Ror* is binding to *Otk* and *Otk2*, which are likewise Wnt co-receptors and have been shown to act together in genital tract development (Linnemannstöns et al., 2014). The possibility exists that *Ror*, *Otk* and *Otk2* all function together in some aspects of *Drosophila* development. To be able to analyze the developmental function of *Ror* alone as well as a

Results

possible combined function of Ror with Otk and Otk2, I have recombined the *Ror*⁴ allele together with the male sterile *otk*, *otk2* double mutant allele *Df(otk,otk2)D72* (Linnemannstöns et al., 2014). This resulting *Ror*, *otk*, *otk2* triple mutant allele was termed *Ror*⁴, *Df(otk,otk2)D72*.

In order to analyze if the absence of Ror alone or Ror, Otk and Otk2 all together leads to defects that cause a decrease in viability, I have performed lethality tests with homozygous embryos of the *Ror*⁴ single mutant and the *Ror*⁴, *Df(otk,otk2)D72* triple mutant. Homozygous embryos of the *Df(otk,otk2)D72* double mutant fly line and wild type (*white*⁻) embryos were used as controls. The average hatching rate of *Df(otk,otk2)D72* embryos is comparable to the wild type control. When compared to the wild type, homozygous *Ror*⁴ mutant embryos display a significantly increased embryonic lethality. However, when compared to *otk*, *otk2* double mutants, the difference is not statistically relevant. The embryonic viability of homozygous *Ror*, *otk*, *otk2* triple mutants was very significantly reduced when compared to all three other lines tested (Figure 22).

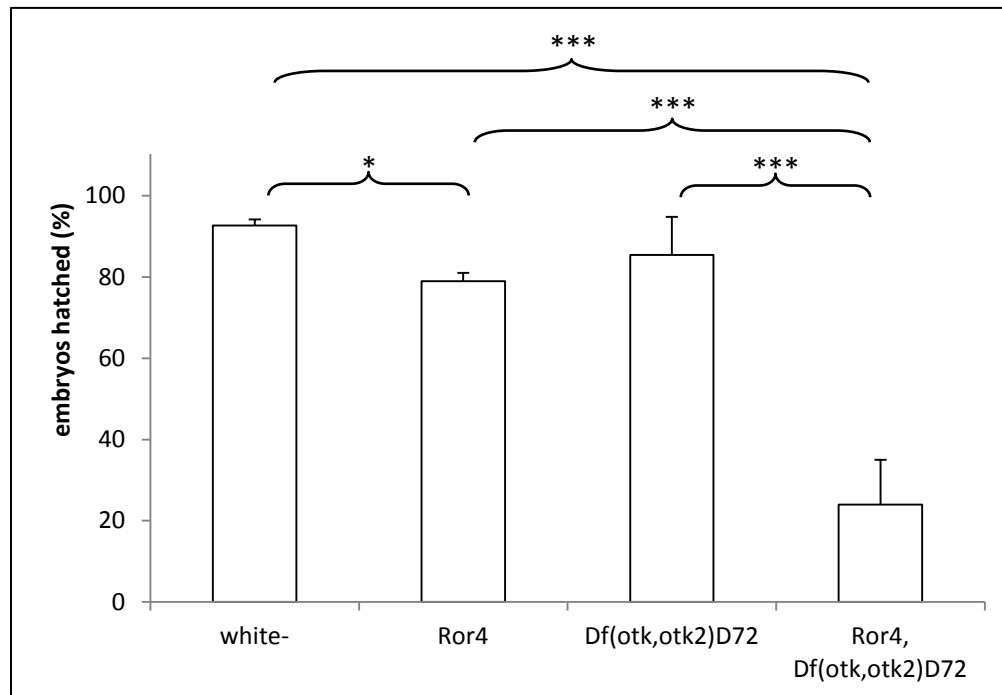


Figure 22: Embryonic viability of *Ror* mutants and *Ror*, *otk*, *otk2* triple mutants compared to wild type and homozygous *otk*, *otk2* double mutants. Homozygous *Ror*⁴ embryos show an increased embryonic lethality when compared to *white*⁻ embryos. Homozygous triple mutants displayed a significant increase in embryonic lethality, on average only 24 % of embryos hatch. Data were obtained by repeating each experiment at least three times. The error bars represent the standard deviation. *: p-value < 0.05; ***: p-value < 0.001.

Results

For the lethality tests, embryos laid by heterozygous flies were sorted by fluorescence of the balancer after aging for 8 h at 25 °C. Typically, the chorion was not removed. A more detailed analysis of the homozygous *Ror*⁴, *Df(otk,otk2)D72* triple mutant embryos which did not hatch revealed that 67 % of unhatched embryos already appear to be dead at the time of their alignment on the agar plate. This fact could only be observed after removing the chorion and it was not possible to remove these eggs prior to the alignment in any of the performed viability tests. The appearance of these eggs resembled unfertilized eggs, indicating that flies mutant for *Ror*, *otk* and *otk2* lay a higher amount of unfertilized eggs than other flies. Since the number of unhatched homozygous embryos is not increased in flies homozygous for only *otk* and *otk2*, this fact cannot be attributed to the existence of sterile male flies in this line. If these unfertilized eggs were taken out of the calculation, the percentaged lethality of homozygous *Ror*⁴, *Df(otk,otk2)D72* triple mutant embryos would only amount to 25 %. Included in these 25 % are 14 % of embryos, which completed embryonic development but failed to hatch. In summary, the general viability of the homozygous triple mutants seems to be affected. In addition to the embryonic lethality rate, I have also analyzed the number of adult flies, which developed from the hatched embryos. Only 27 % of the hatched homozygous triple mutant embryos developed to adulthood, compared to 68 % of the homozygous *otk*, *otk2* double mutants, 70 % of homozygous *Ror*⁴ embryos and 86 % in the wild type control (data not shown).

3.4.2 The embryonic nervous system of homozygous *Ror*⁴ embryos displays a mild CNS phenotype

During embryonic and larval development *Drosophila* *Ror* is primarily expressed in the nervous system. Within the central nervous system, the protein is found in all neuronal cells and in all axonal projections. In the peripheral nervous system it can be found at the membrane of all neurons including the sensory axons (see 3.1). Although the expression pattern of *Ror* is not identical to *Otk* and *Otk2*, they can both also be found in the larval central nervous system as well as in the larval brain. However, the morphology of the nervous system in *otk*, *otk2* double mutants is not affected and homozygous flies are

Results

viable (Linnemannstöns et al., 2014). To analyze if the loss of *Ror* alone or of *Ror*, *otk* and *otk2* together has any effect on the development of the embryonic CNS, I have stained homozygous embryos of the respective mutant lines for the CNS axon marker BP102, for Fasciclin II which marks a subset of CNS axons and for Repo to visualize glial cells. After staining, fillet preparations of the CNS of stage 17 embryos were prepared.

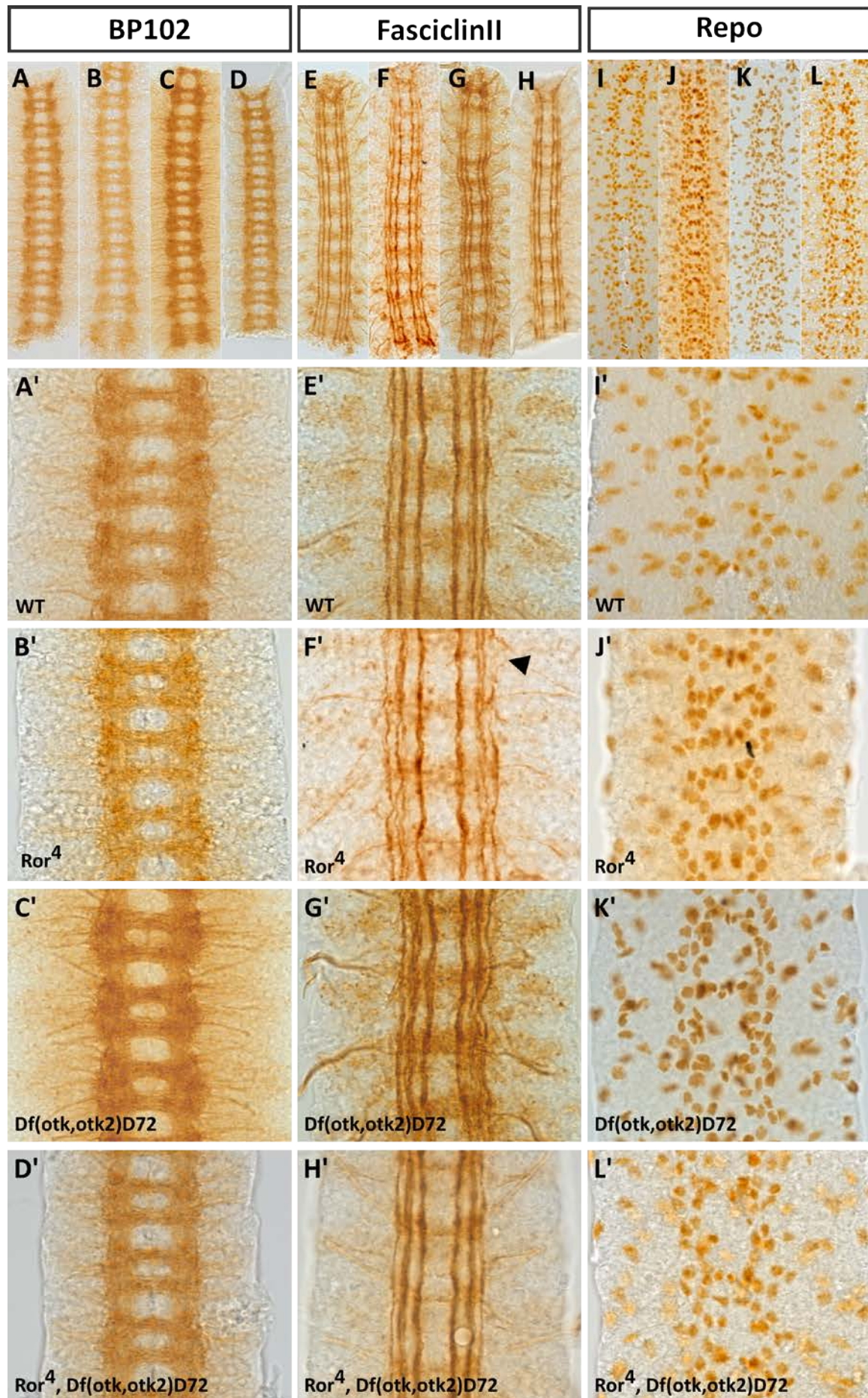
The CNS axon tracts visualized by BP102 in all analyzed mutant nervous systems resembled the wild type. The neuronal processes forming the longitudinal connectives are intact and the anterior and posterior commissures were separated from each other (Figure 23 A-D').

In stage 16/17 embryos, Fasciclin II labels three longitudinal axon bundles, termed fascicles. In wild type and homozygous *Ror*⁴, *Df(otk,otk2)D72* embryos, all three fascicles were well formed and intact (Figure 23 A/A', H/H'). In homozygous *Ror*⁴ embryos every now and then discontinuities in the outermost lateral fascicle were visible (Figure 23 F', arrowhead). However, a detailed analysis of the number of segments in which disrupted fascicles were observed showed that the difference to wild type embryos is not statistically relevant (Figure 24). A closer look at the three fascicles in the *Ror*⁴ embryos revealed that some axons appear wavy and it seems as if not all axons are tightly fasciculated into the bundle (Figure 23 F'). Many *Df(otk,otk2)D72* nervous systems display a similar phenotype. While axons not incorporated into the fascicle are not so frequent, many fascicles are wavy (Figure 23 G'). Surprisingly, most homozygous *Ror*⁴, *Df(otk,otk2)D72* embryos exhibit no axons outside of the bundles and the fascicles themselves are straightly formed (Figure 23 H'). However, some homozygous triple mutant embryos display a more severe CNS phenotype than the *Ror* single mutant. In these samples, the outermost lateral fascicle is disrupted in every segment (Figure 23 M, arrowheads). The remaining fascicles also appear somewhat wavy and unorganized.

The differentiation and maintenance of glial cells is not disturbed in all analyzed mutants. I have not observed any lack or misplacement of glial cells and the pattern in the mutants is comparable to the wild type.

Taken altogether it appears as if *Ror*⁴ mutant embryos and homozygous *Df(otk,otk2)D72* embryos both display a mild axon guidance or fasciculation phenotype.

Results



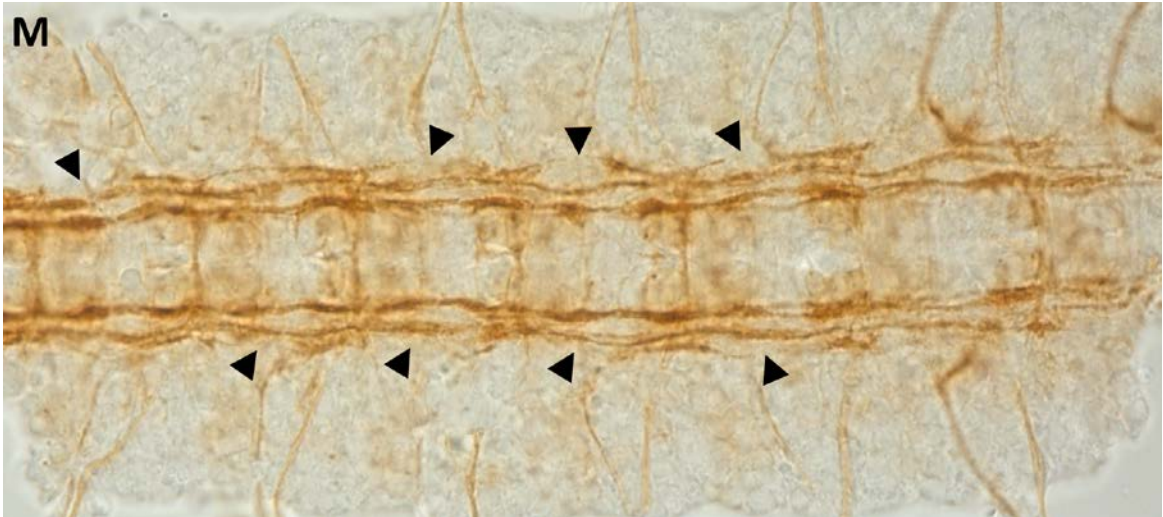


Figure 23: The morphology of the ventral nerve cord in wild type embryos compared to *Ror*, *otk* and *otk2* mutants. (A-D) Axon tracts of the CNS are visualized using the BP102 antibody in wt (A), *Ror*⁴ (B), *Df(otk,otk2)D72* (C) and *Ror*⁴,*Df(otk,otk2)D72* (D) embryos. All mutant embryos resemble the wild type. (E-H) Fasciclin II labels the axons of a subset of neurons within the CNS. In *Ror*⁴ embryos the fascicles have a wavy appearance, and some axons are not tightly incorporated into the fascicles. Some disruptions in the lateral fascicle are also visible (arrowhead); in *otk*, *otk2* double mutants the fascicles appear wavy as well and in *Ror*, *otk*, *otk2* triple mutants all fascicles are intact. (I-L) Glial cells visualized with the anti-Repo antibody. The pattern is not disturbed in any of the investigated mutants. Images A'-L' are magnifications of sections in the images A-L. All images show three abdominal segments of late stage embryos; anterior is up. (M) Some *Ror*, *otk*, *otk2* triple mutant embryos exhibit a stronger CNS phenotype. The lateral fascicle display many breaks (arrowheads).

As mentioned above, the nervous systems of a small amount of homozygous *Ror*⁴, *Df(otk,otk2)D72* triple mutant embryos appear to have an increased number of disrupted fascicles, while the morphology of the other nervous systems was comparable to wild type nervous systems (Figure 23 M). This fact is visible as the high standard error bar in Figure 24. It is possible that these noticeable nervous systems are from embryos mistakenly dissected at an earlier developmental stage or that they are the nervous systems of fully developed but unhatched embryos (mentioned above). The latter would indicate that at least a small percentage of *Ror*, *otk*, *otk2* triple mutant embryos display a lethal phenotype associated with defects in CNS development.

Results

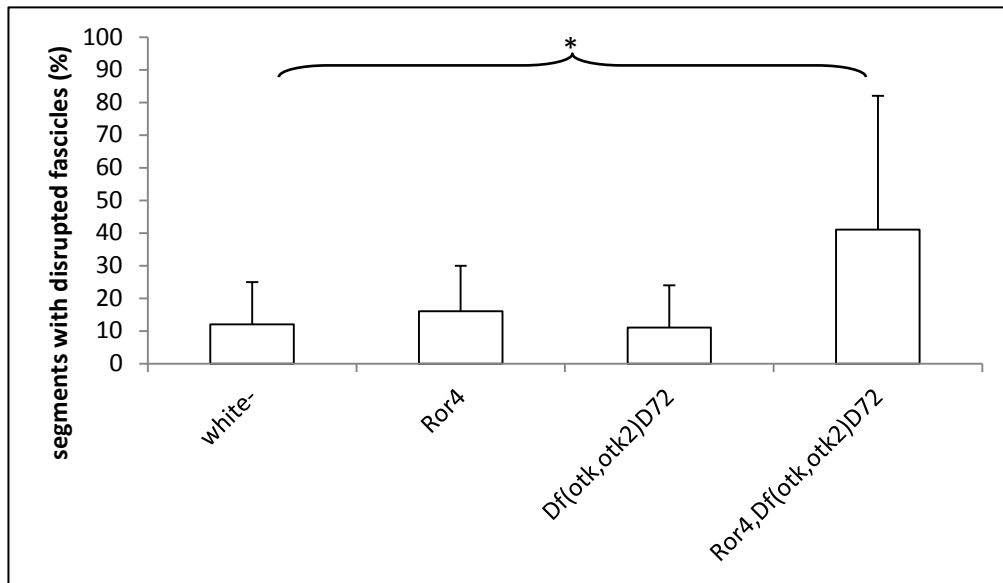


Figure 24: The number of CNS segments with disrupted fascicles in *Ror* and *otk,otk2* mutant embryos is not statistically relevant. In stage 17 *Ror*⁴ mutant embryos the percentage of segments with disrupted fascicles is comparable to the number observed in *white*⁻ and in homozygous *Df(otk,otk2)D72* mutant embryos. In homozygous *Ror*⁴,*Df(otk,otk2)D72* triple mutant embryos, some nervous systems display an increased number of disrupted fascicles. Number of analyzed segments: *white*⁻: n = 105; *Ror*⁴: n = 101; *Df(otk,otk2)D72*: n = 48; *Ror*⁴,*Df(otk,otk2)D72*: n = 47. *: p-value < 0.05.

I have also analyzed the peripheral nervous system of *Ror*⁴ mutants for any defects. For this reason I stained homozygous *Ror*⁴ embryos for the PNS marker 22C10 (Futsch). This marker visualizes all PNS neurons. There are three clusters on the lateral side of the embryo, the dorsal cluster, the lateral cluster and the ventral cluster. The PNS of *Ror* mutant embryos is normally developed. All clusters of neurons are present and axons grow into the CNS as usual (Figure 25).

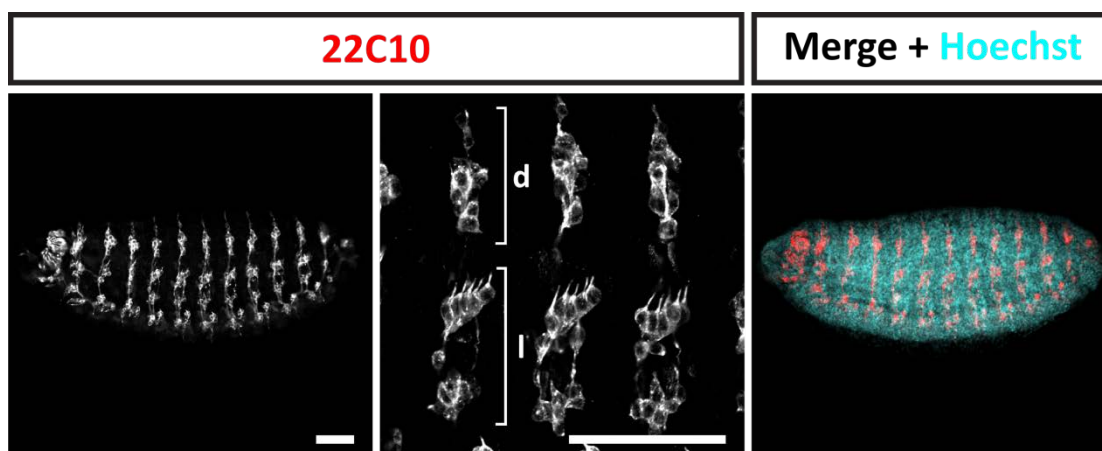


Figure 25: The PNS in *Ror*⁴ mutant embryos is not affected. Stage 17 homozygous *Ror*⁴ embryo stained with 22C10 (Futsch) to reveal the peripheral nervous system. The dorsal cluster (d) and the lateral cluster (l) are shown in a higher magnification. Anterior is to the left, Scale bars = 50 µm.

3.4.3 Adult *Ror*⁴ mutant flies display no obvious defects in planar cell polarity

In mice, the absence of Ror proteins leads to developmental defects dependent on morphogenetic movements (Ho et al., 2012) and classical planar cell polarity (PCP) phenotypes in the cochlea (Yamamoto et al., 2008). Similar effects have been shown in other model organisms. In *Xenopus* for instance, Xror2 is required for convergent extension movements during embryogenesis (Hikasa et al., 2002). This indicates that PCP and convergent extension movements are regulated by Wnt signaling mediated through Ror proteins. While Otk and Otk2 seem to have no function in establishing planar cell polarity (Linnemannstöns et al., 2014), their vertebrate homolog PTK7 has been shown to be involved in PCP signaling in several organisms including mouse, *Xenopus* and zebrafish (Lu et al., 2004; Hayes et al., 2013).

To address whether *Drosophila* Ror plays a role in PCP signaling, I have examined adult mutant flies for PCP defects. One of the planar polarized tissues in *Drosophila* is the eye. Each ommatidium is composed of eight photoreceptor cells, two inner and six outer photoreceptor cells. In sections, these cells resemble the shape of an arrowhead. All the ommatidia in the dorsal half of the eye point dorsally and in the ventral half they all point to the ventral side (Figure 26 A). When this D-V polarity is disturbed, the ommatidia are not oriented in the same direction anymore (Axelrod and McNeill, 2002; Zallen, 2007). In all analyzed mutants, the organization of ommatidia was not disturbed. The ommatidia in the eyes of homozygous *Ror*⁴ mutant flies, *Df(otk,otk2)D72* double mutants and *Ror*⁴, *Df(otk,otk2)D72* triple mutants all form arrow-like shapes that point in the same direction and therefore resemble the wild type (Figure 26 B-E).

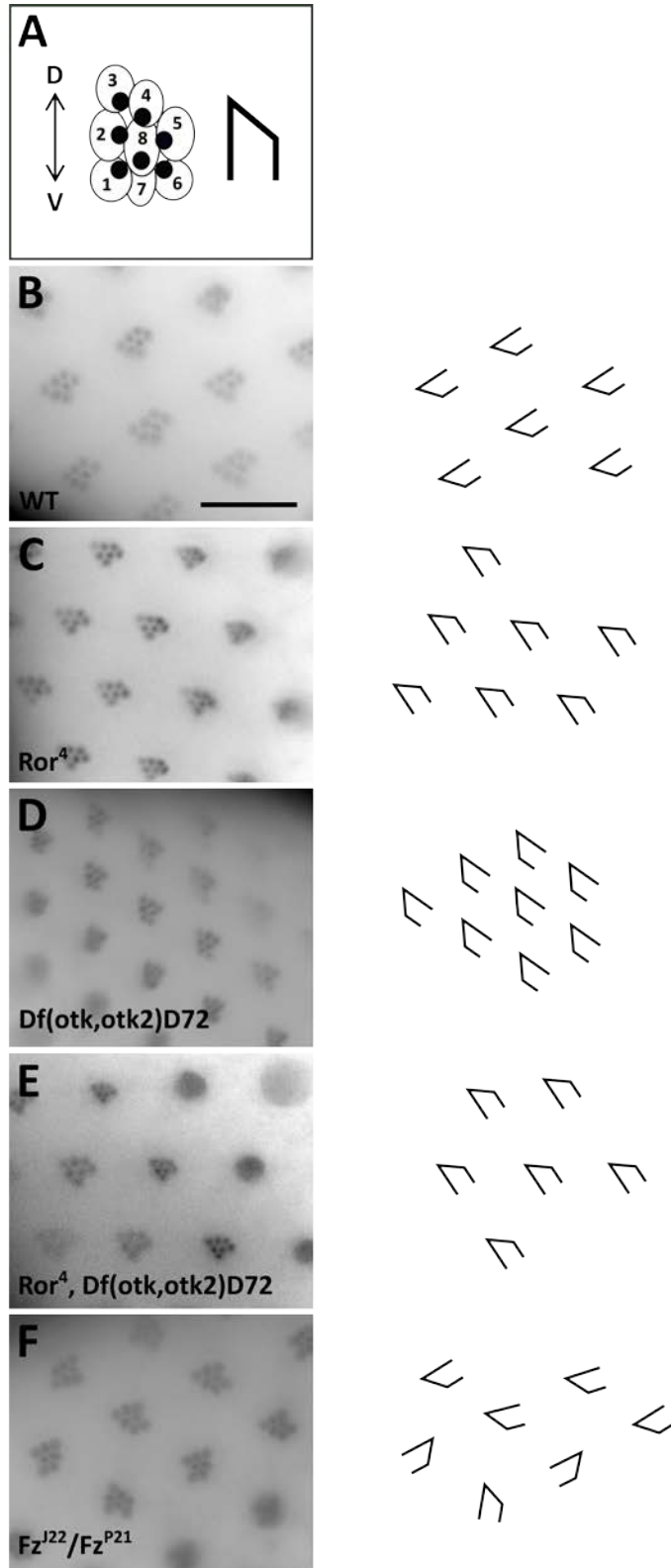


Figure 26: Planar cell polarity in *Ror* mutant eyes is not disturbed. (A) Schematic representation of a *Drosophila* ommatidium. Each ommatidium is formed by 8 photoreceptor cells. In a cross section only one, the S7 or the S8 cell are visible since they are located on top of each other. The visible cells resemble an arrowhead. Ommatidia in the dorsal part of the eye point dorsally. (B) Wild type ommatidia. (C) *Ror⁴* mutant eye (D) *Otk* and *otk2* double mutant *Df(otk,otk2)D72*. (E) Triple mutant *Ror⁴, Df(otk,otk2)D72*. (F) *Fz^{J22}/Fz^{P21}* eye as positive control, the polarity of the ommatidia is disturbed, all arrow-like shapes point in different directions. Scale bar = 1000 μm.

Another planar polarized tissue is the *Drosophila* wing. Here, the planar polarity is evident on the hairs secreted by every cell that all point distally. In the wing, defects in PCP can be easily recognized by disorganization of these hairs (Axelrod and McNeill, 2002; Zallen, 2007). None of the analyzed mutant flies displayed any defect in PCP in the wing. In *Ror*⁴ mutant flies, *Df(otk,otk2)D72* double mutants and *Ror*⁴, *Df(otk,otk2)D72* triple mutants, all wing hairs point in the same direction (Figure 27). The same observation accounts for the bristles on the thorax (data not shown). In contrast to other model organisms, *Drosophila* Ror does not seem to play a role in the establishment of planar cell polarity.

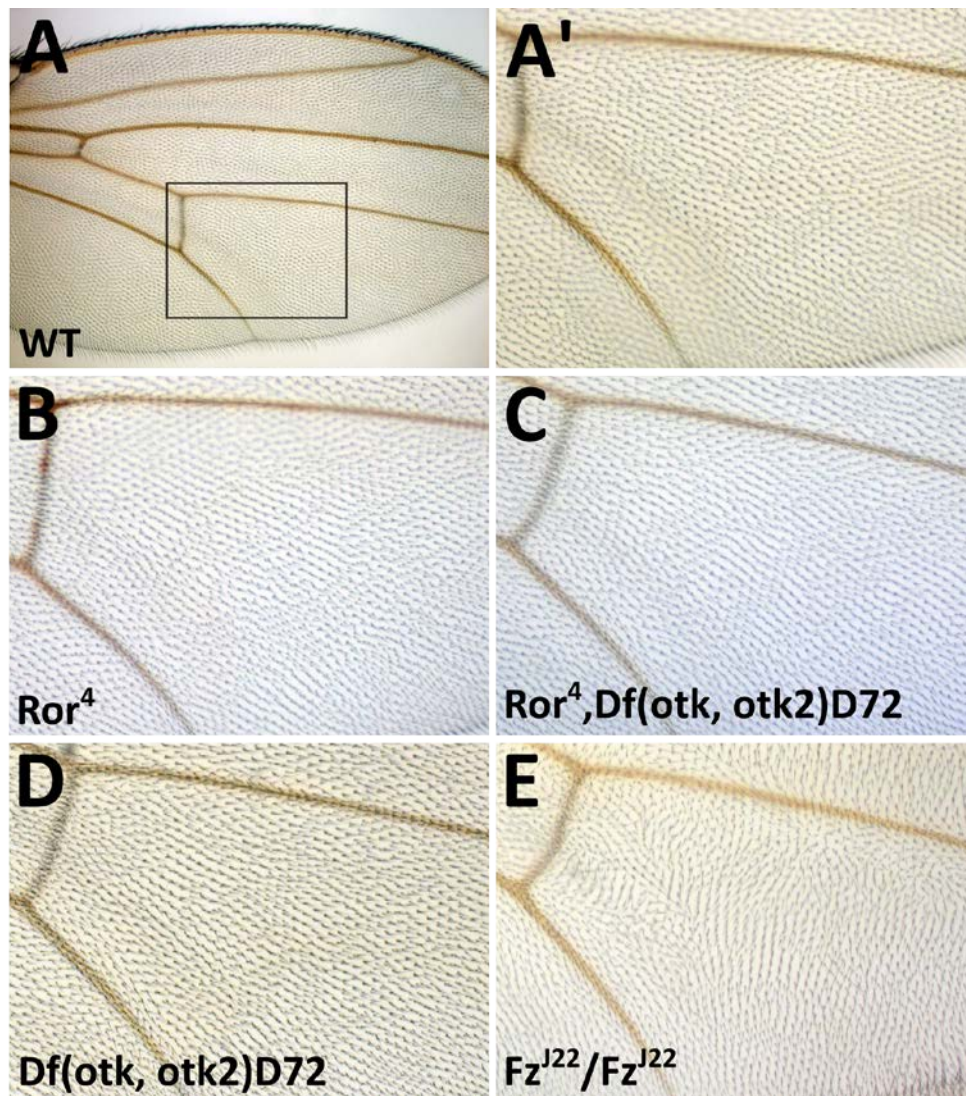


Figure 27: Planar cell polarity in *Ror* mutant wings is not disturbed. The hairs on the wings of all mutants point to the same direction. **(A)** Overview of a *Drosophila* wing. **(A')** Magnification of a wild type wing. **(B)** *Ror*⁴ mutant wing. **(C)** Triple mutant *Ror*⁴, *Df(otk,otk2)D72*. **(D)** *Otk* and *otk2* double mutant *Df(otk,otk2)D72*. **(E)** *Fz*^{J22}/*Fz*^{J22} wing as positive control.

3.5 Ror interacts with members of the Wnt pathways

3.5.1 Ror genetically interacts with the ligand Wnt5

In a first approach to identify the pathway or biological process in which Ror is involved, I have analyzed genetic interactions of *Ror*⁴ with alleles for *fz*, *fz2*, *otk*, *otk2* and *wnt5*. Through the analysis of genetic interactions it is possible to find functional relationships between genes and pathways. For instance, when the double mutant of two genes is showing a more severe phenotype than the two single mutants alone, functional redundancies can be identified. This indicates an *in vivo* relationship between the two proteins.

I have crossed *Ror*⁴ flies together with mutants for *fz*, *fz2*, *otk*, *otk2* and *wnt5* and analyzed their adult progeny for severity of phenotypes and viability. From each allelic combination I have analyzed flies heterozygous for both mutant alleles, flies homozygous for *Ror*⁴ and heterozygous for the second mutation, as well as flies homozygous for both. For *fz* and *fz2* I have additionally analyzed *Ror*⁴ in transheterozygous flies carrying two different alleles for *fz* or *fz2* above each other.

Homozygous *fz*¹²² flies are viable but display PCP defects in eyes, wings and body, the other two tested *fz* alleles are homozygous lethal. Transheterozygous flies for all three allele combinations are also viable with PCP defects. I did not detect any genetic interactions of *Ror*⁴ with *fz* (Table 9). Both *fz2* alleles I used are homozygous lethal, transheterozygous animals are viable and display no PCP defects. However, they are male and female sterile. For *fz2* I did not observe any genetic interactions either.

Flies homozygous mutant for *Wnt5* are viable but display defects in the central nervous system (Fradkin et al., 2004). When additionally removing one copy of *Ror*, this phenotype is not enhanced and the flies are also viable. Only when both copies of *Ror* are missing it is lethal (Table 9). I have analyzed the CNS of late stage *Wnt5*⁴⁰⁰/*Wnt5*⁴⁰⁰; *Ror*⁴/*Ror*⁴ embryos for defects and did not detect a more severe phenotype than in *Wnt5*⁴⁰⁰/*Wnt5*⁴⁰⁰ embryos (data not shown). A lethality test confirmed that the lethality is not embryonic but occurs soon after hatching in the first larval stage (data not shown). Flies homozygous mutant for the *otk* and *otk2* single mutations are viable without any discernible phenotype, double mutants for *otk* and *otk2* are male sterile

Results

(Linnemannstöns et al., 2014). Double mutants for *Ror* and *otk* or *Ror* and *otk2* are viable and fertile. Homozygous flies mutant for all three genes are naturally also male sterile but as demonstrated above, the weak CNS defect observed in *Ror*⁴ embryos cannot be observed (3.4.2). Interestingly, these flies lay an increased number of unfertilized eggs (3.4.1).

In conclusion, I have not observed any functional relationship between *Ror* and *fz*, *fz2*, *otk* or *otk2*. It seems however, that there is a synthetic genetic interaction between *Ror* and *Wnt5*, indicating that the two proteins possibly have a common function during larval or pupal development.

Due to the limited time frame of this study, genetic interactions of *Ror* with the Wnt ligands *Wingless*, *Wnt2* and *Wnt4*, which are all located on the second chromosome as well, were not analyzed. The recombinations between the *Ror*⁴ allele and the single mutants *otk*^{A1} and *otk2*^{C26}, respectively were performed by Dr. Karen Linnemannstöns.

Table 9: *Ror* genetically interacts with *Wnt5*. Genetic interactions of the *Ror*⁴ allele with three *fz* alleles, two *fz2* alleles, single and double mutant alleles for *otk* and *otk2* and one *Wnt5* allele were tested.

Genotype	Viability/Phenotype
<i>Ror</i> ⁴ / <i>Ror</i> ⁴	viable
<i>fz</i> ^{J22} / <i>fz</i> ^{J22}	viable with PCP defects
<i>Ror</i> ⁴ /CyO; <i>fz</i> ^{J22} /TM6	viable
<i>Ror</i> ⁴ / <i>Ror</i> ⁴ ; <i>fz</i> ^{J22} /TM6	viable
<i>Ror</i> ⁴ /CyO; <i>fz</i> ^{J22} / <i>fz</i> ^{J22}	viable with PCP defects
<i>Ror</i> ⁴ / <i>Ror</i> ⁴ ; <i>fz</i> ^{J22} / <i>fz</i> ^{J22} (zygotic)	viable with PCP defects
<i>Ror</i> ⁴ / <i>Ror</i> ⁴ ; <i>fz</i> ^{J22} / <i>fz</i> ^{J22} (maternal)	viable with PCP defects
<i>fz</i> ^{R52} / <i>fz</i> ^{R52}	lethal
<i>Ror</i> ⁴ /CyO; <i>fz</i> ^{R52} /TM6	viable
<i>Ror</i> ⁴ / <i>Ror</i> ⁴ ; <i>fz</i> ^{R52} /TM6	viable
<i>Ror</i> ⁴ /CyO; <i>fz</i> ^{R52} / <i>fz</i> ^{R52}	lethal
<i>Ror</i> ⁴ / <i>Ror</i> ⁴ ; <i>fz</i> ^{R52} / <i>fz</i> ^{R52} (zygotic)	lethal
<i>Ror</i> ⁴ / <i>Ror</i> ⁴ ; <i>fz</i> ^{R52} / <i>fz</i> ^{R52} (maternal)	lethal

Results

fz^{P21}/fz^{P21}	lethal
$Ror^4/CyO; fz^{P21}/TM6$	viable
$Ror^4/Ror^4; fz^{P21}/TM6$	viable
$Ror^4/CyO; fz^{P21}/fz^{P21}$	lethal
$Ror^4/Ror^4; fz^{P21}/fz^{P21}$ (zygotic)	lethal
$Ror^4/Ror^4; fz^{P21}/fz^{P21}$ (maternal)	lethal
fz^{J22}/fz^{P21}	viable with PCP defects
$Ror^4/CyO; fz^{J22}/fz^{P21}$	viable with PCP defects
$Ror^4/Ror^4; fz^{J22}/fz^{P21}$ (zygotic)	viable with PCP defects
$Ror^4/Ror^4; fz^{J22}/fz^{P21}$ (maternal)	viable with PCP defects
fz^{J22}/fz^{R52}	viable with PCP defects
$Ror^4/CyO; fz^{J22}/fz^{R52}$	viable with PCP defects
$Ror^4/Ror^4; fz^{J22}/fz^{R52}$ (zygotic)	viable with PCP defects
$Ror^4/Ror^4; fz^{J22}/fz^{R52}$ (maternal)	viable with PCP defects
fz^{P21}/fz^{R52}	viable with PCP defects
$Ror^4/CyO; fz^{P21}/fz^{R52}$	viable with PCP defects
$Ror^4/Ror^4; fz^{P21}/fz^{R52}$ (zygotic)	viable with PCP defects
$Ror^4/Ror^4; fz^{P21}/fz^{R52}$ (maternal)	viable with PCP defects
$Dfz2^{C2}/Dfz2^{C2}$	lethal
$Ror^4/CyO; Dfz2^{C2}/TM6$	viable
$Ror^4/CyO; Dfz2^{C2}/Dfz2^{C2}$	lethal
$Ror^4/Ror^4; Dfz2^{C2}/TM6$	viable
$Ror^4/Ror^4; Dfz2^{C2}/Dfz2^{C2}$ (zygotic)	lethal
$Df(3L)469-2/Df(3L)469-2$	lethal
$Ror^4/CyO; Df(3L)469-2/TM6$	viable
$Ror^4/CyO; Df(3L)469-2/Df(3L)469-2$	lethal
$Ror^4/Ror^4; Df(3L)469-2/TM6$	viable
$Ror^4/Ror^4; Df(3L)469-2/Df(3L)469-2$ (zygotic)	lethal

Results

<i>Dfz2^{C2}</i> / <i>Df(3L)469-2</i>	viable (sterile)
<i>Ror⁴</i> / <i>CyO</i> ; <i>Dfz2^{C2}</i> / <i>Df(3L)469-2</i>	viable (sterile)
<i>Ror⁴</i> / <i>Ror⁴</i> ; <i>Dfz2^{C2}</i> / <i>Df(3L)469-2</i>	viable (sterile)
<i>Wnt5⁴⁰⁰</i> / <i>Wnt5⁴⁰⁰</i>	viable, CNS defects
<i>Wnt5⁴⁰⁰</i> / <i>Wnt5⁴⁰⁰</i> ; <i>Ror⁴</i> / <i>CyO</i>	viable, CNS defects
<i>Wnt5⁴⁰⁰</i> / <i>Wnt5⁴⁰⁰</i>; <i>Ror⁴</i> / <i>Ror⁴</i>	lethal
<i>otk^{A1}</i> / <i>otk^{A1}</i>	viable
<i>otk2^{C26}</i> / <i>otk2^{C26}</i>	viable
<i>Df(otk,otk2)D72</i> / <i>Df(otk,otk2)D72</i>	viable (male sterile)
<i>Ror⁴</i> , <i>otk^{A1}</i> / <i>Ror⁴</i> , <i>otk^{A1}</i>	viable
<i>Ror⁴</i> , <i>otk2^{C26}</i> / <i>Ror⁴</i> , <i>otk2^{C26}</i>	viable
<i>Ror⁴</i> , <i>Df(otk,otk2)D72</i> / <i>Ror⁴</i> , <i>Df(otk,otk2)D72</i>	viable (male sterile)

3.5.2 Ror binds to the Wnt ligands Wg, Wnt2 and Wnt4

Vertebrate Ror proteins have been shown to bind to several Wnt ligands and also to Fz receptors (Oishi et al., 2003). In order to gain more insight into the function of Ror proteins it is important to identify the Wnt ligands binding to Ror in *Drosophila*. I have studied biochemical interactions of Ror via co-immunoprecipitation. To achieve this, I co-overexpressed GFP-tagged Ror with Myc-tagged Wg, Wnt2 and Wnt4 constructs under the control of the *actin5C* promoter in S2R+ cells. As negative control I co-transfected mCD8-GFP with the same Myc-tagged Wnts. The GFP-tagged proteins were immunoprecipitated from cell lysates using an anti-GFP antibody. Western blotting and detection with an anti-Myc antibody showed that Wg-Myc, Wnt2-Myc as well as Wnt4-Myc were co-immunoprecipitated with Ror-GFP, while none of them were pulled down together with mCD8-GFP (Figure 28). This indicates that all three Wnt ligands bind to Ror-GFP. Although in other experiments I was also able to pull down Wnt5-Myc with Ror-GFP as well, I could not reliably reproduce this result. This was due to a constantly low transfection efficiency of the construct. The transfections, lysate preparations, pull-down and western blotting in this experiment were performed by Julia Loth.

Results

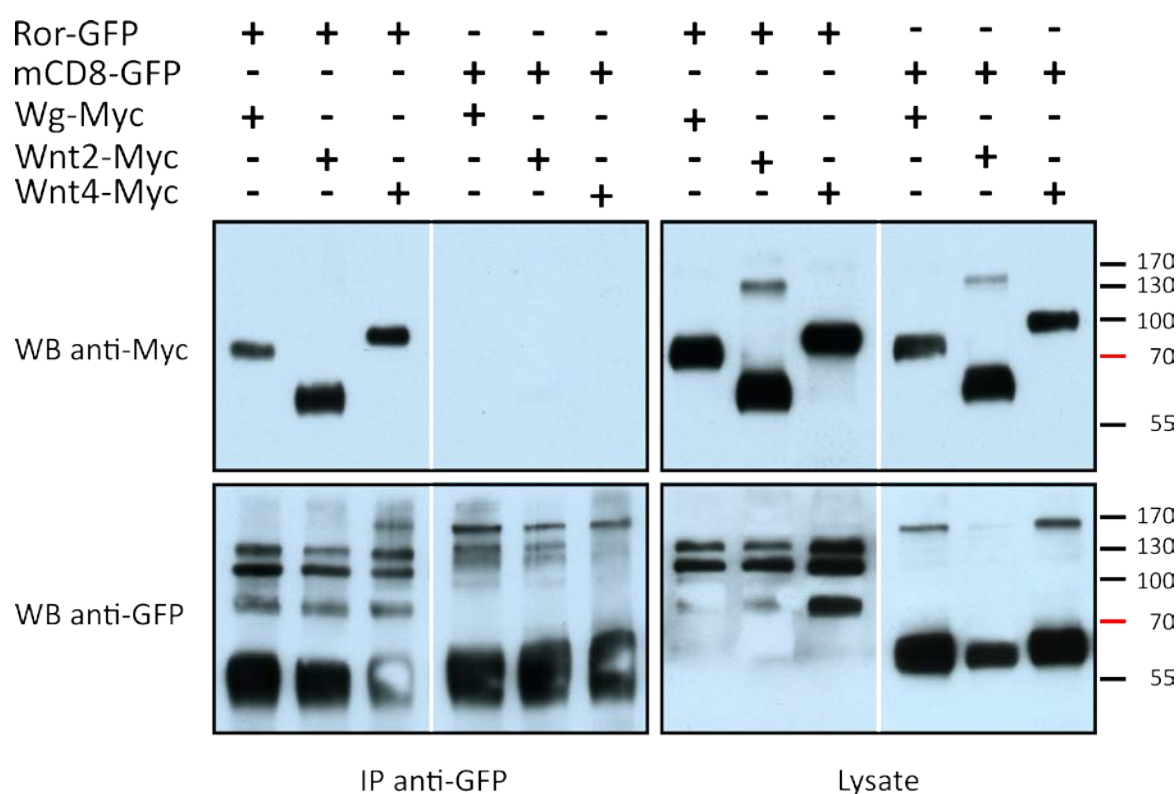


Figure 28: Ror-GFP binds to Myc-tagged Wg, Wnt2 and Wnt4. Indicated constructs were transfected into *Drosophila* S2R+ cells. Co-immunoprecipitation from cell lysates was performed using a rabbit- anti-GFP antibody followed by Western blotting using mouse anti-Myc and rabbit anti-GFP antibodies. In the GFP blot the denatured heavy chain of the antibody used in the IP is visible. IP: immunoprecipitation; WB: Western Blot. Protein sizes are indicated in kDa.

3.5.3 Ror binds to the Wnt receptors Fz and Fz2 and the Wnt co-receptors Otk and Otk2

In *Drosophila*, Fz and Fz2 constitute the core receptors for Wnt signaling (Bhanot et al., 1996, 1999). To receive some indication as to whether Ror acts as an independent Wnt receptor or as a co-receptor together with Fz or Fz2, I performed co-immunoprecipitations with GFP-tagged Ror and Myc-tagged Fz and Fz2 in S2R+ cells. Same as above, I pulled down Ror-GFP with a GFP antibody and after Western blotting detected bound Myc-tagged Fz proteins with a Myc antibody. As negative control mCD8-GFP was used again. At the same time I also analyzed possible biochemical interactions of Ror-GFP with Myc-tagged Otk and Otk2.

All four receptors, Fz, Fz2, Otk and Otk2 co-immunoprecipitated with Ror-GFP (Figure 29). This indicates that Ror is able to bind to all of them and suggests that *Drosophila* Ror may indeed act as a Wnt co-receptor.

Results

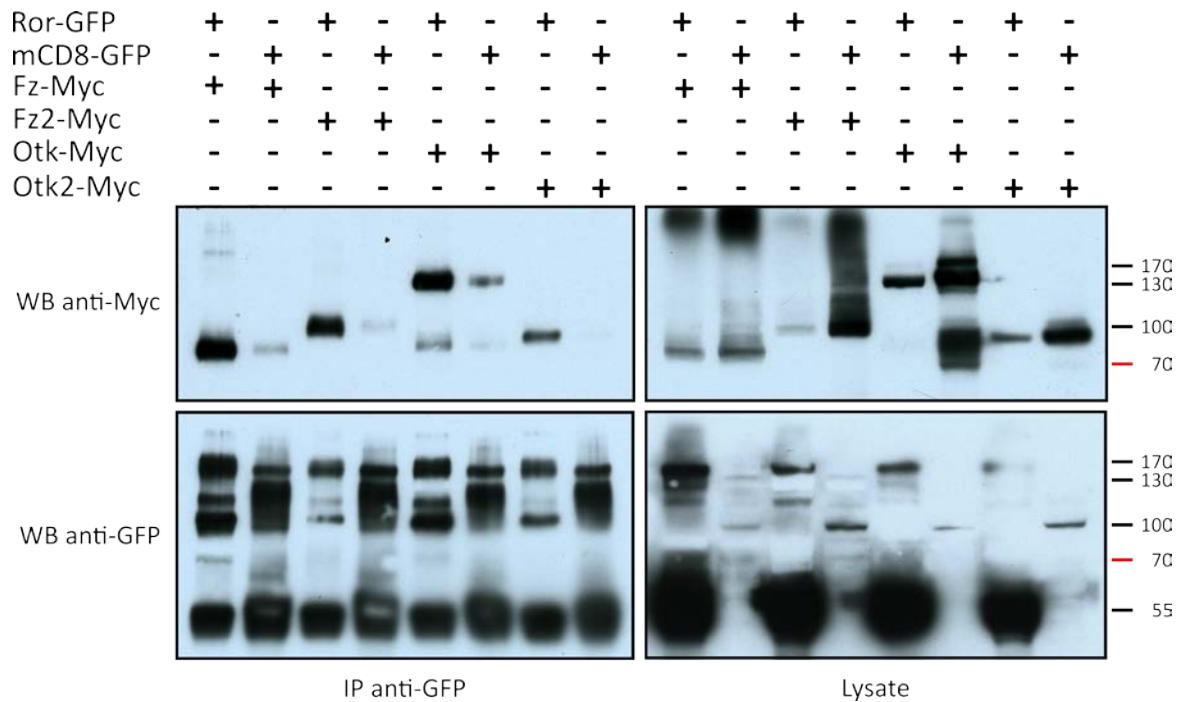


Figure 29: Ror-GFP binds to Myc-tagged Fz, Fz2, Otk and Otk2. Indicated constructs were co-transfected into *Drosophila* S2R+ cells. Co-immunoprecipitation from cell lysates was performed using a rabbit anti-GFP antibody followed by Western blotting using mouse anti-Myc and rabbit anti-GFP antibodies. IP: immunoprecipitation; WB: Western Blot. Protein sizes are indicated in kDa.

3.6. Overexpression of Ror

3.6.1 Ror-Myc overexpression using the Gal4-UAS system

As demonstrated above (3.4.1), Ror is neither essential for embryonic, larval or pupal development, nor for the survival of the adult fly. Also, disruption of *Ror* function does not lead to a strong phenotype. Various genes do not have a loss-of-function phenotype, because there are many redundancies between genes. But many of these genes display a phenotype when ectopically over- or misexpressed. Thereby it is possible to get an indication of the gene's function.

In order to gain some insights into *Ror* gene function, I have ubiquitously overexpressed a Ror-Myc fusion protein using the *daughterless*-Gal4 driver line (*da*-Gal4) and a UAS-Ror-Myc fly line, which was generously provided by the group of J. Noordermeer (Leiden University Medical Center). Figure 30 shows that a Ror-Myc fusion protein can be detected in Western Blot on embryonic lysates from *da*-Gal4/UAS-Ror-Myc embryos.

Results

The predicted size for Ror-Myc is 88 kDa (78 kDa + 6x Myc). In the WB are three distinct bands visible, one at about 100 kDa, one at 80 kDa and the third one at 50 kDa. This indicates that the overexpression of the protein was successful. In the Co-IP experiments, Ror-GFP is represented by three bands as well (see above).

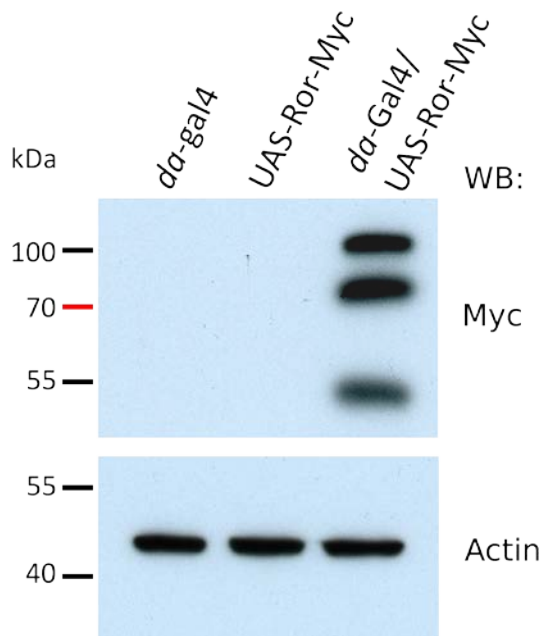


Figure 30: Ror-Myc overexpression via the UAS-Gal4 system. Whole embryo protein lysates of the indicated genotypes were subjected to SDS-PAGE and Western Blotting. The signal for the Ror-Myc fusion protein is clearly visible in the sample from embryos carrying both, the Gal4 driver and the UAS-Ror-Myc transgene.

3.6.2 Viability is not affected by *Ror* overexpression

In order to analyze if the ubiquitous overexpression of Ror-Myc is leading to defects that cause a decrease in viability, I have performed lethality tests with embryos expressing Ror-Myc under control of *da*-Gal4 and with the respective UAS-line and the *da*>Gal4 driver line as controls.

The average hatching rate of Ror-Myc overexpressing embryos is comparable to both control lines. Also, the average number of adult flies is not reduced. Therefore, Ror-Myc overexpression seems to have no general effect on viability (Figure 31).

Results

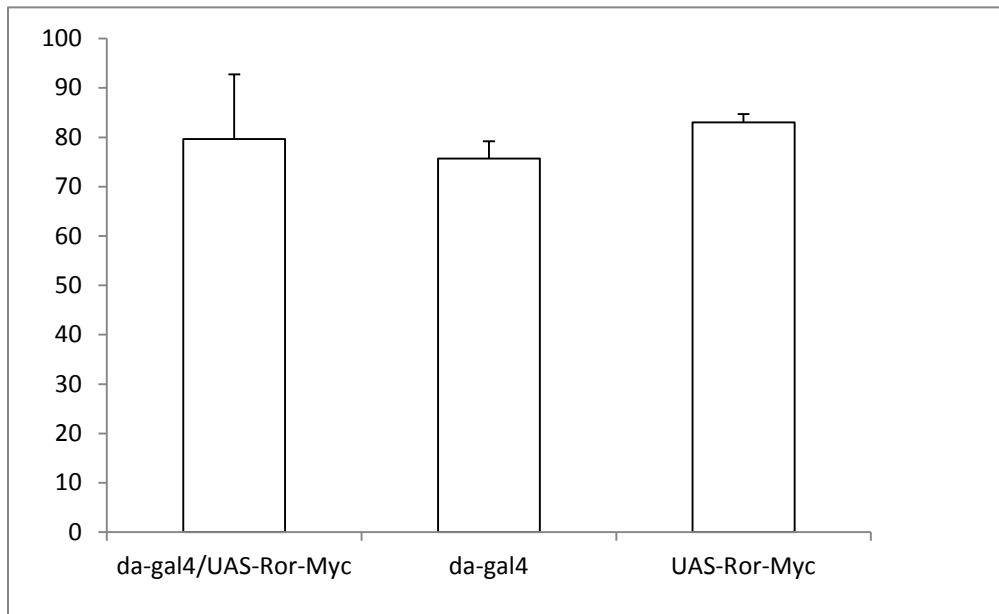


Figure 31: Embryonic viability of Ror-Myc overexpressing embryos compared to the used Gal4 driver and UAS line. The viability of embryo subquitously overexpressing Ror-Myc is not increased compared to *da>Gal4* and UAS-Ror-Myc embryos. Data were obtained by repeating each experiment three times, the error bars represent the standard deviation.

3.6.3 *Ror* overexpression does not lead to any PCP defects in adult flies

Like its absence, the overexpression of Ror-Myc has no influence upon the establishment of planar cell polarity. I have analyzed planar polarized tissues in adult flies, which ubiquitously overexpress Ror-Myc, in the used Gal4 driver line, the used UAS line and in wild type flies.

In homozygous mutant flies for *fz*, the direction of the wing hairs is disturbed. They are misoriented and appear as a swirling pattern (Figure 32 E). The wings of Ror-Myc overexpressing flies displayed no PCP defect. All wing hairs point into the same direction, to the distal side of the wing (Figure 32 D). The same orientation was observed in the negative controls (Figure 32 A-C). The direction of the thoracic bristles of Ror-Myc overexpressing flies was also not disturbed (data not shown).

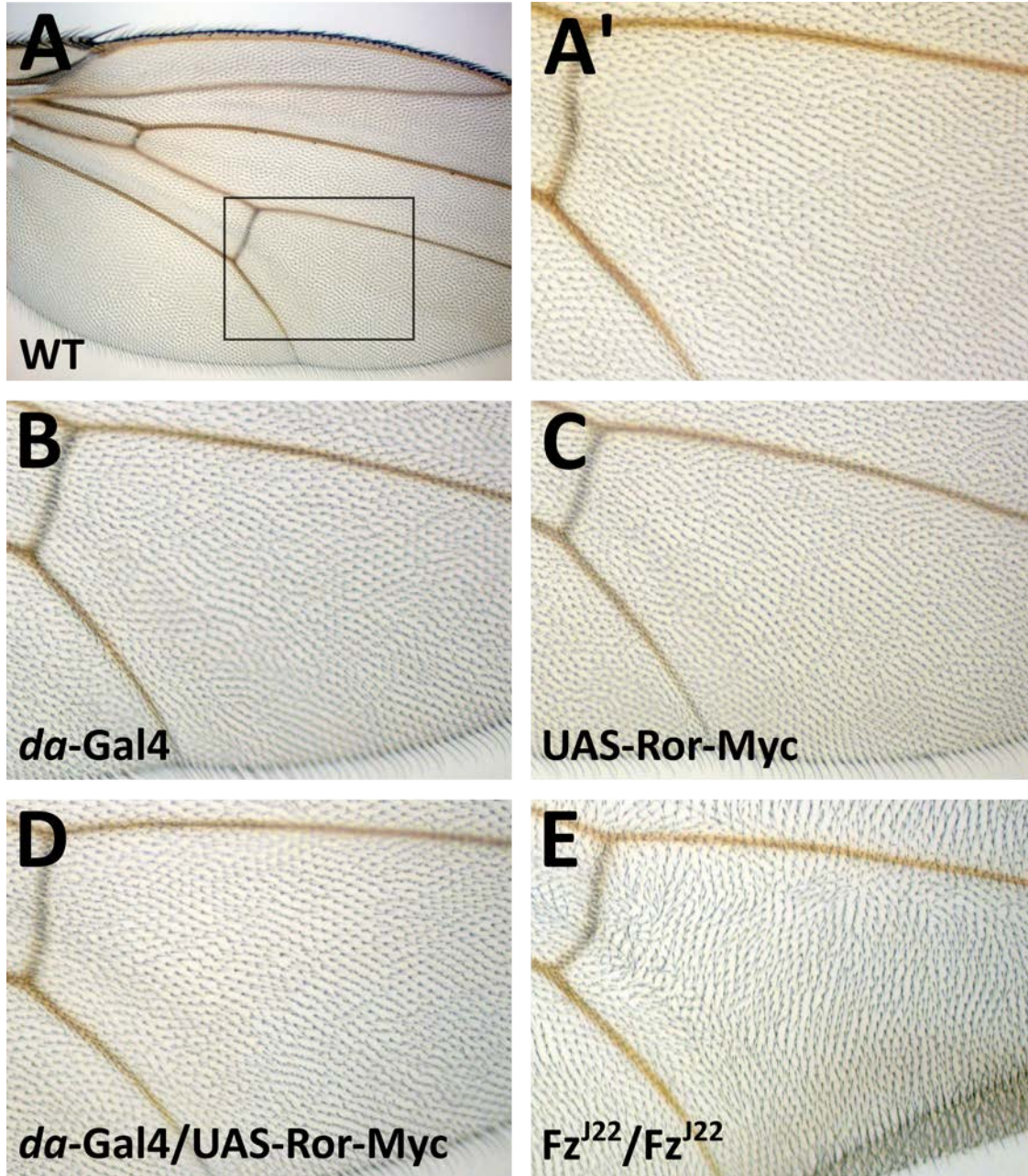


Figure 32: Planar cell polarity in wings of Ror-Myc overexpressing flies is not affected. The hairs on the wings of Ror-Myc overexpressing flies all point in the same direction. **(A)** Overview of a *Drosophila* wing. **(A')** Magnification of a wild type wing. **(B)** *da>Gal4* driver line control wing. **(C)** UAS-Ror-Myc control wing. **(D)** Ror-Myc overexpressing wing. **(E)** *Fz^{J22}/Fz^{J22}* wing as positive control.

Planar cell polarity in the eyes of adult Ror-Myc overexpressing flies was also not disturbed. In cross-sections, the ommatidia all appear as arrow-like shapes pointing into the same direction on each side of the eye (Figure 33 D), which resembles the wild type and the controls (Figure 33 A-C). As a positive control, ommatidia of transheterozygous *fz^{J22}/fz^{P21}* flies are shown. Here, the establishment of planar cell polarity is defective and the ommatidia are oriented into different directions (Figure 33 E).

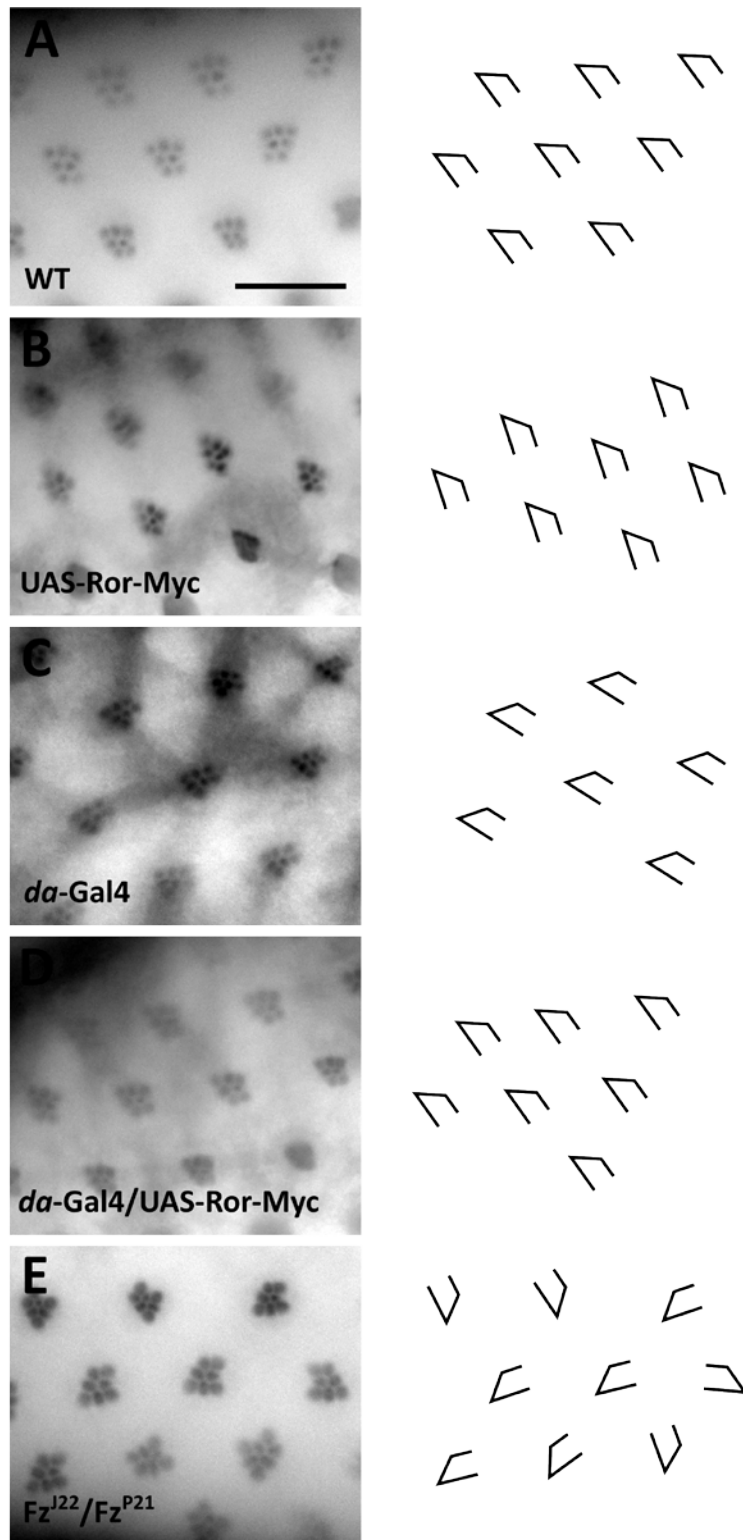


Figure 33: Planar cell polarity in the eyes of Ror-Myc overexpressing flies is not disturbed. (A) Wild type ommatidia. **(B)** UAS-Ror-Myc negative control. **(C)** *da-Gal4* negative control. **(D)** Eye of an adult Ror overexpressing fly. All ommatidia point to the same direction. **(E)** *Fz^{l22}/Fz^{p21}* eye as positive control, the ommatidia point in several different directions. Scale bar = 1000 μ m.

Results

3.6.4 Overexpression of Ror-Myc does not affect nervous system development

I have analyzed the embryonic central nervous system of embryos expressing Ror-Myc ubiquitously under the control of *da>Gal4* for any defects during development. In a staining with the BP102 antibody, which visualizes all CNS axons, the typical ladder-like axon pattern of the CNS could be seen in both, the Ror-Myc overexpressing embryos and in the wild type control. In each CNS segment, two clearly separated commissures are visible and all segments are connected by the longitudinal connectives (Figure 34 A-B').

In a staining for Fasciclin II, the *da>Gal4/UAS-Ror-Myc* embryos also resemble the wild type control. Three parallel axon bundles can be observed on either side of the midline, the lateral, the intermediate and the medial fascicle. I have not observed any breaks in the fascicles, crossings at the midline or any other defects (Figure 34 D/D'). The glial cell pattern in a Repo staining of embryos overexpressing Ror-Myc is not altered and comparable to the wild type. I have not noticed any missing or misplaced glia (Figure 34 E-F').

In addition, I examined the peripheral nervous system of *da>Gal4/UAS-Ror-Myc* embryos. I have stained embryos for the PNS marker 22C10 (Futsch), which marks the processes of all PNS neurons. All neurons within the PNS are present and correctly localized. In each abdominal segment, there are three clusters of neurons visible, the dorsal cluster on the dorsal side of the embryo, the lateral cluster and the ventral cluster on the ventral side (Figure 35).

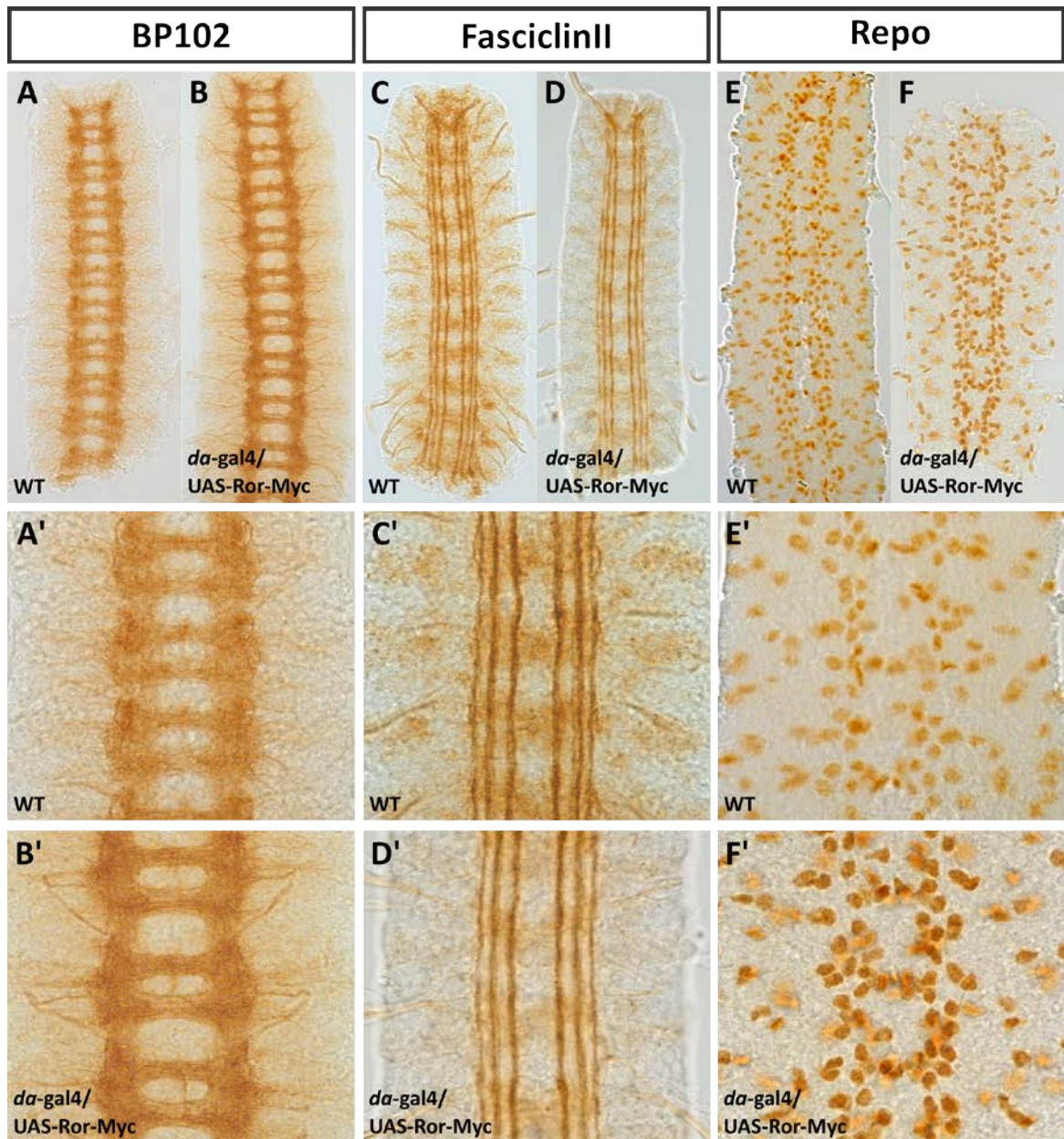


Figure 34: The morphology of the ventral nerve cord in filleted *Ror-Myc* overexpressing embryos compared to wild type embryos. (A/B) Axon tracts of the CNS are visualized using the BP102 antibody in WT (A) and *Ror-Myc* overexpressing embryos (B). The CNS of embryos overexpressing *Ror* resembles the wild type. **(C/D)** Three longitudinal axon tracts are visualized with Fasciclin II. In *da>Gal4/UAS-Ror-Myc* embryos all three fascicles are intact. **(E/F)** Glial cells visualized with the anti-Repo antibody. The pattern in *da/UAS-Ror-Myc* embryos is not disturbed. Images A'-F' are magnifications of sections in the images A-F. All images show three abdominal segments of late stage embryos; anterior is up.

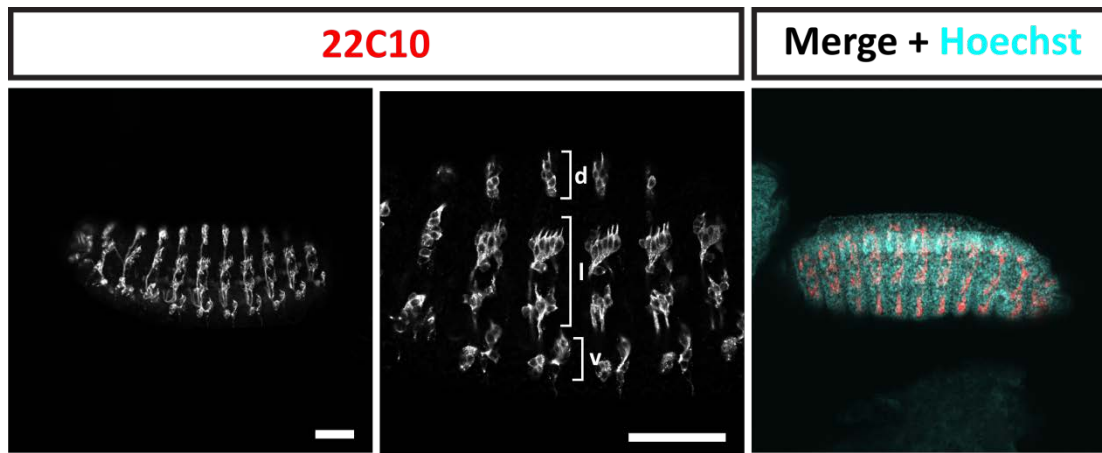


Figure 35: The PNS of Ror-Myc overexpressing embryos. A stage 15 *da>Gal4/UAS-Ror-Myc* embryo stained with 22C10 (Futsch) to visualize the peripheral nervous system. The dorsal cluster (d), the lateral cluster (l) and the central cluster (v) of PNS neurons are shown in a higher magnification. Anterior is to the left, Scale bars = 50 μ m.

To assess a possible phenotype in later development, I also examined the CNS of *da>Gal4/UAS-Ror-Myc* larvae. I have stained brains of third instar larvae with the neuroblast marker Miranda (Mira), the neuronal marker Elav and the glial marker Repo. In all analyzed brains, the morphology and size was not affected. The staining shows normal patterns of neuroblasts and neurons in the brain. Moreover, the number of glial cells is normal (Figure 36). I have also examined neuroblast polarity and did not observe any anomalies (data not shown).

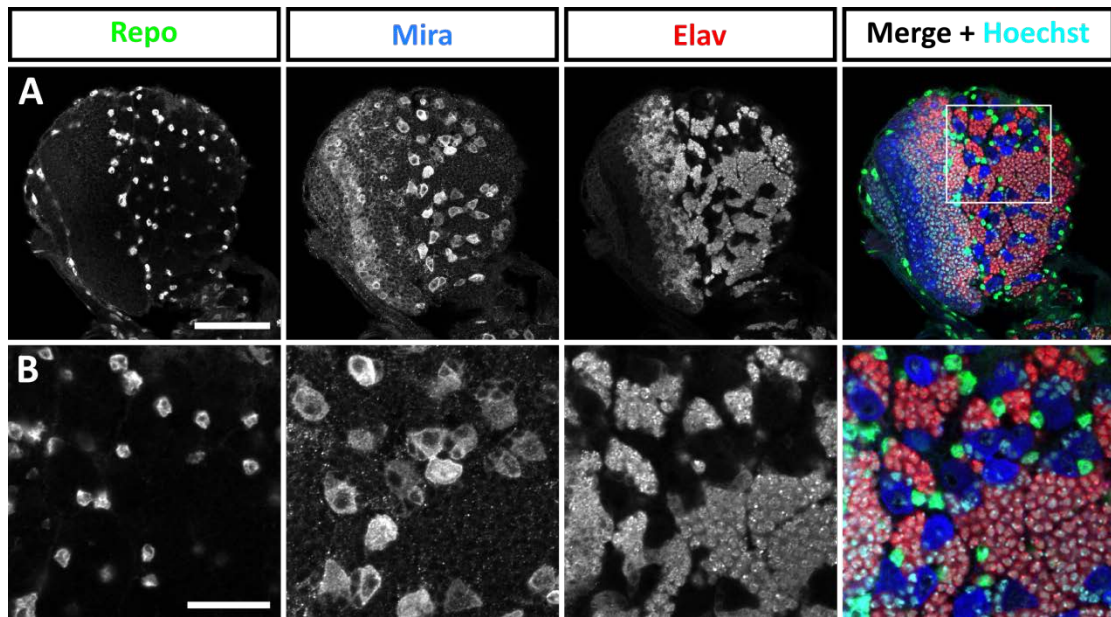


Figure 36: Central nervous system of a third instar *da>Gal4/UAS-Ror-Myc* larva. Pattern of marker protein expression and morphology are normal. **(A)** Overview of a brain hemisphere. **(B)** Higher magnification of the larval brain lobe. Scale bars: A = 50 μ m; B = 20 μ m.

3.7. Transcriptome analysis

Currently, the downstream targets of signaling mediated by *Drosophila* Ror are not known. This is also the case for Otk and Otk2. In co-immunoprecipitation experiments I have demonstrated that Ror is able to bind to the Wnt ligands Wingless, Wnt2 and Wnt4 and to the receptors Frizzled, Frizzled2, Otk and Otk2 (see 3.5). There is no clear indication as to which Wnt signaling pathways might be activated upon ligand binding to Ror and which downstream targets might thereby be regulated. Otk has been shown to bind to Wnt4 and Dsh and has been proposed to antagonize β -catenin dependent Wnt signaling in combination with Fz2 (Peradziryi et al., 2011). Moreover Otk and Otk2 both have been shown bind to Wnt2 (Linnemannstöns et al., 2014). To gain insight into the genetic networks downstream of Ror, Otk and Otk2 I have performed an analysis of genes, differentially expressed in respective mutant fly embryos, using whole transcriptome RNA-sequencing. For this approach, I used total RNA from embryos of homozygous *Ror* mutants (*Ror*⁴), homozygous *otk*, *otk2* mutants (*Df(otk,otk2)D72*) and homozygous *Ror*, *otk*, *otk2* triple mutants (*Ror*⁴, *Df(otk,otk2)D72*). As controls I have used the P-element lines used to generate the mutants (P(GSV3)GS8107 for *Ror*⁴ and

Results

P(XP)d01360 for *Df(otk, otk2)D72*, the *otk* and *otk2* single mutants (*otk*^{A1} and *otk2*^{C26}) as well as *white*⁻ (wt).

3.7.1 Nearly all reads could be mapped to the *Drosophila* genome

The cDNA library preparation and single-end RNA-Sequencing (RNA-Seq, 50 bp read length, single-end) was performed at the transcriptome analysis lab (TAL, GZMB Göttingen).

The reads were later aligned to the *Drosophila melanogaster* genome. In order to be able to interpret RNA-Seq data, one important issue is the assessment of data quality. One measure of data quality is the rate of reads aligned to the genome that can be assigned to transcripts. In my transcriptome analysis, for all eight genotypes an average of 96.9 % of aligned reads could be assigned to transcripts (Figure 37). This indicates that the data quality is good enough for further analysis.

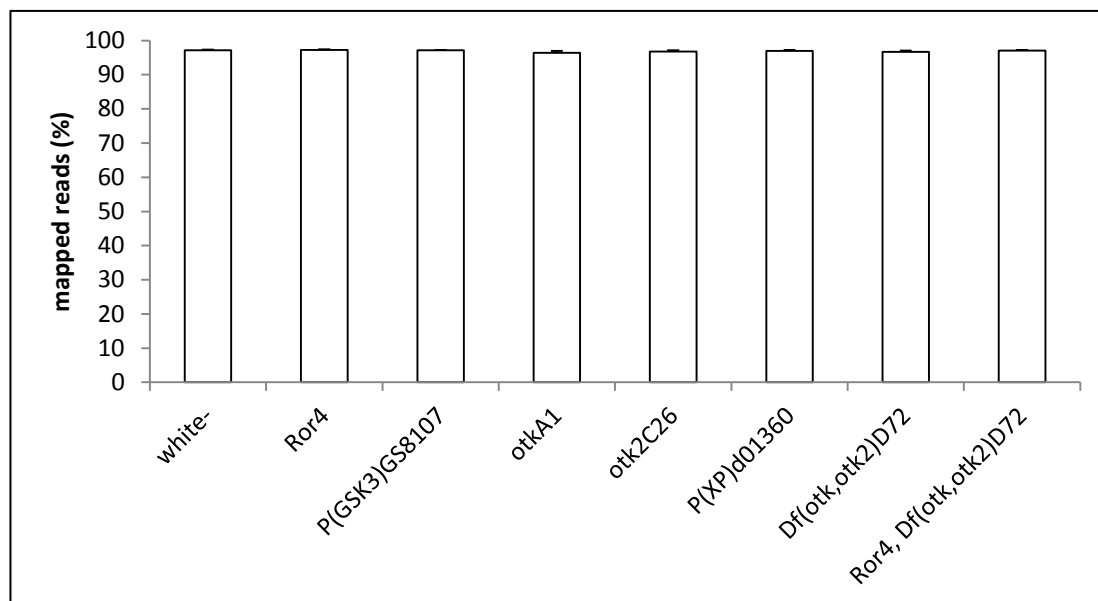


Figure 37: Number of mapped reads in all RNA-Sequencing samples. On average, 96.6 % of all reads could be mapped to the *Drosophila* genome.

3.7.2 The mapped reads in the genomic regions of *Ror*, *otk* and *otk2* correspond to the genotypes of the used fly lines

Another important step is to verify that the obtained data sets correspond to the right genotype. While doing so, one can make sure that the samples have not been interchanged, the RNA samples were not contaminated and the genotypes of the analyzed specimens were as expected. The aligned reads assigned to particular transcripts are stored in a binary format as BAM files. These can be visualized using the Integrative genomics viewer (IGV 2.3.34). In Figure 38 the loci for *Ror*, *otk* and *otk2* are displayed for one of the three *Ror*, *otk*, *otk2* triple mutant samples. As expected, no reads for *otk* were mapped to the *otk* locus (Figure 38 A). Likewise, no reads for *otk2* were present (Figure 38 B). When the *otk* and *otk2* double mutant was generated, the gene *mppe* was also partially removed (Linnemannstöns et al., 2014). This gene is neither necessary for viability, nor for fertility but encodes a metallophosphoesterase, which is involved in the maturation process of Rhodopsin in the eye (Cao et al., 2011). Consistent with the parts of the gene, which are lacking in the mutant, only reads assigned to the 5'UTR of *mppe* were found (Figure 38 B). In the *Ror* mutant allele *Ror*⁴, which was used to generate the triple mutant, only the genomic region between the *Ror* 5'UTR and the end of exon three were removed (Figure 21). This is reflected in the reads assigned to the *Ror* gene. Starting at the end of the third exon, many reads corresponding to *Ror* were detected, whereas upstream no reads were aligned to *Ror* and in the IGV view a clear gap can be observed between *Ror* and the neighboring gene CG31717 (Figure 38 C).

Results

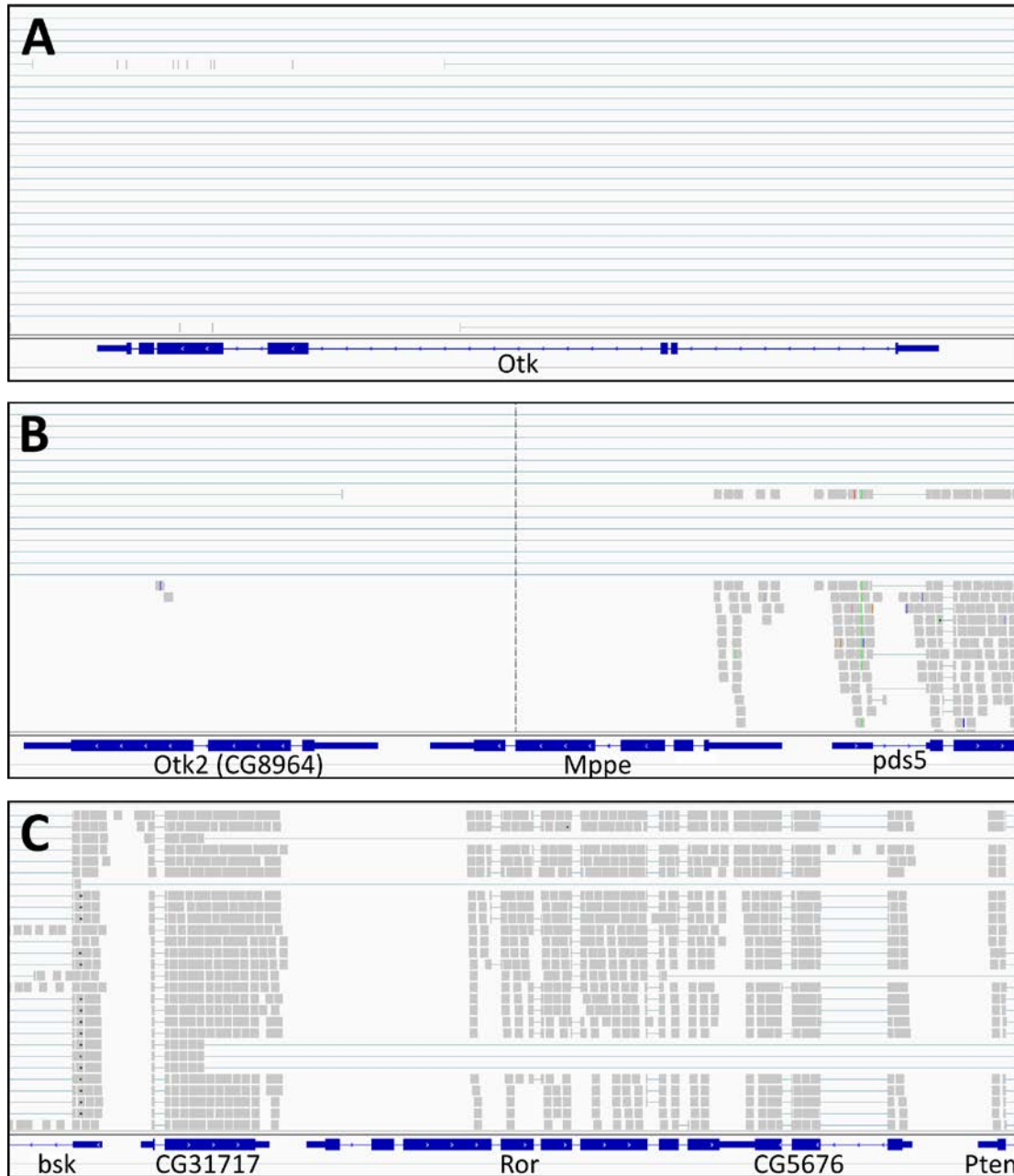


Figure 38: IGV views of the genomic loci for *otk*, *otk2* and *Ror* in a triple mutant RNA-Seq sample. The exons of the indicated genes are represented as dark blue boxes, the introns as dark blue lines. Aligned reads are visualized as grey boxes. **(A)** No reads could be aligned to the *otk* locus. **(B)** To *otk2* and to the majority of the *mppe* locus no reads were aligned, while the *pds5* gene is intact. **(C)** The genes *bsk*, *CG31717*, *CG5676* and *Pten* are intact, many reads could be assigned to their transcripts. Because the first third of the *Ror* gene including the start codon is lacking in the mutant, no reads corresponding to this region can be observed. Size of the pictured genomic regions: A: 22 kb; B: 6.1 kb; C: 6.8 kb.

3.7.3 Differentially expressed genes in *Ror* and *otk*, *otk2* mutant embryos

We have identified various transcripts, which are either up- or downregulated in the analyzed mutant embryos when compared to either a P-element or a wild type control.

Results

The complete lists of differentially expressed genes in the *Ror* single mutant, the *otk*, *otk2* double mutant and the triple mutant compared to the wild type can be found in the appendix. These lists only contain transcripts, which were up- or downregulated at least 2-fold (average \log_2 fold change of 1 or greater). For each genotype between 200 and 650 transcripts were differentially expressed (Table 10). To obtain some of the final data sets, two independent analyses were compared to each other. One data set from our group (AGW, analysis performed by Dr. Manu Tiwari) and the second one from the transcriptome analysis lab (TAL). The data sets for the *otk* and *otk2* single mutants were not included due to space constraints.

Table 10: Number of transcripts up- or downregulated in *Ror*, *otk* and *otk2* mutant embryos. The numbers of differentially expressed genes depicted are the combined result of two independent data analyses (if not indicated otherwise). Single mutants were compared to the wild type control, the *otk*, *otk2* double mutant was compared to the wild type and the two single mutants. The *Ror*, *otk*, *otk2* triple mutant data was compared to the wild type, the *otk*, *otk2* double mutant and to the *Ror* single mutant.

sample	genes upregulated	genes downregulated
<i>otk</i> ^{A1} vs. wt	331 *	306 *
<i>otk2</i> ^{C26} vs. wt	213 *	290 *
<i>Df(otk,otk2)D72</i> vs. wt	100	113
<i>Ror</i> ^A vs. wt	136	127
<i>Ror</i> ^A , <i>Df(otk,otk2)D72</i> vs. wt	118 *	126 *

* numbers are based on data analysis performed by our group (AGW) only

Intersections of the lists of differentially expressed genes in the *Ror* single mutant, the *otk*, *otk2* double mutant and in the triple mutant are depicted as Venn diagrams (Figure 39).

Results

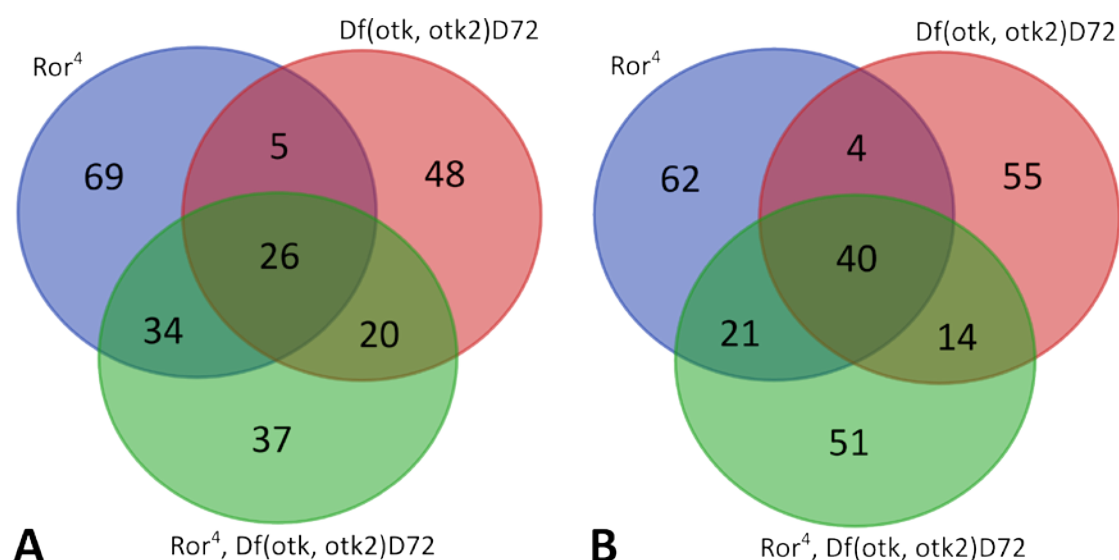


Figure 39: Venn diagrams of up- and downregulated genes. (A) Upregulated genes. **(B)** Downregulated genes. The *Ror* single mutant compared to the *otk, otk2* double mutant as well as the *Ror, otk, otk2* triple mutant.

3.7.4 Cytoscape analysis

For further analysis of the differentially expressed genes, a cluster network analysis was performed by Dr. Manu Tiwari using Cytoscape. This was performed using only the data sets from the *Ror* single mutant, the *otk, otk2* double mutant as well as the *Ror, otk, otk2* triple mutant, all compared to the wild type. Thereby, the obtained data sets were compared to known protein-protein interactions from manually curated interaction databases (IntAct and DIP). The differentially expressed genes and the known interaction partners of the corresponding proteins were then clustered using the GLay algorithm, which is the most relaxed clustering algorithm available. The resulting Figures depict the transcripts identified in the transcriptome analysis in clusters based on documented expression studies.

For better presentability, the symbols for all genes with more than one interaction partner have been indicated next to the cluster. Red nodes correspond to downregulated transcripts, green nodes to upregulated ones. All cyan colored nodes represent known interaction partners of transcripts identified in the transcriptome analysis (Figure 40, Figure 41 and Figure 42).

Results

The clustering resulted in the identification of several transcripts, which are likely regulated by signaling mediated via Ror and/or Otk/Otk2. In *Ror*⁴ mutant embryos for instance, the Forkhead domain 59A protein, which is predicted to be a transcriptional regulator, is highly upregulated (Kaufmann and Knöchel, 1996). Other interesting candidates include the translation initiation factor eIF4E3 and the cytoskeletal component Tektin C (Figure 40).

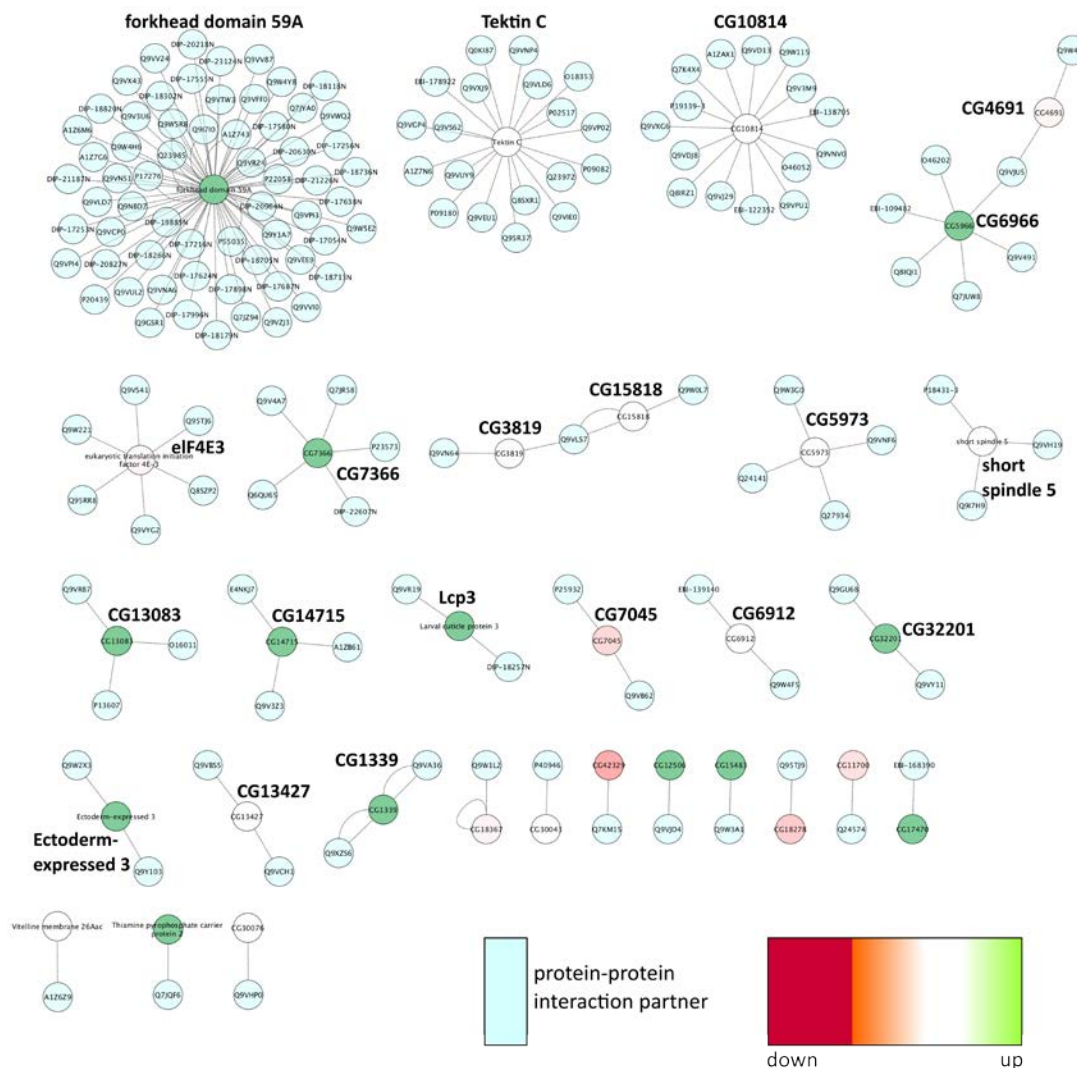
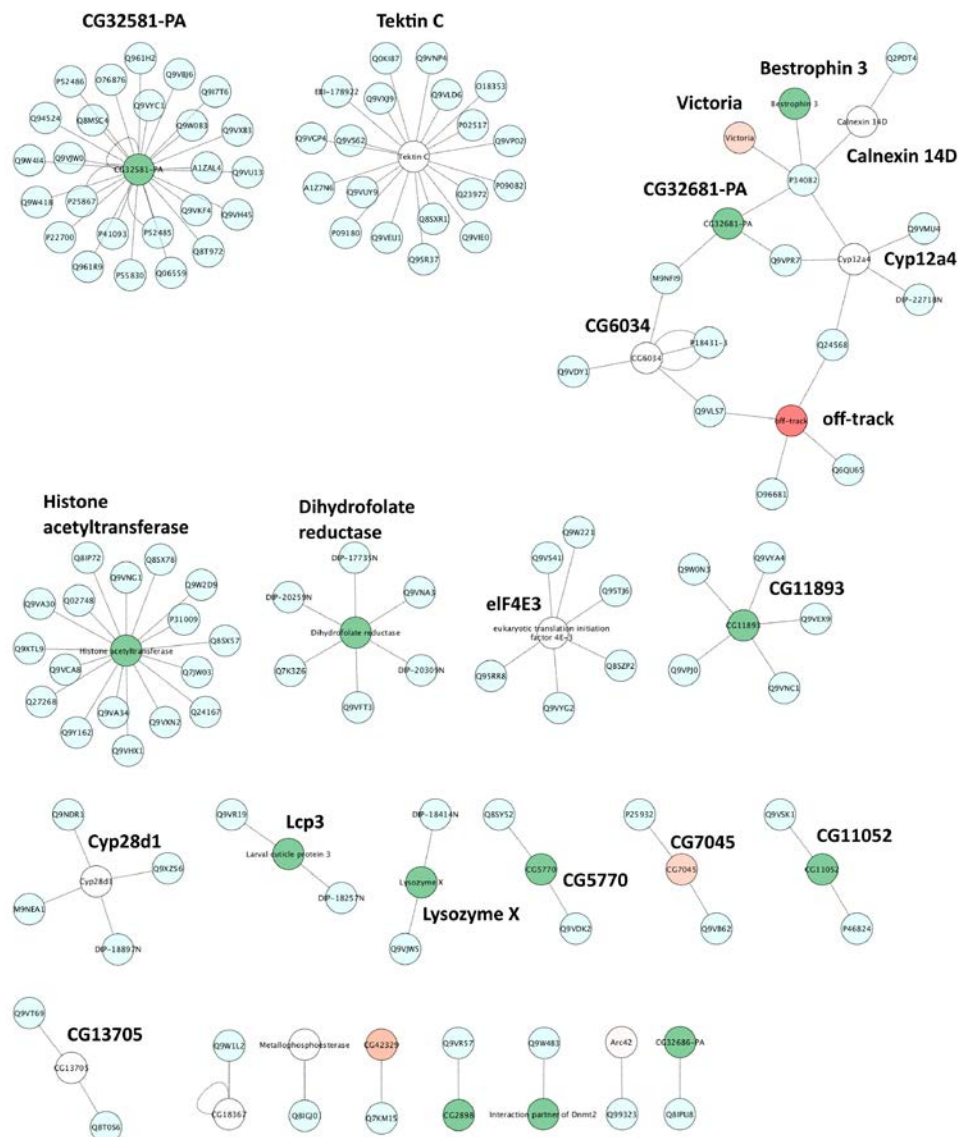


Figure 40: Cluster networks analysis of transcripts up- or downregulated in *Ror*⁴ mutant embryos compared to the wild type. Cyan nodes represent known interaction partners of the proteins corresponding to the differentially expressed transcripts. Green represents upregulation, red represents downregulation. The intensity of the red or green color corresponds to the fold- change expression levels. The interaction partners are not labeled with Flybase symbols but with the Uniprot IDs of the corresponding proteins.

Results

In the cluster networks with genes differentially expressed in *otk*, *otk2* double mutant embryos, the protein with the second most interaction partners is Tektin C, which also appears in the data set from *Ror*⁴ mutants. The center of the largest cluster is the isoform A of the protein encoded by the so far undescribed gene CG32581, which is significantly upregulated. Interestingly, this protein is predicted to be a zinc-finger transcription factor (Flybase, St. Pierre et al., 2014). Other proteins identified in this analysis include the protein encoded by CG6034, which has been demonstrated to bind to the protein encoded by CG8552 (UniProt: Q9VLS7), which in turn was shown to bind Otk (Lowe et al., 2014) (Figure 41).



Results

Figure 41: Cluster networks analysis of transcripts up- or downregulated in *Df(otk, otk2)D72* double mutant embryos compared to the wild type. Cyan nodes represent known interaction partners of the differentially expressed transcripts. Green represents upregulation, red represents downregulation and the intensity of the color corresponds to the change in expression levels. For legend see Figure 40. All interaction partners are labeled with the Uniprot IDs of the corresponding proteins.

As expected, the two proteins Tektin C as well as isoform A of CG32581 appear in the cluster network for the *Ror, otk, otk2* triple mutant as well. Most other genes in this network are differentially expressed in the *otk, otk2* double mutant (see list appendix). But the protein encoded by CG9452 for instance is highly upregulated in embryos mutant for all three genes only (Figure 42).

Results

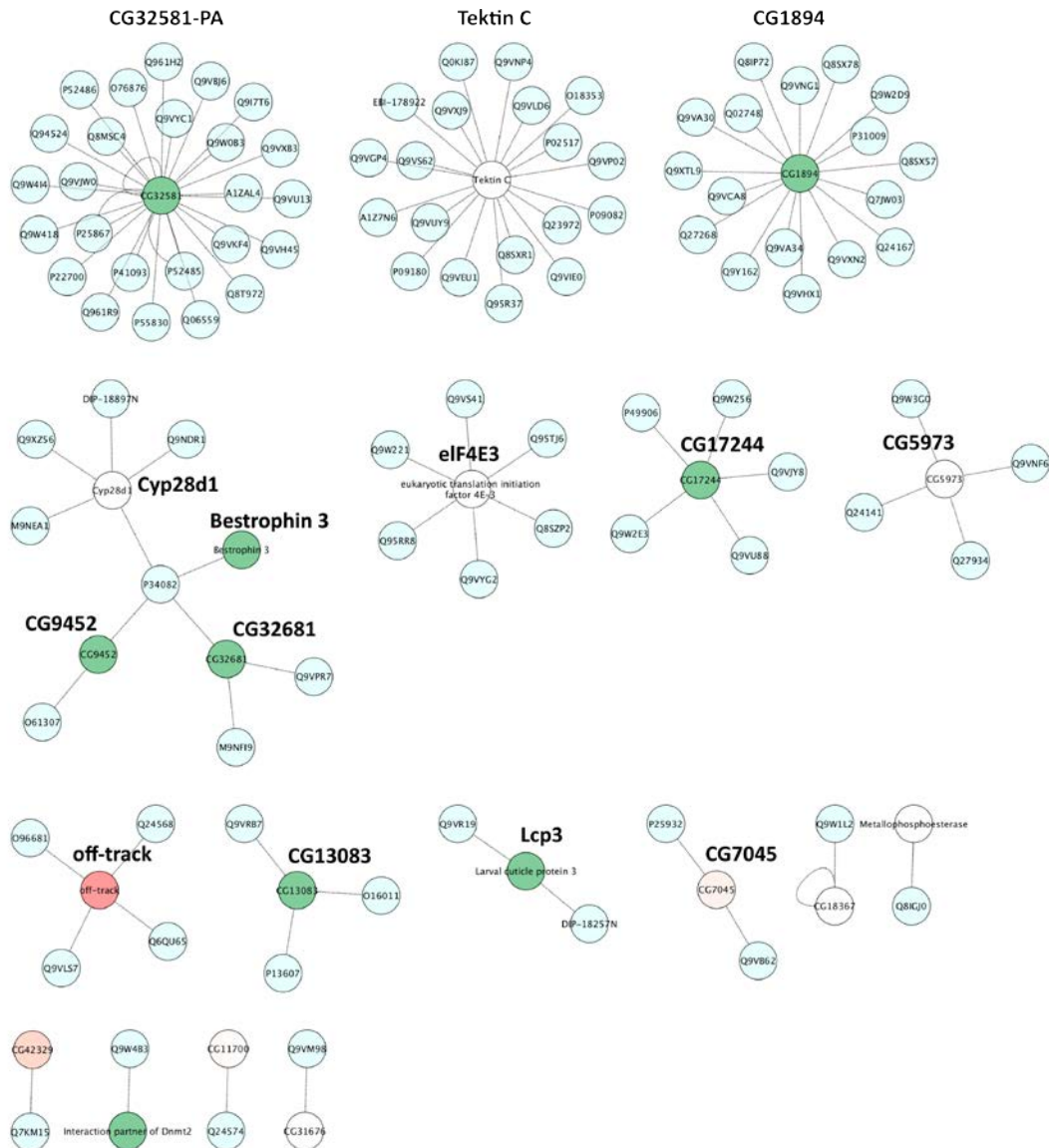


Figure 42: Cluster networks analysis of transcripts up- or downregulated in *Ror⁴, Df(otk, otk2)D72* triple mutant embryos compared to the wild type. The cyan colored nodes represent known interaction partners of the differentially expressed transcripts, all labeled with the Uniprot IDs of the corresponding proteins. The green nodes represent upregulated proteins, the red nodes downregulated proteins. The intensity of the color corresponds to the change in expression levels. For legend see Figure 40.

4. Discussion

4.1 Expression of *Ror>Ror-eGFP*

4.1.1 *Ror>Ror-eGFP* is primarily expressed in the nervous system

One indication to the function of a protein comes from looking at where and when it is expressed. Since in a previous study only the embryonic transcript expression was analyzed (Wilson et al., 1993) and my attempts to generate a specific antibody against *Ror* failed, I have established a fly line expressing a C-terminally tagged *Ror-eGFP* fusion protein under control of the endogenous *Ror* promoter. I could show that the *Ror>Ror-eGFP* signal (*Ror-eGFP*) becomes apparent at stage 11 and persists through embryonic development. The fact that a previous report states that the transcript level decays at the end of embryogenesis (Wilson et al., 1993) indicates that the fusion protein is quite stable. It was primarily found in the ventral nerve cord and the brain (Figure 13). As expected for a transmembrane protein, *Ror-eGFP* could be found at the membrane and in axonal processes (Figure 14). Although I have observed the fusion protein at the membrane of NBs (Figure 15), I could not reach a final conclusion about the cell types in which it is expressed due to the low expression level and high background.

In the larval brain the expression level is stronger and could clearly be seen in NBs and their neuronal progeny, excluding glial cells (Figure 17). The protein was also detected in the adult brain (data not shown).

The expression of *Ror-eGFP* could not only be found within the CNS but also in the membrane of the sensory cells of the PNS. This could be observed from embryonic stage 13 onwards and included sensory organs in the abdominal segments and in the head (Figure 14).

Interestingly, *Ror-eGFP* displayed a very specific expression pattern in the imaginal discs. Within all analyzed discs it could be observed in distinct cell clusters (Figure 18). These cells likely represent proneural clusters before the specification of SOPs, and/or specified SOPs. Some SOPs emerge already hours before puparium formation, while others become specified during early pupal development (Cubas et al., 1991; Huang et al.,

1991). To further illuminate this matter, co-immunostainings with different proneural markers (e.g Atonal, Amos, Achaete, Scute) or markers expressed in SOPs (e.g Senseless, Deadpan, Asense) would have to be performed. The discs shown in Figure 18 were all dissected any time during the third larval stage, which lasts about 30 h at 25°C. Thus, for this analysis one should dissect the imaginal discs at specific time points and also include early pupal stages. It would also be interesting to see, whether Ror is still expressed in neurons of differentiated adult sensory organs.

On the basis of the temporal and spatial expression pattern of Ror-eGFP it is probable that the protein functions during development of the nervous system. Ror-eGFP expression within the CNS begins at stage 11. At this stage segregation of NBs is completed and they are already dividing (Hartenstein and Campos-Ortega, 1984). The embryonic SOPs are already specified as well (Bodmer et al., 1989). Therefore, Ror function seems to be important rather later in NS development. Since the protein was still observed in the adult brain, it likely also takes part in the subsequent maintenance and function of the nervous system.

Several Wnt receptors are also expressed within the embryonic CNS. Transcript expression for the neurospecific receptor kinase NrK, which is considered the second *Drosophila* Ror homolog, resembles Ror in the embryo. It is also restricted to neural cells and can be detected within CNS and PNS (Oishi et al., 1999). To examine NrK expression more precisely, we have cloned a NrK>NrK-C-eGFP fusion construct with the same technique used for Ror>Ror-eGFP (Loth, 2014). However, to date we have not successfully established a transgenic fly line carrying this construct. Expression of the PTK7 homologs Otk and Otk2 within the CNS can also be observed from stage 11 onwards, but they are not exclusively found in the nervous system. Within the CNS they co-localize with Ror, but while Ror-eGFP is evenly distributed, Otk and Otk2 are both enriched at the anterior commissure and their expression level differs along different classes of neuronal cells. Additionally, they are only expressed in a subset of sensory organs (Pulido et al., 1992; Linnemannstöns et al., 2014). Another known Wnt receptor whose expression partly overlaps with Ror-eGFP is Drl, which is predominantly found on the growth cones and axons of neurons, which project through the AC (Callahan et al., 1995).

4.1.2 Ror-eGFP expression does not depend on Wg, Wnt2, Wnt4 or Wnt5

The expression of *otk* is dependent on Wnt2 signaling. While the Otk protein level is strongly reduced in *wnt2* mutant embryos, this is not the case for *otk2*. Additionally, Otk expression within the CNS is slightly reduced in *wnt5* mutant embryos (Linnemannstöns et al., 2014). The embryonic expression of Ror-eGFP was not influenced by the lack of *wg*, *wnt2*, *wnt4* or *wnt5* (Figure 19). It has to be noted that the Ror-eGFP construct including the regulatory region is located on the third chromosome, while the endogenous *Ror* gene is located on the second chromosome. Along with the fact that in addition to the GFP-tagged version, the analyzed embryos still expressed the endogenous *Ror* gene. Thus, if only the endogenous Ror protein was regulated by Wnt signaling one would not be able to detect it since no specific Ror antibody is available. Also, if Ror expression would be regulated post-transcriptionally, it is possible that the C-terminal GFP tag would be interfering.

4.2 Loss-of-function and overexpression of *Ror*

4.2.1 Ror loss of function does not lead to lethality but results in a mild fasciculation

defect while overexpression does not affect development

The lack of Ror protein was not lethal, indicating that the proteins function is not essential. The viability however was decreased, but only when compared to the wild type control. When compared to *otk*, *otk2* double mutant embryos, the difference was not statistically relevant (Figure 22). This was also the case when compared to other fly lines (e.g. *da>Gal4* or *UAS-Ror-Myc*). So this increased embryonic lethality is probably artificial. In order to clarify this matter, one would have to increase the number of analyzed embryos (n=300) and also compare to the viability of the P-element line, which was used for the generation of the *Ror^Δ* allele. The ubiquitous overexpression of Ror-Myc clearly did not influence the viability (Figure 31).

Because of the specific expression of *Ror* in the nervous system, I was interested to see if I could uncover any defects in neural development. When looking at all axon tracts of the CNS or at the pattern of glial cells, the mutant embryos were unremarkable (Figure

Discussion

23 B'/J'). But in the FasII staining several differences to the wt control became obvious. The first one, disruptions in the lateral fascicles, was not statistically significant (Figure 24). More noticeable was that all three fascicles appeared to be wavy and many axons appeared not tightly associated with the fascicles (Figure 23 F'). This defect was more pronounced in the lateral and intermediate fascicles than in the medial one. The fact that these defects are not visible in the BP102 staining could indicate that only a subset of the longitudinal axons was affected. The pathway choices of all axons seemed not to be disturbed, all major axon tracts were formed and no defects in midline crossing were observed. So although Ror expression in the CNS begins at a point in development when differentiating axons begin to extend axons, the main requirement for the protein might be in the late stages of CNS development. To confirm this, it is necessary to examine the establishment of the longitudinal pathways in earlier embryos. Without a thorough analysis of *Ror* mutant CNS development covering all stages between stage 12 and stage 17 one cannot be sure if the observed phenotype is due to a defect in inter-axonal adhesion, axon guidance or axon fasciculation. Also important would be to see whether the observed defect is still visible in the larval and adult CNS.

To verify that the observed phenotype is specific to the loss of Ror function, one would have to examine whether it can be rescued by supplying wild type Ror either by expressing a UAS-Ror construct using a neuronal driver line (e.g. *elav>Gal4*) or by simply analyzing the CNS of Ror-eGFP embryos in a *Ror*⁴ mutant background. If this was indeed the case, one could identify the required protein domain(s) by performing rescue experiment with different deletion constructs.

Interestingly, a phenotype with similarities has been described for the double mutant of two receptor protein tyrosine phosphatases (RPTPs), Ptp4E and Ptp10D (Jeon et al., 2008). In *Drosophila*, all six existing RPTPs are involved in CNS and motor axon guidance. Among them, there is extensive redundancy and the observed phenotypes are of varying severity (Jeon et al., 2008; Sun et al., 2001; Schindelholz et al., 2001). In Ptp4E¹, Ptp10D¹ double mutant embryos, the longitudinal fascicles appear wavy and exhibit some fraying. The longitudinally projecting SemalB-positive axons also do not form a tight bundle and appear frayed. However, sometimes there are also discontinuities in the fascicles and additionally they exhibit defects in motor axon guidance (Jeon et al., 2008).

It would be important to look for motor axon guidance defects in *Ror* mutants and quite interesting to analyze the CNS of embryos mutant for *Ror* and one or several RPTPs.

Genetic redundancy between Wnt signaling components has been shown several times already (see 1.2 and 1.4). Therefore is likely that this is also the case between the two *Drosophila* Ror family members. The second member *Nrk* has been implicated in the maintenance of adult muscles and in axon guidance and rhabdomere elongation during eye development (Kucherenko et al., 2011; Marrone et al., 2011). We have analyzed larval brains in which we downregulated *Nrk* via RNAi, but did not observe any obvious defects (Loth, 2014) and also downregulated *Ror* and *Nrk* together via RNAi. The resulting flies were viable, displayed no PCP defects but we did not examine their CNS (data not shown). A first indication as to whether *Ror* and *Nrk* act together could come from co-overexpressing the two proteins, but to fully understand the function of *Drosophila* Ror proteins, the generation of a *Ror*, *Nrk* double mutant is crucial.

In some of the analyzed *otk*, *otk2* mutant embryos, the fascicles appeared wavy as well, but breaks or fraying could be seen (Figure 23 G'). For *otk* it has previously been suggested that its loss leads to guidance defects of motor axons and aberrant photoreceptor axon projections in the brain (Winberg et al., 2001; Cafferty et al., 2004). However, the allele used in these reports (*otk*³) is lethal, which is in contrast to our recently published *otk* single and double mutant alleles (Linnemannstöns et al., 2014). Thus, the lethality of the published phenotype might be due to a second site lethal mutation and all previous findings concerning *otk* function might be misleading (Linnemannstöns, 2012). The analysis of the morphology of the *otk*, *otk2* mutant nervous system was not within the scope of this thesis. The CNS of *otk*, *otk2* double mutant embryos was used as a control for the *Ror*, *otk*, *otk2* triple mutant line. This was done in order to ensure that possible defects observed in the triple mutant cannot be attributed to the lack of *otk* and *otk2* and the number of *otk*, *otk2* double mutant nervous systems analyzed was quite low. Until the morphology of the *otk*, *otk2* mutant nervous system has been thoroughly re-examined, the involvement of the two proteins in nervous system development remains unclear.

4.2.2 Neither *Ror* loss of function nor *Ror* overexpression affect PCP

In vertebrates, the absence of either Ror2 or PTK7 leads to characteristic PCP defects such as disturbed orientation of the hairs in the mouse inner ear and characteristic gastrulation and neurulation defects (Lu et al., 2004; Paudyal et al., 2010; Hikasa 2002; Yamamoto 2008; Ho et al., 2012). However, in *Drosophila*, the absence of *Ror*, *otk* and *otk2* by themselves or in combination has no influence upon the establishment of planar cell polarity (Figure 26; Figure 27; Linnemannstöns et al., 2014). The same is true for the overexpression of Ror-Myc (Figure 32 and Figure 33). This is not surprising, since Ror-eGFP expression in the imaginal discs is only expressed in small very distinct clusters. For a protein with an essential function in PCP signaling, one would expect a much broader expression domain.

4.2.3 The combined loss of *Ror*, *Otk* and *Otk2* increases the lethality rate and some embryos display CNS defects

The combined loss of *Otk* and *Otk2* did not increase the embryonic lethality (Figure 22; Linnemannstöns et al., 2014) and the loss of *Ror* alone did not seem to influence the viability as well. However, when all three genes were lacking, the embryonic lethality appeared to be significantly increased (Figure 22). But this increase is not due to embryos dying during embryogenesis but rather to an increased number of unfertilized eggs. Noticeable was that of all embryos that hatched, only 27 % developed to adulthood. So the lack of *Ror*, *Otk* and *Otk2* together increases the overall lethality during post-embryonic stages of development.

Some triple mutant embryos displayed a phenotype within the CNS (Figure 23 M). These embryos explain the high standard deviation in Figure 24 and most likely represent embryos, which would not survive to adulthood. The outermost fascicle in these nervous systems is discontinuous and displays numerous fascicle breaks (Figure 23 M). This phenotype is somewhat unexpected since the CNS of *Ror*⁴ mutant embryos displayed different defects. The FasII staining of the CNS of other triple mutant embryos resembled the wild type (Figure 23 H') and in the BP102 staining showing all CNS axons, all analyzed embryos were unremarkable (Figure 23 D'). To quantify the fraction of nervous systems

carrying the severe phenotype, it is necessary to examine a much higher number of embryos. To ensure that the analyzed embryos are indeed late staged and their CNS is fully developed, it would be wise to co-stain for a second protein, which makes it possible to follow CNS condensation (e.g. Even-skipped).

While the intermediate fascicle was mostly intact in the triple mutant CNS and they displayed no commissural phenotype, their CNS phenotype was still somewhat similar to that of *wnt5* mutant embryos. Due to the failure of the inner and outer fascicle to defasciculate from each other during stage 14, their intermediate fascicle shows breaks, and the outer fascicle is discontinuous as well (Fradkin et al., 2004).

The formation of the longitudinal axon pathways requires interactions between neurons and glial cells. While earlier in CNS development the pioneer axons act as support for glia cells, later the longitudinal glia cells provide axon guidance cues and direct fasciculation and defasciculation (Hidalgo et al., 2000). However, since the number and positions of longitudinal glia were neither affected in the *Ror*⁴ single mutant embryos nor in the triple mutant embryos (Figure 23 J'/L'), this can be ruled out as the cause of the observed phenotypes.

To ensure that the observed phenotype is indeed due to the lack of *Ror*, *otk* and *otk2*, rescue experiments with *Ror*, *otk* or *otk2* alone have to be performed.

4.3 Ror acts as receptor for Wnt ligands

4.3.1 Ror genetically interacts with Wnt5

Double homozygous mutants for *wnt5* and *Ror* die after hatching as L1 larvae. As mentioned above, the phenotypes of the two single mutants differ from each other, although both seem to affect axon guidance and/or defasciculation. Both, *Ror* and *wnt5* single mutants are viable, although 19 % of *wnt5* mutant embryos fail to hatch, probably due to a more severe phenotype (Fradkin et al., 2004). The lethality of the double mutants is 100 % penetrant and indicates a genetic interaction of the two genes. The two proteins might act in partly redundant, parallel pathways both affecting CNS development. While lethality tests demonstrated that the embryos hatch and die shortly afterwards, the morphology of their nervous systems could not be analyzed yet due time

constraints. This would be very important to further clarify the relationship of the two genes.

As noted above, some *Ror*, *otk*, *otk2* triple mutant embryos exhibit a phenotype that displays similarities to the *wnt5* mutant CNS. Therefore it would be also interesting to analyze the nervous system of *wnt5*, *otk*, *otk2* triple mutant embryos and of embryos lacking all four genes.

Interestingly, vertebrate Ror2 has been shown to act as receptor for Wnt5 and together they play roles in morphogenetic processes such as convergent extension movements and neural tube closure. The loss of Ror2 phenocopies Wnt5a loss-of-function in *Xenopus* explants as well as in mouse embryos (Schambony and Wedlich, 2007; Ho et al., 2012). However, *Drosophila* Wnt5 is also a known ligand for Drl and together they direct axon and myotubes growth (1.2.4). It is likely, that Wnt5 interacts with several receptors during nervous system development, which also explain the differences of the phenotypes.

4.3.2 Biochemical interactions with other Wnt family members

One aim of this study was the identification of the extracellular ligands of *Drosophila* Ror. It has been demonstrated that vertebrate Ror proteins can regulate β -catenin-dependent and -independent Wnt signaling by binding to Wnt ligands and that the *C. elegans* Ror homolog Cam-1 which amongst others regulates cell motility and asymmetric cell division, binds to the Wnt homologs *cwn-1*, *egl-20* and *mom-2* (Billiard et al., 2005; Mikels and Nusse, 2006; Green et al., 2007; Forrester et al., 1999; Kim and Forrester, 2003). Therefore we asked whether *Drosophila* Ror could also interact with Wnt proteins. Co-immunoprecipitation experiments between Ror-GFP and different Myc-tagged Wnt proteins in *Drosophila* S2R+ cells showed that Wg, Wnt2 and Wnt4 are able to bind to Ror (Figure 28). However, it does not seem as if Ror shows any specificity in its interaction with Wnts. A biochemical interaction with Wnt5, which displayed a genetic interaction with *Ror* and is considered the primary Ror ligand in vertebrates, could not be reliably reproduced. Although the binding was observed several times (data not shown), the Western blot signal was always weak and could never be confirmed with absolute certainty. It has been stated that tagged Wnt proteins have a significantly lower

activity, which might explain the weak signal in the Wnt5 IPs. Due to the reduced biological activity of tagged Wnts, one should exercise caution when interpreting data produced with tagged Wnts (Willert and Nusse, 2012). It is possible that Ror transduces signals from several Wnts and until the NS of *Ror* mutant embryos has not been thoroughly analyzed, one can only speculate in which processes Ror signaling might be involved. Additionally, it has to be noted that the IPs were performed with Ror and Wnt ligands overexpressed within the same cells. Thus, some of the observed interactions might be artificial and may not occur *in vivo*. In theory, the expression patterns of several Wnts are compatible with a function together with Ror. As mentioned above, Wnt5 can be found in the embryonic brain and in CNS axons, but is primarily enriched at the PC (Fradkin et al., 1995; Fradkin et al., 2004). A fraction of Wnt4 transcript can also be found in the late CNS (Fisher et al., 2012). And although Wnt2 cannot be found within the nervous system, it might still reach Ror by diffusion.

4.4 Possible signal transduction mechanism of *Drosophila* Ror

In vertebrates it is likely that PTK7 and Ror2 act together in some aspects of development as loss-of-function animals for both proteins display similar phenotypes (see 4.2.2) and both proteins have been shown to antagonize β -catenin dependent signaling (Mikels and Nusse, 2006; Li et al., 2008; Yuan et al., 2011). Additionally, it has been shown that ectopic expression of Ror2 in cultured cells can induce filopodia formation, a phenotype also observed when PTK7 was overexpressed in MCF7 cells (Nishita et al., 2006; Podleschny, 2011). Since both protein families are structurally highly conserved (Forrester et al., 2002; Jung et al., 2002), a functional interaction between their corresponding *Drosophila* homologs is possible. However, it has to be noted that *Drosophila* Ror is slightly closer related to the vertebrate Ror1 proteins, while Nrk displays more sequence homology to Ror2 (Wilson et al., 1993; Oishi et al., 1997). For example mouse and human Ror2 as well as Nrk, but not Ror1 and *Drosophila* Ror possess a tyrosine-containing motif within their kinase domains, which can interact with SH2 domains of Shc adapter proteins as well as Src and PI3K kinases upon phosphorylation (Oishi et al., 1999; Songyang and Cantley, 1995).

We have shown that Ror is able to bind to both, Otk and Otk2 (Figure 29). This has also been demonstrated for Nrk (Loth, 2014) and for Drl (Mandile, 2013). But the fact that some *Ror*, *otk*, *otk2* triple mutant embryos display a more severe CNS phenotype than *Ror* single mutants or *otk*, *otk2* double mutants alone indicates a functional connection between Ror and Otk/Otk2.

Currently, it is unclear whether *Drosophila* Ror is an active tyrosine kinase. PTK7/Otk and Ryk/Drl have been classified as pseudokinases but still appear to have roles in signal transduction (Winberg et al., 2001; Kroiher et al., 2001; Yoshikawa et al., 2001). Although human Ror2 has been associated with kinase activity *in vitro* (Masiakowski and Carroll, 1992), both human Rors were recently also classified as inactive RTKs because they contain non-consensus amino acid residues within the kinase domain regions, which are critical for enzyme activity (Hanks et al., 1988; Bainbridge et al., 2014). However, *Drosophila* Ror and *C. elegans* Cam-1 both retain the consensus sequence and the kinase domain of Nrk has been shown to possess autophosphorylation activity *in vitro* (Bainbridge et al., 2014; Forrester et al., 1999; Oishi et al., 1999).

Consequently, there are several possible mechanisms how Ror might transduce a signal. Ror and Nrk might form homo- and heterodimers. So if Ror were an active kinase, its signal transduction mechanism would be the one of a typical RTK. But if it were to be an inactive kinase, it would be very likely that upon ligand binding Ror and Nrk would dimerize and Nrk would phosphorylate Ror. This would then create a docking site for phosphotyrosine-binding signaling molecules, which would further transduce the signal (Kroiher et al., 2001). Alternatively, Ror could become activated by cytosolic tyrosine kinases, which had been activated via another pathway. This mechanism would be the most probable when Ror would be signaling together with Otk and/or Otk2. Otk and Otk2 also form homo- and heterodimers and most probably interact via their transmembrane domains (Linnemannstöns et al., 2014). PTK7 has also been proposed to exert its signaling activity through interactions with functional kinases at the plasma membrane (Boudeau et al., 2006) and surely has been found to be a substrate of Src and to directly interact with the SH3 and SH2 domains of Src when signaling together at epithelial cell-cell contacts (Andreeva et al., 2014). Similarly, in chondrocytes Ror2 recruits the non-receptor tyrosine kinase Src and becomes phosphorylated (Akbarzadeh et al., 2008) and Wnt5a/Ror2 signaling in osteosarcoma cell lines also involves the

activation of a Src-family kinase (Enomoto et al., 2009). It would be important to examine whether Ror and Nrk are interacting with the *Drosophila* Src kinases Src42A or Src46B.

4.5 Transcriptomic analysis

A key challenge to a clearer understanding of the genetic and molecular function of Ror, Otk and Otk2 is the identification of processes occurring downstream of Ror-, Otk/Otk2- and possibly also Ror/Otk/Otk2-signaling. To identify their co-interactors, modulators and possible downstream targets, we performed transcriptomic analysis and analyzed differentially expressed genes in the respective single, double and triple mutants as compared to a wild type control. We then used Cytoscape and community clustering to visualize molecular interaction networks from our expression data. In essence, we overlaid the differential expression results from late stage embryos of the *Ror* single mutant, the *otk*, *otk2* double mutant and the *Ror*, *otk*, *otk2* triple mutants onto protein-protein interactions from curated databases. By this means it was possible to identify several protein complexes which may be regulated by Ror, and/or Otk and Otk2 and hypothesize about possible downstream events.

4.5.1 The forkhead domain protein Fd59A is upregulated in *Ror*⁴ mutant embryos

We have identified 263 transcripts, which were up- or downregulated at least 2-fold (average log₂ fold change of 1 or greater) when Ror was missing (136 upregulated; 127 downregulated) (appendix). The protein Forkhead domain 59A (Fd59A) was upregulated 4.23-fold, displayed a high significance (adjusted p-value = 6,6E⁻⁶²) and was found to directly interact with various other proteins (Figure 40). Fd59A belongs to a family of transcription factors containing a forkhead/HNF-3 DNA-binding motif, which is also called winged-helix domain. Many members of this family have been shown to be involved in the establishment of the body axis as well as in the differentiation and specification of various tissues (Kaufmann and Knöchel, 1996). Like *Ror*, transcript expression of *fd59A* commences at stage 11. At first transcript and protein can be observed in cell clusters, which probably consist of neuroblasts and their progeny. Later,

it is visible in a segmented pattern of neuronal cell clusters in the ventral nerve cord as well as in a pair of thoracic sensory organs and in the embryonic brain (Häcker et al., 1992; Lacin et al., 2014). The expression is maintained during development and can still be observed in the adult brain; there it is prominently visible in the lamina and medulla of the optic lobe (Lacin et al., 2014). Its expression is activated by the homeodomain transcription factors Hb9 and Nkx6 and can be assigned to two distinct sets of neurons: Hb9⁺ and octopaminergic neurons (Lacin et al., 2014). While in octopaminergic neurons it acts to regulate egg-laying behavior, the function in Hb9-expressing neurons has not been identified yet (Lacin et al., 2014). Interestingly, in mice the forkhead transcription factor FOXN1 has been implicated to be regulated by Bone morphogenic proteins (BMPs) and Wnt proteins. Wnt signaling through the stabilization of beta-catenin as well as through phosphatidylinositol 3-kinase (PI3K) was shown to contribute to FOXN1 expression (Coffer et al., 2004).

Both, Fd59A and Ror are expressed during the same stages of development and both within the CNS as well as the PNS. Therefore it seems probable that Ror-mediated signaling regulates *fd59A* expression. Since *fd59A* is upregulated when *Ror* is missing, its expression might be negatively regulated by Ror in the wild type. To confirm this, a first step would be to perform a quantitative real-time PCR. The next steps would be the analysis of *fd59A* mutant and overexpressing embryos for phenotypes within the nervous system and stainings of *Ror* mutant embryos with an existing anti-Fd59A antibody (Lacin et al., 2014).

4.5.2 The microtubule-binding protein Tektin C is downregulated in *Ror*⁴ mutant embryos as well as in *Df(otk, otk2)*D72 embryos

In *otk, otk2* double mutant embryos the levels of 113 transcripts were reduced and the levels of 100 transcripts were increased (see appendix). One gene whose expression was very significantly downregulated in *Ror* single mutants ($\log_2\text{FC} = +5.5$) as well as in *otk, otk2* double mutants (+7) was Tektin C, a microtubule-binding protein predicted to be a cytoskeletal component (Goldstein and Gunawardena, 2000). In a LC-MS-based proteomics study, Tektin C was identified as a sperm protein within the seminal vesicle

(Dorus et al., 2006). So far no phenotypic data is available, since the downregulation of *tektin C* via RNAi has been found to be pupal lethal (Mummery-Widmer et al., 2010). Tektin C has been shown to directly interact with various other proteins including the translational repressor Smaug (Dahanukar et al., 1999) and the transcription factor Gooseberry that, amongst other tissues, is also expressed in the developing CNS (Urbach and Technau, 2003). It can therefore be observed as the base of the second largest protein cluster in the *Ror* mutant, the *otk, otk2* double mutant and subsequently also in the *Ror, otk, otk2* triple mutant when compared to the wild type (Figure 40, Figure 41, Figure 42). It can be speculated that Otk and Otk2 might be able to change the cytoskeletal organization by regulating Tektin C expression. Thereby they could affect cell shape and motility and were involved in various developmental events.

The downregulation of Tektin C in the analyzed mutant embryos suggests that Ror/Otk/Otk2 signaling might indeed be regulating changes in the cytoskeletal organization of cells. Besides a quantitative real-time PCR, further experiments are necessary to elucidate the biological relevance of this finding. It has to be noted that downregulation of *tektin C* via RNAi is pupal lethal while the analyzed mutants in which *tektin C* appears to be significantly downregulated are viable and do not display an increased lethality.

4.5.3 A potential zinc-finger transcription factor encoded by the gene CG32581 is downregulated in Df(*otk, otk2*)D72 embryos

The gene CG32581 encodes for two transcripts. Only the isoform CG32581-RA is affected in the *otk, otk2* double mutants. This explains as to why many reads are present for CG32581 in IGV. The proteins encoded by CG32581 are predicted to contain a zinc-finger domain and therefore are most likely transcription factors. Based on the sequence similarity with human RNF-5 they have also been predicted to display ubiquitin-protein transferase activity (Flybase, 2008; St. Pierre et al., 2014). As per IntAct and DIP databases, CG32581-RA exhibits binary interaction with 26 proteins, all in two-hybrid screens (Figure 41). These include several ribosomal proteins, an ubiquitin-conjugating enzyme as well as a helix-loop-helix protein, which is also predicted to have transcription

factor activity (Flybase, 2008; St. Pierre et al., 2014). Besides the above mentioned qRT-PCRs to confirm the downregulation of CG32581-PA, in the future it will be important to confirm all protein-protein interactions by co-immunoprecipitation and subsequently analyze the knockout- as well as the overexpression phenotype of mutants for CG32581. One gene, which is only differentially expressed in embryos mutant for *Ror*, *otk* and *otk2* is CG9452, which has been predicted to possess acid phosphatase activity (Flybase; St. Pierre et al., 2014). In the triple mutant it is upregulated (+2) and has been shown to interact with FasciclinII, which controls growth cone guidance during nervous system development (Lin et al., 1994) and with the filamin-binding protein Teneurin-m, which is involved in neural development as well (Zheng et al., 2011; Lowe et al., 2014) (Figure 42). Besides CG9452, there are 26 other proteins upregulated only in the triple mutant and 51 are downregulated (Figure 39).

5. References

- Aberle, H., Bauer, A., Stappert, J., Kispert, A., Kemler, R. (1997). β -catenin is a target for the ubiquitin–proteasome pathway. *The EMBO Journal* **16** (13):3797-3804
- Adler, P. N., Vinson, C., Park, W. J., Conover, S., Klein, L. (1990). Molecular structure of frizzled, a *Drosophila* tissue polarity gene. *Genetics* **126** (2):401-416
- Adler, P. N., Lee, H. (2001). Frizzled signaling and cell-cell interactions in planar polarity. *Curr Opin Cell Biol.* **13** (5):635-40
- Adler, P. N., Taylor, J. (2001). Asymmetric cell division: plane but not simple. *Curr Biol.* **11** (6):R233-6
- Adler, P. N. (2002). Planar Signaling and Morphogenesis in *Drosophila*. *Developmental Cell* **(2)** (5):525-535
- Akbarzadeh S., Wheldon, L. M., Sweet, S. M., Talma, S., Mardakheh, F. K., Heath, J. K. (2008). The deleted in brachydactyly B domain of ROR2 is required for receptor activation by recruitment of Src. *Plos One* **3** (3):e1873
- Amit, S., Hatzubai, A., Birman, Y., Andersen, J. S., Ben-Shushan, E., Mann, M., Ben-Neriah, Y., Alkalay, I. (2002). Axin-mediated CKI phosphorylation of beta -catenin at Ser 45: a molecular switch for the Wnt pathway. *Genes and Development* **16** (9):1066-1076
- Angers, S., Moon, R.T. (2009). Proximal events in Wnt signal transduction. *Nature Reviews Molecular Cell Biology* **10** (7):468-477
- Andreeva, A., Lee, J., Iohia, M., Wu, X., Macara, I.G., Lu, X. (2014) PTK7-Src signaling at epithelial cell contacts mediates spatial organization of actomyosin and planar cell polarity. *Developmental Cell* **29** (1):20-33
- Axelrod, J. D., Miller, J. R., Shulman, J. M., Moon, R. T., Perrimon, N. (1998) Differential recruitment of Dishevelled provides signaling specificity in the planar cell polarity and Wingless signaling pathways. *Genes and Development* **12** (6):2610-2622
- Axelrod, J. D., McNeill, H. (2002). Coupling Planar Cell Polarity Signaling to Morphogenesis. *The Scientific World Journal* **2**:434-454
- Bainbridge, T. W., DeAlmeida, V. I., Izrael-Tomasevic, A., Chalouni, C., Pan, B., Goldsmith, J., Schoen, A. P., Quiñones, G. A., Kelly, R., Lill, J.R., Sandoval, W., Costa, M., Polakis, P., Arnott, D., Rubinfeld, B., Ernst, J. A. (2014). Evolutionary divergence in the catalytic activity of the CAM-1, ROR1 and ROR2 kinase domains. *Plos One* **9** (7):e102695
- Bänziger, C., Soldini, D., Schütt, C., Zipperlen, P., Hausmann, G., Basler, K. (2006). Wntless, a Conserved Membrane Protein Dedicated to the Secretion of Wnt Proteins from Signaling Cells. *Cell* **125** (3):509-522

References

- Bartscherer, K., Pelte, N., Ingelfinger, D., Boutros, M. (2006). Secretion of Wnt Ligands Requires Evi, a Conserved Transmembrane Protein. *Cell* **125** (3):523-533
- Basson, M. (2012). Signaling in cell differentiation and morphogenesis. *Cold Spring Harbor Perspectives in Biology* **4** (6).
- Bate and Martinez-Arias (1993). The Development of *Drosophila melanogaster*. Cold Spring Harbor Laboratory Press
- Behrens, J., von Kries, J. P., Kühl, M., Bruhn, L., Wedlich, D., Grosschedl, R., Birchmeier, W. (1996). Functional interaction of beta-catenin with the transcription factor LEF-1. *Nature* **382** (6592):638-42
- Bejsovec, A., Martinez-Arias, A. (1991). Roles of wingless in patterning the larval epidermis of *Drosophila*. *Development* **113** (2):471-485
- Benzing, T., Simons, M., Walz, G. (2007). Wnt Signaling in Polycystic Kidney Disease. *Journal of the American Society of Nephrology* **18** (5):1389-1398
- Bhanot, P., Brink, M., Samos, C., Hsieh, J., Wang, Y., Macke, J. P., Andrew, D., Nathans, J., Nusse, R. (1996). A new member of the frizzled family from *Drosophila* functions as a Wingless receptor. *Nature* **382** (6588):225-230
- Bhanot, P., Fish, M., Jemison, J. A., Nusse, R., Nathans, J., Cadigan, K.M. (1999). Frizzled and Dfrizzled-2 function as redundant receptors for Wingless during *Drosophila* embryonic development. *Development* **126** (18):4175-86
- Bhat, K. M. (1996). The patched signaling pathway mediates repression of gooseberry allowing neuroblast specification by wingless during *Drosophila* neurogenesis. *Development* **122** (9):2921-2932
- Bienz, M. (1994). Homeotic genes and positional signalling in the *Drosophila* viscera. *Trends in Genetics* **10** (1):22-26
- Billiard, J., Way, D. S., Seestaller-Wehr, L. M., Moran, R. A., Mangine, A., Bodine, P. V. N. (2005). The Orphan Receptor Tyrosine Kinase Ror2 Modulates Canonical Wnt Signaling in Osteoblastic Cells. *Molecular Endocrinology* **19** (1):90-101
- Bin-Nun, N., Lichtig, H., Malyarova, A., Levy, M., Elias, S., Frank, D. (2014). PTK7 modulates Wnt signaling activity via LRP6. *Development* **141** (2):410-421
- Bodmer, R., Carretto, R., Jan, Y.N. (1989) Neurogenesis of the peripheral nervous system in *Drosophila* embryos: DNA replication patterns and cell lineages. *Neuron* **3** (1):21-32
- Bonkowski, J., Yoshikawa, S., O'Keefe, D., Scully, A., Thomas, J.B. (1999). Axon routing across the midline controlled by the *Drosophila* Derailed receptor. *Nature* **402** (6761):540-544
- Boudeau, J., Miranda-Saavedra, D., Barton, G.J., Alessi, D.R. (2006). Emerging roles of pseudokinases. *Trends in Cell Biology* **16** (9):443-452

References

- Boutros, M., Mlodzik, M. (1999). Dishevelled: at the crossroads of divergent intracellular signaling pathways. *Mechanisms of Development* **83** (1-2):27-37
- Boutros, M., Mihaly, J., Bouwmeester, T., Mlodzik, M. (2000). Signaling Specificity by Frizzled Receptors in *Drosophila*. *Science* **288** (5472):1825-1828
- Brand, A. H., Perrimon, N. (1993). Targeted gene expression as a means of altering cell fates and generating dominant phenotypes. *Development* **118** (2):401-415
- Brennan, K., Gonzalez-Sancho, J. M., Castelo-Soccio, L. A. Howe, L. R., Brown, A. M. C (2004). Truncated mutants of the putative Wnt receptor LRP6/Arrow can stabilize β -catenin independently of Frizzled proteins. *Oncogene* **23** (28):4873-4884
- Brown, A. M. C., Papkoff, J., Fung, Y. K., Shackleford, G. M., Varmus, H. E. (1987). Identification of protein products encoded by the proto-oncogene int-1. *Molecular and Cellular Biology* **7** (11):3971-3977
- Buratovich, M. A., Anderson, S., Gieseler, K., Pradel, J., Wilder, E.L. (2000). DWnt-4 and Wingless have distinct activities in the *Drosophila* dorsal epidermis. *Development Genes and Evolution* **210** (3):111-119
- Cadigan, K. and Nusse, R. (1997) Wnt signaling: a common theme in animal development, *Genes and Development* **11** (24):3286–3305
- Cadigan, K., Fish, M., Rulifson, E., Nusse, R. (1998). Wingless Repression of *Drosophila* frizzled 2 Expression Shapes the Wingless Morphogen Gradient in the Wing. *Cell* **93** (5):767-777
- Cafferty, P., Lu, L., Rao, Y. (2004). The receptor tyrosine kinase Off-track is required for layer-specific neuronal connectivity in *Drosophila*. *Development* **131** (21):5287-5295
- Callahan, C. A., Muralidhar, M. G., Lundgren, S. E., Scully, A. L., Thomas, J. B. (1995). Control of neuronal pathway selection by a *Drosophila* receptor protein-tyrosine kinase family member. *Nature* **376** (6536):171-174
- Cao, J., Li, Y., Xia, W., Reddig, K., Hu, W., Xie, W., Li, H. S., Han, J. (2011). A *Drosophila* metallophosphoesterase mediates deglycolylation of rhodopsin. *The EMBO Journal* **30** (18):3701-13
- Cavallo, R. A., Cox, R. T, Moline, M. M., Roose, J., Plevoy, G. A., Clevers, H., Peifer, M., Bejsovec, A. (1998). *Drosophila* Tcf and Groucho interact to repress Wingless signalling activity. *Nature* **395** (6702):604-608
- Chen, C. M., Struhl, G. (1999). Wingless transduction by the Frizzled and Frizzled2 proteins of *Drosophila*. *Development* **126** (23):5441-52
- Chen C. M., Strapps, W., Tomlinson, A., Struhl, G. (2004). Evidence that the cysteine-rich domain of *Drosophila* Frizzled family receptors is dispensable for transducing Wingless. *Proceedings of the National Academy of Sciences USA* **101** (45):15961-15966

References

- Ching, W., Hang, H. C., Nusse, R. (2008). Lipid-independent Secretion of a *Drosophila* Wnt Protein. *Journal of Biological Chemistry* **283** (25):17092-17098
- Chu-LaGriff, Q., Doe, C. Q. (1993). Neuroblast specification and formation regulated by wingless in the *Drosophila* CNS. *Science* **261** (5128):1594-1597
- Clevers, H. (2006) Wnt/ β -Catenin Signaling in Development and Disease, *Cell* **127** (3):469-80
- Coffer, P. J., Burgering, B. M. (2004). Forkhead-box transcription factors and their role in the immune system. *Nature Reviews Immunology* **4** (11):889-899
- Cohen, D., Mariol, M., Wallace, R., Weyers, J., Kamberov, Y. G., Pradel, J., Wilder, E.L. (2002). DWnt4 Regulates Cell Movement and Focal Adhesion Kinase during *Drosophila* Ovarian Morphogenesis. *Developmental Cell* **2** (4):437-448
- Cselenyi, C. S., Jernigan, K. K., Tahinci, E., Thorne, C. A., Lee, L. A, Lee, E. (2008). LRP6 transduces a canonical Wnt signal independently of Axin degradation by inhibiting GSK3's phosphorylation of β -catenin. *PNAS* **105** (23):8032-8037
- Cubas, P., De Celis, J. F., Campuzano, S., Modolell, J. (1991). Proneural clusters of achaete-scute expression and the generation of sensory organs in the *Drosophila* imaginal wing disc. *Genes and Development* **5** (6):996-1008
- Curtin, J. A., Quint, E., Tshipouri, V., Arkell, R. M., Cattanach, B., Copp, A. J., Henderson, D. J., Spurr, N., Stanier, P., Fisher, E. M., Nolan, P. M., Steel, K. P., Brown, S., Gray, I. C., Murdoch, J. N. (2003). Mutation of *Celsr1* Disrupts Planar Polarity of Inner Ear Hair Cells and Causes Severe Neural Tube Defects in the Mouse. *Current Biology* **13** (13):1129-33
- Dahanukar, A., Walker, J. A., Wharton. R. P. (1999). Smaug, a novel RNA-binding protein that operates a translational switch in *Drosophila*. *Molecular Cell* **4** (2):209-218
- Daniels, D. L., Weis, W. I. (2005). β -catenin directly displaces Groucho/TLE repressors from Tcf/Lef in Wnt-mediated transcription activation. *Nature Structural and Molecular Biology* **12** (4):364-371
- Davidson, G., Wu, W., Shen, J., Bilic, J., Fenger, U., Stannek, P., Glinka, A., Niehrs, C. (2005). Casein kinase 1 γ couples Wnt receptor activation to cytoplasmic signal transduction. *Nature* **438** (7069):867-872
- De, A. (2011) Wnt/ Ca^{2+} signaling pathway: a brief overview, *Acta Biochimica et Biophysica Sinica* **43** (10):745-756
- DeChiara, T. M., Kimble, R. B., Poueymirou, W. T., Rojas, J., Masiakowski, P., Valenzuela, D. M., Yancopoulos, G. D. (2000). Ror2, encoding a receptor-like tyrosine kinase, is required for cartilage and growth plate development. *Nature Genetics* **24** (3):271-274
- DeFalco, T., Camara, N., Bras, S., Doren, M. (2008). Nonautonomous Sex Determination Controls Sexually Dimorphic Development of the *Drosophila* Gonad. *Developmental Cell* **14** (2):275-286

References

- DiNardo, S., Heemskerk, J., Dougan, S., O'Farrell, P. H. (1994). The making of a maggot: patterning the *Drosophila* embryonic epidermis. *Current Opinion in Genetics and Development* **4** (4):529-534
- Dorus, S., Busby, S. A., Gerike, U., Shabanowitz, J., Hunt, D. F., Karr, T. L. (2006) Genomic and functional evolution of the *Drosophila melanogaster* sperm proteome. *Nature Genetics* **38** (12):1440-1445
- Du, S. J., Purcell, S. M., Christian, J. L., McGrew, L. L., Moon, R. T. (1995). Identification of distinct classes and functional domains of Wnts through expression of wild-type and chimeric proteins in *Xenopus* embryos. *Molecular and Cellular Biology* **15** (5):2625–2634
- Dura, J., Preat, T., Tully, T. (1993). Identification of *linotte*, a new gene affecting learning and memory in *Drosophila melanogaster*. *Journal of Neurogenetics* **9** (1):1-14.
- Easty, D. J., Mitchell, P. J., Patel, K., Florenes, V. A., Spritz, R. A., Bennett, D.C. (1997). Loss of expression of receptor tyrosine kinase family genes PTK7 and SEK in metastatic melanoma. *International Journal of Cancer* **71** (6):1061-1065
- Eisenberg, L. M., Ingham, P.W., Brown, A. (1992). Cloning and characterization of a novel *Drosophila* Wnt gene, *Dwnt-5*, a putative downstream target of the homeobox gene *Distal-less*. *Developmental Biology* **154** (1):73-83
- Endoh, H., Tomida, S., Yatabe, Y., Konishi, H., Osada, H., Tajima, K., Kuwano, H., Takahashi, T., Mitsudomi, T. (2004). Prognostic Model of Pulmonary Adenocarcinoma by Expression Profiling of Eight Genes As Determined by Quantitative Real-Time Reverse Transcriptase Polymerase Chain Reaction. *Journal of Clinical Oncology* **22** (5):811-819
- Enomoto, M., Hayakawa, S., Itsukushima, S., Ren, D. Y., Matsuo, M., Tamada, K., Oneyama, C., Okada, M., Takumi, T., Nishita, M., Minami, Y. (2009). Autonomous regulation of osteosarcoma cell invasiveness by Wnt5a/Ror2 signaling. *Oncogene* **28** (36):3197-3208
- Fisher, B., Weiszmam, R., Frise, E., Hammonds, A., Tomancak, P., Beaton, A., Berman, B., Quan, E., Shu, S., Lewis, S., Rubin, G., Barale, C., Laguertas, E., Quinn, J., Ghosh, A., Hartenstein, V., Ashburner, M., Celniker, S. (2012). BDGP in situ homepage: <http://insitu.fruitfly.org/cgi-bin/ex/insitu.pl>
- FlyBase Curators (2008--). Assigning Gene Ontology (GO) terms by sequence similarity in FlyBase.
- Fradkin, L., Noordermeer, J., Nusse, R. (1995). The *Drosophila* Wnt Protein DWnt-3 Is a Secreted Glycoprotein Localized on the Axon Tracts of the Embryonic CNS. *Developmental Biology* **168** (1):202-213
- Fradkin, L., Van Schie, M., Wouda, R., De Jong, A., Kamphorst, J., Radjkoemar-Bansraj, M., Noordermeer, J. (2004). The *Drosophila* Wnt5 protein mediates selective axon fasciculation in the embryonic central nervous system. *Developmental Biology* **272** (2):362-375
- Fradkin, L. G., Dura, J., Noordermeer, J. (2010). Ryks: new partners for Wnts in the developing and regenerating nervous system. *Trends in Neurosciences* **33** (2):84-92

References

- Forrester, W. C., Dell, M., Perens, E., Garriga, G. (1999). A C. elegans Ror receptor tyrosine kinase regulates cell motility and asymmetric cell division. *Nature* **400** (6747):881-885
- Forrester, W. C. (2002). The Ror receptor tyrosine kinase family. *Cellular and Molecular Life Sciences* **59** (1):83-96
- Fung, Y. K., Shackleford, G. M., Brown, A. M., Sanders, G. S., Varmus, H. E. (1985). Nucleotide sequence and expression in vitro of cDNA derived from mRNA of int-1, a provirally activated mouse mammary oncogene. *Molecular and Cellular Biology* **5** (12):3347-3344
- Ganguly, A., Jiang, J., Ip, T. Y. (2005). Drosophila WntD is a target and an inhibitor of the Dorsal/Twist/Snail network in the gastrulating embryo. *Development* **132** (15):3419-3429
- Gieseler, K., Mariol, M. C., Sagnier, T., Graba, Y., Pradel, J. C. (1995). Wingless and DWnt4, 2 Drosophila Wnt genes, have related expression, regulation and function during the embryonic development. *Comptes Rendus de l'Académie des Sciences III* **318** (11):1101-1110
- Gieseler, K., Graba, Y., Mariol, M., Wilder, E. L., Martinez-Arias, A., Lemaire, P., Pradel, J. (1999). Antagonist activity of DWnt-4 and wingless in the Drosophila embryonic ventral ectoderm and in heterologous Xenopus assays. *Mechanisms of Development* **85** (1-2):123-131
- Gieseler, K., Wilder, E., Mariol, M., Buratovitch, M., Bérenger, H., Graba, Y., Pradel, J. (2001). DWnt4 and wingless Elicit Similar Cellular Responses during Imaginal Development. *Developmental Biology* **232** (22):339-350
- Glinka, A., Wu, W., Delius, H., Monaghan, A. P., Blumenstock, C., Niehrs, C. (1998). Dickkopf-1 is a member of a new family of secreted proteins and functions in head induction. *Nature* **391** (6665):357-362
- Goldstein, L. S., Gunawardena, S. (2000). Flying through the drosophila cytoskeletal genome. *Journal of Cell Biology* **150** (2):63-68
- Gong, Y., Mo, C., Fraser, S. E. (2004). Planar cell polarity signalling controls cell division orientation during zebrafish gastrulation. *Nature* **430** (7000):689-693
- Gonzalez, F., Swales, L., Bejsovec, A., Skaer, H., Martinez-Arias, A. (1991). Secretion and movement of wingless protein in the epidermis of the Drosophila embryo. *Mechanisms of Development* **35** (1):43-54
- Gordon, M., Dionne, M., Schneider, D. S., Nusse, R. (2005). WntD is a feedback inhibitor of Dorsal/NF- κ B in Drosophila development and immunity. *Nature* **437** (7059):746-749
- Gordon, M. D., Nusse, R. (2006). Wnt Signaling: Multiple Pathways, Multiple Receptors, and Multiple Transcription Factors. *Journal of Biological Chemistry* **281** (32):22429-22433
- Graba, Y., Gieseler, K., Aragnol, D., Laurenti, P., Mariol, M. C., Berenger, H., Sagnier, T., Pradel, J. (1995). DWnt-4, a novel Drosophila Wnt gene acts downstream of homeotic complex genes in the visceral mesoderm. *Development* **121** (1):209-18

References

- Green, J. L., Inoue, T., Sternberg, P. W. (2007). The *C. elegans* ROR receptor tyrosine kinase, CAM-1, non-autonomously inhibits the Wnt pathway. *Development* **134** (22):4053-4062
- Green, J. L., Inoue, T., Sternberg, P. W. (2008). Opposing Wnt Pathways Orient Cell Polarity during Organogenesis. *Cell* **134** (4):646-656
- Gross, J., Chaudhary, V., Bartscherer, K., Boutros, M. (2012). Active Wnt proteins are secreted on exosomes. *Nature Cell Biology* **14** (10):1036-1045
- Grillenzoni, N., Flandre, A., Lasbleiz, C., Dura, J. (2007). Respective roles of the DRL receptor and its ligand WNT5 in *Drosophila* mushroom body development. *Development* **134** (17):3089-3097
- Gubb, D., García-Bellido, A. (1982). A genetic analysis of the determination of cuticular polarity during development in *Drosophila melanogaster*. *Journal of Embryology and Experimental Morphology* **68**:37-57
- Guo, N., Hawkins, C., Nathans, J. (2004). Frizzled6 controls hair patterning in mice. *Proceedings of the National Academy of Sciences USA* **101** (26):9277-9281
- Habas, R., Kato, Y., He, X. (2001). Wnt/Frizzled activation of Rho regulates vertebrate gastrulation and requires a novel Formin homology protein Daam1. *Cell* **107** (7):843-54
- Hanks, S.K., Quinn, A.M., Hunter, T. (1988) The protein kinase family: conserved features and deduced phylogeny of the catalytic domains. *Science* **241** (4861):42-52
- Hart, M. J., De los Santos, R., Albert, I. N., Rubinfeld, B., Polakis, P. (1998). Downregulation of β -catenin by human Axin and its association with the APC tumor suppressor, β -catenin and GSK3 β . *Current Biology* **8** (10):573-581
- Hartenstein, V., Campos-Ortega, J. A. (1984). Early neurogenesis in wild-type *Drosophila melanogaster*. *Roux's Archives of Developmental Biology* **193**(5):308-325
- Harterink, M., Korswagen, H. C. (2012). Dissecting the Wnt secretion pathway: key questions on the modification and intracellular trafficking of Wnt proteins. *Acta Physiologica* **204** (1):8-16
- Hayes, M., Naito, M., Daulat, A., Angers, S., Ciruna, B. (2013). Ptk7 promotes non-canonical Wnt/PCP-mediated morphogenesis and inhibits Wnt/ β -catenin-dependent cell fate decisions during vertebrate development. *Development* **140** (10):2245-2245
- He, X., Saint-Jeannet, J., Wang, Y., Nathans, J., David, I., Varmus, H. E. (1997). A Member of the Frizzled Protein Family Mediating Axis Induction by Wnt-5A. *Science* **275** (5306):1652-1654
- He, X., Semenov, M., Tamai, K., Zeng, X. (2004). LDL receptor-related proteins 5 and 6 in Wnt/ β -catenin signaling: Arrows point the way. *Development* **131** (8):1663–1677

References

- Heisenberg, C., Tada, M., Rauch, G., Saúde, L., Concha, M. L., Geisler, R., Stemple, D. L., Smith, J. C., Wilson, S. W. (2000). Silberblick/Wnt11 mediates convergent extension movements during zebrafish gastrulation. *Nature* **405** (6782):76-81
- Herr, P., Hausmann, G., Basler, K. (2012) Wnt secretion and signalling in human disease. *Trends in molecular medicine* **18** (8):483–93
- Hidalgo, A., Booth, G. E. (2000) Glia dictate pioneer axon trajectories in the Drosophila embryonic CNS. *Development* **127** (2):393-402
- Hikasa, H., Shibata, M., Hiratani, I., Taira, M. (2002). The Xenopus receptor tyrosine kinase Xror2 modulates morphogenetic movements of the axial mesoderm and neuroectoderm via Wnt signaling. *Development* **129** (22):5227-5239
- Hikasa, H., Sokol, S. (2013) Wnt signaling in vertebrate axis specification. *Cold Spring Harbor Perspectives in Biology* **5** (1):a007955
- Ho, H. H., Susman, M. W., Bikoff, J. B., Ryu, Y. K., Jonas, A. M., Hu, L., Kuruvilla, R., Greenberg, M. E. (2012). Wnt5a–Ror–Dishevelled signaling constitutes a core developmental pathway that controls tissue morphogenesis. *Proceedings of the National Academy of Sciences* **109** (11):4044-4051
- Hoffmans, R., Städeli, R., Basler, K. (2005). Pygopus and Legless Provide Essential Transcriptional Coactivator Functions to Armadillo/ β -Catenin. *Current Biology* **15** (13):1207-1211
- Holstein, T. (2012) The evolution of the Wnt pathway. *Cold Spring Harbor Perspectives in Biology* **4**:a007922
- Hovens, C. M., Stacker, S. A., Andres, A. C., Harpur, A. G., Ziemiecki, A., Wilks, A. F. (1992). RYK, a receptor tyrosine kinase-related molecule with unusual kinase domain motifs. *Proceedings of the National Academy of Sciences* **89** (24):11818-11822
- Hsieh, J., Kodjabachian, L., Rebbert, M. L., Rattner, A., Smallwood, P. M., Harryman Samos, C., Nusse, R., Dawid, I. B., Nathans, J. (1999). A new secreted protein that binds to Wnt proteins and inhibits their activities. *Nature* **398** (6726):431-436
- Huang, F., Dambly-Chaudière, C., Ghysen, A. (1991) The emergence of sense organs in the wing disc of Drosophila. *Development* **111** (4):1087-95
- Hurlstone, A., Clevers, H. (2002). T-cell factors: turn-ons and turn-offs. *The EMBO Journal* **21** (10):2303–2311
- Ikeda, S., Kishida, S., Yamamoto, H., Murai, H., Koyama, S., Kikuchi, A. (1998). Axin, a negative regulator of the Wnt signaling pathway, forms a complex with GSK-3 β and β -catenin and promotes GSK-3 β -dependent phosphorylation of β -catenin. *The EMBO Journal* **17** (5):1371–1384
- Ikeya, M., Lee, S., Johnson, J. E., McMahon, A. P., Takada, S. (1997). Wnt signalling required for expansion of neural crest and CNS progenitors. *Nature* **389** (6654):966-970

References

- Immerglück, K., Lawrence, P. A., Bienz, M. (1990). Induction across germ layers in *Drosophila* mediated by a genetic cascade. *Cell* **62** (2):261-268
- Inaki, M., Yoshikawa, S., Thomas, J. B., Aburatani, H., Nose, A. (2007). Wnt4 Is a Local Repulsive Cue that Determines Synaptic Target Specificity. *Current Biology* **17** (18):1574–1579
- Inoue, T., Oz, H. S., Wiland, D., Gharib, S., Deshpande, R., Hill, R.J., Katz, W. S., Sternberg, P. W. (2004). *C. elegans* LIN-18 Is a Ryk Ortholog and Functions in Parallel to LIN-17/Frizzled in Wnt Signaling. *Cell* **118** (6):795–806
- Itasaki, N., Jones, C. M., Mercurio, S., Rowe, A., Domingos, P. M., Smith, J. C., Krumlauf, R. (2003). Wise, a context-dependent activator and inhibitor of Wnt signalling. *Development* **130** (18):4295-4305
- Itoh, K., Brott, B. K., Bae, G., Ratcliffe, M. J., Sokol, S. Y. (2005). Nuclear localization is required for Dishevelled function in Wnt/ β -catenin signaling. *Journal of Biology* **4** (1):3
- Janda, C., Waghray, D., Levin, A. M., Thomas, C., Garcia, K. C. (2012). Structural basis of Wnt recognition by Frizzled. *Science* **337** (6090):59-64
- Janson, K., Cohen, E. D., Wilder, E. L. (2001). Expression of DWnt6, DWnt10, and DFz4 during *Drosophila* development. *Mechanisms of Development* **103** (1-2):113-120
- Jeon, M., Nguyen, H., Bahri, S., Zinn, K. (2008). Redundancy and compensation in axon guidance: genetic analysis of the *Drosophila* Ptp10D/Ptp4E receptor tyrosine phosphatase subfamily. *Neural Development* **3**:3
- Jiang, J., Struhl, G. (1998). Regulation of the Hedgehog and Wingless signalling pathways by the F-box/WD40-repeat protein Slimb. *Nature* **391** (6666):493-496
- Jing, L., Lefebvre, J., Gordon, L., Granato, M. (2009). Wnt Signals Organize Synaptic Prepattern and Axon Guidance through the Zebrafish unplugged/MuSK Receptor. *Neuron* **61** (5):721-733
- Jue, S. F., Bradley, R. S., Rudnicki, J. A., Varmus, H. E., Brown, A. M. (1992). The mouse Wnt-1 gene can act via a paracrine mechanism in transformation of mammary epithelial cells. *Molecular and Cellular Biology* **12** (1):321-328
- Jung, J. W., Ji, A. R., Lee, J., Kim, U. J., Lee, S. T. (2002). Organization of the human PTK7 gene encoding a receptor protein tyrosine kinase-like molecule and alternative splicing of its mRNA. *Biochimica et Biophysica Acta* **1579** (2-3):153-163
- Katzen, F. (2007). Gateway® recombinational cloning: a biological operating system. *Expert Opinion Drug Discovery* **2** (4):571-89
- Kaufmann, E., Knöchel, W. (1996). Five years on the wings of fork head. *Mechanisms of Development* **57**:3-20

References

- Keeble, T. R., Halford, M. M., Seaman, C., Kee, N., Macheda, M., Anderson, R. B., Stacker, S. A., Cooper, H. M. (2006). The Wnt receptor Ryk is required for Wnt5a-mediated axon guidance on the contralateral side of the corpus callosum. *Journal of Neuroscience* **26** (21):5840-5848
- Keeble, T. R., Cooper, H. M. (2006). Ryk: a novel Wnt receptor regulating axon pathfinding. *International Journal of Biochemistry and Cell Biology* **38** (12):2011-2017
- Keller, R. (2002). Shaping the Vertebrate Body Plan by Polarized Embryonic Cell Movements. *Science* **298** (5600):1950-1954
- Kennerdell, J. R., Carthew, R. W. (1998). Use of dsRNA-Mediated Genetic Interference to Demonstrate that frizzled and frizzled 2 Act in the Wingless Pathway. *Cell* **95** (7):1017-1026
- Kibar, Z., Salem, S., Bosoi, C. M., Pauwels, E., Marco, P., Merello, E., Bassuk, A. G., Capra, V., Gros, P. (2011). Contribution of VANGL2 mutations to isolated neural tube defects. *Clinical Genetics* **80** (1):76-82
- Kieserman, E. K., Wallingford, J. B. (2009). In vivo imaging reveals a role for Cdc42 in spindle positioning and planar orientation of cell divisions during vertebrate neural tube closure. *Journal of Cell Biology* **122** (Pt 14):2481-2490
- Kikuchi, A. (1999) Roles of Axin in the Wnt Signalling Pathway. *Cellular Signalling* **11** (11):777-788
- Kilian, B., Mansukoski, H., Barbosa, F. C., Ulrich, F., Tada, M., Heisenberg, C. P. (2003). The role of Ppt/Wnt5 in regulating cell shape and movement during zebrafish gastrulation. *Mechanisms of Development* **120** (4):467-476
- Kim, C., Forrester, W. C. (2003). Functional analysis of the domains of the C. elegans Ror receptor tyrosine kinase CAM-1. *Developmental Biology* **264** (2):376-390
- Kim, G. H., Her, J. H., Han, J. K. (2008). Ryk cooperates with Frizzled 7 to promote Wnt11-mediated endocytosis and is essential for Xenopus laevis convergent extension movements. *Journal of Cell Biology* **182** (6):1073-1082
- Kim, S., Gailite, I., Moussian, B., Luschnig, S., Goette, M., Fricke, K., Honemann-Capito, M., Grubmüller, H., Wodarz, A. (2009). Kinase-activity-independent functions of atypical protein kinase C in Drosophila. *Journal of Cell Science* **122** (Pt 20):3759-71
- Kishida, S., Yamamoto, H., Ikeda, S., Kishida, M., Sakamoto, I., Koyama, S., Kikuchi, A. (1998). Axin, a Negative Regulator of the Wnt Signaling Pathway, Directly Interacts with Adenomatous Polyposis Coli and Regulates the Stabilization of β -Catenin. *Journal of Biological Chemistry* **273** (18):10823-10826
- Klein, T. J., Mlodzik, M. (2005). Planar Cell Polarization: An Emerging Model Points in the Right Direction. *Cell and Developmental Biology* **21**:155-176
- Komekado, H., Yamamoto, H., Chiba, T., Kikuchi, A. (2007). Glycosylation and palmitoylation of Wnt-3a are coupled to produce an active form of Wnt-3a. *Genes to Cells* **12** (4):521-534

References

- Komiya, Y., Habas, R. (2008) Wnt signal transduction pathways. *Organogenesis* **4** (2):68-75
- Konsavage, W. M. Jr, Yochum, G. S. (2013). Intersection of Hippo/YAP and Wnt/ β -catenin signaling pathways. *Acta Biochimica et Biophysica Sinica* **45** (2):71-9
- Kozopas, K., Nusse, R. (2002). Direct Flight Muscles in *Drosophila* Develop from Cells with Characteristics of Founders and Depend on DWnt-2 for Their Correct Patterning. *Developmental Biology* **243** (2):312-325
- Kozopas, K., Samos, C. H., Nusse, R. (1998). DWnt-2, a *Drosophila* Wnt gene required for the development of the male reproductive tract, specifies a sexually dimorphic cell fate. *Genes and Development* **12** (8):1155–1165
- Kramps, T., Peter, O., Brunner, E. Nellen, D., Froesch, B., Chatterjee, S., Murone, M., Züllig, S., Basler, K. (2002). Wnt/Wingless Signaling Requires BCL9/Legless-Mediated Recruitment of Pygopus to the Nuclear β -Catenin-TCF Complex. *Cell* **109** (1):47-60
- Kroiher, M., Miller, M., Steele, R. (2001). Deceiving appearances: signaling by “dead” and “fractured” receptor protein-tyrosine kinases. *Bioessays* **23** (1):69-76
- Kucherenko, M. M., Marrone, A. K., Rishko, V. M., Magliarelli, Hde F., Shcherbata, H. R. (2011) Stress and muscular dystrophy: a genetic screen for dystroglycan and dystrophin interactors in *Drosophila* identifies cellular stress response components. *Developmental Biology* **352** (2):228-242
- Kühl, M., Sheldahl, L., Park, M., Miller, J., Moon, R. (2000) The Wnt/Ca²⁺ pathway: a new vertebrate Wnt signaling pathway takes shape. *Trends in Genetics* **16** (7):279–283
- Kurayoshi, M., Yamamoto, H., Izumi, S., Kikuchi, A. (2007). Post-translational palmitoylation and glycosylation of Wnt-5a are necessary for its signalling. *Biochemical Journal* **402** (3):515-523.
- Lacin, H., Zhu, Y., Wilson, B. A., Skeath, J. B. (2014). Transcription factor expression uniquely identifies most postembryonic neuronal lineages in the *Drosophila* thoracic central nervous system. *Development* **141** (5):1011-1021
- Lahaye, L., Wouda, R. R. De Jong, A. W., Fradkin, L. G., Noordermeer, J. N. (2012). WNT5 Interacts with the Ryk Receptors Doughnut and Derailed to Mediate Muscle Attachment Site Selection in *Drosophila melanogaster*. *PLoS One* **7** (3):e32297
- Latres, E., Chiaur, D. S., Pagano, M. (1999). The human F box protein β -Trcp associates with the Cul1/Skp1 complex and regulates the stability of β -catenin. *Oncogene* **18** (4):849-854
- Lee, J., Ishimoto, A., Yanagawa, S. (1999). Characterization of Mouse Dishevelled (Dvl) Proteins in Wnt/Wingless Signaling Pathway. *Journal of Biological Chemistry* **274** (30):21464-21470
- Lee, T., Luo, L. (1999). Mosaic analysis with a repressible cell marker for studies of gene function in neuronal morphogenesis. *Neuron* **22** (3):451–461

References

- Li, V. S., Ng, S. S., Boersema, P. J., Low, T. Y., Karthaus, W. R., Gerlach, J. P., Mohammed, S., Heck, A. J., Maurice, M. M., Mahmoudi, T., Clevers, H. (2012). Wnt Signaling through Inhibition of β -Catenin Degradation in an Intact Axin1 Complex. *Cell* **149** (6):1245-1256
- Lin, D. M., Fetter, R. D., Kopczynski, C., Grenningloh, G., Goodman, C. S. (1994). Genetic analysis of Fasciclin II in *Drosophila*: defasciculation, refasciculation, and altered fasciculation. *Neuron* **13**(5):1055-69
- Lin, G., Xu, N., Xi, R. (2008). Paracrine Wingless signalling controls self-renewal of *Drosophila* intestinal stem cells. *Nature* **455** (7216):1119-1123
- Linnemannstöns, K. (2012). The transmembrane receptors Otk and Otk2 function redundantly in *Drosophila* Wnt signal transduction. Dissertation, University of Göttingen
- Linnemannstöns, K., Ripp, C., Honemann-Capito, M., Brechtel-Curth, K., Hedderich, M., Wodarz, A. (2014). The PTK7-Related Transmembrane Proteins Off-track and Off-track 2 Are Co-receptors for *Drosophila* Wnt2 Required for Male Fertility. *PLoS Genetics* **10** (7):e1004443
- Liu, C., Li, Y., Semenov, M., Han, C., Baeg, G., Tan, Yi., Zhang, Z., Lin, X., He, X. (2002). Control of β -Catenin Phosphorylation/Degradation by a Dual-Kinase Mechanism. *Cell* **108** (6):837-847
- Liu, Y., Shi, J., Lu, C., Wang, Z., Lyuksyutova, A.I., Song, X., Song, X., Zou, Y. (2005). Ryk-mediated Wnt repulsion regulates posterior-directed growth of corticospinal tract. *Nature Neuroscience* **8** (9):1151-1159
- Llimargas, M., Lawrence, P. (2001). Seven Wnt homologues in *Drosophila*: A case study of the developing tracheae. *Proceedings of the National Academy of Sciences* **98** (25):14487-14492
- Logan, C., Nusse, R. (2004) The Wnt Signaling Pathway in Development and Disease. *Cell and Developmental Biology* **20**:781–810
- Loth, J. (2014). Functional analysis of the neurospecific receptor kinase Dnrk in *Drosophila melanogaster*. MSc. Thesis, University of Göttingen
- Lowe, N., Rees, J. S., Roote, J., Ryder, E., Armean, I. M., Johnson, G., Drummond, E., Spriggs, H., Drummond, J., Magbanua, J. P., Naylor, H., Sanson, B., Bastock, R., Huelsmann, S., Trovisco, V., Landgraf, M., Knowles-Barley, S., Armstrong, J. D., White-Cooper, H., Hansen, C., Phillips, R. G., UK *Drosophila* Protein Trap Screening Consortium, Lilley, K. S., Russell, S., St Johnston, D. (2014). Analysis of the expression patterns, subcellular localisations and interaction partners of *Drosophila* proteins using a pigP protein trap library. *Development* **141** (20):3994-4005
- Lu, W., Yamamoto, V., Ortega, B., Baltimore, D. (2004a). Mammalian Ryk is a Wnt coreceptor required for stimulation of neurite outgrowth. *Cell* **119** (1):97-108

References

- Lu, X., Borchers, A., Jolicoeur, C., Rayburn, H., Baker, J. C., Tessier-Lavigne, M. (2004). Wnt proteins are lipid-modified and can act as stem cell growth factors. *Nature* **423** (6938):448-452
- MacDonald, B. T., Tamai, K., He, X. (2009). Wnt/ β -Catenin Signaling: Components, Mechanisms, and Diseases. *Developmental Cell* **17** (1):9-26
- Macheda, M., Sun, W. W., Kugathasan, K., Hogan, B. M., Bower, N.I., Halford, M. M., Zhang, Y. F., Jacques, B. E., Lieschke, G. J., Dabdoub, A., Stacker, S. A. (2012). The Wnt Receptor Ryk Plays a Role in Mammalian Planar Cell Polarity Signaling. *Journal of Biological Chemistry* **287** (35):29312-29323
- Mandile, E. (2013). Role of Otk and Otk2 in Wnt5/Derailed signaling in Drosophila, MSc. Thesis, University of Göttingen
- Mao, J., Wang, J., Liu, B., Pan, W., Farr, G. H. III, Flynn, C., Yuan, H., Takada, S., Kimelman, D., Li, L., Wu, D. (2001). Low-Density Lipoprotein Receptor-Related Protein-5 Binds to Axin and Regulates the Canonical Wnt Signaling Pathway. *Molecular Cell* **7** (4):801-809
- Marikawa, Y., Elinson, R. P. (1998) β -TrCP is a negative regulator of the Wnt/ β -catenin signaling pathway and dorsal axis formation in Xenopus embryos. *Mechanisms of Development* **77** (1):75-80
- Marrone, A. K., Kucherenko, M. M., Wiek, R., Göpfert, M. C., Shcherbata, H. R. (2011) Hyperthermic seizures and aberrant cellular homeostasis in Drosophila dystrophic muscles. *Scientific Reports* **1**:47
- Martinez-Arias, A., Lawrence, P. A. (1985). Parasegments and compartments in the Drosophila embryo. *Nature* **313** (6004):639-642
- Masiakowski, P., Carroll, R. D. (1992) A novel family of cell surface receptors with tyrosine kinase-like domain. *Journal of Biological Chemistry* **267** (36):26181-26190
- Matsuda, T., Nomi, M., Ikeya, M., Kani, S., Oishi, I., Terashima, T., Takada, S., Minami, Y. (2001). Expression of the receptor tyrosine kinase genes, Ror1 and Ror2, during mouse development. *Mechanisms of Development* **105** (1-2):153-156
- Matsuyama, M., Aizawa, S., Shimono, A. (2009). Sfrp Controls Apicobasal Polarity and Oriented Cell Division in Developing Gut Epithelium. *PLoS Genetics* **5** (3):e1000427
- McElwain, M., Ko, D. C., Gordon, M. D., Fyrst, H., Saba, J. D., Nusse, R. (2011). A Suppressor/Enhancer Screen in Drosophila Reveals a Role for Wnt-Mediated Lipid Metabolism in Primordial Germ Cell Migration. *PLoS One* **6** (11):e26993
- McMahon, A., Moon, R. T. (1989). Ectopic expression of the proto-oncogene int-1 in Xenopus embryos leads to duplication of the embryonic axis. *Cell* **58** (6):1075-1084
- Mikels, A., Nusse, R. (2006). Purified Wnt5a Protein Activates or Inhibits β -Catenin–TCF Signaling Depending on Receptor Context. *PLoS Biology* **4** (4):e115

References

- Miller, M., Steele, R. (2000). Lemon Encodes an Unusual Receptor Protein-Tyrosine Kinase Expressed during Gametogenesis in Hydra. *Developmental Biology* **224** (2):286-298
- Minami, Y., Oishi, I., Endo, M., Nishita, M. (2010). Ror-family receptor tyrosine kinases in noncanonical Wnt signaling: Their implications in developmental morphogenesis and human diseases. *Developmental Dynamics* **239** (1):1-15
- Molenaar, M., Van de Wetering, M., Oosterwegel, M., Peterson-Maduro, J., Godsave, S., Korinek, V., Roose, J., Destree, O., Clevers, H. (1996). XTcf-3 Transcription Factor Mediates β -Catenin-Induced Axis Formation in Xenopus Embryos. *Cell* **86** (3):391–399
- Moon, R. T. (1993). In pursuit of the functions of the Wnt family of developmental regulators: Insights from Xenopus laevis. *Bioessays* **15** (2):91-97
- Moreau-Fauvarque, C., Taillebourg, E., Boissoneau, E., Mesnard, J., Dura, J. M. (1998). The receptor tyrosine kinase gene linotte is required for neuronal pathway selection in the Drosophila mushroom bodies. *Mechanisms of Development* **78** (1-2):47–61
- Moreau-Fauvarque, C., Taillebourg, E., Pr  at, T., Dura, J. M. (2002). Mutation of linotte causes behavioral defects independently of pigeon in Drosophila. *NeuroReport* **13** (17):2309-2312
- M  ller-Tidow, C., Schw  ble, J., Steffen, B., Tidow, N., Brandt, B., Becker, K., Schulze-Bahr, E., Halfter, H., Vogt, U., Metzger, R., Schneider, P. M., B  chner, T., Brandts, C., Berdel, W. E., Serve, H. (2004). High-Throughput Analysis of Genome-Wide Receptor Tyrosine Kinase Expression in Human Cancers Identifies Potential Novel Drug Targets. *Clinical Cancer Research* **10** (4):1241-1249
- Mulligan, K. A., Fuerer, C., Ching, W., Fish, M., Willert, K., Nusse, R. (2012). Secreted Wingless-interacting molecule (Swim) promotes long-range signaling by maintaining Wingless solubility. *Proceedings of the National Academy of Sciences* **109** (2):370-377
- Mummery-Widmer, J. L., Yamazaki, M., Stoeger, T., Novatchkova, M., Bhalerao, S., Chen, D., Dietzl, G., Dickson, B. J., Knoblich, J. A. (2009). Genome-wide analysis of Notch signalling in Drosophila by transgenic RNAi. *Nature* **458** (7241):987-992
- Mu  oz, R., Moreno, M., Oliva, C., Orbenes, C., Larra  n, J. (2006). Syndecan-4 regulates non-canonical Wnt signalling and is essential for convergent and extension movements in Xenopus embryos. *Nature Cell Biology* **8** (5):492-500
- Neumann, C. J., Cohen, S. M. (1997). Long-range action of Wingless organizes the dorsal-ventral axis of the Drosophila wing. *Development* **124** (4):871-880
- Neumann, S., Coudreuse, D. Y. M., Van Der Westhuyzen, D. R., Eckhardt, E. R. M., Korswagen, H. C., Schmitz, G., Sprong, H. (2009). Mammalian Wnt3a is Released on Lipoprotein Particles. *Traffic* **10** (3):334-343
- Niehrs, C. (2012) The complex world of WNT receptor signalling, *Nature Reviews Molecular Cell Biology* **13** (12):767–779

References

- Nishita, M., Yoo, S. K., Nomachi, A., Kani, S., Sougawa, N., Ohta, Y., Takada, S., Kikuchi, A., Minami, Y. (2006). Filopodia formation mediated by receptor tyrosine kinase Ror2 is required for Wnt5a-induced cell migration. *Journal of Cell Biology* **175**(4):555-62
- Nishita, M., Itsukushima, S., Nomachi, A., Endo, M., Wang, Z., Inaba, D., Qiao, S., Takada, S., Kikuchi, A., Minami, Y. (2010). Ror2/Frizzled Complex Mediates Wnt5a-Induced AP-1 Activation by Regulating Dishevelled Polymerization. *Molecular and Cellular Biology* **30** (14):3610-3619
- Nomachi, A., Nishita, M., Inaba, D., Enomoto, M., Hamasaki, M., Minami, Y. (2008). Receptor Tyrosine Kinase Ror2 Mediates Wnt5a-induced Polarized Cell Migration by Activating c-Jun N-terminal Kinase via Actin-binding Protein Filamin A. *Journal of Cell Biology* **283** (241):27973-27981
- Nusse, R., Varmus, H. (1982) Many tumors induced by the mouse mammary tumor virus contain a provirus integrated in the same region of the host genome. *Cell* **31** (1):99–109
- Nusse, R., Brown, A., Shackleford, G., McMahon, A., Moon, R., Varmus, H. (1991) A New Nomenclature for int-1 and Related Genes: The Wnt Gene Family. *Cell* **64** (2):231
- Nüsslein-Vollhardt, C., Wieschaus, E. (1980). Mutations affecting segment number and polarity in *Drosophila*. *Nature* **287** (5785):795-801.
- Oates, A., Bonkovsky, J. L., Irvine, D. V., Kelly, L. E., Thomas, J. B., Wilks, A. F. (1998). Embryonic expression and activity of doughnut, a second RYK homolog in *Drosophila*. *Mechanisms of Development* **78** (1-2):165-169
- Oldridge, M., Fortuna, A. M., Maringa, M., Propping, P., Mansour, S., Pollitt, C., DeChiara, T. M., Kimble, R. B., Valenzuela, D. M., Yancopoulos, G. D., Wilkie, A. O. M. (2000). Dominant mutations in ROR2, encoding an orphan receptor tyrosine kinase, cause brachydactyly type B. *Nature Genetics* **24** (3):275-278
- Oishi, I., Sugiyama, S., Liu, Z., Yamamura, H., Nishida, Y., Minami, Y. (1997). A Novel *Drosophila* Receptor Tyrosine Kinase Expressed Specifically in the Nervous System. *Journal of Cell Biology* **272** (18):11916-11923
- Oishi, I., Takeuchi, S., Hashimoto, R., Nagabukuro, A., Ueda, T., Liu, Z. J., Hatta, T., Akira, S., Matsuda, Y., Yamamura, H., Otani, H., Minami, Y. (1999). Spatio-temporally regulated expression of receptor tyrosine kinases, mRor1, mRor2, during mouse development: implications in development and function of the nervous system. *Genes to Cells* **4** (1):41-56
- Oishi, I., Suzuki, H., Onishi, N., Takada, R., Kani, S., Ohkawara, B., Koshida, I., Suzuki, K., Yamada, G., Schwabe, G. C., Mundlos, S., Shibuya, H., Takada, S., Minami, Y. (2003). The receptor tyrosine kinase Ror2 is involved in non-canonical Wnt5a/JNK signalling pathway. *Genes to Cells* **8** (7):645-654.
- Panáková, D., Sprong, H., Marois, E., Thiele, C., Eaton, S. (2005). Lipoprotein particles are required for Hedgehog and Wingless signalling. *Nature* **435** (7038):58-65

References

- Park, W., Liu, J., Adler, P. N. (1994). frizzled Gene expression and development of tissue polarity in the *Drosophila* wing. *Developmental Genetics* **15** (4):383-389
- Park, M., Wu, X., Golden, K., Axelrod, J. D., Bodmer, R. (1996). The Wingless Signaling Pathway Is Directly Involved in *Drosophila* Heart Development. *Developmental Biology* **177** (1):104-116
- Parr, B. A., McMahon, A. P. (1995). Dorsalizing signal Wnt-7a required for normal polarity of D–V and A–P axes of mouse limb. *Nature* **374** (6520):350-353
- Parr, B. A., McMahon, A. P. (1998). Sexually dimorphic development of the mammalian reproductive tract requires Wnt-7a. *Nature* **395** (6703):707-710
- Patel, M. S., Karsenty, G. (2002) Regulation of Bone Formation and Vision by LRP5, *New England Journal of Medicine* **346** (20):1572–1574
- Patthy L. (2000). The WIF module. *Trends in Biological Science* **25** (1):12-13
- Paudyal, A., Damrau, C., Patterson, V.L., Ermakov, A., Formstone, C., Lallane, Z., Wells, S., Lu, X., Norris, D. P., Dean, C. H., Henderson, D. J., Murdoch, J. N. (2010). The novel mouse mutant, *chuzhoi*, has disruption of Ptk7 protein and exhibits defects in neural tube, heart and lung development and abnormal planar cell polarity in the ear. *BMC Developmental Biology* **10**:87
- Payre, F., Vincent, A., Carreno, S. (1999). *Ovo/svb* integrates Wingless and DER pathways to control epidermis differentiation. *Nature* **400** (6741):271-275
- Peradziryi, H., Kaplan, N. A., Podleschny, M., Liu, X., Wehner, P., Borchers, A., Tolwinski, N. (2011). PTK7/Otk interacts with Wnts and inhibits canonical Wnt signalling. *The EMBO Journal* **30** (18):3729-3740
- Petrova, I. M. (2014). Non-canonical Wnt Signaling via the Ryk and Ror Receptors in the *Drosophila* Nervous System. PhD thesis, Leiden University
- Piao, S., Lee, S., Kim, H., Yum, S., Stamos, J. L., Xu, Y., Lee, S., Lee, J., Oh, S., Han, J., Park, B., Weis, W. I., Ha, N. (2008). Direct Inhibition of GSK3 β by the Phosphorylated Cytoplasmic Domain of LRP6 in Wnt/ β -Catenin Signaling. *PLOS One* **3** (12):e4046
- Podleschny, M. (2011) Analyzing the Function of PTK7 in Cell Migration. Dissertation, Georg-August-University Göttingen
- Polakis, P. (2012) Wnt signaling in cancer., *Cold Spring Harbor Perspectives in Biology* **4** (5)
- Pulido, D., Campuzano, S., Koda, T., Modolell, J., Barbacid, M. (1992) *Dtrk*, a *Drosophila* gene related to the *trk* family of neurotrophin receptors, encodes a novel class of neural cell adhesion molecule. *The EMBO Journal* **11** (2):391-404
- Puppo, F., Thomé, V., Lhoumeau, A., Cibois, M., Gangar, A., Lembo, F., Belotti, E., Marchetto, S., Lécine, P., Prébet, T., Sebbagh, M., Shin, W., Lee, S., Kodjabachian, L., Borg, J. (2011). Protein tyrosine kinase 7 has a conserved role in Wnt/ β -catenin canonical signalling. *EMBO Reports* **12** (1):43-49

References

- Qian, D., Jones, C., Rzadzinska, A., Mark, S., Zhang, X., Steel, K. P., Dai, X., Chen, P. (2007). Wnt5a functions in planar cell polarity regulation in mice. *Developmental Biology* **306** (1):121–133
- Reya, T., Clevers, H. (2005). Wnt signalling in stem cells and cancer. *Nature* **434** (7035):843–850
- Rijsewijk, F., Schuermann, M., Wagenaar, E., Parren, P., Weigel, D., Nusse, R. (1987) The Drosophila homology of the mouse mammary oncogene int-1 is identical to the segment polarity gene wingless. *Cell* **50** (4):649-657
- Rulifson, E. J., Wu, C. H., Nusse, R. (2000). Pathway Specificity by the Bifunctional Receptor Frizzled Is Determined by Affinity for Wingless. *Molecular Cell* **6** (1):117-126
- Russell, J., Gennissen, A., Nusse, R. (1992). Isolation and expression of two novel Wnt/wingless gene homologues in Drosophila. *Development* **115** (2):475-485
- Sakane, H., Yamamoto, H., Matsumoto, S., Sato, A., Kikuchi, A. (2012). Localization of glypican-4 in different membrane microdomains is involved in the regulation of Wnt signaling. *Journal of Cell Science* **125** (Pt 2):449–460
- Sakurai, M., Aoki, T., Yoshikawa, S., Santschi, L. A., Saito, H., Endo, K., Ishikawa, K., Kimura, K., Ito, K., Thomas, J. B., Hama, C. (2009). Differentially Expressed Drl and Drl-2 Play Opposing Roles in Wnt5 Signaling during Drosophila Olfactory System Development. *The Journal of Neuroscience* **29** (15):4972-4980
- Sambrook, J., Fritsch, E. F., Maniatis, T. (1989). Molecular cloning: a laboratory manual, 2nd edition. Cold Spring Harbor Laboratory, Cold Spring Harbor, New York.
- Sato, A., Kojima, T. Ui-Tei, K., Miyata, Y., Saigo, K. (1999). Dfrizzled-3, a new Drosophila Wnt receptor, acting as an attenuator of Wingless signaling in wingless hypomorphic mutants. *Development* **126** (20):4421-30
- Sato, A., Khadka, D. K., Liu, W., Bharti, R., Runnels, L. W., Dawid, I. B., Habas, R. (2006). Profilin is an effector for Daam1 in non-canonical Wnt signaling and is required for vertebrate gastrulation. *Development* **133** (21):4219-4231
- Savant-Bhonsale, S., Friese, M., McCoon, P., Montell, D. J. (1999). A Drosophila Derailed homolog, Doughnut, expressed in invaginating cells during embryogenesis. *Gene* **231**:155-161
- Schambony, A., Wedlich, D. (2007). Wnt-5A/Ror2 Regulate Expression of XPAPC through an Alternative Noncanonical Signaling Pathway. *Developmental Cell* **12** (5):779-792
- Schindelfholz, B., Knirr, M., Warrior, R., Zinn, K. (2001). Regulation of CNS and motor axon guidance in Drosophila by the receptor tyrosine phosphatase DPTP52F. *Development* **128** (21):4371-4382
- Schneider, I. (1972). Cell lines derived from late embryonic stages of Drosophila melanogaster. *Journal of Embryology and Experimental Morphology* **27** (2):353-65

References

- Schmidt-Ott, U., Technau, G. M. (1992). Expression of *en* and *wg* in the embryonic head and brain of *Drosophila* indicates a refolded band of seven segment remnants. *Development* **116** (1):111-125
- Sharma, R. P., Chopra, V. L. (1976). Effect of the Wingless (*wg1*) mutation on wing and haltere development in *Drosophila melanogaster*. *Developmental Biology* **48** (2):461-465
- Shimizu, H., Julius, M. A., Giarre, M., Zheng, Z., Brown, A. M., Kitajewski, J. (1997). Transformation by Wnt family proteins correlates with regulation of beta-catenin. *Cell Growth and Differentiation* **8** (12):1349-1358
- Shnitsar, I., Borchers, A. (2008). PTK7 recruits dsh to regulate neural crest migration. *Development* **135** (24):4015-4024
- Siegfried, E., Perrimon, N. (1994) *Drosophila* wingless: A paradigm for the function and mechanism of Wnt signaling. *Bioessays* **16** (6):395-404
- Simons, M., Mlodzik, M. (2008). Planar cell polarity signaling: from fly development to human disease. *Annual Review of Genetics* **42**:517-540
- Sivasankaran, R., Calleja, M., Morata, G., Basler, K. (2000). The Wingless target gene *Dfz3* encodes a new member of the *Drosophila* Frizzled family. *Mechanisms of Development* **91** (1-2):427-431
- Songyang, Z., Cantley, L. C. (1995). Recognition and specificity in protein tyrosine kinase-mediated signalling. *Trends in Biochemical Science* **20** (11):470-475
- Sossin, W.S. (2006). Tracing the Evolution and Function of the Trk Superfamily of Receptor Tyrosine Kinases. *Brain, Behavior and Evolution* **68** (3):145-156
- Staal, F. J., Luis, T. C., Machteld, M. M. Tiemessen (2008). WNT signalling in the immune system: WNT is spreading its wings. *Nature Reviews Immunology* **8** (8):581-593
- Stacker S.A., Hovens, C. M., Vitali, A., Pritchard, M. A., Baker, E., Sutherland, G. R., Wilks, A. F. (1993). Molecular cloning and chromosomal localisation of the human homologue of a receptor related to tyrosine kinases (RYK). *Oncogene* **8** (5):1347-1356
- St. Pierre, S. E., Ponting, L., Stefancsik, R., McQuilton, P. and the FlyBase Consortium (2014). FlyBase 102 - advanced approaches to interrogating FlyBase. *Nucleic Acids Research* **42**:D780-788
- Strapps, W. S.; Tomlinson, A. (2001). Transducing properties of *Drosophila* Frizzled proteins. *Development* **128** (23):4829-4835
- Struhl, G., Basler, K. (1993). Organizing activity of wingless protein in *Drosophila*. *Cell* **72** (4):527-540
- Strutt, D. I. (2001). Asymmetric Localization of Frizzled and the Establishment of Cell Polarity in the *Drosophila* Wing. *Molecular Cell* **7** (2):367-375

References

- Strutt, D., Johnson, R., Cooper, K., Bray, S. (2002). Asymmetric Localization of Frizzled and the Determination of Notch-Dependent Cell Fate in the *Drosophila* Eye. *Current Biology* **12** (10):813-824
- Strutt, D. (2003). Frizzled signalling and cell polarisation in *Drosophila* and vertebrates. *Development* **130** (19):4501-4513
- Su, Y., Fu, C., Ishikawa, S., Stella, A., Kojima, M., Shitoh, K., Schreiber, E. M., Day, B. W., Liu, B. (2008). APC is essential for targeting phosphorylated beta-catenin to the SCF β -TrCP ubiquitin ligase. *Molecular Cell* **32** (5):652-61.
- Sun, Q., Schindelfholz, B., Knirr, M., Schmid, A., Zinn, K. (2001). Complex Genetic Interactions among Four Receptor Tyrosine Phosphatases Regulate Axon Guidance in *Drosophila*. *Molecular and Cellular Neuroscience* **17** (2):274-291
- Swarup, S., Verheyen, E. M. (2012). Wnt/Wingless signaling in *Drosophila*. *Cold Spring Harbor Perspectives in Biology* **4** (6)
- Tada, M., Smith, J. (2000). Xwnt11 is a target of *Xenopus* Brachyury: regulation of gastrulation movements via Dishevelled, but not through the canonical Wnt pathway. *Development* **127** (10):2227-2238
- Taillebourg, E., Moreau-Fauvarque, C., Delaval, K., Dura, J. M. (2005). In vivo evidence for a regulatory role of the kinase activity of the linotte/derailed receptor tyrosine kinase, a *Drosophila* Ryk ortholog. *Development Genes and Evolution* **215** (3):158-163
- Takada, R., Satomi, Y., Kurata, T., Ueno, N., Norioka, S., Kondoh, H., Takao, T., Takada, S. (2006). Monounsaturated Fatty Acid Modification of Wnt Protein: Its Role in Wnt Secretion. *Developmental Cell* **11** (6):791-801
- Takeuchi, S., Takeda, K., Oishi, I., Nomi, M., Ikeya, M., Itoh, K., Tamura, S., Ueda, T., Hatta, T., Otani, H., Terashima, T., Takada, S., Yamamura, H., Akira, S., Minami, Y. (2000). Mouse Ror2 receptor tyrosine kinase is required for the heart development and limb formation. *Genes to Cells* **5** (1):71-78
- Tamai, K., Semenov, M., Kato, Y., Spokony, R., Liu, C., Katsuyama, Y., Hess, F., Saint-Jeannet, J., He, X. (2000). LDL-receptor-related proteins in Wnt signal transduction. *Nature* **407** (6803):530-535
- Tao, Q., Yokota, C., Puck, H., Kofron, M., Birsoy, B., Yan, D., Asashima, M., Wylie, C., Lin, W., Heasman, J. (2005). Maternal Wnt11 Activates the Canonical Wnt Signaling Pathway Required for Axis Formation in *Xenopus* Embryos. *Cell* **120** (6):857-871
- Thomas, K. R., Capecchi, M. R. (1990). Targeted disruption of the murine int-1 proto-oncogene resulting in severe abnormalities in midbrain and cerebellar development. *Nature* **346** (6287):847-850
- Tolwinski, N. S., Wehrli, M., Rives, A., Erdeniz, N., DiNardo, S., Wieschaus, E. (2003). Wg/Wnt Signal Can Be Transmitted through Arrow/LRP5,6 and Axin Independently of Zw3/Gsk3 β Activity. *Developmental Cell* **4** (3):407-418

References

- Umbhauer, M., Djiane, A., Goisset, C., Penzo-Méndez, A., Riou, J., Boucaut, J., Shi, D. (2000). The C-terminal cytoplasmic Lys-Thr-X-X-X-Trp motif in frizzled receptors mediates Wnt/ β -catenin signalling. *The EMBO Journal* **19** (18):4944-4954
- Urbach, R., Technau, G.M. (2003). Segment polarity and DV patterning gene expression reveals segmental organization of the Drosophila brain. *Development* **130** (16): 3607--3620
- Urbach, R., Technau, G. M. (2008) Dorsoventral patterning of the brain: a comparative approach. *Advances in Experimental Medicine and Biology* **628**:42-56
- Van Amerongen, R., Mikels, A., Nusse, R. (2008). Alternative wnt signaling is initiated by distinct receptors. *Science Signaling* **1** (35):re9
- Van Ooyen, A., Nusse, R. (1984). Structure and nucleotide sequence of the putative mammary oncogene int-1; proviral insertions leave the protein-encoding domain intact. *Cell* **39** (1):233-240
- Van Ooyen, A., Kwee, V., Nusse, R. (1985). The nucleotide sequence of the human int-1 mammary oncogene; evolutionary conservation of coding and non-coding sequences. *The EMBO Journal* **4** (11):2905-2909
- Vinson, C., Conover, S., Adler, P. (1989). A Drosophila tissue polarity locus encodes a protein containing seven potential transmembrane domains. *Nature* **338** (6212):263-264
- Venken, K. J., Carlson, J. W., Schulze, K. L., Pan, H., He, Y., Spokony, R., Wan, K. H., Koriabine, M., De Jong, P. J., White, K. P., Bellen, H. J., Hoskins, R. A. (2009). Versatile P[acman] BAC libraries for transgenesis studies in Drosophila melanogaster. *Nature Methods* **6** (6):431-434
- Wallingford, J. B., Harland, R. M. (2001). Neural tube closure requires Dishevelled-dependent convergent extension of the midline. *Development* **129** (24):5815-5825
- Wallingford, J. B., Habas, R. (2005). The developmental biology of Dishevelled: an enigmatic protein governing cell fate and cell polarity. *Development* **132** (20):4421-4436
- Wang, J., Mark, S., Zhang, X., Qian, D., Yoo, S. J. (2005). Regulation of polarized extension and planar cell polarity in the cochlea by the vertebrate PCP pathway. *Nature Genetics* **37** (9):980–985
- Wang, Y., Zhang, J., Mori, S., Nathans, J. (2006). Axonal Growth and Guidance Defects in Frizzled3 Knock-Out Mice: A Comparison of Diffusion Tensor Magnetic Resonance Imaging, Neurofilament Staining, and Genetically Directed Cell Labeling. *The Journal of Neuroscience* **26** (2):355-364
- Wang, Y., Guo, N., Nathans, J. (2006b). The Role of Frizzled3 and Frizzled6 in Neural Tube Closure and in the Planar Polarity of Inner-Ear Sensory Hair Cells. *The Journal of Neuroscience* **26** (8):2147-2156

References

- Wang, B., Sinha, T., Jiao, K., Serra, R., Wang, J. (2011). Disruption of PCP signaling causes limb morphogenesis and skeletal defects and may underlie Robinow syndrome and brachydactyly type B. *Human Molecular Genetics* **20** (2):271-285
- Wang, J., Sinha, T., Wynshaw-Boris, A. (2012) Wnt Signaling in Mammalian Development: Lessons from Mouse Genetics, *Cold Spring Harbor Perspectives in Biology* **4**:a007963
- Warming, S., Costantino, N., Court, D. L., Jenkins, N. A., Copeland, N. G. (2005). Simple and highly efficient BAC recombineering using galK selection. *Nucleic Acids Research* **33** (4):e36
- Wehner, P., Shnitsar, I., Urlaub, H., Borchers, A. (2011). RACK1 is a novel interaction partner of PTK7 that is required for neural tube closure. *Development* **138** (7):1321-1327
- Wehrli, M., Dougan, S. T., Caldwell, K., O'Keefe, L., Schwartz, S., Vaizel-Ohayon, D., Schejter, E., Tomlinson, A., DiNardo, S. (2000). Arrow encodes an LDL-receptor-related protein essential for Wingless signalling. *Nature* **407** (6803):527-530
- Willert, K., Brink, M., Wodarz, A., Varmus, H., Nusse, R. (1997). Casein kinase 2 associates with and phosphorylates Dishevelled. *The EMBO Journal* **16** (11):3089-3096
- Willert, K., Brown, J. D., Danenberg, E., Duncan, A. W., Weissman, I. L., Reya, T., Yates, Y. R., Nusse, R. (2003). Wnt proteins are lipid-modified and can act as stem cell growth factors. *Nature* **423** (6938):448-452
- Willert, K., Nusse, R. (2012). Wnt Proteins. *Cold Spring Harbor Perspectives in Biology* **4** (9):a007864
- Wilson, C., Goberdhan, D. C., Steller, H. (1993). Dror, a potential neurotrophic receptor gene, encodes a Drosophila homolog of the vertebrate Ror family of Trk-related receptor tyrosine kinases. *Proceedings of the National Academy of Sciences* **90** (15):7109-7113
- Winberg, M. L., Tamagnone, L., Bai, J., Comoglio, P. M., Montell, D., Goodman, C. S. (2001). The transmembrane protein Off-track associates with Plexins and functions downstream of Semaphorin signaling during axon guidance. *Neuron* **32** (1):53-62
- Wodarz, A., Nusse, R. (1998). Mechanisms of Wnt Signaling in Development. *Cell and Developmental Biology* **14**:59–88
- Wong, G. T., Gavin, B. J., McMahon, A. P. (1994). Differential transformation of mammary epithelial cells by Wnt genes. *Molecular and Cellular Biology* **14** (9):6278-6286
- Wong, H., Bourdelas, A., Krauss, A., Lee, H., Shao, Y., Wu, D., Mlodzik, M., Shi, D., Zheng, J. (2003). Direct Binding of the PDZ Domain of Dishevelled to a Conserved Internal Sequence in the C-Terminal Region of Frizzled. *Molecular Cell* **12** (5):1251–1260
- Wouda, R., Bansraj, M., De Jong, A. W. M., Noordermeer, J N., Fradkin, L. G. (2008). Src family kinases are required for WNT5 signaling through the Derailed/RYK receptor in the Drosophila embryonic central nervous system. *Development* **135** (13):2277-2287

References

- Wu, C., Nusse, R. (2002). Ligand Receptor Interactions in the Wnt Signaling Pathway in *Drosophila*. *Journal of Biological Chemistry* **277** (44):41762-41769
- Wu, J., Roman, A., Carvajal-Gonzalez, J., Mlodzik, M. (2013). Wg and Wnt4 provide long-range directional input to planar cell polarity orientation in *Drosophila*. *Nature Cell Biology* **15** (9):1045-1055.
- Yamaguchi, T. P., Bradley, A., McMahon, A. P., Jones, S. (1999). A Wnt5a pathway underlies outgrowth of multiple structures in the vertebrate embryo. *Development* **126** (6):1211-1223
- Yamaguchi, T. (2001) Heads or tails: Wnts and anterior–posterior patterning. *Current Biology* **11** (17):R713-724
- Yamamoto, S., Nishimura, O., Misaki, K., Nishita, M., Minami, Y., Yonemura, S., Tarui, H., Sasaki, H. (2008). Cthrc1 Selectively Activates the Planar Cell Polarity Pathway of Wnt Signaling by Stabilizing the Wnt-Receptor Complex. *Developmental Cell* **15** (1):23-36
- Yanagawa, S., Van Leeuwen, F., Wodarz, A., Klingensmith, J., Nusse, R. (1995) The dishevelled protein is modified by wingless signaling in *Drosophila*. *Genes and Development* **9** (9):1087-1097
- Yanagawa, S., Lee, J. S., Ishimoto, A. (1998). Identification and characterization of a novel line of *Drosophila* Schneider S2 cells that respond to wingless signaling. *Journal of Biological Chemistry* **273** (48):32353-32359
- Yanagawa, S., Matsuda, Y., Lee, J., Matsubayashi, H., Sese, S., Kadowaki, T., Ishimoto, A. (2002). Casein kinase I phosphorylates the Armadillo protein and induces its degradation in *Drosophila*. *The EMBO Journal* **21** (7):1733-1742
- Yao, Y., Wu, Y., Yin, C., Ozawa, R., Aigaki, T., Wouda, R., Noordermeer, J., Fradkin, L. G., Hing, H. (2007). Antagonistic roles of Wnt5 and the Drl receptor in patterning the *Drosophila* antennal lobe. *Nature Neuroscience* **10** (11):1423-1432
- Yen, W., Williams, M., Periasamy, A., Conaway, M., Burdsal, C., Keller, R., Lu, X., Sutherland, A. (2009). PTK7 is essential for polarized cell motility and convergent extension during mouse gastrulation. *Development* **136** (12):2039-2048
- Yoda, A., Oishi, I., Minami, Y. (2003). Expression and Function of the Ror-Family Receptor Tyrosine Kinases During Development: Lessons from Genetic Analyses of Nematodes, Mice, and Humans. *Journal of Receptors and Signal Transduction* **23** (11):1-15
- Yoshikawa, S., Bonkowsky, J. L., Kokel, M., Shyn, S., Thomas, J. B. (2001). The derailed guidance receptor does not require kinase activity in vivo. *Journal of Neuroscience* **21** (1):RC119
- Yoshikawa, S., McKinnon, R. D., Kokel, M., Thomas, J. B. (2003). Wnt-mediated axon guidance via the *Drosophila* Derailed receptor. *Nature* **422** (6932):583-588

References

- Yuan, R. H., Jeng, Y. M., Hu, R. H., Lai, P. L., Lee, P. H., Cheng, C. C., Hsu, H. C. (2011). Role of p53 and β -catenin mutations in conjunction with CK19 expression on early tumor recurrence and prognosis of hepatocellular carcinoma. *Journal of Gastrointestinal Surgery* **15** (2):321-329
- Zallen, J. A., Wieschaus, E. (2004). Patterned Gene Expression Directs Bipolar Planar Polarity in *Drosophila*. *Developmental Cell* **6** (3):343-355
- Zallen, J.A. (2007). Planar Polarity and Tissue Morphogenesis. *Cell* **129** (6):1051-1063
- Zeng, X., Tamai, K., Doble, B., Li, S., Huang, H., Habas, R., Okamura, H., Woodgett, J., He, X. (2005). A dual-kinase mechanism for Wnt co-receptor phosphorylation and activation. *Nature* **438** (7069):873-877
- Zheng, L., Zhang, J., Carthew, R. W. (1995). Frizzled regulates mirror-symmetric pattern formation in the *Drosophila* eye. *Development* **121** (9):3045-3055
- Zheng, L., Michelson, Y., Freger, V., Avraham, Z., Venken, K. J., Bellen, H. J., Justice, M. J., Wides, R. (2011). *Drosophila* Ten-m and filamin affect motor neuron growth cone guidance *PLoS One* **6** (8):e22956

6. Appendix

Log2FC: log₂ fold change

patj: adjusted p-value

AGW: AG Wodarz (M. Tiwari)

TAL: Transcriptome analysis lab

red highlights indicate genes removed in the respective mutants

Genes upregulated in *Ror*⁴ mutant vs. WT

	Gene_ID	Description	log2FC		patj	
			AGW	TAL	AGW	TAL
1	Cyp4p2	Cyp4p2	6,04	6,01	1,8808E-248	0
2	CG13083	-	5,84	5,73	8,47245E-92	2,46E-136
3	CG42822	-	4,02	3,55	6,6086E-62	5,85E-42
4	Lcp3	Larval cuticle protein 3	3,5	3,15	6,12934E-18	1,7E-17
5	CG15483	-	3,45	3,23	3,68633E-08	5,68E-13
6	CG31769	-	3,31	3,13	2,60385E-11	1,96E-19
7	TotF	Turandot F	2,87	2,67	2,67169E-34	3,45E-23
8	lectin-24A	lectin-24A	2,85	2,6	2,8498E-10	1,74E-11
9	CG40472	-	2,78	2,8	3,13362E-18	1,14E-36
10	CG13947	-	2,61	2,45	2,34438E-08	8,26E-13
11	CG31918	-	2,57	2,2	1,93644E-28	1,52E-44
12	Phae2	Phaedra 2	2,56	2,3	1,41648E-11	8,33E-12
13	CG12868	-	2,55	2,2	2,59425E-41	6,13E-11
14	CG14715	-	2,48	2,23	4,78575E-34	1,45E-18
15	CG5866	-	2,43	2,04	0,000012986	0,00000323
16	CG40298	-	2,4	2,34	1,74788E-14	1,19E-19
17	CG17633	-	2,38	2,04	3,82134E-07	9,18E-08
18	CG42365	-	2,32	1,83	2,45391E-07	0,0000406
19	CG8620	-	2,32	1,39	0,001045579	0,0139
20	Cpr30F	Cuticular protein 30F	2,29	2,43	0,002826022	0,00000117
21	CR43460	-	2,28	2	3,82617E-05	0,000000857
22	CG7366	-	2,21	2,02	1,26751E-08	1,89E-10
23	CG43630	-	2,21	1,66	0,000163847	0,0000708
24	CG3355	-	2,16	2,04	1,76913E-09	1,55E-09

Appendix

25	CG17470	-	2,14	2,02	0,000195682	0,000000499
26	Tpc2	Thiamine pyrophosphate carrier protein 2	2,13	1,32	4,23133E-08	0,00118
27	Ect3	Ectoderm-expressed 3	2,1	2,03	3,65901E-63	1,58E-44
28	fd59A	forkhead domain 59A	2,08	2,07	6,6086E-62	6,69E-153
29	CG32201	-	2,02	1,54	0,012628479	0,00606
30	Lsp1alpha	Larval serum protein 1 alpha	1,97	1,27	0,015504217	0,0332
31	CG5770	-	1,94	2,02	0,000684382	0,000000214
32	Victoria	Victoria	1,93	1,56	1,96458E-06	0,0000216
33	gom	gomdanji	1,92	1,99	6,74427E-05	1,07E-12
34	b6	b6	1,92	1,59	6,61494E-06	0,0000497
35	CG42367	-	1,9	2,02	0,008629519	0,00000194
36	Phae1	Phaedra 1	1,9	1,85	0,004367657	0,0000029
37	CG33299	-	1,89	1,73	0,015504217	0,000566
38	CG17127	-	1,89	1,51	3,54956E-05	0,000634
39	CG31913	-	1,86	1,53	0,02350322	0,00493
40	Ir76a	Ionotropic receptor 76a	1,82	1,75	2,87653E-18	5,29E-19
41	CG12917	-	1,73	1,86	0,04844124	0,000473
42	CG13154	-	1,73	1,65	7,55042E-09	1,06E-10
43	CG6280	-	1,72	1,68	1,33067E-13	1,78E-25
44	mthl11	methuselah-like 11	1,72	1,65	0,045697815	0,00282
45	Ir87a	Ionotropic receptor 87a	1,72	1,6	2,7494E-08	0,000000506
46	CG17681	-	1,71	1,8	0,003539685	0,00000142
47	CG8568	-	1,7	1,58	2,16576E-08	8,8E-09
48	CG8170	-	1,7	1,52	3,23871E-05	0,00000361
49	Cpr92A	Cuticular protein 92A	1,69	1,67	0,048257148	0,000818
50	CG14642	-	1,69	1,44	1,45073E-11	0,000000197
51	CG1698	-	1,68	1,62	3,71016E-08	2,26E-12
52	CG4398	-	1,67	1,58	9,26163E-12	1,98E-10
53	CG10924	-	1,67	1,56	2,57938E-32	0,00000155
54	ana2	anastral spindle 2	1,65	1,63	1,18563E-12	1,76E-17
55	CG14770	-	1,63	1,38	0,000069769	0,000369
56	CG33468	-	1,62	1,2	0,028786156	0,0325
57	CG9737	-	1,59	1,34	2,06671E-06	0,000197
58	Lcp4	Larval cuticle protein 4	1,58	1,4	6,49688E-07	0,000178
59	snoRNA:la-c	-	1,58	1,23	0,039183256	0,0278
60	CG10131	-	1,57	1,59	0,000762777	0,000000162
61	Cpr64Ad	Cuticular protein 64Ad	1,54	1,24	0,000236156	0,00299

Appendix

62	CG30091	-	1,53	1,54	0,015162893	0,0000238
63	CG15005	-	1,53	1,5	9,82944E-50	1,4E-37
64	CG14625	-	1,52	1,37	0,004930692	0,00083
65	CG5928	-	1,51	1,2	0,010128742	0,0131
66	CG11060	-	1,49	1,51	0,005476343	0,00000251
67	CG42854	-	1,48	1,58	0,0007775	0,00000589
68	ChLD3	ChLD3	1,48	1,41	8,15265E-13	2,02E-10
69	CG9518	-	1,47	1,33	0,018842248	0,00222
70	CG14257	-	1,46	1,36	1,69115E-10	0,000000153
71	CG8908	-	1,45	1,45	0,000035768	0,0000305
72	CG6290	-	1,43	1,35	0,001617215	0,00022
73	snoRNA: Me28S- C788b	-	1,43	1,29	0,006011853	0,000319
74	TwldG	TweedleG	1,43	1,2	0,001336991	0,00369
75	GstE9	Glutathione S transferase E9	1,42	1,37	0,000291323	0,00000265
76	CG4998	-	1,42	1,26	0,008306299	0,00146
77	TwldF	TweedleF	1,41	1,13	0,029647965	0,0297
78	Muc91C	Mucin 91C	1,4	1,14	0,012994245	0,0162
79	TwldE	TweedleE	1,4	1,01	8,21664E-05	0,0324
80	phr	photorepair	1,38	1,37	7,62336E-23	2,6E-39
81	CG32548	-	1,38	1,18	0,000401977	0,00223
82	CG5621	-	1,36	1,31	0,00013959	6,83E-08
83	CG14892	-	1,34	1,16	6,39783E-05	0,000942
84	CG12540	-	1,34	1,15	1,67179E-05	0,00107
85	CG6357	-	1,33	1,24	3,56188E-06	3,38E-08
86	CG6347	-	1,33	1,2	0,000109816	0,000463
87	CG4440	-	1,32	1,28	0,049952229	0,00177
88	CG3777	-	1,31	1,26	2,50697E-05	4,15E-08
89	CG8854	-	1,31	1,2	1,9895E-08	0,0000178
90	CG6106	-	1,3	1,34	9,88442E-13	4,73E-17
91	CG34382	-	1,3	1,14	0,002798307	0,000895
92	CG32302	-	1,3	1,07	0,000588724	0,00882
93	CG8757	-	1,28	1,26	0,000956992	5,71E-08
94	CG5756	-	1,27	1,22	0,000000001	4,51E-10
95	CG14757	-	1,26	1,24	3,80555E-05	0,00000171
96	Cht6	Cht6	1,26	1,19	0,010106291	0,000562
97	CG7201	-	1,25	1,18	1,09464E-05	0,00000534

Appendix

98	CG42319	-	1,25	1,15	1,46573E-05	0,000137
99	CG30380	-	1,24	1,16	0,00249365	0,000261
100	CG34221	-	1,24	1,15	0,015398857	0,00458
101	GstD10	Glutathione S transferase D10	1,24	1,05	0,007789481	0,00614
102	CG34057	-	1,24	1,03	4,64093E-07	0,0000576
103	CG14089	-	1,24	1,01	0,044529516	0,0285
104	CG30187	-	1,23	1,24	4,47325E-05	3,92E-11
105	HP6	Heterochromatin protein 6	1,23	1,21	0,007014414	0,00000653
106	Spn85F	Serpin 85F	1,23	1,19	0,031571765	0,000293
107	CG31810	-	1,23	1,18	6,45911E-05	0,0000932
108	Gadd45	Gadd45	1,22	1,16	2,09859E-12	2,36E-08
109	lambdaTry	lambdaTry	1,21	1,16	0,006404457	0,00164
110	CG5011	-	1,21	1,14	7,02917E-05	0,00144
111	CG6470	-	1,2	1,29	0,016643114	0,0000115
112	CG6409	-	1,2	1,08	3,66653E-07	0,000357
113	CG9664	-	1,19	1,2	1,24199E-17	2,45E-33
114	CG13216	-	1,19	1,03	0,000155251	0,00338
115	Cralbp	Cellular retinaldehyde binding protein	1,17	1,11	0,001944975	0,001
116	TwdIT	TweedleT	1,17	1,05	0,000184914	0,00132
117	CR43883	-	1,15	1,14	0,027287774	0,000514
118	CG8192	-	1,15	1,06	5,19366E-05	0,000243
119	CG18641	-	1,14	1,05	7,12936E-05	0,000215
120	CG4686	-	1,14	1,05	9,64126E-07	0,000000709
121	CG42821	-	1,14	1,01	0,016643114	0,0118
122	CG13868	-	1,13	1,1	3,40338E-07	0,000000317
123	CG7330	-	1,13	1,04	0,001733277	0,00465
124	CG10264	-	1,13	1,02	0,002217922	0,00362
125	Msr-110	Msr-110	1,12	1,09	0,000000019	9,37E-09
126	Tequila	Tequila	1,11	1,07	3,70654E-05	0,0000188
127	CG4415	-	1,09	1,1	0,001236483	0,000000383
128	CG34220	-	1,09	1,03	0,001655147	0,0000188
129	CG17329	-	1,08	1,07	0,030096959	0,00194
130	Cda4	Chitin deacetylase-like 4	1,08	1,05	6,31847E-05	0,0000115
131	CG9747	-	1,06	1,01	0,000151094	0,0000191
132	CG9411	-	1,05	1,03	2,6019E-31	1,47E-16
133	CG5527	-	1,04	1,02	0,000017236	1,02E-08
134	CR43859	-	1,02	1,01	0,004955632	0,000023

Appendix

135	CG15545	-	1,01	1	0,040371759	0,00622
136	Gr28b	Gustatory receptor 28b	1	1,01	0,020097701	0,0000888

Genes downregulated in *Ror*⁴ mutant vs. WT

	Gene_ID	Description	log2FC		patj	
			AGW	TAL	AGW	TAL
1	CG42329	-	-4,57	-4,41	2,23381E-76	4,88E-71
2	CG18278	-	-3,89	-4,01	3,57656E-11	1,05E-20
3	CG34437	-	-3,85	-3,47	1,28739E-29	9,58E-49
4	CG7045	-	-3,62	-3,82	9,54458E-12	1,85E-26
5	CG33128	-	-3,6	-3,08	7,276E-11	5,14E-24
6	Ada1-1	transcriptional Adaptor 1-1	-3,48	-3,82	5,80706E-08	5,32E-19
7	CG11700	-	-3,44	-3,3	2,14442E-36	3,22E-56
8	Or71a	Odorant receptor 71a	-3,35	-3,24	3,21093E-14	4,68E-27
9	CG42853	-	-3,31	-3,58	0,000000061	7,19E-19
10	CG43291	-	-3,3	-2,71	1,31935E-09	1,82E-14
11	CG9822	-	-3,21	-3,57	1,06284E-06	4,02E-17
12	CG18088	-	-3,1	-2,97	1,24251E-16	7,89E-28
13	Mal-B1	Maltase B1	-3,09	-3,1	2,13732E-41	8,66E-80
14	PH4alphaSG2	prolyl-4-hydroxylase-alpha SG2	-3,05	-2,91	4,83782E-51	9,01E-64
15	CG18367	-	-3,01	-2,75	5,68428E-17	3,69E-13
16	CG4691	-	-3	-3,37	8,17979E-06	1,68E-14
17	eIF4E-3	eukaryotic translation initiation factor 4E-3	-2,96	-2,89	1,25785E-12	3,95E-20
18	CCHa2	CCHamide-2	-2,81	-2,57	4,68712E-33	2,42E-26
19	kek4	kekkon4	-2,77	-2,66	2,37579E-21	6,48E-26
20	CG33120	-	-2,58	-2,54	5,71331E-46	8,65E-58
21	CR33013	-	-2,55	-2,58	7,41957E-06	8,2E-14
22	CG10814	-	-2,54	-1,86	0,000017236	0,000145
23	CG11459	-	-2,49	-2,19	7,46068E-10	4,21E-16
24	Tektin-C	Tektin C	-2,45	-2,43	6,2095E-41	4,88E-47
25	CG30076	-	-2,36	-1,82	3,36885E-05	0,000011
26	CG6908	-	-2,36	-1,94	4,45304E-07	6,36E-08
27	Oatp58Dc	Organic anion transporting polypeptide 58Dc	-2,26	-2,1	4,95557E-16	2,01E-17
28	CG6912	-	-2,25	-2,15	8,73834E-27	2,55E-27

Appendix

29	CG5973	-	-2,23	-2,22	7,94152E-17	1,46E-28
30	CG30043	-	-2,18	-2,17	1,8846E-10	1,32E-19
31	Cht4	Chitinase 4	-2,18	-2,19	0,002871711	9,07E-08
32	Vm26Ac	Vitelline membrane 26Aac	-2,17	-1,97	0,005659788	0,0000317
33	Ugt35b	UDP-glycosyltransferase 35b	-2,15	-1,83	0,002525123	0,00000253
34	CG13998	-	-2,14	-2,57	0,006546662	4,72E-08
35	CG13427	-	-2,09	-1,97	0,000134291	9,32E-09
36	AttB	Attacin-B	-2,07	-1,94	0,00122461	5,94E-08
37	CG15818	-	-2,06	-2,04	5,07318E-27	3,51E-47
38	ssp5	short spindle 5	-2,04	-1,24	0,011087528	0,0214
39	CG43400	-	-2	-1,73	4,17597E-05	0,0000598
40	CG10257	-	-1,98	-1,8	0,010775027	0,000149
41	CG5002	-	-1,98	-1,95	4,41596E-09	1,24E-17
42	yar	yellow-achaete intergenic RNA	-1,96	-1,89	4,18039E-16	1,31E-19
43	CG43057	-	-1,96	-2,18	0,016647375	0,00000727
44	CG15905	-	-1,94	-1,92	0,000585045	0,000000661
45	CG13813	-	-1,89	-1,57	1,90911E-13	7,4E-09
46	CG4757	-	-1,88	-1,6	0,022543737	0,00261
47	Vm26Aa	Vitelline membrane 26Aa	-1,86	-1,91	0,001485053	0,000000312
48	Toll-9	Toll-9	-1,85	-1,56	0,000011063	0,000000162
49	CG14736	-	-1,84	-1,75	0,009390055	0,00000739
50	CG4650	-	-1,84	-1,79	1,00612E-05	1,87E-11
51	CG9624	-	-1,8	-1,9	0,028340665	0,0000152
52	CG33474	-	-1,77	-1,9	3,01654E-10	1,34E-12
53	CG15128	-	-1,77	-2,29	0,041307481	0,000000337
54	Lip4	Lipase 4	-1,75	-1,68	1,35838E-23	1,67E-18
55	CG13334	-	-1,75	-1,81	0,012512689	0,00000155
56	GstE4	Glutathione S transferase E4	-1,74	-1,61	0,000573574	0,0000554
57	CG31676	-	-1,74	-1,69	1,50727E-13	5,34E-15
58	Ugt37c1	UDP-glycosyltransferase 37c1	-1,74	-1,7	5,29676E-21	2,98E-22
59	Cyp6a9	Cytochrome P450-6a9	-1,73	-1,75	0,011611066	0,0000354
60	CG13428	-	-1,72	-1,72	0,030360539	0,000116
61	CG7213	-	-1,72	-2,01	0,033434714	0,0000123
62	Prat2	Phosphoribosylamidotransferase 2	-1,71	-1,35	4,84257E-12	0,000223
63	Ugt86De	Ugt86De	-1,71	-1,89	0,039761401	0,0000714
64	alphaTub84D	alpha-Tubulin at 84D	-1,7	-1,67	2,53368E-25	9,87E-45
65	Mis12	Mis12	-1,69	-1,53	1,10781E-06	0,00000143
66	CG13962	-	-1,66	-1,49	0,001916118	0,00000221

Appendix

67	CG10799	-	-1,66	-1,65	1,64805E-06	1,05E-15
68	CG11997	-	-1,61	-1,62	8,71666E-06	2,16E-11
69	CG43799	-	-1,61	-1,62	9,65201E-23	6,12E-33
70	CG32985	-	-1,61	-1,77	0,019028928	0,0000137
71	mus304	mutagen-sensitive 304	-1,59	-1,61	5,84258E-10	3,33E-20
72	CG5386	-	-1,58	-1,32	0,049814179	0,00194
73	CG42831	-	-1,57	-1,42	0,0007775	0,00000102
74	PH4alphaMP	prolyl-4-hydroxylase-alpha MP	-1,57	-1,51	0,005682934	0,000000728
75	Cyp4e2	Cytochrome P450-4e2	-1,56	-1,54	4,57455E-21	6,55E-22
76	CG31955	-	-1,54	-1,48	0,001359749	0,000000708
77	CG6034	-	-1,54	-1,48	3,4215E-07	0,00000141
78	pncr009:3L	putative noncoding RNA 009:3L	-1,47	-1,32	0,028925959	0,0000266
79	Dscam4	Down syndrome cell adhesion molecule 4	-1,46	-1,4	7,44514E-05	0,0000145
80	psd	palisade	-1,46	-1,47	2,40018E-09	1,02E-17
81	Cpr49Ac	Cuticular protein 49Ac	-1,45	-1,4	1,39685E-14	4,25E-18
82	Muc96D	Mucin 96D	-1,43	-1,33	0,011611066	0,00317
83	Adh	Alcohol dehydrogenase	-1,4	-1,38	0,043422598	0,0000335
84	Ror	Ror	-1,39	-1,38	6,56031E-36	3,66E-43
85	CG13793	-	-1,38	-1,29	0,032858923	0,00134
86	Cyp6a20	Cyp6a20	-1,38	-1,39	0,001557324	0,0000248
87	CG9394	-	-1,37	-1,31	0,018949224	0,00143
88	Cyp310a1	Cyp310a1	-1,37	-1,33	2,21102E-10	1E-11
89	Est-Q	Esterase Q	-1,35	-1,29	0,000006038	2,09E-09
90	CG30154	-	-1,33	-1,28	4,10016E-05	0,000000025
91	CG18135	-	-1,31	-1,2	7,91374E-12	0,000004
92	CG13857	-	-1,3	-1,15	0,007789481	0,006
93	IntS12	Integrator 12	-1,3	-1,28	1,96973E-10	2,45E-18
94	CG33093	-	-1,3	-1,32	2,74347E-06	2,57E-08
95	CG14502	-	-1,29	-1,28	0,005738587	0,0000224
96	CG2614	-	-1,28	-1,28	1,13208E-14	3,83E-30
97	CG9444	-	-1,26	-1,08	3,32676E-07	0,000334
98	CG10026	-	-1,25	-1,19	0,037252633	0,00289
99	Cyp4ad1	Cyp4ad1	-1,25	-1,2	6,45911E-05	0,0000428
100	CG14694	-	-1,23	-1,13	1,67401E-05	0,0000189
101	CG9961	-	-1,23	-1,22	0,006119787	0,00238
102	gfzf	GST-containing FLYWCH zinc-finger protein	-1,22	-1,18	2,68474E-09	4,48E-17

Appendix

103	poe	purity of essence	-1,21	-1,03	0,04663317	0,0485
104	CG5828	-	-1,21	-1,21	1,29615E-11	1,52E-20
105	CG33136	-	-1,19	-1,37	0,027392158	0,000144
106	CG13055	-	-1,17	-1,03	0,043422598	0,00568
107	neo	neyo	-1,17	-1,03	0,002246284	0,00252
108	CG31002	-	-1,17	-1,1	0,000324906	0,0000136
109	CG33099	-	-1,17	-1,15	1,10781E-06	1,02E-14
110	mre11	meiotic recombination 11	-1,17	-1,16	0,000131716	0,000000622
111	alpha-Est7	alpha-Esterase-7	-1,17	-1,17	3,01725E-12	2,79E-21
112	Elp2	Elongator complex protein 2	-1,16	-1,16	1,21801E-23	1,13E-26
113	nvd	neverland	-1,16	-1,16	0,000058718	0,000000025
114	CG31728	-	-1,15	-1,13	0,000000012	1,28E-14
115	CG4408	-	-1,15	-1,14	0,000468779	1,03E-08
116	Ady43A	Ady43A	-1,13	-1,11	4,36799E-10	1,16E-16
117	Cyp309a2	Cyp309a2	-1,12	-1,06	0,001466153	0,0000274
118	Gprk1	G protein-coupled receptor kinase 1	-1,12	-1,11	1,85587E-20	3,55E-24
119	fusl	fuseless	-1,1	-1	4,53656E-25	0,0000641
120	DopEcR	Dopamine/Ecdysteroid receptor	-1,1	-1,02	0,000843702	0,000616
121	CG13983	-	-1,1	-1,05	0,015163931	0,000547
122	tap	target of Poxn	-1,1	-1,08	3,37598E-14	1,24E-15
123	CG7296	-	-1,06	-1,01	0,002499162	0,000223
124	RluA-2	RluA-2	-1,06	-1,05	7,276E-11	1,69E-16
125	CG11437	-	-1,04	-1,05	0,000109038	2,18E-10
126	CG42806	-	-1,01	-1	4,29141E-08	3,78E-18
127	CG9672	-	-1	-1,02	0,028850888	0,00041

Appendix

Genes upregulated in Df(*otk,otk2*)D72 double mutant vs. WT

	Gene_ID	Description	log2FC		patj	
			AGW	TAL	AGW	TAL
1	CG32581	-	6,55	4,02	3,08382E-73	1,46E-119
2	Cyp4p2	Cyp4p2	6,34	6,47	3,1061E-238	0
3	CG32572	-	4,64	4,51	1,26831E-38	1,51E-47
4	CG31231	-	3,26	4,11	9,10657E-13	7,49E-19
5	CG32681	-	3,22	3,62	7,9782E-26	1,98E-54
6	Mst89B	Mst89B	3,11	4	3,58339E-11	1,91E-15
7	lectin-24A	lectin-24A	3,05	3,2	5,18022E-14	4,63E-12
8	Ipod	Interaction partner of Dnmt2	3,03	4,86	2,11878E-08	7,58E-20
9	CG30148	-	2,89	2,96	5,20619E-42	3,08E-19
10	Lcp3	Larval cuticle protein 3	2,84	3,46	9,15483E-09	1,04E-15
11	CG13970	-	2,72	3,43	7,70711E-10	1,46E-14
12	Best3	Bestrophin 3	2,71	3,67	2,83672E-07	8,9E-11
13	ninaD	neither inactivation nor afterpotential D	2,66	3,05	2,70111E-11	6,47E-17
14	CG18754	-	2,59	2,84	3,26423E-10	2,23E-16
15	CG5770	-	2,57	2,94	4,27788E-09	1E-10
16	CG33128	-	2,56	2,79	1,00364E-21	8,73E-30
17	CG31918	-	2,51	2,21	2,13314E-26	1,03E-44
18	CG1894	-	2,51	2,87	3,00752E-10	6,77E-18
19	CG40472	-	2,5	2,65	2,46997E-15	6,89E-31
20	CG8100	-	2,48	2,78	8,17679E-10	2,54E-09
21	CG17352	-	2,45	2,48	5,76445E-66	1,43E-47
22	CG10924	-	2,45	2,78	7,09005E-10	8,15E-16
23	CR32745	-	2,35	2,68	1,7216E-12	5,47E-24
24	CG2898	-	2,32	2,82	4,01586E-06	0,000000336
25	CG32686	-	2,26	2,64	0,000004427	0,000013
26	LysX	Lysozyme X	2,26	2,81	0,0000015	5,28E-11
27	CG8908	-	2,22	2,44	6,62656E-09	2,12E-11
28	CG5644	-	2,17	2,58	1,7866E-07	2,46E-16
29	CG6282	-	2,16	2,26	5,64394E-20	1,21E-24
30	CG32750	-	2,14	2,18	6,48946E-38	7,85E-72
31	CG13560	-	2,14	2,68	0,00012636	0,00000217
32	CG11893	-	2,12	2,35	2,21925E-09	9,23E-15
33	CG11052	-	2,1	2,35	2,11878E-08	2,17E-19
34	CG42854	-	2,09	2,47	1,09606E-09	6,49E-12

Appendix

35	CG43646	-	2,08	2,45	0,000000017	5,03E-18
36	Dhfr	Dihydrofolate reductase	2,01	2,1	8,32185E-13	7,51E-17
37	CG32368	-	2,01	2,4	1,93315E-05	2,92E-09
38	CG13360	-	2	2,06	6,45892E-06	5,56E-10
39	CG31427	-	1,96	2,54	3,89648E-05	8,84E-11
40	CG12868	-	1,94	2,15	1,19417E-05	0,000000141
41	CR33294	-	1,93	2,21	6,70326E-06	9,04E-08
42	CG40298	-	1,91	2,06	0,000000427	1,13E-13
43	gom	gomdanji	1,89	2,19	3,36705E-05	1,24E-14
44	CG42365	-	1,78	1,95	0,001239132	0,00221
45	CG7191	-	1,75	2,01	3,36718E-05	1,2E-10
46	CG1571	-	1,74	1,99	4,73802E-05	0,00000068
47	Ir87a	Ionotropic receptor 87a	1,66	1,81	6,49964E-05	0,000000226
48	Hsp27	Heat shock protein 27	1,66	1,82	7,55847E-06	0,000000107
49	CG10131	-	1,65	1,84	9,86131E-05	2,61E-08
50	CG11300	-	1,6	2,47	0,020341418	0,000493
51	CG32641	-	1,59	5,91	0,000023939	2,62E-29
52	TM4SF	Transmembrane 4 superfamily	1,58	1,71	2,98462E-05	0,00000327
53	CG42367	-	1,57	2,23	0,022061672	0,0000148
54	CG32984	-	1,54	1,68	8,02287E-07	1,33E-09
55	Muc30E	Mucin 30E	1,5	2,1	0,021807108	0,0000571
56	CG6470	-	1,46	1,65	0,000286524	1,36E-08
57	CR43870	-	1,46	1,87	0,010511704	0,00000488
58	CG11951	-	1,45	1,47	3,3559E-06	0,000000172
59	CG9664	-	1,45	1,48	9,20982E-28	3,03E-51
60	CG14564	-	1,45	1,79	0,016939382	0,00144
61	snRNA:7SK	small nuclear RNA 7SK	1,37	1,5	0,018449751	0,029
62	CG31810	-	1,34	1,46	0,000962781	0,00000567
63	CG2064	-	1,34	1,52	0,003489205	0,000055
64	lambdaTry	lambdaTry	1,31	1,4	0,002122013	0,000964
65	CG30091	-	1,31	1,42	0,006158585	0,00164
66	CG6279	-	1,29	1,32	5,46194E-07	4,89E-12
67	GstE9	Glutathione S transferase E9	1,27	1,3	0,000617939	0,000102
68	Tequila	Tequila	1,26	1,27	3,51266E-08	0,00000103
69	CG15545	-	1,26	1,33	0,004334111	0,000565
70	RpS19b	Ribosomal protein S19b	1,24	1,35	0,00125662	0,0000324
71	LKR	lysine ketoglutarate reductase	1,23	1,3	1,04088E-06	0,0000004
72	CR12460	-	1,23	1,45	0,03251539	0,000112

Appendix

73	Arc1	Activity-regulated cytoskeleton associated protein 1	1,21	1,22	0,003830025	0,0412
74	CG31516	-	1,21	1,33	0,007061058	0,000775
75	CG31414	-	1,2	1,18	2,92599E-17	1,44E-31
76	GNBP3	Gram-negative bacteria binding protein 3	1,19	1,23	1,29446E-08	1,23E-16
77	snoRNA:Or-CD12	-	1,18	1,42	0,049996284	0,00101
78	CG7860	-	1,17	1,18	2,08259E-07	0,000368
79	CG6891	-	1,14	1,15	1,12037E-19	4,36E-19
80	CG14528	-	1,12	1,15	2,06593E-10	7,58E-10
81	PGRP-LA	Peptidoglycan recognition protein LA	1,12	1,15	0,000000102	4,13E-11
82	Yp3	Yolk protein 3	1,12	1,19	0,000902846	0,000165
83	CG16965	-	1,11	1,2	0,001692597	0,000000772
84	CG14526	-	1,11	1,21	0,000773309	0,0000031
85	CG13868	-	1,1	1,13	5,84576E-06	0,000000723
86	CG32335	-	1,1	1,13	1,72628E-07	0,000000492
87	CG5854	-	1,1	1,13	7,97844E-13	2E-31
88	CG14898	-	1,1	1,15	0,000644214	0,000105
89	CG13813	-	1,09	1,15	0,000194221	0,000385
90	CG10089	-	1,07	1,14	0,000783473	0,000000131
91	Ir76a	Ionotropic receptor 76a	1,06	1,13	0,003583804	0,00000035
92	CG6357	-	1,05	1,05	0,003457629	0,0000165
93	CG17244	-	1,05	1,08	1,87862E-05	0,000371
94	CG17329	-	1,05	1,16	0,04293801	0,00266
95	ana2	anastral spindle 2	1,04	1,1	0,003183357	0,000000228
96	CG1698	-	1,02	1,05	0,002084614	0,000137
97	Ubi-p5E	Ubiquitin-5E	1,02	1,05	6,68945E-10	5,31E-16
98	CR43859	-	1,02	1,1	0,010866296	0,00000706
99	GstE5	Glutathione S transferase E5	1	1,05	0,002262135	0,000226
100	CG43647	-	1	1,1	0,028597451	0,000463

Appendix

Genes downregulated in Df(*otk,otk2*)D72 double mutant vs. WT

	Gene_ID	Description	log2FC		patj	
			AGW	TAL	AGW	TAL
1	otk	off-track	-8,88	-8,83	5,6106E-238	7,42E-115
2	CG8964		-8,02	-8,37	2,9278E-170	1,3E-190
3	mthl8	methuselah-like 8	-7,9	-8,23	1,0312E-128	1,6E-113
4	CG7045	-	-4,29	-5,75	1,69342E-20	2,15E-21
5	CG42329	-	-5	-5,22	2,31341E-88	3,62E-72
6	CG10514	-	-4,4	-4,8	5,89852E-41	5,68E-61
7	CG40498	-	-4,49	-4,71	3,22258E-62	6,09E-128
8	Victoria	Victoria	-4,11	-4,67	4,6569E-21	5,5E-25
9	CG13705	-	-2	-3,87	0,00126017	8,98E-09
10	Cnx14D	Calnexin 14D	-2,72	-3,83	3,46925E-26	9,14E-55
11	CG33093	-	-3,26	-3,6	3,13139E-23	3,95E-44
12	Arc42	Arc42	-2,97	-3,1	1,11053E-36	2,16E-52
13	Or71a	Odorant receptor 71a	-2,7	-3,1	7,81732E-12	6,05E-18
14	CG34057	-	-2,92	-3,08	7,82634E-19	2,99E-23
15	Mal-B1	Maltase B1	-2,99	-3	4,7348E-102	1,77E-71
16	eIF4E-3	eukaryotic translation initiation factor 4E-3	-2,59	-2,97	3,43253E-10	3,22E-15
17	Tektin-C	Tektin C	-2,83	-2,87	8,49287E-62	1,65E-60
18	kek4	kekkon4	-2,53	-2,85	5,21876E-12	4,72E-24
19	Mppe	Metallophosphoesterase	-2,59	-2,73	9,12924E-24	2,08E-61
20	CG18367	-	-2,21	-2,65	1,33346E-06	0,00000019
21	CG13033	-	-2,42	-2,62	2,56512E-08	0,00000171
22	Cyp12a4	Cyp12a4	-2,36	-2,59	1,8228E-11	5,26E-21
23	Cyp6a9	Cytochrome P450-6a9	-1,74	-2,27	0,00369442	0,0000546
24	Ugt86De	Ugt86De	-1,7	-2,27	0,009215835	0,00183
25	CG1315	-	-1,62	-2,23	0,011591251	0,000117
26	CG9466	-	-1,72	-2,21	0,006579257	0,00186
27	CG6034	-	-2,14	-2,2	1,83057E-14	5,99E-11
28	Ada	Adenosine deaminase	-2,03	-2,18	3,0812E-11	5,12E-17
29	CG9509	-	-1,96	-2,18	7,9251E-08	2,01E-10
30	CG9903	-	-2,03	-2,1	1,13129E-24	2,36E-43
31	CR33013	-	-1,78	-2,02	0,00015773	0,00000572
32	CG15905	-	-1,7	-1,99	0,001180681	0,000097
33	CG5973	-	-1,96	-1,99	4,52401E-19	1,12E-20
34	CG10562	-	-1,5	-1,98	0,025321814	0,00155

Appendix

35	CG5397	-	-1,91	-1,94	2,07089E-25	4,55E-20
36	Tsp42Ec	Tetraspanin 42Ec	-1,62	-1,93	0,00813589	0,00612
37	mus304	mutagen-sensitive 304	-1,83	-1,92	3,07338E-13	1,9E-26
38	phr6-4	(6-4)-photolyase	-1,81	-1,92	3,3751E-10	1,55E-18
39	CG4991	-	-1,49	-1,9	0,030815501	0,011
40	CG34166	-	-1,46	-1,85	0,031416034	0,0121
41	CG3823	-	-1,66	-1,82	3,53479E-05	0,00000281
42	CG9451	-	-1,47	-1,8	0,012830419	0,000486
43	GstE4	Glutathione S transferase E4	-1,6	-1,8	0,001521978	0,000439
44	CCHa2	CCHamide-2	-1,79	-1,77	1,97044E-20	5,35E-11
45	CG33474	-	-1,5	-1,77	6,13468E-08	2,92E-09
46	CG15279	-	-1,45	-1,76	0,020545831	0,00492
47	CG3734	-	-1,64	-1,76	2,83672E-07	9,27E-10
48	CG12539	-	-1,5	-1,72	0,001895923	0,000000167
49	CG11700	-	-1,71	-1,71	4,34587E-13	5,11E-17
50	CG43799	-	-1,66	-1,7	1,42883E-19	8,82E-35
51	kappaTry	kappaTry	-1,51	-1,69	0,003532391	0,00262
52	Cyp6a20	Cyp6a20	-1,6	-1,68	7,17536E-06	0,00000706
53	CG32364	-	-1,52	-1,66	0,000019319	4,6E-12
54	CG32243	-	-1,59	-1,64	6,22662E-16	5,29E-37
55	Cyp9b2	Cytochrome P450-9b2	-1,41	-1,59	0,003605357	0,000394
56	Tsp42Ei	Tetraspanin 42Ei	-1,57	-1,59	2,67397E-18	1,15E-14
57	CG10000	-	-1,29	-1,58	0,045751073	0,00153
58	CG7149	-	-1,55	-1,57	1,22385E-26	1,6E-32
59	CG10086	-	-1,44	-1,56	4,62735E-05	3,25E-08
60	psd	palisade	-1,48	-1,54	0,000000002	3,62E-19
61	Mis12	Mis12	-1,44	-1,53	8,33314E-05	0,0000365
62	CG31288	-	-1,37	-1,52	0,00123817	0,000000772
63	CG4302	-	-1,44	-1,51	0,000233921	0,00158
64	CG30043	-	-1,41	-1,5	5,33137E-05	1,17E-08
65	CG4098	-	-1,42	-1,5	6,0311E-06	4,38E-09
66	CG5171	-	-1,42	-1,5	2,36613E-05	0,000000633
67	Cyp4ad1	Cyp4ad1	-1,41	-1,48	1,52377E-05	0,00000341
68	CG9989	-	-1,32	-1,44	0,000294506	0,000000133
69	CG9961	-	-1,31	-1,42	0,004686855	0,00467
70	CG15530	-	-1,19	-1,41	0,036270015	0,0000708
71	CG15661	-	-1,34	-1,4	2,39067E-05	0,000104
72	CG9394	-	-1,31	-1,39	0,006392319	0,0089

Appendix

73	CG13743	-	-1,2	-1,38	0,032771183	0,00168
74	Adgf-D	Adenosine deaminase-related growth factor D	-1,19	-1,36	0,042984375	0,00727
75	CG31477	-	-1,21	-1,36	0,007415583	0,00000751
76	CG42335	-	-1,3	-1,36	8,00725E-06	7,19E-09
77	CG8665	-	-1,33	-1,36	2,6012E-10	4,01E-10
78	CG31955	-	-1,19	-1,35	0,010353506	0,0000611
79	CG32115	-	-1,28	-1,35	7,55847E-06	1,38E-13
80	CG13024	-	-1,34	-1,34	0,000161168	0,0137
81	CG11892	-	-1,23	-1,33	0,003631171	0,0000052
82	CG6236	-	-1,3	-1,33	1,04582E-13	1,77E-41
83	CG13427	-	-1,16	-1,32	0,045751073	0,00395
84	CG6431	-	-1,2	-1,31	0,001844148	0,000118
85	Dscam4	Down syndrome cell adhesion molecule 4	-1,26	-1,29	0,000209644	0,000986
86	CG10184	-	-1,21	-1,28	0,000294506	0,000000582
87	Ada2a	transcriptional Adaptor 2a	-1,2	-1,26	7,18234E-19	1,53E-67
88	CG7194	-	-1,2	-1,25	0,000108123	0,0000204
89	CG8419	-	-1,15	-1,25	0,002289438	1,32E-09
90	Lip4	Lipase 4	-1,23	-1,25	4,01361E-08	1,84E-09
91	CG5828	-	-1,22	-1,24	3,09492E-11	5,55E-21
92	alpha-Est9	alpha-Esterase-9	-1,15	-1,24	0,010289241	0,00342
93	CG17841	-	-1,19	-1,21	1,53845E-09	1,6E-10
94	CG13565	-	-1,16	-1,2	1,52377E-05	0,000000349
95	CG9672	-	-1,06	-1,16	0,025529687	0,00019
96	CG4335	-	-1,14	-1,15	1,615E-11	1,42E-12
97	mre11	meiotic recombination 11	-1,09	-1,15	0,00325565	0,00000472
98	CG31664	-	-1,05	-1,14	0,016495256	0,000144
99	Oatp58Dc	Organic anion transporting polypeptide 58Dc	-1,08	-1,13	0,001153868	0,000154
100	CG10602	-	-1,12	-1,12	7,86862E-12	3,17E-18
101	CG7299	-	-1,1	-1,12	0,010289241	0,0241
102	Fmo-1	Flavin-containing monooxygenase 1	-1,12	-1,12	1,50618E-06	0,000224
103	CG33120	-	-1,09	-1,11	9,64701E-07	1,64E-13
104	CG4408	-	-1,09	-1,11	7,65819E-05	4,92E-08
105	Elp2	Elongator complex protein 2	-1,1	-1,11	1,24214E-15	3,81E-24
106	Cyp4e2	Cytochrome P450-4e2	-1,09	-1,09	4,88328E-14	2,16E-10
107	CG15818	-	-1,06	-1,08	9,58835E-09	1,04E-12
108	CG18814	-	-1,05	-1,07	0,00000085	3,45E-10

Appendix

109	yar	yellow-achaete intergenic RNA	-1,07	-1,07	5,68383E-06	0,00000657
110	Treh	Trehalase	-1	-1,06	0,019667621	0,0053
111	alpha-Est7	alpha-Esterase-7	-1,04	-1,06	6,23882E-08	5,47E-18
112	CG6912	-	-1,04	-1,05	9,80811E-06	0,00000489
113	CG9186	-	-1	-1	9,25045E-13	7,59E-27

Appendix

Genes upregulated in *Ror*⁴, *Df(otk,otk2)D72* triple mutant (only AGW data)

	Gene_ID	Description	log2FC	padj
1	CR44417	-	6,19	2,87507E-08
2	CG42514	-	6,06	0,000991563
3	CG6357	-	5,96	0,002888638
4	Ect3	Ectoderm-expressed 3	4,41	1,86812E-07
5	CG6279	-	4,34	0,000282043
6	CG10863	-	4,32	6,47705E-08
7	Cyp6a13	Cyp6a13	3,48	0,045839555
8	CG14715	-	3,45	0,007889418
9	CG32641	-	3,41	0,024566009
10	CG31075	-	3,12	7,16338E-06
11	Gr28b	Gustatory receptor 28b	2,99	0,003384306
12	CG6280	-	2,98	1,9166E-08
13	CG4872	-	2,90	7,2227E-09
14	CG8665	-	2,84	5,28713E-10
15	CG14257	-	2,79	2,08259E-08
16	CG7173	-	2,75	4,21063E-23
17	CG32195	-	2,70	1,21202E-07
18	hng3	hinge3	2,69	0,000121503
19	CG9518	-	2,64	0,039457263
20	CG14898	-	2,62	0,000375984
21	CG17127	-	2,40	0,04790834
22	Arc2	Arc2	2,32	0,024528757
23	CG7366	-	2,16	0,013417388
24	CG32695	-	2,16	0,004326925
25	CG7763	-	2,15	0,000915865
26	CG7330	-	2,13	0,000250159
27	CG30345	-	2,10	0,006868999
28	CG8568	-	2,08	0,000180283
29	CG4398	-	1,99	1,00705E-06
30	CG5621	-	1,98	0,000920701
31	CG7384	-	1,96	0,010445353
32	TM4SF	Transmembrane 4 superfamily	1,96	0,001857423
33	CR43883	-	1,94	0,007168896
34	CG11395	-	1,92	2,26442E-12
35	snoRNA:Or-CD12	-	1,92	0,014953388

Appendix

36	GstE9	Glutathione S transferase E9	1,91	0,000504132
37	CG30091	-	1,90	0,003080616
38	CG10581	-	1,89	4,97247E-07
39	CG7135	-	1,89	0,043980132
40	CG30187	-	1,88	1,37325E-05
41	CG31810	-	1,87	1,5507E-05
42	CG32259	-	1,86	0,005464599
43	CG4415	-	1,82	2,53376E-05
44	CG33468	-	1,81	0,027017744
45	CG11060	-	1,77	0,006838315
46	CG9664	-	1,75	6,8144E-19
47	Phae1	Phaedra 1	1,71	0,035309782
48	Ir40a	Ionotropic receptor 40a	1,69	0,003921705
49	CG13868	-	1,69	1,309E-15
50	ana2	anastral spindle 2	1,66	8,96163E-10
51	lambdaTry	lambdaTry	1,63	1,0288E-05
52	CG15545	-	1,62	1,86761E-05
53	CG30148	-	1,61	0,001574994
54	CG14275	-	1,60	4,68729E-53
55	Ir76a	Ionotropic receptor 76a	1,59	2,99227E-10
56	CG1698	-	1,59	1,09254E-07
57	phr	photorepair	1,58	2,5035E-24
58	CG10131	-	1,58	0,000566046
59	gom	gomdanji	1,58	0,000890897
60	CR45451	-	1,52	0,000840407
61	CG42822	-	1,44	2,52853E-05
62	CG14567	-	1,42	2,51926E-22
63	CG5770	-	1,40	0,001628694
64	CG32368	-	1,39	0,000863503
65	CG8620	-	1,39	0,00398911
66	CG12896	-	1,38	0,000389813
67	CR43460	-	1,36	0,000200899
68	Lcp4	Larval cuticle protein 4	1,35	1,2967E-05
69	CG6470	-	1,34	6,7254E-06
70	CR43432	-	1,32	4,0481E-11
71	CG5687	-	1,31	5,8821E-05
72	Cyt-b5-r	Cytochrome b5-related	1,30	1,77363E-13
73	CG32686	-	1,29	0,00074447

Appendix

74	CG11052	-	1,28	5,31246E-07
75	Victoria	Victoria	1,27	1,34976E-05
76	Arc1	Activity-regulated cytoskeleton associated protein 1	1,26	6,44784E-07
77	fd59A	forkhead domain 59A	1,26	3,05372E-57
78	CR45140	-	1,25	2,26731E-05
79	antr	antares	1,25	1,73275E-06
80	Dhfr	Dihydrofolate reductase	1,25	5,24504E-13
81	CG17681	-	1,24	1,769E-05
82	CG13947	-	1,23	2,45146E-07
83	Eip71CD	Ecdysone-induced protein 28/29kD	1,23	1,03459E-08
84	Phae2	Phaedra 2	1,23	8,39554E-07
85	CG17633	-	1,20	9,37366E-06
86	CG31913	-	1,19	0,000200899
87	CG8908	-	1,19	7,1043E-09
88	GstD5	Glutathione S transferase D5	1,18	3,23965E-08
89	CG2898	-	1,18	4,10179E-05
90	CG10924	-	1,17	1,18973E-35
91	CG13946	-	1,17	4,20763E-05
92	CG1894	-	1,17	2,55629E-08
93	CG17244	-	1,15	3,20709E-33
94	fdy	flagrante delicto Y	1,14	1,09847E-05
95	CG3355	-	1,14	1,16061E-14
96	CG8369	-	1,12	6,52783E-12
97	CG40298	-	1,10	1,713E-15
98	CG31769	-	1,10	1,42511E-07
99	lectin-24A	lectin-24A	1,09	1,65214E-10
100	CG31918	-	1,09	1,42058E-36
101	TotF	Turandot F	1,08	8,40304E-20
102	CG42854	-	1,07	3,12141E-25
103	Best3	Bestrophin 3	1,06	1,6414E-09
104	CG12868	-	1,06	5,38773E-25
105	CG42365	-	1,06	3,33995E-16
106	CG9452	-	1,04	1,37465E-22
107	CG32681	-	1,04	6,36017E-26
108	Lcp3	Larval cuticle protein 3	1,02	2,21562E-14
109	CG31231	-	1,02	2,61006E-14
110	CG40472	-	1,02	8,79878E-46

Appendix

111	CG18754	-	1,02	4,26696E-24
112	CR44383	-	1,02	2,37372E-17
113	CR45319	-	1,02	5,69633E-27
114	CG32572	-	1,01	3,26055E-37
115	Ipod	Interaction partner of Dnmt2	1,01	1,20542E-31
116	CG13083	-	1,01	4,6136E-163
117	Cyp4p2	Cyp4p2	1,01	5,2743E-285
118	CG32581	-	1,00	1,60855E-80

Appendix

Genes downregulated in *Ror*⁴, *Df(otk,otk2)D72* triple mutant (only AGW data)

	Gene_ID	Description	log2FC	padj
1	otk	off-track	-8,41	1,7403E-200
2	CG8964		-7,69	2,1608E-181
3	CG7046	-	-5,09	5,34769E-55
4	CR45625	-	-4,27	1,42458E-24
5	CG18577	-	-4,23	3,90396E-28
6	CG42329	-	-4,19	1,04069E-38
7	CR44743	-	-3,48	4,87729E-17
8	CR43105	-	-3,45	3,43536E-14
9	CG7045	-	-3,28	1,41618E-16
10	Mal-B1	Maltase B1	-3,08	1,3556E-101
11	CG11700	-	-2,93	1,47269E-33
12	Mppe	Metallophosphoesterase	-2,81	5,54165E-38
13	CG33128	-	-2,79	2,81123E-10
14	CG18088	-	-2,75	1,44618E-24
15	CG43291	-	-2,70	8,6414E-10
16	Tektin-C	Tektin C	-2,53	8,98966E-70
17	CG43799	-	-2,45	2,14133E-46
18	CG33120	-	-2,45	7,5598E-53
19	CR33013	-	-2,35	3,35394E-07
20	Or71a	Odorant receptor 71a	-2,26	2,11015E-09
21	CG43400	-	-2,20	1,4658E-08
22	eIF4E-3	eukaryotic translation initiation factor 4E-3	-2,19	6,18679E-09
23	Cyp28d1	Cyp28d1	-2,15	1,42008E-05
24	CG5171	-	-2,14	2,47471E-14
25	CG18367	-	-2,10	6,23841E-06
26	kek4	kekkon4	-2,06	4,50608E-15
27	CG31676	-	-2,06	2,67516E-16
28	CG5973	-	-2,03	5,97339E-22
29	CG10514	-	-2,01	1,10556E-13
30	Ugt86De	Ugt86De	-2,01	9,02212E-05
31	CG9903	-	-1,99	1,7653E-30
32	CG30043	-	-1,97	3,56386E-09
33	CG5002	-	-1,96	2,55028E-28
34	CG11370	-	-1,94	0,000172505

Appendix

35	yar	yellow-achaete intergenic RNA	-1,87	2,16908E-14
36	Cyp6a20	Cyp6a20	-1,86	6,95058E-11
37	Ugt37c1	UDP-glycosyltransferase 37c1	-1,82	2,80646E-22
38	CG6034	-	-1,81	1,6638E-16
39	CG15905	-	-1,81	0,00021437
40	mus304	mutagen-sensitive 304	-1,80	8,13677E-13
41	CG9449	-	-1,80	4,90148E-06
42	NimC1	Nimrod C1	-1,75	1,04378E-06
43	Bace	beta-site APP-cleaving enzyme	-1,73	0,001350296
44	CG33474	-	-1,72	7,3506E-10
45	psd	palisade	-1,70	6,17466E-10
46	CG3868	-	-1,70	0,001508252
47	CG11892	-	-1,69	1,43719E-05
48	CG33093	-	-1,68	1,14294E-09
49	CG11997	-	-1,64	1,42315E-05
50	Cyp12a4	Cyp12a4	-1,63	8,44817E-06
51	CG9672	-	-1,54	5,7569E-05
52	CG9509	-	-1,52	2,72103E-05
53	CR45600	-	-1,49	2,83133E-05
54	CG33966	-	-1,48	6,52025E-07
55	CG4650	-	-1,48	0,000169405
56	CG13857	-	-1,46	0,000387805
57	kappaTry	kappaTry	-1,43	0,000116802
58	CR43186	-	-1,41	0,017941562
59	CG31955	-	-1,41	0,000211959
60	CG3819	-	-1,41	0,017941562
61	CG32444	-	-1,41	0,018991986
62	CG31288	-	-1,39	0,000250159
63	CG5391	-	-1,38	0,009096974
64	CG10026	-	-1,38	2,72389E-05
65	CG31103	-	-1,37	1,90735E-07
66	CCHa2	CCHamide-2	-1,36	3,82051E-06
67	Mal-A8	Maltase A8	-1,36	0,025837953
68	Ror	Ror	-1,36	2,49961E-47
69	GstE4	Glutathione S transferase E4	-1,36	0,002000682
70	Lip4	Lipase 4	-1,35	1,0493E-11
71	CG10912	-	-1,34	0,029672193
72	CR44230	-	-1,34	0,012156132

Appendix

73	Mis12	Mis12	-1,34	0,000511496
74	Dscam4	Down syndrome cell adhesion molecule 4	-1,34	6,40069E-05
75	CG17636	-	-1,34	0,001608265
76	CG33136	-	-1,33	0,002653911
77	CG9961	-	-1,33	0,002839893
78	CG13024	-	-1,33	0,001733379
79	Lsp1gamma	Larval serum protein 1 gamma	-1,31	1,05289E-07
80	CG9394	-	-1,30	0,000350681
81	CR44292	-	-1,29	7,07618E-05
82	CG8562	-	-1,29	0,000182386
83	CG7484	-	-1,28	0,001733379
84	CG13427	-	-1,27	0,011342947
85	CG15818	-	-1,26	1,39521E-14
86	fru	fruitless	-1,25	0,04790834
87	CG34437	-	-1,25	4,13103E-18
88	CG31098	-	-1,25	2,51926E-22
89	CG40160	-	-1,24	0,000451226
90	CG5828	-	-1,24	2,67401E-14
91	CG6293	-	-1,22	1,35747E-16
92	CG11459	-	-1,22	0,000772775
93	CG2614	-	-1,21	3,70941E-14
94	mt:ND2	mitochondrial NADH-ubiquinone oxidoreductase chain 2	-1,20	0,006868999
95	Bearded family member	Enhancer of split m4	-1,20	3,2608E-05
96	CR43950	-	-1,20	0,000211959
97	CG42335	-	-1,19	2,65161E-06
98	CG13160	-	-1,19	0,046816091
99	Nha1	Na ⁺ /H ⁺ hydrogen antiporter 1	-1,18	0,044925743
100	Ag5r2	Antigen 5-related 2	-1,18	0,047204932
101	helix-loop-helix	Enhancer of split m5	-1,17	0,001647194
102	CG31321	-	-1,16	0,037625548
103	Elp2	Elongator complex protein 2	-1,15	3,56797E-16
104	nvd	neverland	-1,15	9,07559E-06
105	CG31102	-	-1,14	6,58771E-08
106	fs(1)N	female sterile (1) Nasrat	-1,14	0,030948731
107	ZnT77C	Zinc transporter 77C	-1,13	1,22962E-15

Appendix

108	CG14183	-	-1,13	4,36963E-05
109	plx	pollux	-1,12	3,03647E-05
110	CG32687	-	-1,12	1,76704E-08
111	RluA-2	RluA-2	-1,10	2,87204E-14
112	htt	huntingtin	-1,09	1,22473E-05
113	CG30154	-	-1,09	0,000208455
114	CG3344	-	-1,08	1,17696E-06
115	CG6912	-	-1,08	2,85772E-10
116	mthl8	methuselah-like 8	-1,07	1,445E-06
117	Oatp58Dc	Organic anion transporting polypeptide 58Dc	-1,07	0,00198621
118	CG17732	-	-1,06	0,03606966
119	alpha-Est7	alpha-Esterase-7	-1,06	6,52783E-12
120	mre11	meiotic recombination 11	-1,06	0,001123791
121	CG5039	-	-1,05	0,001017489
122	CG18661	-	-1,05	0,009964165
123	CG33003	-	-1,03	4,49343E-05
124	CG11437	-	-1,02	7,24702E-09
125	Cyp310a1	Cyp310a1	-1,02	1,07233E-07
126	Ugt86Dc	Ugt86Dc	-1,00	0,041422878

7. Curriculum vitae

Caroline Ripp

Date of birth: March 1st 1983

Place of birth: Stuttgart

Nationality: German

Education

Since Jan 2011	<p>Doctoral studies at the Göttingen Graduate School for Neurosciences, Biophysics and Molecular Biosciences (GGNB) within the program “Genes and Development”, University of Göttingen, Germany</p> <p>Dept. of Anatomy and Cell Biology, Georg August University Göttingen</p> <p>Prof. Dr. A. Wodarz</p>
May 2010 – Dec 2010	<p>Research assistant in the Department of Developmental Biology, Centre for Organismal Studies (COS), University of Heidelberg, Germany</p>
Oct 2007 – Oct 2009	<p>Master’s Degree Program “Molecular and Cellular Biology” at the University of Marburg, Germany</p> <p>Degree: Master of Science (M.Sc.) (grade 1,3)</p> <ul style="list-style-type: none"> ➤ Infection Biology ➤ Molecular Genetics ➤ Developmental Biology
July 2007 – Oct 2007	<p>Student research assistant in the Department of Organismic Interactions, Max Planck Institute for Terrestrial Mikrobiologie, Marburg, Germany</p>
Oct 2004 – June 2007	<p>Bachelor’s Degree Program “Biology” at the University of Marburg, Germany</p> <p>Degree: Bachelor of Science (B.Sc.) (grade 2,3)</p> <ul style="list-style-type: none"> ➤ Genetics ➤ Mikrobiologie ➤ Cell Biology

Curriculum vitae

June 2002 General qualification for university entrance at the
Wirtschaftsgymnasium (commercial high school) Hermann-
Gundert Schule Calw, Germany

Stay in a foreign country

Dec 2002 – June 2004 AuPair stay in Melville, NY, USA

Publications

Böhmer, C., **Ripp, C.**, and Bölker, M. (2009). The germinal centre kinase Don3 triggers the dynamic rearrangement of higher-order septin structures during cytokinesis in *Ustilago maydis*. *Molecular Microbiology* **74** (6):1484-1496

Linnemannstöns K., **Ripp C.**, Honemann-Capito M., Brechtel-Curth K., Hedderich M., Wodarz A. (2014) .The PTK7-related transmembrane proteins off-track and off-track 2 are co-receptors for Drosophila Wnt2 required for male fertility. *PLoS Genetics* **10** (7):e1004443